Enhanced Production of Microbial Exocellular Biopolymers for Removal of Phosphate from Water

Thesis submitted in fulfillment
of the requirements
for the award of degree of

DOCTOR OF PHILOSOPHY

IN

BIOTECHNOLOGY

By

Taranpreet Kaur

(Regn no. 901000004)

Supervisor

Dr. Moushumi Ghosh

(Professor)

Department of Biotechnology

Thapar University, Patiala-147004, India

July, 2015

Dedicated To

My Beloved Family

THAPAR UNIVERSITY

CERTIFICATE

This is to certify that, the work entitled "***Enhanced production of microbial exocellular biopolymers for phosphate removal from water***" by Taranpreet kaur, in fulfillment of the requirement for the award of the degree of **Doctor of Philosophy** in the Department of Biotechnology, Thapar University, Patiala, is a record of the candidate's own independent and original research work was carried out under my direct supervision. Further, I certify that this work has not been submitted for any other degree.

Dr. Moushumi Ghosh
Professor
Department of Biotechnology
Thapar University, Patiala, Punjab,
India

Dr. Dinesh Goyal
Professor and Head
Department of Biotechnology,
Thapar University, Patiala, Punjab,
India

CANDIDATES DECLARATION

THAPAR UNIVERSITY

I hereby declare that, the present work embodied in this thesis titled "***Enhanced production of microbial exocellular biopolymers for phosphate removal from water***" was carried out by me under direct supervision of **Dr. Moushumi Ghosh** (Professor), Department of Biotechnology, Thapar University, Patiala and is the original record of my own independent and original research work. This work has not been submitted in part or in full in any other university for any degree or diploma.

Date: 31/07/2015
Place: Patiala

Taranpreet Kaur

Taranpreet Kaur
Department of Biotechnology
Thapar University, Patiala, Punjab, India

Acknowledgements

It gives me immense pleasure to thank all those individuals who have extended their help, directly or indirectly, during my stay at Thapar University, Patiala.

I would like to express my deep gratitude to my supervisor ***Dr. Moushumi Ghosh****, Professor, Department of Biotechnology, Thapar University, Patiala. Her constructive criticism, keen observation and meticulous planning were the driving forces during the course of my Ph.D. The moral support and liberty provided by her helped me hone my technical and scientific skills which will help me a long way in my life.*

I am thankful to ***Prof. Prakash Gopalan****, Director, Thapar University,* ***Prof. Abhijit Mukherjee****, former Director, Thapar University,* ***Dr. O.P Pandey****, Dean (Research and sponsored projects), Thapar University and* ***Prof. P.K Bajpai****, former Dean (Research and sponsored projects), Thapar University for providing a stimulating research environment and infrastructure for conducting research.*

I take this opportunity to thank ***Prof. Dinesh Goyal*** *(Head, Department of Biotechnology), and* ***Prof. M. Sudhakara Reddy****, Ex-Head, Department of Biotechnology, Thapar University, for their constant support during the course of my study. I am thankful to* ***Dr. H. S Bhunia*** *Department of Chemical engineering, Thapar University and* ***Prof. N. Tejo Prakash****, School of Energy and Environment, Thapar University for their valuable suggestions, guidance and support during the course of my Ph.D.*

I would also like to acknowledge the financial support received from ***University Grants Commission, New Delhi*** *for providing Maulana Azad National Fellowship to carry out the research. I would also like to acknowledge Venus Remedies Ltd, Baddi, for providing Animal House Facility to carry out in vivo studies, Sophisticated Analytical Instruments Facility, Thapar University, for providing analytical facilities, Department of chemistry, Thapar University, Centre for DNA Fingerprinting and Diagnostics, Hydrabad and Central Salt & Marine Chemicals Research Institute, Gujrat for their valuable technical help in biopolymer characterization.*

I owe special thanks to ***Dr. Abhijit Ganguli****, Associate Professor, Thapar University for his constant support and up boost during my stay at Thapar University. I would also like to acknowledge my senior labmates cum friends* ***Dr. Santosh Pathak, Dr. Mukesh Kumar, Dr.***

Meenakshi Malik Verma, Dr. Richu *and* ***Dr. Seema Bhanwar*** *for their constant support and encouragement.*

I am especially thankful to my friends ***Dr. Gurpreet Kaur Khaira, Gaatha Sharma****,* ***Mahiti Gupta, Vineet, Neha Kapoor, Neha Lohia, Parul, Supriya, Vivek*** *and* ***Pawandeep Singh*** *for their great support and valuable suggestions for carrying out research.*

I would also like to acknowledge lab assistants ***Mr. Ram Newal, Mr. Lallan Yadav, Mr. Surinder*** *and* ***Mr Mohinder*** *for their support and help in my research.*

I fell short to words to express my gratitude to my parents and in laws for the prayers, love, constant support, motivation and sacrifices they have made to make my life comfortable and helped me to complete the task. I would like to thank my dearest sister cum best friend ***Tanmeet Kaur*** *for her love, encouragement, care and never ending support.*

Last, but not the least, my special heartfelt gratitude to my loving husband ***Dr. Raman Preet Singh*** *for his endless motivation, love, patience, companionship, understanding and stimulating scientific discussions. Without his immense support, I would not be able to complete my thesis.*

Above all, Thank you ***GOD*** *for giving me patience and strength to complete my thesis*

Date:

Place:

TARANPREET KAUR

List of publications

Publications in peer-reviewed journals

1. **Kaur T**, Ganguli A and **Ghosh M**. Development of exobiopolymer-based biosensor for detection of phosphate in water, Water Science and Technology, 2013; 68:2619-25.

2. **Kaur T**, Sharma J, Ganguli A and **Ghosh M**. Application of biopolymer produced from metabolic engineered *Acinetobacter* sp. for the development of phosphate optoelectronic sensor. Composite Interfaces, 2013; 21:143-145.

3. **Kaur T and Ghosh M**. *Acinetobacter haemolyticus* MG606 produces a novel, phosphate binding exobiopolymer, Carbohydrate Polymers, 2015; 132:72-79

4. **Kaur T and Ghosh M**. Characterization and upregulation of bifunctional phosphoglucomutase/phosphomannomutase enzyme in an exobiopolymer overproducing strain of *Acinetobacter haemolyticus,* Microbiological Research, 2015; 181, 8–14.

Conference proceedings

1. **Kaur T and Ghosh M**, Overexpression of phosphoglucomutase (PGM) enzyme in metabolically engineered *Acinetobacter* sp. 54th Annual Conference of Association of Microbiologists of India (AMI) held at Maharshi Dayanand University, Rohtak , Haryana, Nov. 17-20, 2013.

2. **Kaur T**, Sharma J and **Ghosh M**, Novel phosphate biosensor based on biopolymer. International conference on Industrial Biotechnology, 2012, Punjabi University, Patiala. Nov. 21-23, 2012.

3. **Kaur T**, Sharma J and **Ghosh M**, Development of phosphate selective biopolymer-sensor using metabolically engineered strain of *Acinetobacter sp*. ICNP-International Conference on Natural Polymers, Kottayam Kerala. Oct. 26-28, 2012.

4. **Kaur T** and **Ghosh M**, Modeling of phosphate –exobiopolymer interactions, 2nd. International Conference on. "Agriculture, Food Technologies and. Environment- New Approaches". (AFTENA- 2013), JawaharLal Nehru University, New Delhi, Oct 19-20, 2013.

Table of contents

List of abbreviations

ADP	Adenosine diphosphate
ATP	Adenosine triphosphate
AICc	Corrected Akaike's information criterion
BET	Brunauer, Emmett and Teller
BJH	Barrett, Joyner and Halenda
BSA	Bovine serum albumin
CB	Commassie blue
CFU	Colony forming unit
CPC	Cetylpyridinium chloride
CTAB	Cetyltriammonium bromide
DEAE	Diethylaminoethyl
DMEM	Dulbecco's modified Eagle's medium
DMSO	Dimethyl sulfoxide
DNA	Deoxyribonucleic acid
EBP	Exobiopolymers/Exocellular biopolymers
EDTA	Ethylenediamine-tetra acetic acid
EDS	Energy dispersive X-ray spectroscopy
FBS	Fetal bovine serum
F1P	Fructose-1-phosphate
F6P	Fructose-6-phosphate
FTIR	Fourier transform infrared spectroscopy
G1P	Glucose-1-phosphate
G6P	Glucose-6-phosphate
GPC	Gel permeation chromatography
GCMS	Gel chromatography- Mass spectroscopy
GST	Glucosyltransferases
HYBRID	Hybrid fractional error function
LB	Luria Bertani
LPS	Lipopolysaccharide

LD	Lethal dose
MPSD	Marquardt's percent standard deviation
MMT	Million Metric Tons
MTT	3-(4,5-dimethylthiazol-2-yl)-2,5-diphenyltetrazolium bromide
M1P	Mannose-1-phosphate
M6P	Mannose-6-phosphate
OD	Optical density
PAGE	Polyacrylamide gel electrophoresis
PBS	Phosphate-buffered saline
PDI	Polydispersity index
PGM	Phosphoglucomutase
R.T	Retention time
RT-PCR	Real time polymeric chain reaction
rpm	Revolutions per minute
SD	Standard deviation
SEM	Scanning electron microscope
SLS	Sodium lauryl sulphate
SSE	Sum squares error
Td	Degradation temperature
TGA	Thermogravimetric analysis
UDP	Uridine diphosphate
XRD	X-ray diffraction spectrum

List of symbols

%	Percentage
µ	Micron
µg	Microgram
µL	Microliter
µM	Micromolar
°C	Degree celcius
cm	Centimeter
g	Gram
h	Hours
Kb	Kilo base
KDa	Kilo Dalton
Kg	Kilo gram
L	Liter
min	Minutes
M	Molar
mA	Miliampere
mL	Milliliter
mM	Millimolar
mg	Milligram
mV	Milivolt
nm	Nanometer
Pa	Pascal
Sec	Seconds
U	Units
v/v	Volume by volume
w/v	Weight by volume

List of Tables

List of Figures

Abstract

Phosphorus is an essential element required by all life forms for their survival and growth. Recent decades have witnessed expansion of agriculture, human population and industry resulting in increased use, and consequent elevations in discharge of phosphorus. In view of the untoward outcomes of excessive phosphorus discharge in water bodies, regulatory bodies have posed limits on phosphorus concentration in waste water. Permissible limits of phosphorus discharge are achieved through physical/chemical and biological methods of phosphate (the only bioavailable form of phosphorus) removal. However, installation and operational costs, availability of resources, phosphorus removal efficiency, recovery and reusability of phosphorus following treatment, waste management and occupational hazards are the major impediments in wide application of these methods. Sorbents derived from biological sources have gained immense interest in recent years as sustainable, non-toxic and cost effective alternatives for removal of pollutants. Despite their increasing popularity in remediation of other pollutants, biosorbents for phosphorus removal from waste water have not been extensively investigated. In fact, biosorbent-mediated phosphorus remediation has been restricted to sorbents prepared from agricultural wastes while microbial polymers have remained unexplored.

The present study exploited the potential of bacterial exobiopolymer (EBP) as a biosorbent for phosphorus removal. An isolate producing phosphate-binding EBP was isolated from sludge and designated *Acinetobacter haemolyticus* TK15. In an attempt to potentiate EBP production, mutants were generated using Tn5 transposon mutagenesis and screened for EBP yield and phosphate removal. An insertional mutant which showed enhanced EBP production and high phosphate binding affinity was selected and designated *A. haemolyticus* MG606. Sequencing of Tn5 flanking regions revealed that insertion occurred in a 9 bp motif located 89 bp upstream of a bifunctional enzyme, phosphoglucomutase/ phosphomannomutase (PGM/PMM). The Tn5 insertion resulted in increased transcription of *pgm* gene and subsequent elevation in PGM

activity in *A. haemolyticus* MG606 cell lysates. Contrastingly, enzyme activities of other enzymes involved in EBP biosynthesis (UDP-glucose epimerase, phosphoglucoisomerase and glucosyltransferase) was comparable in *A. haemolyticus* MG606 and *A. haemolyticus* TK15. The increase in PGM activity was accompanied by an increase in a downstream metabolite, UDP-glucose, which also serves as a precursor in EBP biosynthesis. Purified PGM/PMM exhibited optimal activity at 35°C and pH 7.5.

EBP produced by *A. haemolyticus* MG606 was characterized by physical, chemical and spectroscopic methods to understand its composition and physicochemical properties. Scanning electron microscopy and X-ray diffraction analysis revealed porous and amorphous nature of EBP while nitrogen sorption studies revealed surface area of 87.8 cm^2/g. The biopolymer was found to be polysaccharide in nature consisting of 48.9 KDa heteropolysaccharide composed of galactose, glucose, xylose, lyxose, allose, ribose, arabinose, mannose and fructose units. The exobiopolymer was found to be thermal stable with degradation temperature of 290°C. Aqueous solution of EBP exhibited viscoelastic properties characteristic of shear-thinning, non-Newtonian, pseudoplastic liquids. Toxicity studies revealed LD_{50} of 12.11 log CFU/mouse for *A. haemolyticus* MG606 and 92.31 mg/kg for EBP following intraperitoneal administration in Swiss albino mice. No apparent toxicity was observed in cell lines (RAW 264.7 and A549) for up to 400 µg/mL EBP.

To elucidate the nature of phosphate binding with EBP, phosphate binding was determined as a function of contact time, EBP concentration and phosphate concentration. Phosphate binding was maximal at 100 mg/L EBP and 240 min contact time. Phosphate sorption on EBP was modeled by various isotherm equations and was best described by Langmuir isotherm with maximum phosphate binding capacity of 25 mg/g of EBP. In order to further characterize the nature of phosphate-EBP interactions, the mechanism of phosphate binding was determined by

physicochemical and spectroscopic methods. Phosphate binding was attributed to polysaccharides and protein fractions of biopolymer and involved ligand exchange mechanism via hydroxyl groups and electrostatic interactions via amino groups.

The culture conditions were optimized to enhance EBP production by *A. haemolyticus* MG606. The pH, temperature, carbon and nitrogen sources were optimized in shake flask using one factor at a time method and optimal conditions were found to be temperature 35°C, pH 6.5, inoculum size 1%, agitation speed 120 rpm, glucose and acetate as carbon source and ammonium sulphate as nitrogen source. The concentrations of carbon and nitrogen sources were further optimized in a 5 L bioreactor using central composite design of response surface methodology. The highest EBP yield was observed at 5.454 g/L glucose, 4.506 g/L sodium acetate and 0.358 g/L ammonium sulphate. The growth kinetics and EBP production under optimized conditions was modeled using Leudeking-Piret model and EBP production was found to be partially growth associated.

To determine the applicability of EBP in phosphate detection, an optoelectronic biosensor was fabricated. The biosensor response was linear in the concentration range 1-10 mg/L phosphate. The limit of detection and limit of quantification of biosensor were 0.5 and 1 mg/L of phosphate, respectively. The applicability of EBP in remediation of water was determined in column studies using EBP-containing calcium alginate hydrogel beads. Phosphate removal by hydrogel beads followed Thomas model. Overall, the results of the present study suggest EBP produced by *A. haemolyticus* MG606 has potential applications in phosphate sensing and remediation.

Keywords: *Acinetobacter haemolyticus*, phosphate binding exobiopolymer, phosphoglucomutase, sorption isotherms, biosensor

1.INTRODUCTION

Sustainable management of water quality is a global issue of paramount importance. The diverse nature of pollutants as well natural constituents released intentionally or unintentionally through industrial and agricultural processes (UNEP, 2012a; UNEP, 2012b) poses a significant challenge to water quality management.

The complexity of affording water quality through appropriate interventions is compounded on account of the magnitude of untreated water discharged; as much as 80% of global waste water is neither collected nor treated, approximately 90% waste water in developing countries flows untreated in water bodies and about 70% of industrial waste originating is disposed off untreated in water. The presence of certain natural components such as phosphorous in untreated water have impacted the environment (Thakur 2006a; Thakur 2006b; Rockstrom et al., 2009). High phosphorus levels in runoff from agricultural, industrial, and domestic sources have contributed to significant detrimental environmental changes throughout entire ecosystems. Enrichment of aquatic ecosystems from agricultural runoff is attributed to algal blooms and to the formation of hypoxic zones caused by the death and decomposition of aquatic vegetation, affecting plant biodiversity in natural ecosystems and upsetting the biological balance (EC, 2013; Jarvie et al., 2013; Oliveira and Machado, 2013).

Current global budgeting indicates input of phosphates into water bodies in the tune of 13 MMT P/yr- being released to soil by weathering of phosphate-rich rocks, 46 MMT/yr from fertilizers, 24 MMT/yr by livestock and animal wastes. Phosphorus losses from lithosphere into freshwaters have been estimated as 18.7-31.4 MMT P/yr and losses to leaching and runoff are estimated at 0.16 million tons per year (Liu et al., 2008). These data indicate continued discharge of phosphorous in water bodies with a prediction of gruesome consequences on ecosystem and utilizable natural water resources. Though regulatory guidelines suggest phosphate levels within

0.05 mg/L if streams discharge into lakes or reservoirs, 0.025 mg/L within a lake or reservoir, and 0.1 mg/L in streams or flowing waters not discharging into lakes or reservoirs, few validated economical methods for phosphate removal methods have shown desirable results in terms of compliance (EPA, 2013).

Given the sensitivity of native biological population even to a small change in phosphorous concentration and the economic impact in restoration of any ecosystem, additional water quality improvement measures are necessary as an important remedial measure for the environment. Such strategies must be effective, sustainable such that they can go along with best management practices and be implemented for achieving adequate water quality. To this end, several physical, chemical and biological methods have been developed and deployed for removal of phosphate from water. Ion exchange, electrodialysis, membrane filtration are among physical treatment methods. Amongst the chemical methods, treatment with iron and aluminum salts has been successfully employed for treatment of water. These salts react with phosphorus resulting in precipitation of metal phosphate. However, the large amount of products generated and the safety of workers coming in contact with corrosive chemicals are concerns while implementing chemical precipitation methods (Beutel, 2012; EPA, 2013).

Biological methods of phosphorus removal have been advocated in recent years due to cost effectiveness as well as ease of phosphate recovery (EPA, 2013). Bioremediation of phosphates is achieved through enhanced biological phosphorus removal (EBPR) process which harnesses microbial potential to use phosphorus from water to provide energy for metabolism and building blocks for cell synthesis. EBPR process involves treatment of wastewater using polyphosphate accumulating organisms (PAOs) which accumulate phosphates intracellularly in the form of polyphosphates and by extracellular chelation through EBP produced by these PAOs.

Microorganisms such as *Pseudomonas* sp, *Acinetobacter sp, Moraxella* sp, *Aerobacter* sp, *Mycobacterium* sp, *Klebsiella* sp etc. are capable of utilizing phosphorus and its compounds in water (Blackall et al., 2002; Gebremariam et al., 2011).

Prospects of phosphate chelation by exobiopolymers (EBP) have assumed significance recently, based on cumulative reports indicating EBP producing bacterial strains with higher phosphate removal capacity as compared to the non-EBP producers. The possibility of selective enrichment by microbial EBP and its subsequent separation offer a rapid and efficient method for removal of phosphate from high phosphate contaminated sites (Cloete and Oosthuizen, 2001; Liu et al., 2006a; Liu et al., 2006b).

In fact, EBP from diverse microbial genera have been investigated for potential applications in removal of other ionic contaminations, most notably heavy metals, as well as organic contaminants like pesticides and oil spills. Thus far, several groups have reported affinity of EBP for cationic contaminants such as arsenic, lead, mercury, chromium, other heavy metal ions (More et al., 2014) as well as cation-binding capacity of EBP. The contribution of anion-binding by EBP has largely remained unexplored and studies aimed in elucidating the binding mechanisms of anions such as phosphate would be an interesting proposition.

The successful commercial application has been limited by high production and downstream processing costs for EBPs; therefore for developing real time process involving selective phosphate removal, systematic studies for optimizing EBP production by suitable strains are mandatory. To account for commercial feasibility it is equally important that EBPs are produced in sufficient quantities (high yield) by the target bacterial culture(s) (Freitas et al., 2011).

EBP production is a complex process in bacteria and is formed during exponential and stationary phase of growth. Conversion of glucose-6-phosphate (G6P) to glucose-1-phosphate (G1P) by

enzyme phosphoglucomutase (PGM) forms the starting point of the EBP biosynthetic pathway. This enzyme catalyses a representing step i.e a branch point in carbohydrate metabolism; G6P enters catabolic processes to yield energy and reducing power, whereas G1P is a precursor of sugar nucleotides that are used by cells in the synthesis of various polysaccharides leading to the synthesis of other nucleotide sugar precursors viz UDP D- Glucose UDP-D-Galactose, and dTDP - L-Rhamnose which are the donors of monomers for biosynthesis of the long chain of the EBP are synthesised by enzymes phosphorylases, epimerases etc. (Rehm, 2009). Therefore, the key regulatory enzymes are deemed as possible targets for metabolic engineering (Nigam, 2013). The common approaches for EBP overproduction is through mutagenesis- random or site directed for selection and screening of mutants for its maximal EBP production (Escalante et al., 2002; Adrio and Demain, 2006). On the other hand, using low-cost raw materials has proven to be a direct and efficient way to lower the cost of EBP while optimization of the cultivation process is a powerful approach to improve the production of EBP (Nigam and Pandey, 2009). Therefore a successful strategy must encompass development of high EBP yielding strains, formulation and optimization of a low cost media and validation of characteristics and functionality of EBP for phosphate removal.

In view of the dearth of scientific data on phosphate removal capacity of EBP by PAOs, the present study was conducted with an overall objective to investigate the nature of EBP-phosphate interactions in an EBP-overproducing strain (designated as MG606) of *Acinetobacter haemolyticus*. Specifically, the current investigation was aimed at identifying the EBP components responsible for phosphate binding and physiochemical characterization of the interacting component(s). Further, the nature and mechanism of phosphate interaction with the polysaccharide and protein fractions of EBP was investigated by physical and chemical methods.

EBP production considering one-factor-at-a-time (OFAT) method was used to investigate the effect of carbon and nitrogen sources on EBP production. The effect of significant variables influencing EBP production and their mutual interactions were investigated by central composite design (CCD) of response surface methodology (RSM) (Domingos et al., 2008; Dubey et al., 2011). Besides, the kinetics of EBP production and cell growth under optimal conditions identified by CCD were also modeled and composition of EBP produced under optimized conditions was determined. Finally, to ensure commercial feasibility of the phosphate binding EBP, biosensor and hydrogel based systems were developed and validated.

The aforementioned study was conducted under the framework of following objectives

1. Isolation, screening and identification of EBP producing bacteria

2. Development of mutants for enhanced EBP production

3. Statistical optimization of cultural parameters for high yielding mutants.

Layout of Thesis

The thesis is divided into five major chapters.

Chapter 1: Introduction contains the brief overview about the area of present study, gaps and significance of study objectives of research.

Chapter 2: Review of Literature discusses the background information on phosphate in water and environment. It entails information on current remediation technologies that are used to treat phosphate with their advantages and disadvantages, along with sources and types of exobiopolymer produced by microbes along and strategies for exobiopolymer enhancement with relevant literature.

Chapter 3: Materials and methods describe the approach and details of all the experiments that were performed in carrying out different studies are collated together.

Chapter 4: Results contains detailed results of the study and is divided into sections corresponding to study objectives. **Section 1** describes screening and isolation of microbial strains capable of producing phosphate-binding exobiopolymer and identification of the most promising isolate. **Section 2** describes insertional mutagenesis for enhanced exobiopolymer production, mechanism of exobiopolymer overproduction, pathogenicity/toxicity of the mutant and its exobiopolymer, properties of exobiopolymer and mechanism of phosphate-exobiopolymer interactions**. Section 3** describes optimization of culture conditions in shake flask along with statistical optimization and kinetic modeling at bioreactor scale. **Section 4** describes real time applications of exobiopolymer for environmental monitoring and bioremediation.

Chapter 5: Discussion discusses the results and outcomes with reports available in literature.

Chapter 6: Conclusion: the last chapter contains a summary of salient findings and conclusions of this thesis. The scope of future work is also included in this chapter.

References used in all chapters and sections are compiled at the end of the thesis.

2. REVIEW OF LITERATURE

Water is an essential component of sustainable social and economic development as well as environmental sustainability. The increasing demand of water for domestic, agricultural and industrial usage has stressed fresh water resources due to overutilization to levels much beyond sustainable limits as well as accumulation of pollutants. Nitrogen and phosphorous have been identified as the most common contaminants in fresh water and contribute to eutrophication (WWAP, 2015). Phosphorus discharges to freshwater are expected to increase more drastically than nitrogen and silicon, and hence, phosphorus poses a more imminent environmental problem than other nutrient pollutants (UNDESA, 2012).

2.1 Phosphorus in water

The rising level of phosphorus in freshwater and marine ecosystems has necessitated the need to relook into sources contributing to increased phosphorus discharge in water. The phosphorus cycle is a slow process and typically requires over a million years to complete one cycle. However, the influx has increased several folds compared to pre-industrialization era due to increased use of fertilizers and livestock as well as increased rate of soil erosion (Liu et al., 2008).

2.1.1 Global phosphorus cycle

The biogeochemical cycling of phosphorus is unique from other elements in several aspects. One of the distinctive characteristics of phosphorus cycle is that, under natural conditions, phosphorus does not exist in elemental form but as salts. The second distinctive feature is the cycle operates primarily in lithosphere, hydrosphere and biosphere with insignificant involvement of atmosphere (Filippelli, 2008).

In the lithosphere, most of the phosphorus exists in rocks in the form of apatite minerals. Apatite minerals are composed of phosphate oxyanions and calcium cations with chemical formula

$Ca_4(PO_4)_3X$ where X = OH (hydroxyapatite), F (fluorapatite) or Cl (chlorapatite) (Filippelli, 2002). The withering of rocks results in formation of soil, and thus soil serves as a phosphorus sink. In soil, the apatite material reacts with dissolved carbon dioxide or organic acids resulting in dissolution of apatite and release of phosphate. The released phosphate is incorporated by plants into biomolecules. Additionally, the released phosphorus could also co-precipitate with or adsorb on iron and magnesium oxyhydroxides and remain occluded in soil for long durations (Filippelli, 2008). The erosion of soil drains soil-bound phosphorus to rivers which carry phosphorus into seas and oceans. The eroded phosphorus sediments in deep sea and on continental margins are returned to surface by subduction or accretion (Filippelli, 2008; Liu et al., 2008). This cycling of phosphorus completes the cycle between lithosphere and hydrosphere. Phosphorus could enter biosphere in lithosphere and hydrosphere whereby plants and phytoplankton consume the dissolved phosphorus and convert to organic phosphorus. The phosphorus then moves up in the food chain from plants to animals and then returned to soil and water by excretion and decomposition processes (Filippelli, 2008; Liu et al., 2008).

Phosphorus speciation bears spatial and temporal relations at a given point in phosphorus cycle. Phosphorus exists as apatite in rocks; however, the soil formed by erosion of rocks progressively becomes enriched in organic, occluded and non-occluded fractions with a concomitant decrease in apatite forms (Filippelli, 2008; Liu et al., 2008). Following soil erosion, riverine phosphorus is delivered to oceans in two forms: particulate and dissolved. The particulate phosphorus is transported to oceans and deposited in deep sea and on continental margins, while the dissolved phosphorus is biologically available (Filippelli, 2008). The total amount of phosphorus transported to oceans via rivers is estimated at $17.7\text{-}30.4 \times 10^{12}$ g/yr. The particulate organic and inorganic phosphorus contribute 0.9×10^{12} g/yr and $15.8\text{-}27.9 \times 10^{12}$ g/yr, respectively. On the

other hand, dissolved organic and inorganic phosphorus (orthophosphate, $H_2PO_4^-$, HPO_4^{2-}, PO_4^{3-}) contribute $0.2x10^{12}$ g/yr and $0.8x10^{12}$ g/yr, respectively (Compton et al., 2000; Filippelli, 2002). Recent estimates suggest that total phosphorus influx from land to oceans is 4-6 $x10^{12}$ g/yr (Filippelli, 2008). The phosphorus cycle is summarized below (Figure 2.1).

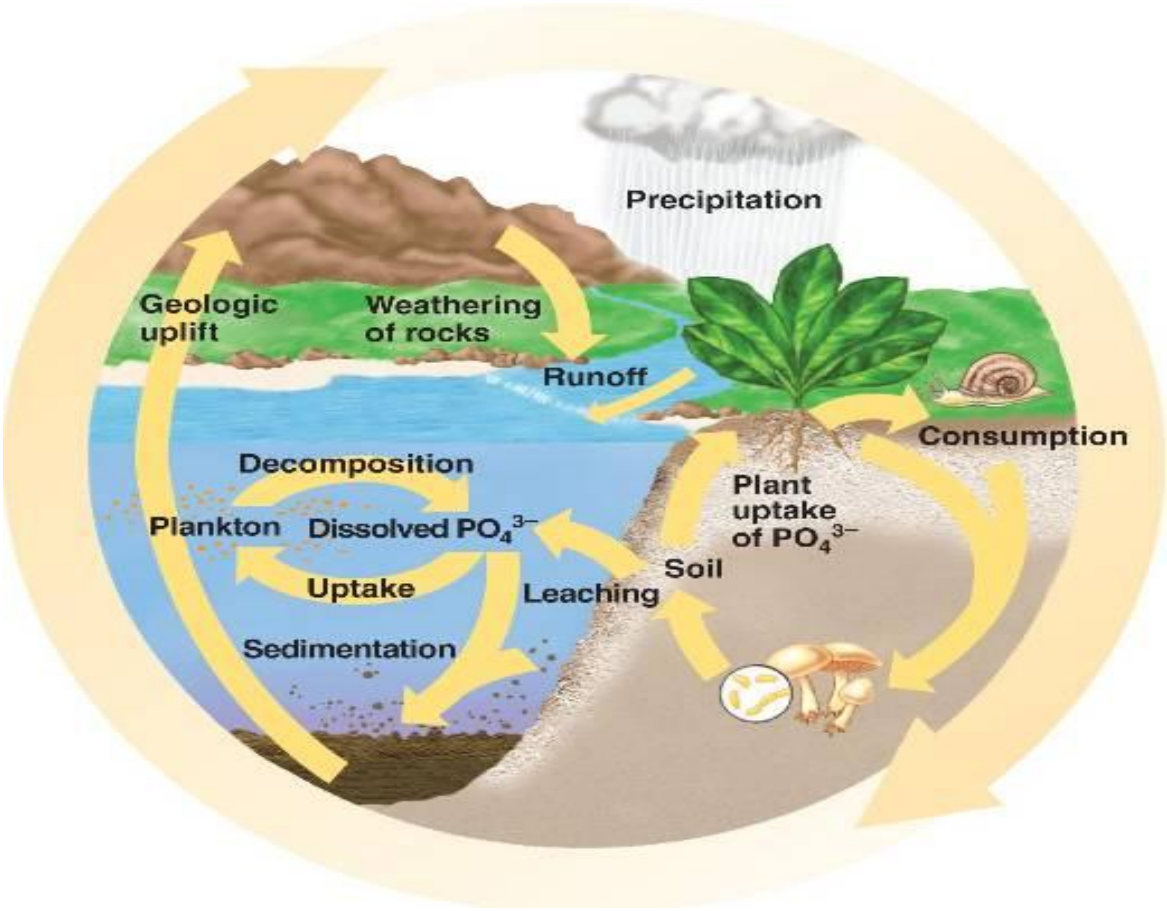

Figure 2.1: Global phosphorus cycle.
(Source: EFHS biology I: Biogeochemical cycles)

Polyphosphates are frequently used in treatment of boiler water and present in detergents sand soaps. In fact, the detergents could contain upto 7% weight fraction of phosphorus. These polyphosphates are not biologically available but could be converted to the biologically available, orthophosphates form in water (Filippelli, 2008; WWAP, 2015).

2.1.2 Phosphorus pollution: magnitude and environmental impact

Phosphorus disposal in water bodies has increased several folds in the last century due to soil erosion and agriculture runoff as well as agricultural, domestic and industrial wastes. The current phosphorus content in fresh water is at least 75% higher than pre-industrialization levels while annual inputs in oceans have increased over 5 folds (Childers et al., 2011; Bouwman et al., 2013).

Phosphate rock is the major source of phosphorus used for commercial purposes. Approximately, 158 million tonnes of phosphate rock is mined annually and 80-90% of the mined phosphorus is used in agriculture while 5% is used in animal feed and 15% for industrial applications. Of the total phosphorus applied, nearly 33% is lost due to soil erosion and only 15-30% of the applied phosphorus is utilized by crops. The phosphorus losses in livestock stand at 45% and arise due to mismanagement of manure. Therefore, soil erosion, surface runoff and agricultural wastes account for the major proportion of phosphorus reaching water bodies (Tirado and Allsopp, 2012; Bouwman et al., 2013).

The background levels of phosphorus are in the range of 0.005-0.05 mg/L and an increase in phosphorus flux to water bodies could result in eutrophication – a condition of excess nutrient accumulation. Phosphorous is a growth limiting nutrient and is generally present in low concentrations. However, an increase in phosphorus content to 0.1 mg/L provides conditions conducive for growth of phytoplanktons. This results in depletion of dissolved oxygen and algal growth. Additionally, the surface algal blooms and the increased turbidity prevent sunlight from reaching floor of water bodies thereby interfering with photosynthesis of aquatic/submerged plants. The resulting hypoxic conditions are detrimental to survival of fish and other aquatic life forms and hence result in “dead zones” where no life can survive. The noxious algal blooms also

produce toxins which could exert untoward effects on human and animal health (Chislock et al., 2013). Small proportions of the accumulated phosphorus are also converted to a highly toxic gas, phosphine, which can adversely impact human health and aquatic life (Hou et al., 2011; Ding et al., 2014).

The permissible or safe limits of phosphorus discharge have been estimated for fresh water and oceans. It is estimated that the safe limits might have exceeded by 3 to 20 times (Carpenter and Bennett, 2011) and recent estimates suggest that over 400 coastal dead zones exist (Childers et al., 2011). The eutrophication of freshwater and coastal zones will continue to increase in developed countries until 2030 and then stabilize while eutrophication will continue to increase beyond 2030 in developing countries. By 2050, the number of eutrophic lakes is expected to increase by at least 20% with phosphorus being the major nutrient pollutant contributing to eutrophication (UNDESA, 2012; WWAP, 2015).

2.2 Phosphorus removal from water

Phosphorus removal from waste water is a key factor in preventing eutrophication of water bodies. The dissolved form of phosphorus is the only fraction which participates in and contributes to the eutrophication process while the particulate forms do not participate in the biogenic cycle (Filippelli, 2002; Filippelli, 2008; Aydin et al., 2009). Amongst the dissolved forms, only inorganic phosphorus compounds are involved in eutrophication process (Bi et al., 2012; Samadi-Maybodi et al., 2013; Zhuang et al., 2014). Therefore, phosphorus removal strategies have mainly focused on removal of soluble inorganic, most notably being the phosphate ion (UNEP, 2008; Nguyen et al., 2012). Based on the mechanism of removal, the phosphorus removal methods could be classified into three major types: chemical, physical and biological (Nguyen et al., 2012). Although the mechanisms and means of phosphorus removal

differ among these methods, these methods involve two basic steps – 1) conversion of soluble phosphorus to insoluble form and, 2) removal/recovery of the insoluble form.

2.2.1 Physical/chemical treatment methods

Physical and chemical methods of phosphate removal are the most common methods of waste water treatment. Although phosphorus removal by a given process can be described predominantly as physical or chemical, it is non-pragmatic to draw clear distinctions between the two processes. This is because the removal processes involve both, physical and chemical, processes either simultaneously or in tandem (Arnaldos and Pagilla, 2010; Hasan et al., 2014). Therefore, it is generally appropriate to classify the methods as physical/chemical methods (EPA, 2013).

Filtration and/or membrane-based technologies

A large number of variants of membrane processes have been developed which employ different membrane media to filter phosphate contaminated water. The membrane filters use a pressure gradient to force contaminated water through the membrane, leaving contaminants behind. Phosphate removal by membranes is based on physical separation based on the size as well as molecular weight or by electrostatic separation by charged membranes. These membranes have been used for microfiltration (Zhang et al., 2006; Cho et al., 2009; Gerardo et al., 2013), ultrafiltration (Dietze et al., 2002; Remy et al., 2014; Yang et al., 2014), floating plastic media filtration (Chiemchaisri et al., 2003), sand filtration (Erickson et al., 2012), nanofiltration (Leo et al., 2013; Luo et al., 2014) and reverse osmosis (Kumar et al., 2007b; Leo et al., 2013; Xu et al., 2013a; Luo et al., 2014). Although separation and purification through membranes can be modulated by modulating different driving forces such as pressure, concentration, electric potential and temperature, these processes are not able to remove salts, acids, sugars etc. A

combination of reverse/forward osmosis and ultrafiltration with nanofiltration rejects macromolecules and multivalent ions effectively at moderate operating pressure. Apart from phosphate, this process is able to remove heavy metals, colour, viruses, bacteria and parasites from waste water (Qiu et al., 2015). The phosphorus removal efficiency could be upto 95%. The main disadvantages of these processes are higher cost and energy consumption along with requirement of additional ancillary equipment occupying building space.

Coagulation and flocculation

Phosphorus removal by coagulation and flocculation is the most commonly used method and include chemical precipitation/coagulation and electrocoagulation methods. Chemical precipitation is the most commonly used method whereby phosphate is precipitated with calcium, aluminum, and iron salts (Chimenos et al., 2003). The negatively charged phosphate ions react with positively charged aluminum and iron salts to form insoluble metal complexes which can be conveniently removed by filtration techniques (Zeng et al., 2004; Chimenos et al., 2006; Arnaldos and Pagilla, 2010). This chemical precipitation process depends on numerous factors like initial metal concentration, pH, temperature, ionic strength and presence of other ionic species (Szabo et al., 2008; Muster et al., 2013). Iron precipitates phosphates in the form of $FePO_4.2H_2O$ while aluminium forms $AlPO_4.2H_2O$. These forms are predominant below pH of 6. Calcium forms $CaHPO_4.2H_2O$, $CaHPO_4$, $Ca_4H(PO_4)_3.2.5H_2O$, $Ca_3(PO_4)_2$, $Ca_5(PO_4)_3OH$ etc and the complexes are formed with higher solubility under alkaline conditions (Figure 2.2) (Barat et al., 2011; Yagi and Fukushi, 2012). The efficiency of coagulation process can be further improved by combination with magnetic separation (Liu et al., 2013a; Kim, 2015; Kim et al., 2015).

Electrocoagulation is also being employed for phosphate removal by using aluminium and iron electrodes with polyaluminium chloride and other synthetic molecules as destabilizing agent (Zheng et al., 2009; Tchamango et al., 2010; Mahvi et al., 2011; Yagi and Fukushi, 2012; Kim and Chung, 2014; Stafford et al., 2014; Wang et al., 2014c).

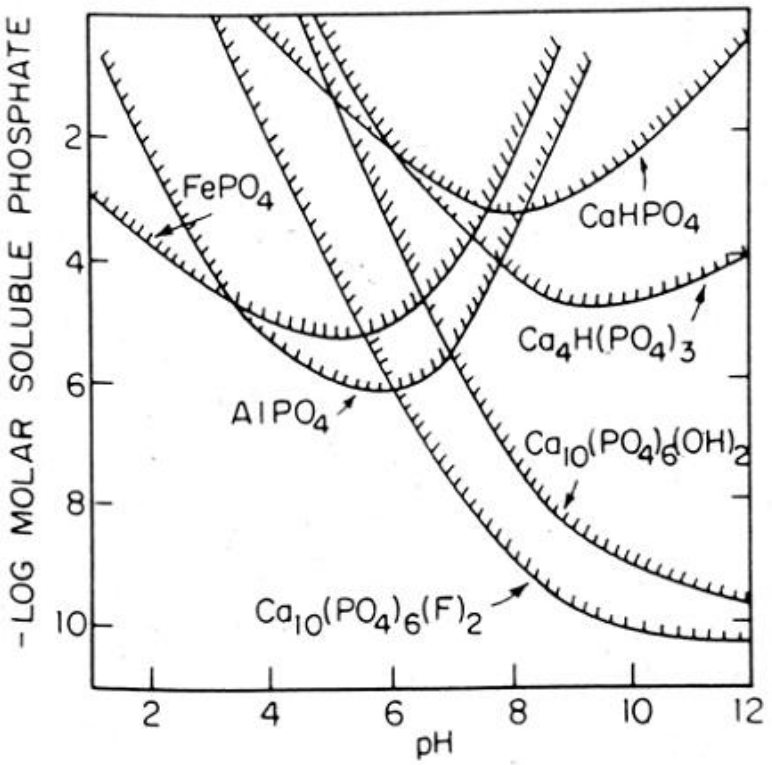

Figure 2.2: Solubility of the metal phosphates at different pH ranges.
(Source: (Stumm, 1981))

Despite the high efficiency of phosphorus removal by coagulation methods, this method has several shortcomings. One of the major disadvantages of coagulation method is the cost associated with use of metal salts and pH-controlling additives. The effluent generated after phosphorus removal requires a neutralization step which adds further costs in the process. Another disadvantage to this method is excess sludge production (metal-hydroxides and metal phosphates) which poses disposal problems. Additionally, the recovered phosphorus could not be

easily recycled and reused since other pollutants are co-precipitated with phosphorus (Nguyen et al., 2012).

Sorption

Phosphorus removal by chemical sorption is constantly gaining popularity. Sorption involves binding of phosphorus on a solid support by ionic, van der Waal's and covalent interactions. The bound phosphorus can then be recovered and reused. Several adsorbents are currently being used employed for wastewater treatment such granular activated carbon, granular iron-based media and powdered activated carbon (EPA, 2013).

In addition to standalone adsorbent systems, adsorption-based methods are also used in conjunction with other methods to improve efficiency and throughput of remediation systems (EPA, 2013). Adsorptive removal of phosphorus using wastes derived from agriculture, mining and food industry has received considerable attention in recent years because these wastes offer a cost-effective, viable, biodegradable and sustainable source of sorbents (Jellali et al., 2011; Nguyen et al., 2012; Littler et al., 2013; Nguyen et al., 2015). Some of the recently studied sorbents and their phosphorus/phosphate removal capacities are listed in table 2.1.

The main advantage of adsorption of phosphorus is the possibility of phosphorus desorption from the adsorbent and regeneration of the recovered phosphate from wastewater. A major disadvantage of this method is the low binding capacity of most sorbents thus requiring large amounts of the sorbent (Chitrakar et al., 2006; Jellali et al., 2010; Jellali et al., 2011; Wahab et al., 2011). Another disadvantage is affinity towards other anions which leads to low removal capacities under field conditions. However, chemical modifications of natural sorbents could increase affinity and selectivity for phosphorus binding (Nguyen et al., 2012). Apart from the above mentioned disadvantages, a major limitation in using sorbents is their low solubility,

viscous nature and difficulty to recover after completion of sorption. These issues have been addressed by incorporating sorbents in hydrogels prepared from natural, semi-synthetic and synthetic polymers (Singh and Kumar, 2013; Mittal et al., 2014; Mittal et al., 2015).

Table 2.1: Phosphorus removal by various adsorbants.

Material	**Adsorption capacity(mg P/g)**	**References**
Apatite	1.09- 4.76	Molle et al., 2005; Bellier et al., 2006
Woodfiber	4.3	Eberhardt et al., 2006
Date Palm fibres	4.35	Riahi et al., 2009
Posidonia oceanica fibers	7.45	Wahab et al., 2011
Bauxite	0.61-2.95	Drizo et al., 1999; Altundogan , 2002
Dolomite	0.168	Prochaska, 2006
Gravels	3.6	Vohla et al., 2005
Limestone	0.3-0.67	Drizo et al., 1999; Johansson, 1999
Sand	0.42-2.45	Pant et al., 2001; Vohla et al., 2005
Zeolite	2.15-2.19	Sakadevan and Bavor, 1998; Wu et al., 2006
Shellsand	8-9.6	Sovik and Klove, 2005; Adam et al., 2007
Phosphate mine slimes	7.45	Jellali et al., 2011
Fly ash	3.65-90.09	Chen et al., 2007; Pengthamkeerati et al., 2008; Xu et al., 2010
Alum sludge	10.20	Babatunde and Zhao, 2010

2.2.2 Biological treatment methods

Biological methods of phosphorus removal rely on phosphorus accumulating capacity of organisms. These methods employ plants or microorganisms for phosphorus removal and the biomass generated can be directly applied as fertilizer or accumulated phosphorus can be recovered by physicochemical methods (EPA, 2013).

Phytoremediation

Phytoremediation involves accumulation of phosphorus in biomass of plants like hyacinth and water lettuce as well as several species of algae/cyanobacteria (Awuah et al., 2004; Xiang et al., 2009; Gupta et al., 2012; Matsui et al., 2013; Renuka et al., 2013; Arbib et al., 2014; Li et al., 2014a; Thongtha et al., 2014; Akinbile et al., 2015; Di Luca et al., 2015; Gu et al., 2015). These organisms are used in constructed wetlands for phosphorus removal from wastewater and the biomass generated can be used as a phosphorus source. However, the high cost of collection and disposal of biomass are important concerns for habitat management. Additionally, the impact of phytoremediants on preexisting ecosystems also hampers their wide application (Chalot et al., 2012; Foucault et al., 2013; Jeong et al., 2013; Tak et al., 2013; Vigil et al., 2015).

Microbial removal of phosphorus

Enhanced biological phosphorus removal (EBPR) is a method of phosphorus removal using polyphosphate accumulating organisms (PAO). These microorganisms accumulate phosphorus from sludge in the form of intracellular polyphosphate. EBPR is divided into two major steps: anaerobic and aerobic. The activated sludge is mixed with waste water under anaerobic conditions whereby PAOs consume organic carbon (volatile fatty acids) from water and convert to intracellular poly-β-hydroxyalkanoates. PAOs also degrade intracellular glycogen and polyphosphate for energy generation and breakdown of polyphosphates releases phosphate into surrounding water. The waste water is then passed through aerobic conditions where these microorganisms take up phosphates and store it in the form of intracellular polyphosphates. The intracellular poly-β-hydroxyalkanoates are used for energy generation and glycogen production (Figure 2.3). A key to the functionality of this process is the utilization of phosphate by microorganisms both as energy source and a building block of genetic material. The main

advantages of EBPR include low operating cost, reduced sludge production, easier management and reuse potential of produced sludge (Blackall et al., 2002).

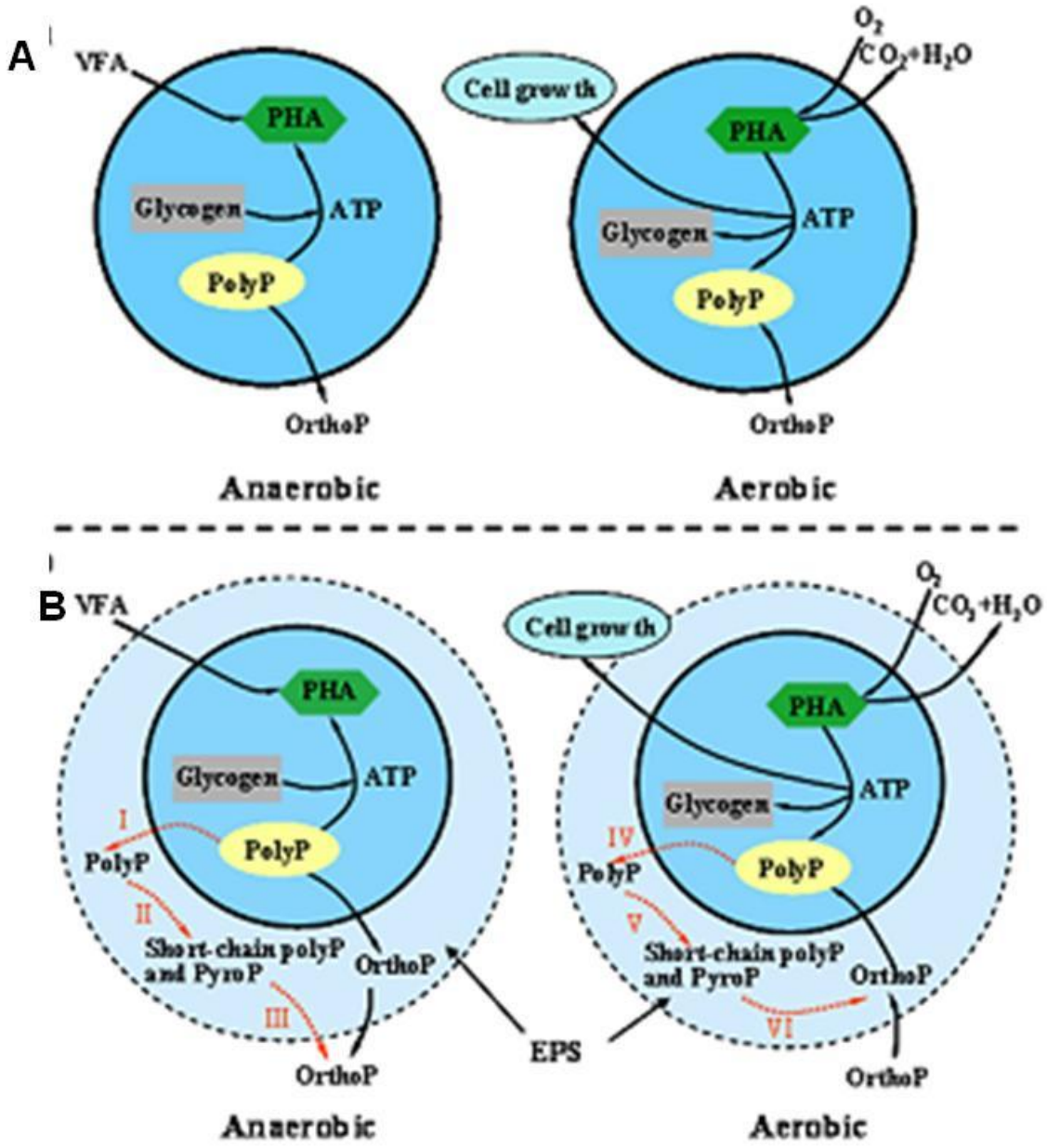

Figure 2.3: A) Metabolic model for enhanced biological phosphorus removal B) Metabolic model involving role of exobiopolymers in enhanced biological phosphorus removal.
Source (Zhang et al., 2013b)

During the initial days of development of EBPR, *Acinetobacter* sp. was the first PAO to be identified in sludge and was the most commonly identified microorganism in sludge samples

(Fuhs and Chen, 1975). Thereafter, several environmental and typed strains of various *Acinetobacter* sp. have been identified as possible PAOs in sludge samples and in experimental studies (Pauli, 1994; Muyima and Cloete, 1995; Pauli and Kaitala, 1997; Mino, 2000; Boswell et al., 2001; Gebremariam et al., 2011; Pasayeva et al., 2011; Ren et al., 2013). Other microorganisms involved in EBPR process are *Lampropedia* spp. (Stante et al., 1997), *Microlunatus phosphovorus* (Nakamura et al., 1995), *Micropruina glycogenica* (Shintani et al., 2000), *Tetrasphaera elongate* (Hanada et al., 2002) *and Candidatus Nostocoida limicola* (Blackall et al., 2000), *Pseudomonas* spp. (Li et al., 2003), *Moraxella* spp. (Lotter, 1984), *Aeromonas* spp. (Li et al., 2003), *Klebsiella* spp. (Gersberg and Allen, 1985), *Pseudomonas cesicularis* (Suresh et al., 1985), etc.. Approximately, one-third of the bacterial population of EBPR plant is comprised of Actinobacteria while another one-third of betaproteobacteria and nearly one-tenth of gammaproteobacteria. The Acinetobacter are one of the major PAOs and account for 3-6% bacterial population (Blackall et al., 2002; OECD, 2010).

In recent years, it has been realized that extracellular biopolymers or exobiopolymer (EBP) present in activated sludge can also bind phosphorus and contribute to EBPR as shown in figure 2.3 (Lee et al., 2003; Wang et al., 2014a). It is estimated that EBP can bind phosphorus upto 10% of its weight. This is comparable to phosphorus removal by highly efficient EBPR processes where phosphorus ratio is 8-12%. In presence of conditions stimulating EBP production, the efficiency of EBPR could further increase upto 14% phosphorus weight ratio due to contributions by EBP (Liu et al., 2006a; Liu et al., 2006b). According to one estimate, EBP fraction could contribute as high as 30% of the total phosphorus removal in EBPR (Wang et al., 2014a). However, these studies were either restricted to quantitative analysis of phosphorus content (Cloete and Oosthuizen, 2001; Oosthuizen and Cloete, 2001; Zhou et al., 2008; Li et al.,

2010a; Fang et al., 2011; Long et al., 2012; Liu et al., 2006a; Liu et al., 2006b) or phosphorus speciation in EBP (Zhang et al., 2009; Zhang et al., 2013a; Zhang et al., 2013b). A major shortcoming of these studies is the fact that the EBP present in EBPR sludge is heterogenous in nature with contributions from all EBP-producing organisms present in sludge. The identity of organism(s) contributing to phosphate-binding fraction of EBP is elusive.

2.3 Microbial exobiopolymers

EBPs are produced by microorganisms and secreted by microbial cells which account for their slimy character. The extracellular EBP helps in water retention and minimise desiccation of cells. EBP is also involved in aggregation of bacterial cells, adherence to surfaces, flocs and cellular communications. EBP is a key structural element of biofilm and forms a protective barrier against chemical stress. Due to the resistance conferred by EBP, microbes are able to survive in fresh water, salt water, soil, sludge, cold or hot environment (Iyer et al., 2006; Kumar et al., 2007a; Singh et al., 2011b; Kreyenschulte et al., 2014; Madhuri and Rabhakar, 2014; Zhurina et al., 2014).

EBP is mainly composed of carbohydrates, proteins, nucleic acids, lipids and uronic acids along with substitutions by acetate, pyruvate, succinate and other acids. Proteins and carbohydrates are predominant components and comprises about 75-90% of the polymer. Other components, present in relatively smaller amounts, are lipopolysaccharides, glycoproteins and lipoproteins (Singh et al., 2011a; More et al., 2014). Microorganisms exhibit significant interspecies and intraspecies (interstrain) differences in EBP composition and structure. Based on their composition, EBP can be classified into homopolysaccharides and heteropolysaccharides (Satpute et al., 2010; More et al., 2014).

Table 2.2: Some exobiopolymers with their applications.

Polymer	Organism	Monomers	Application	Reference
Dextran	*L. mesenteroides, Pediococcus* sp. *Streptococcus* sp	Glucose	Blood plasma extender, microcarrier in tissue culture, immobilization in biosensors	Bhavani and Nisha, 2010; Samal and Dubruel, 2014
Alternan	*L. mesenteroides*	Glucose	Low-glycemic sweetener	Patel et al., 2012
Inulin	*L johnsonii, L citreum*	Fructose	Prebiotics, targeted drug delivery	Patel et al., 2012
Curdlan	*A. faecalis, C. flauigena*	Glucose	Gelling agent	Zhang and Edgar, 2014
Pullulan	*A. pullulans*	Maltotriose, Maltotetrose	manufacture of edible films	Singh et al., 2008; Cheng et al., 2011
Xanthan	*X. campestris*	glucose, mannose, glucuronic acid	Emulsification, gelatination	Garcia-Ochoa et al., 2000
Alginate	*A. vinelandii* *P. aeruginosa*	mannuronic acid, guluronic acid	Immobilization, Microencapsulation	Lee and Mooney, 2012
Levan	*Z. mobilis* *B. subtilis*	Fructose	Cholesterol lowering agent, blood plasma extender	Combie, 2006
Gellan gum	*Sphingomonas sp.*	D-glucose, L-rhamnose and D-glucuronic	Gelling agent	Bajaj et al., 2007
Hyaluronic acid	*Streptococcus spp., L.lactis, B. subtilis, P. multocida, P. aeruginosa*	D-glucuronic acid and D-N-acetylglucosamine	Moisturization, Synovial fluid replica	Liu et al., 2011b; Boeriu et al., 2013
Emulsan	*A. calcoaceticus, A. venetianus RAG-1*	N-acyl D-galactosamine, N-acyl L-	Emulsification, Immobilization	Dams-Kozlowska et al., 2008

		galactosamine uronic acid and 2,4-diamino-6-deoxy-D-glucosamine, fatty acids		
Welan gum	*Alcaligenes sp*	L-mannose , L-rhamnose, D-glucose, and D-glucuronic acid	Stabilizer, viscosifier	Kaur et al., 2014
Ethapolan	*Acinetobacter sp*	glucose, mannose, galactose, and rhamnose	Emulsification	Grinberg et al., 1995; Pirog et al., 2004
Alasan	*A. radioresistens* KA53	galactosamine, D-galactosaminuronic acid, and diaminodideoxy glucosamine, alanine	Emulsification	Navon-Venezia et al., 199)
Biodispersan	*A. calcoaceticus* A2	glucosamine, a 6-methyl aminohexose, galactosamine uronic acid,amino sugars	Biodispersion and Emulsification	Rosenberg et al., 1988a
Liposan	*C. lipolytica*	glucose, galactose, galactosamine, and galacturonic acid.	Emulsification and stabilization	Cirigliano and Carman, 1985
Poly-gamma-glutamate	*B. anthracis and B. subtilis*	D-glutamate	Bioflocculant	Rehm, 2010; Bajaj and Singhal, 2011
polyL-lysine	*S. albulus*	L-lysine	Bioflocculant	Nishikawa and Ogawa, 2002
Kefiran	*L. kefiranofaciens, L. delbrueckii subsp. bulgaricus*	Galactose, Glucose	Thickener, stabilizer, emulsifier, gelling agent	Maeda et al., 2004

Other Exobiopolymers	*L. casei*	Rhamnose, glucose, galactose, glucosamine. Galactosamine	Artificial thickners, viscosifiers, stabilizers, emulsifying agents, gelling and water-binding agents, texturizers	Sutherland, 1986; De Vuyst et al., 1998; De Vuyst and Degeest, 1999; Mozzi et al., 2006; Madhuri and Rabhakar, 2014
	L. delbrueckii subsp.bulgaricus	Galactose, Glucose, rhamnose		
	L. debrueckii subsp. Lactis	Galactose, Glucose		
	S. thermophilus	Galactose, glucose and N-acetyl glucosamine, N-acetyl galactosamine		
	L. rhamnosus	Glucose, Galactose, rhamnose		
	L. lactis ssp. Cremoris	Galactose, glucose and rhamnose		
	L. paracasei	Glucose, galactose		
	L. helveticus	Glucose, Galactose, rhamnose, and N-acetyl glucosamine		
	L. sake	Glucose, rhamnose		

Structurally, the EBP could be classified as alpha- and beta-linked, or linear and branched glycans. These structural differences transform into different physicochemical characteristics and are crucial for functionality of EBP (Satpute et al., 2010; More et al., 2014). For example, dextran is (1→6)-linked α-D-glucan , curdlan is (1→3)-linked β-D-glucan where as cellulose is (1→4)-linked β-D-glucan. Among the heteropolysaccharides, alginate is one of the most important polymer which is composed of linear non-repeats of (1→4)-linked β-D-mannuronic acid and α-L-guluronic acid. On the other hand, xanthan gum is composed of glucose, acetylated mannose, glucouronic acid and pyruvate while gellan gum is composed of glucose, glucuronic acid and rhamnose units (More et al., 2014; Roca et al., 2015). Some of the commercially useful EBP are listed in table 2.2 with their applications.

2.3.1 Biosynthesis of EBP

EBP is a complex mixture of different classes of biomolecules and hence, EBP biosynthesis is a complex process. Amongst the various biochemical components, polysaccharide fraction is the major component both in terms of composition and functionality. Hence, biosynthesis of polysaccharide fraction has remained the key area in understanding and elucidating EBP biosynthesis (More et al., 2014; Roca et al., 2015).

Polysaccharide biosynthesis can be divided into four steps: 1) sugar transport into cytoplasm, 2) synthesis of sugar-1-phosphates, 3) activation and coupling of sugars and 4) polymerization and export. Sugars represent the principal carbon source of microorganisms and their movement into cytoplasm is tightly regulated by control proteins. The inward transport of sugar is carried out by transport systems like phosphoenolpyruvate-sugar phosphotransferase system and permease transport system. This system is involved in phosphorylation of the transported sugars to prevent their outward movement by diffusion. The transported sugars are then converted to different

phosphosugars and then into sugar nucleotides. Under experimental conditions, glucose is generally used as the sole carbon source and hence, the production of different sugar nucleotides follows the biosynthetic pathway as outlined in figure 2.4. However, in case other sugars (galactose, lactose, etc.) are used as carbon, these are converted to glucose 1-phosphate via Leloir and other pathways and therefore, the pathway converges to that shown in figure 2.4 (Looijesteijn et al., 1999; Rocchetta et al., 1999; Bonin and Reiter, 2000; Richau et al., 2000; Escalante et al., 2002; Harper and Bar-Peled, 2002; Hofmann et al., 2005; Oka and Jigami, 2006; Gu et al., 2011; Wu et al., 2014b; Roca et al., 2015). The production of the polysaccharide is under genetic control and several genes involved in EBP biosynthesis are located in an operon. Under appropriate environmental and/or nutritional conditions, the genes located on the operon are activated resulting in EBP production. Microorganisms like *Pseudomonas* can simultaneously produce more than one type of polysaccharide and in such cases, the enzymes required for synthesis of EBP precursors could be shared among different operons and pathways (Franklin et al., 2011; Ghafoor et al., 2011; Ma et al., 2012; Chew et al., 2014; Laverty et al., 2014; Wang et al., 2014b). The sugar nucleotides produced through the biochemical cascade are assembled into the polysaccharide backbone through glycosyltransferases and exported outside the cell. The extracellular translocation could be mediated through a lipid-mediated or a non-lipid-mediated mechanism. The polysaccharide could undergo further modifications, such as acetylation, before exporting outside the cell (Franklin et al., 2011; Dimopoulou et al., 2014; Hidalgo-Cantabrana et al., 2014; Laverty et al., 2014).

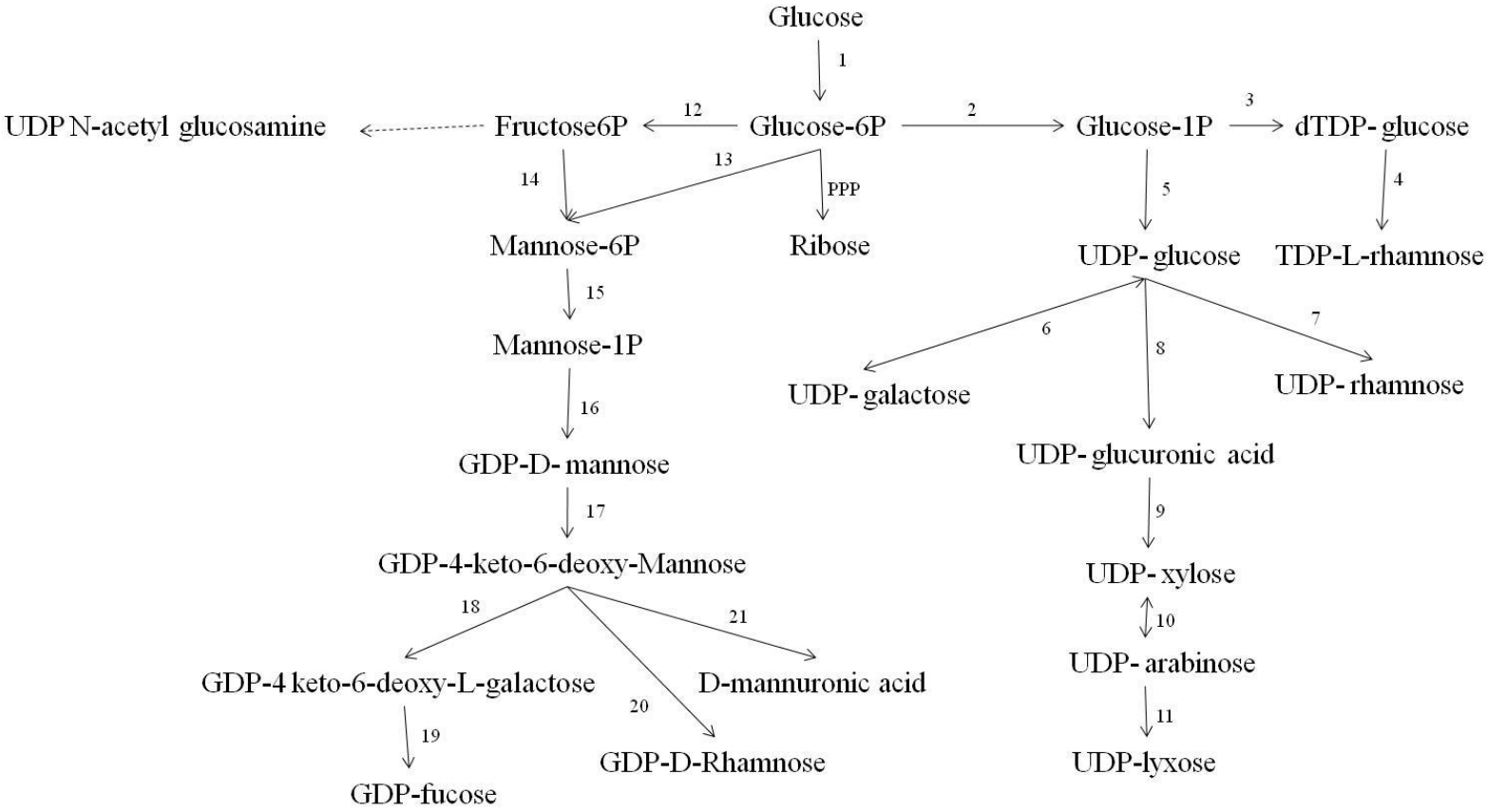

Figure 2.4: Postulated pathway leading of nucleotide sugar precursors presumed to be involved in exobiopolymer biosynthesis. 1 = Hexokinase; 2 = Phosphoglucomutase; 3 = dTDP-glucose pyrophosphorylase; 4 = TDPR synthatase complex; 5 = UDP-D-glucose pyrophosphorylase; 6 = UDP-glucose 4 epimerase; 7 = UDP-L-rhamnose synthase; 8 = UDP-glucose dehydrogenases; 9 = UDP-glucuronic acid decarboxylases; 10 = UDP-xylose 4-epimerase; 12 = Phosphoglucose isomerase; 13,14 = Mannose 6-phosphate isomerase; 15 = Phosphomannomutase; 16 = Mannose 1-phosphate guanyltransferase; 17 = GDP-D-mannose 4,6-dehydratase;18 = GDP-4-keto-6-deoxy-D-Man 3,5 epimerase; 19 = GDP-4-keto-6-deoxy-L-galactose-4-reductase; 20 = GDP-4-keto-6-deoxy-D-Man reductase;21-GDP-D-Man dehydrogenase

2.3.2 Environmental applications of EBP

In recent years, EBP produced by microorganisms have been identified as a novel, safe, biodegradable platform for environmental remediation due to their flocculant and sorptive properties. EBP stabilize microbial aggregates by polymer entanglement, ion bridging mechanism, electrostatic interactions, van der Waal's forces and hydrogen bonding and hence, helps in removal of microbes and particulate matter by flocculation (Mayer et al., 1999; Mikkelsen and Nielsen, 2001; Klausen et al., 2004; Satpute et al., 2010; More et al., 2014). EBP can also adsorb pollutants by physical adsorption, ion exchange, complexation and precipitation mechanism (Wingender et al., 1999; Satpute et al., 2010; More et al., 2014). Due to these properties, EBP from a large number of microorganisms, such as *Bacillus subtilis, Pseudomonas putida, pseudomonas aeruginosa, Pseudomonas plecoglossicida Exiguobacterium acetylicum, Klebsiella terrigena, Bacillus licheniformis, Staphylococcus aureus, Pseudomonas, Halomonas, Herbaspirasillum* and *Paenibacillus* have potential applications in dye, metal ion and oil spill removal as well as wastewater and land leachate treatment (Loaec et al., 1997; Deng et al., 2003; Guibaud et al., 2003; Priester et al., 2006; Zhang et al., 2007; Li et al., 2009; Liu et al., 2009; Buthelezi et al., 2010; Satpute et al., 2010; Jia et al., 2011; Chassenieux et al., 2013; Chien et al., 2013; More et al., 2014).

2.3.3 Constrains in application of EBP

Commercial applications of EBP are restricted due to low productivity and high costs. This is because, under natural conditions, these polymers are produced in very low quantities and hence, only a few polymers with desirable properties can be manufactured in a commercially viable manner. The low productivity also requires several downstream processes of purification which results in losses at each processing step which further reduce the yield and increase production costs. Further, in several cases, the strains may produce several types of biopolymers and separation of the desired fraction requires additional purification steps.

Thus, there is a potential need to develop strategies to enhance extracellular turnover of these biopolymers (Freitas et al., 2011; Kaur et al., 2014; Kreyenschulte et al., 2014; More et al., 2014; Roca et al., 2015).

2.4 Strategies for enhancing extracellular turnover of EBP

The commercial production of EBP production is governed by 4 important variables: raw material (carbon and nitrogen sources), fermentation process (type and design of bioreactor, operational conditions), strain and downstream processing. The culture medium is by far the most expensive component which can account for as much as 40% of the total production costs. The downstream processing costs are an important constraint when high purity biopolymers are required for food and pharmaceutical applications but the processing costs generally contribute to relatively smaller proportion of total production costs. The production costs bear an inverse relation with production volume and hence, with an increase in production volume and yield, the overall production costs could be significantly reduced (Kreyenschulte et al., 2014). Considering, the importance of enhancing EBP production, several strategies are used which include strain improvement (metabolic or cellular engineering, selection of spontaneous mutants) as well as optimizing upstream and downstream processes (Kurane and Matsuyama, 1994; Adrio and Demain, 2006; Rehm, 2009; Rehm, 2010; Freitas et al., 2011; Kreyenschulte et al., 2014; Roca et al., 2015).

2.4.1 Strain improvement

Strain improvement is the most commonly employed method for augmenting EBP production. This strategy involves selection of EBP overproducing mutants generated by random or targeted mutagenesis.

Random mutagenesis results in unbiased mutations throughout the genome resulting in generation of a large number of mutants. These mutations can be introduced by use of physical mutagens such as ultraviolet and X-ray radiations or chemical mutagens such as

ethyl methane sulfonate, methyl methane sulfonate, diethylsulfate and nitrosoguanidine. Physical mutagenesis has been successfully applied for selecting mutants which overproduce xylanase, bacitracin, monacolin K, clavulanic acid and other industrially important enzymes but with limited success for EBP overproduction (Korbekandi et al., 2010; Awan et al., 2011; Sun et al., 2011; Xu et al., 2011a; Aftab et al., 2012; Ghazi et al., 2014). Similarly, chemical mutagenesis has also been extensively used for enhanced production of several exoproducts (Frengova et al., 2004; Pratush et al., 2010; Chen et al., 2013; Khanam and Prasuna, 2013; Li et al., 2014b) including exobiopolymer production (Escalante et al., 2002; Welman et al., 2003; Derkx et al., 2014). Although physical and chemical mutagenesis is useful for generation of mutants with complex phenotypes without prior knowledge of genetic composition and regulatory networks, these methods suffer from several disadvantages such as mutation hot spots, screening of a large number of mutants and reversibility of mutations (Derkx et al., 2014). These issues with physical and chemical mutagenesis have paved the way for development of insertional mutagenesis methods.

Insertional mutagenesis is a random mutagenesis technique which employs mobile elements, called transposons, as mutagens. Transposons are short pieces of DNA that replicate by inserting into other pieces of DNA (plasmids, chromosomes, viruses). These mobile elements have been employed for random mutagenesis at genomic level to identify organization of individual genes and decipher genes involved in complex, multigenic phenotypes. Transposon mutagenesis offers several advantages over chemical and physical mutagenesis. First, transposon insertion generally occurs at a single point in the whole genome therefore a single gene is affected in a mutant unlike physical and chemical mutagens which can induce multiple mutations in one mutant. Second, transposon insertion introduces a marker gene (such as antibiotic resistance) in the mutant which helps in easy selection of mutants from the background while all colonies need to be screened after physical and chemical mutagenesis.

Third, the transposon insertion site can be easily determined by inverse PCR and primer walking techniques while genome sequencing is required for mapping mutations introduced by physical and chemical mutagens (Judson and Mekalanos, 2000; Bosse et al., 2006; Xu et al., 2011b; Barquist et al., 2013; Stahl and Stintzi, 2015).

A large variety of transposons [Tn(s)] have been developed for bacterial mutagenesis such as Tn3, Tn5, Tn7, Tn10, Tn552, Mu and mariner (Choi and Kim, 2009). These transposons are composed of a central region coding for antibiotic resistance gene(s) with insertion sequences at both ends. The insertion sequences help insert the transposon into host DNA and these insertions could either be biased towards specific sequence motifs as observed in Tn5 and Mu or relatively unbiased as observed in Tn7 (Manna et al., 2001; Kumar et al., 2004; Seringhaus et al., 2006; Green et al., 2012). Tn5 is the most extensively studied transposon in bacterial mutagenesis and has been used for identifying genes involved in complex biological processes such as exobiopolymer production (Nogales et al., 2006; Pehl et al., 2012; Janczarek and Urbanik-Sypniewska, 2013; Malamud et al., 2013; Cursino et al., 2015). This strategy has been applied for modifying production of multi-gene products such as fatty acids and enzymes (Civerolo et al., 1987; Chatterjee et al., 1995; Dunne et al., 2000; Amiri-Jami et al., 2006). Further, Tn5-mediated mutagenesis has also been employed to identify genes responsible in EBP production and enhance biopolymer production by Tn5 insertional mutagenesis (Reeve et al., 1997; Gibson et al., 2006; Rodriguez et al., 2006; Neeraj et al., 2009; Nunez et al., 2009; Jones, 2012; Cursino et al., 2015).

2.4.2 Metabolic engineering

Metabolic engineering is another commonly used strategy for overproducing microbial products through engineering of biosynthetic pathways. This method involves modulation of metabolite flux between competing pathways with an aim to divert the flux towards the pathway involved in biosynthesis of product of interest. Since EBP biosynthesis is dependent

on the availability of sugar nucleotides, metabolic engineering of EBP production has focused on overexpression of genes involved in EBP biosynthesis. Considering the complexity of EBP biosynthetic pathway and the multitude of enzymes involved, a large number of enzymes could serve as potential targets. However, only a few of these enzymes have been explored and validated so far (Papagianni, 2012). Phosphoglucomutase is a key enzyme in EBP biosynthetic pathway and is a branching point between glycolysis and EBP biosynthesis pathway. Overexpression of phosphoglucomutase in lactic acid bacteria resulted in amplification of EBP production presumably through diversion of carbon flux towards production of sugar nucleotides (Levander et al., 2002; Svensson et al., 2005; Papagianni, 2012). Similarly, engineered lactic acid bacteria overexpressing epimerase and glycosyltransferases also exhibited enhanced EBP production (van Kranenburg et al., 1999; Boels et al., 2001; Levander et al., 2002; Mozzi et al., 2003; Koo et al., 2010; Chai et al., 2012).

2.4.3 Alteration of culture conditions

Culture conditions are an important factor governing production of microbial products and hence, their optimization presents an arduous task in developing an efficient fermentation process. EBP production from bacteria is widely affected by culture conditions such as temperature, pH, incubation conditions and nutritional sources.

The optimum growth temperature for maximum EBP production depends on the type of microorganism as well as temperature of its natural habitat. Some reports suggest that EBP synthesis is growth associated and the optimal temperature required for bacterial growth and EBP production are the same. This is because optimal temperature increases synthesis of sugar precursors and a decrease in temperature results in decreased growth rate and biosynthesis of sugar precursors. On the other hand, a reduction in growth at sub-optimal temperatures could divert metabolic flux towards EBP biosynthesis (More et al., 2014).

According to literature, most of the microorganisms produce EBP at temperature ranging from 25°C to 30°C but in some cases unfavorable conditions could trigger EBP production in response to self protection. In case of mesophilic strains, growth of bacterial strain and EBP production is uncoupled but the opposite is true for thermophilic strains (Cerning et al., 1994; Gamar-Nourani et al., 1998; De Vuyst and Degeest, 1999; Looijesteijn et al., 1999; Degeest et al., 2001; Shene et al., 2008; Torres et al., 2012; More et al., 2014; Yilmaz et al., 2014).

EBP production by microorganism is greatly influenced by cultural pH however, the effect of pH on EBP synthesis largely depends on microorganism, operating conditions and media used for cultivation. The pH-induced morphological changes in cells could result in reduction in EBP biosynthesis (More et al., 2014). In most bacteria, the optimal pH for EBP production varies between 5 to 7 (Williams and Wimpenny, 1977; De Vuyst et al., 1998; Gamar-Nourani et al., 1998; Grobben et al., 1998; Looijesteijn and Hugenholtz, 1999; More et al., 2014) while pH 2.6 was found optimal for *Lactobacillus salivarius* (Sanhueza et al., 2015).

Carbon and nitrogen sources significantly impact EBP yield, composition and molecular weight. Although bacteria can assimilate a wide range of carbon and nitrogen sources, EBP production is supported on selected nutritional sources only (Ravella et al., 2010; More et al., 2014). It is believed that EBP producing genes could be induced in presence of specific substrates and hence, only a few substrates support EBP synthesis (Audy et al., 2010; Liu et al., 2011a; Seviour et al., 2011; Andersen et al., 2013; Lee et al., 2013; Shi et al., 2014). Further, use of alternating carbon sources such as whey, molasses, soyabean oil and agro-wastes or by-products such as spent malt grains, apple pomace, grape pomace, and citrus peels offer cheaper alternatives to costlier nutritional sources (Cerning et al., 1994; Sutherland, 1998; Shivakumar and Vijayendra, 2006; Muhammadi and Afzal, 2014).

2.5 Pathogenicity of exobiopolymer-producing organisms

The pathogenicity of producer strain is a major concern. These concerns attract even more

attention in case the producer strain is genetically modified to induce production of a foreign molecule or augment production of an endogenous compound. According to OECD and WHO (Laboratory Biosafety Manual), the possibility of alterations (augmentation or attenuation) in pathogenicity of a genetically engineered bacterium depends on a host of factors including, but not limited to, the genetic background of donor and recipient strains (WHO, 2004; OECD, 2011). OECD guidelines on application of microorganisms for environmental bioremediation states that the pathogenicity of wild type isolates may be altered by genetic engineering and suggest characterization of pathogenicity factors in the engineered strains. These studies are crucial to determine biosafety at laboratory and production scale as well as assess the impact of intentional or unintentional release of engineered strains in environment (OECD, 2011).

The correlation between pathogenicity factors and pathogenicity may appear to be plausible but the OECD guideline itself states that the correlation may not be straightforward. In fact, the mere introduction of a foreign pathogenic factor or augmentation of an endogenous pathogenic determinant may not be enough to escalate pathogenicity (OECD, 2011). Therefore, the molecular characterization of pathogenic factors could not be completely relied on but serve as indicators or provide supplementary information when data is available from more reliable assay methods. The most straightforward approach in establishing pathogenicity of bacterial strains is the mouse lethality assay which determines death/survival of mice after injection of different doses of bacteria (Giacometti et al., 2004; Lindback et al., 2011). This approach is similar to toxicity screening of chemicals since bacterial pathogenicity is also determined in terms of LD50 values.

2.6 Toxicological evaluation of exobiopolymer

The commercial application of a new chemical, irrespective of its application, is subject to regulatory clearance and approval. A key component of the regulatory clearance process is

submission of toxicity data to ascertain untoward effects of the chemical on human health. The toxicity studies are generally conducted in rodents (mice or rats) and may be divided into single dose (acute) or repeated dose (subacute or chronic) studies. The acute toxicity studies are generally the first step in a toxicity screening program and allow calculation of median lethal dose (LD50). LD50 value serves as an indicator of toxicity and a metric to compare toxicities of different compounds. Although any dose (and dose range) can theoretically be used to calculate LD50, OECD has set forth a limit of 5000 mg/kg as the maximum permissible dose for acute toxicity considering the relevance to human exposure levels.

Microbial EBPs are generally considered devoid of toxicity and thus, extensive studies on EBP toxicity are not available except for EBPs approved for use in food, cosmetics and pharmaceuticals. On the other hand, a host of beneficial effects of EBP have been reported such as antioxidant, anticancer, immunomodulatory, etc. which have further fostered the assertions on inherent biocompatibility of EBPs (Ramberg et al., 2010). A systemic review of 34 microbial polysaccharide gums used in cosmetics was published by Cosmetic Ingredients Review panel and found to be safe based on available literature. The LD50 values of beta-glucan, gellan gum, pullulan and xanthan gum were found to be >1000 mg/kg following oral administration while those of beta-glucan and high molecular weight dextran were <1000 mg/kg following parenteral administration. Similarly, WHO has also recognized gellan gum, pullulan and xanthan gum as sufficiently safe for food applications. Dextran has been approved as an indirect food additive as well as a pharmaceutical ingredient for eye drops and as plasma substitute (Long et al., 2012). Despite the availability of extensive toxicity studies on a few high molecular weight EBPs, a generalization on non-toxic nature of all EBPs could not be drawn and further studies are warranted to address this issue.

3. MATERIALS AND METHODS

3.1 Reagents and chemicals

All chemicals were either procured from Sigma (USA) or HiMedia (India) unless otherwise specified. Luria-Bertani agar (LA), Luria-Bertani broth (LB), bacterial culture media components, Dulbecco's modified Eagle's medium and fetal bovine serum (FBS) were purchased from HiMedia, Mumbai. Culture media used for EBP production was composed of ammonium sulphate (1 g/L), calcium chloride dihydrate (0.7 g/L), dextrose (1 g/L), dipotassium hydrogen phosphate (1 g/L), magnesium sulphate heptahydrate (0.3 g/L), peptone (5 g/L), potassium dihydrogen orthophosphate (1 g/L), sodium chloride (0.1 g/L) and agar (3 g/L). The final pH of medium was adjusted to 7.0 ± 0.2. Culture media was sterilized by autoclaving at 121°C for 20 min and allowed to cool below 50°C before use. Other details of reagent and media preparation are described in Annexure I.

3.2 Isolation and screening of exobiopolymer producing bacteria capable of phosphate binding

3.2.1 Collection of water and sludge samples

Water and sludge samples were collected from eight different sites expected to receive high phosphate inflow (Table 3.1). Triplicate water samples were collected in sterile plastic containers previously rinsed and sterilized with isopropyl alcohol from each sampling site. The sludge samples were collected in sterile plastic bags (HiMedia, Mumbai) and transported to the laboratory on ice and analyzed within 6-8 h post collection.

3.2.2 Screening of exocellular biopolymer producing bacteria

Total bacteria present in water and sludge samples were isolated by thoroughly mixing one gram of sample to 100 mL of sterile saline. After vortexing for 5 min, 1 mL of sample was withdrawn and mixed with 9 mL of saline in a sterile test tube and marked the test tube as 10^0 dilution.

Similarly, 10-fold dilutions were made up to 10^{-5}. Hundred microliters from each dilution was spread evenly on LA plates. The inoculated plates were incubated at 37°C for 24-48 h for isolation of individual colonies. EBP producing microorganisms were screened on the basis of mucoid appearance on EBP production media. From the total of 280 isolates, 130 isolates having mucoid appearance were selected. Further, the selected isolates were grown in LA/LB for routine maintenance and preserved in cryovials at -80°C using 40% glycerol as cryoprotectant. The culture isolates were grown in 1000 mL of EBP production media for 48 h at 37°C and EBP production from these isolates was examined.

Table 3.1: Number of bacterial isolates from different sites.

Sites	Number of isolates
Bhakhra Canal, Patiala	23
Eutrophic pond, Rajpura Road, Patiala	58
Drain 1, Rajpura Road, Patiala	54
River drain 2, Rajpura Road, Patiala	29
Federal Mogul Industry, Patiala (Site 1)	24
Federal Mogul Industry, Patiala (Site 2)	32
Federal Mogul Industry, Patiala (Site 3)	40
Rainbow Denim Ltd., Lalru	20

3.2.3 Exocellular biopolymer extraction and purification

For EBP extraction, isolates were centrifuged at 12,000 g for 30 min at 4°C. The cell free supernatant was concentrated to one tenth of its original volume by lyophilizing. Double volume of chilled ethanol was added to precipitate the crude EBP and kept overnight at 4°C. The crude

EBP precipitates were collected by centrifugation at 12,000 g for 30 min at 4°C. The pellet formed was dissolved in equal volume of deionized water and precipitated with 10% of cetyl pyridinium chloride and resuspended in 10% NaCl. The suspension formed was again centrifuged at 10,000 g for 20 min and pellet was dialyzed extensively for 48 h with deionized water. The EBP formed was lyophilized to obtain purified powdered product (Ghosh et al., 2009).

3.2.4 Screening of bacteria producing phosphate binding exocellular biopolymer

The crude EBP extracted from isolates was further screened on the basis of binding ability with phosphate. Standard concentration of EBP (1 mg/mL) and potassium dihydrogen orthophosphate (1 µg/mL) were prepared and mixed. The mixture was incubated for 12-24 h at 30°C. After incubation, the mixture was then filtered through 0.22 µm membrane filter and phosphate concentration was determined by molybdenum blue stannous chloride method (APHA, 1998). Two milliliters of sample was mixed with 2.5 mL of ammonium molybdate solution (2.5%) and 2 mL of stannous chloride (2.5%) (Annexure I). The reaction was allowed to proceed for 10 min at room temperature and absorbance was recorded at 690 nm.

The isolates were selected on the basis of percentage phosphate removal. Out of 130 EBP producers, only 5 isolates produced EBP which could bind phosphate. Based on maximum binding ability, one strain was selected for further studies and designated as TK15.

3.3 Morphological and biochemical characterization of strain TK15

The isolated TK15 was characterized on the basis of morphological, biochemical and microscopic observations. The identification was done according to the methods described in *Bergey's Manual of Determinative Bacteriology* (Bergey and Holt, 1994). Some of the biochemical methods are described as below

Hydrogen sulfide test

To differentiate between sulfur reducers and non-reducers, SIM agar (Annexure I) tubes were inoculated with log phase cultures and incubated at 37^{o}C for 24 h. Sulfate reducers convert sulfur compounds to sulfide and leads to formation of black precipitates. An uninoculated tube was used as negative control.

Urease test

Urea broth (Annexure I) was inoculated with log phase culture of TK15 and incubated at 37ºC for 24 h. After incubation, phenol red was added and change in color was observed. The urease positive bacteria produce pink color with phenol red due to formation of ammonia. An uninoculated tube was used as negative control.

Methyl red test

Methyl red Voges-Proskauer (MR-VP) broth (Annexure I) was inoculated with log phase culture of TK15 and incubated at 37ºC for 24-48 h. After incubation, few drops of methyl red indicator (Annexure I) was added to the culture. An uninoculated tube was used as negative control.

Voges-Proskauer test

MR-VP broth was inoculated with log phase culture of TK15 and incubated at 37ºC for 24-48 h. After incubation, few drops of Barritt's reagent A (Annexure I) was added, with continuous shaking for 10 min. Then, few drops of Barritt's reagent B (Annexure I) was added. The development of a deep rose color represents a positive result. An uninoculated tube was used as negative control.

Citrate utilization test

Simmon citrate agar (Annexure I) was streaked with log phase culture of TK15 and incubated at 37ºC for 24-48 h. Citrate positive cultures were identified by the presence of blue colored growth on the surface of slant. An uninoculated tube was used as negative control.

Indole production test

SIM agar tubes were inoculated with log phase culture of TK15 and incubated at 37ºC for 24 h. Cultures producing a red layer on the addition of Kovac's reagent (Annexure I) represents a positive test. An uninoculated tube was used as negative control.

Starch hydrolysis test

TK15 isolate was streaked on starch agar plates (Annexure I) and incubated at 37ºC for 24-48 h. After incubation, the plates were flooded with Gram's iodine solution for 30 sec and then the excess of iodine was decanted. Appearance of clear zone surrounding the colonies was monitored for starch hydrolyzing ability of isolate.

3.4 16S molecular characterization of strain TK15

Total genomic DNA was isolated from isolate TK15 by phenol-chloroform precipitation method (Sambrook and Russell, 2001). The log phase cells of TK15 were washed twice with saline, resuspended in saline EDTA and then lysed with cell lysis solution (Annexure I) at 37°C for 10 min. Equal volume of phenol:chloroform:isoamyl alcohol solution (25:24:1) was added and centrifuged at 8,000 g, for 10 min. Equal volume of isopropyl alcohol was then added to upper aqueous phase layer and centrifuged at 12,000 g for 30 min followed by washing with 70% ethanol at 10,000 g for 10 min. The pellet was then air dried and dissolved in 30 µL of Tris EDTA (TE) buffer. The extracted DNA was resolved on 0.8% of agarose gel by electrophoresis.

DNA was amplified with universal primers P0 (5'-GAGAGTTTGATCCTGGCTCAG-3') and P6 (5'-CTACGGCTACCTTGTTACGA-3'). The PCR mixture contained 1 µL *Taq* (10 X) buffer, 5 µL purified DNA (50-100 ng), 150 µM of each dNTP, 500 ng of each primer and 2.5 U *Taq* polymerase. The reaction mixture volume was adjusted to 100 µL with MilliQ water. The reaction mixture was first incubated for 5 min at 95°C for initial denaturation, and then cycled for 36 cycles for denaturation, annealing and extension (94°C/1 min, 55°C /1 min, 72°C/2 min), followed by a final extension for 10 min at 72°C, on a Bio Rad thermal cycler (Bio Rad, MyCycler, USA). The amplicon so obtained was sequenced using automated sequencer. DNA sequencing was performed by the Genei Molecular Biology Resource Facility at Bangalore India, using an ABI Prism 310 Genetic Analyzer (PE Applied Biosystems, USA) with Big Dye Terminator Cycle Sequencing v 2.0. The sequence of isolate TK15 was searched in NCBI BLAST and related sequences were aligned in MEGA5 using CLUSTAL W (Tamura et al., 2011). The evolutionary analysis was performed by neighbor-joining method in MEGA5 and Kimura 2-parameter method was used to compute evolutionary distances (Saitou and Nei, 1987) (Kimura, 1980).

The isolate TK15 was characterized to be *Acinetobacter haemolyticus*, thus was represented as *Acinetobacter haemolyticus* TK15. The 16S rDNA sequence of *A. haemolyticus* TK15 was deposited in GenBank database with Accession No KP701480.

3.5 Amplified Ribosomal DNA Restriction Analysis (ARDRA)

ARDRA was used to verify the authenticity of the isolated *A. haemolyticus* TK15 strain and for molecular fingerprinting. The 16S amplicon generated in section 3.4 was digested with tetracutter restriction enzymes by incubation. The reaction mixture included: 16 µL PCR reaction product, 1.0 µL of *Alu*I or *Sau*3A (5U) separately and 2.0 µL Buffer. The reactions were allowed

to incubate at 37°C for 1 h. The restriction profile were resolved by electrophoresis on 1.4% (w/v) agarose gel (Vaneechoutte et al., 1995).

3.6 Evaluation of virulence markers in *A. haemolyticus* TK15

The virulence markers were determined in *A. haemolyticus* TK15 based on markers commonly found in Acinetobacter sp. and enterobacteriaceae (Doughari et al., 2011; Bitrian et al., 2012; Tayabali et al., 2012).

Haemolysis

Haemolytic assay was performed in 5% (v/v) sheep blood agar plates (Himedia, Mumbai). Bacterial culture was spot inoculated on to blood agar plates and incubated for 48 h at 37ºC. The plates were visually inspected for clear zone (hemolysis) around the colony (Bitrian et al., 2012).

Cell mobility

To determine cell motility, an isolated colony of *A. haemolyticus* TK15 was picked with a sterile needle and medium containing triphenyl tetrazolium chloride was stabbed to a depth of 1 cm in the tube. The tubes were incubated at 37°C for 18 h. A positive motility test is indicated by a red turbid area extending away from the line of inoculation (Bitrian et al., 2012).

Antibiotic sensitivity profile

Antibiotic susceptibility profile of *A. haemolyticus* TK15 was analyzed by Bauer-Kirby disc diffusion method (Bauer et al., 1966). Briefly, 250 µL of log phase bacterial culture was added to 25 mL of LA medium and poured on 90 mm petridish. The uniform sized paper discs (diameter 6 mm) was placed on the surface of LA and impregnated with antibiotics at the concentration of 25 µg/mL. The antibiotics used (ampicillin, chloramphenicol, ciprofloxacin, gentamicin, kanamycin, rifampicin and streptomycin) were selected based on previous reports on antibiotic

sensitivity profile of *A. haemolyticus* and related species (Wolff et al., 1999; Bitrian et al., 2012; Tayabali et al., 2012).

Protease activity

Protease estimation was performed in culture supernatant of *A. haemolyticus* TK15. To the 1 mL of supernatant, 3 mL of phosphate buffer (pH 7.5) was added followed by 1% casein (3 mL) as substrate and the mixture was incubated at 35°C for 30 min. The reaction was stopped by addition of 5 mL trichloroactetic acid and filtered. To1 mL of filtrate, 2 ml of 20% Na_2CO_3 and 1 mL of Folin's reagent was added followed by incubation for 30 min at room temperature. The absorbance was recorded at 650 nm by diluting the mixture with 6 mL of distilled water and compared with blank (Cupp-Enyard, 2008).

Lipase activity

Nutrient agar plates containing 2.5% trioleylglycerol and 0.001% rhodamine B solution (w/v in sterile water) were prepared. The plates were bored with 3 mm borer and 100 µL of culture supernatant was added in these wells. The plates were incubated at 37°C for 16 h. The presence of lipase activity in the culture was confirmed by formation of orange colored product around wells (Willerding et al., 2011).

N-acylhomoserine lactones (AHLs) production assay

Fifty microliters of log phase culture of *Chromobacterium violaceum* CV026 was added to 5 mL of molten semi-solid LA (3% w/v) and poured over the surface of prewarmed LA plates. After solidification of overlaid agar, wells were punched with a sterile cork borer. These wells were filled with supernatant of *A. haemolyticus* TK15. The petri dishes were incubated at 30°C for 24 h and examined for the stimulation of violacein synthesis indicated by blue purple pigmentation of the bacterial lawn around wells (McClean et al., 1997).

Biofilm production

A. haemolyticus TK15 isolate was grown in LB medium overnight at 30ºC. Culture was inoculated in polystyrene 96-well plates containing 200 µL media. After 24 h incubation, samples were carefully removed, the wells were gently washed three times with 200 µL of phosphate buffer saline (PBS), dried in an inverted position, and stained with 1% (w/v) crystal violet (CV) for 20 min. The wells were then washed five times with 400 µL of PBS, the CV-stained cells were solubilized in 200 µL of ethanol, and the samples were incubated for 30 min with gentle mixing. The absorbance of the solubilized biofilm was measured at 585 nm. A blank was processed under the same conditions using LB medium (Djordjevic et al., 2002).

3.7 Transposon mutagenesis for development of exocellular biopolymer overproducing mutants

3.7.1 Generation of spontaneous mutants

In order to obtain an antibiotic selection marker for *A. haemolyticus* TK15, spontaneous mutants were generated by spreading log phase culture of TK15 on streptomycin (25 to 100 µg/mL) containing LA. The survivor colonies that appeared after overnight incubation were picked and grown on streptomycin-containing LA for ten subsequent generations to confirm resistance against streptomycin. This colony was referred as spontaneous mutant (Wang et al., 2001).

3.7.2 Screening of exocellular biopolymer overproducing mutant

Transposon mutagenesis was carried out by conjugation between donor *Escherichia coli* JB110 harboring Tn5-containing pGS9 (suicidal vector) and recipient spontaneous mutant *A. haemolyticus* TK15 (Ghosh et al., 2006). The antibiotic resistant strains were selected using kanamycin (50 µg/mL) and streptomycin (200 µg/mL) as selection markers for donor and recipient, respectively. Mid-log phase cultures of donor and recipient cells were harvested,

washed twice with saline and mixed in different ratios (1:1, 1:2, 2:1 and 1:3). The mixed cells were placed on filter paper discs supported on LA plates and incubated at 30°C for 24 h. The filter paper discs were transferred to 50 mL LB containing 50 µg/mL kanamycin and 200 µg/mL streptomycin. The cells were incubated in selection medium for 8 h at 30°C. An aliquot of 0.1 mL was withdrawn from antibiotic-containing LB and spread on LA plate. The EBP-producing exconjugants were selected from a library of 998 mutants on the basis of mucoid appearance of colonies. Mucoid colonies were transferred to EBP production media and crude EBP was extracted to determine EBP yield and phosphate removal. The mutant showing highest EBP yield with phosphate removal capacity was selected and as designated as *A. haemolyticus* MG606.

3.7.3 Confirmation of Tn5 insertion

Total genomic DNA form *A. haemolyticus* TK15 and its mutant strain *A. haemolyticus* MG606 were extracted as described in section 3.4. PCR reactions were conducted using Tn5-specific forward primer (5'-CATTGACCACACCACCTCT-3') and reverse primer (5'-CAGCAACAACCATTTCAACG-3'). The PCR mixture (100 µL) contained 1 µL *Taq* (10 X) commercial buffer, 5 µL of purified DNA, 150 µM of each dNTP, 500 ng of each primer and 2.5 U *Taq* polymerase. The reaction mixture volume was adjusted to 100 µL with MilliQ water. The 100 µL of reaction mixture was incubated at 95°C for 5 min for initial denaturation followed by 36 cycles of denaturation, annealing and extension (94°C/1 min, 51°C/1 min, 72°C/2 min), followed by a final extension for 10 min at 72°C on a Bio Rad thermal cycler (Bio Rad, MyCycler, USA). The amplified Tn5 DNA was resolved on 1.4% agarose gel.

3.8 Identification of insertion site by inverse PCR

The site of Tn5 insertion was mapped by inverse PCR. This technique involves restriction digestion of genomic DNA followed by intramolecular ligation to generate circular DNA. The

circularized DNA is then amplified by PCR using primers directed outwards of Tn5 which allows amplification of sequences in flanking region of Tn5 insertion point. The experimental procedure is outlined in figure 3.1 and primers used listed in table 3.2.

Table 3.2: List of primers used in the study.

Gene/Primer	Primer sequence	References
Tn5	5'-CCATTGACCACACCACCTCT-3' 5'-CAGCAACAACCATTTCAACG-3'	Self designed
IR2	5'-CGGGATCCTCACATGGAAGTCAGATCCTG-3'	(Huang et al., 2000)
BR	5'-CATTCCTGTAGCGGATGGAGATC-3'	(Huang et al., 2000)
BG	5'-GCCAAGGATCCGATGGCGCAGG-3'	Self designed
pgm	5'-CCGTGTAGTGATGGTTGATAAGTTCGGTAAC-3' 5'-GCTTTTTCAAGTGCCACTTCAAGTGCC-3'	Self designed
tuf	5'-TGGGAAGCGAAAATCCTG-3' 5'-CAGTACAGGTAGACTTCTG-3'	Self designed

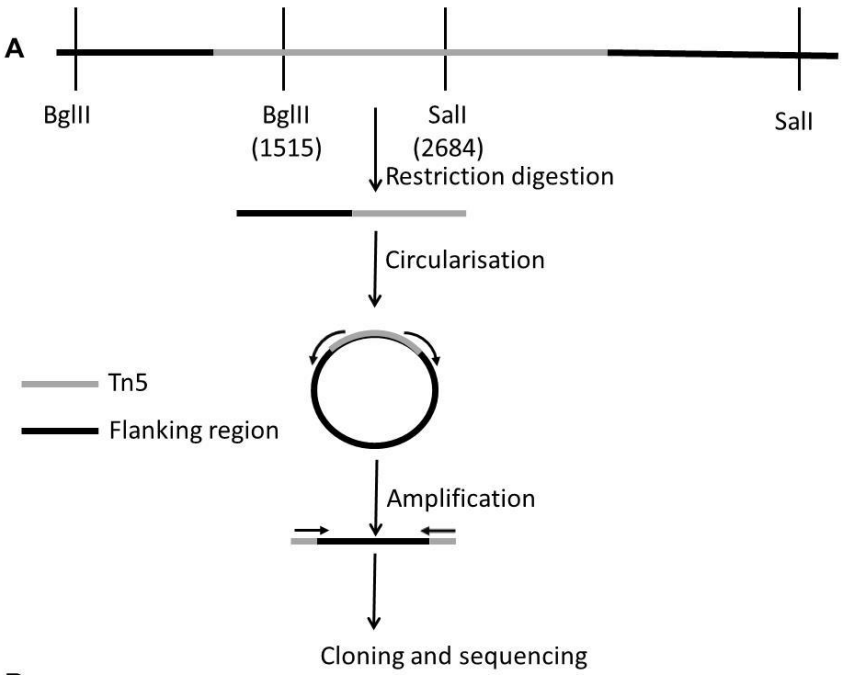

Figure 3.1: Outline of inverse PCR procedure and position of restriction sites.

Genomic DNA of *A. haemolyticus* MG606 was separately digested with 10 U of *Sal*I or *Bgl*II (Promega, USA). After overnight digestion at 37°C, self-ligation was performed using Rapid DNA Ligation Kit (Roche Applied Science, Germany). The restriction digested DNA (10 µL; 0.1µg/mL) was mixed with 10 µL ligation buffer (5X) and 4 µL T4 DNA ligase (6 U/µL). The reaction mixture was incubated overnight at 22°C and then, heated to 70°C for 5 min to stop the reaction. Inverse PCR was performed using self-ligated DNA as template. The PCR reaction mixture comprised of 1X reaction buffer, 2 mM $MgCl_2$, 200 µM of dNTPs, 0.5 µM forward and reverse primers (Table 3.2), 2.5 units *Taq* polymerase and 6-8 ng template DNA. The template DNA was amplified by 1 cycle of initial denaturation (95°C/5 min), 35 cycles of denaturation, annealing and extension (94°C/1min, 53°C/1min, 72°C/3min) and 1 cycle of final extension (72°C/5 min). The PCR product was purified with Wizard SV Gel and PCR Clean-Up System (Promega, USA). The purified amplicons and pGEM-T easy vector (Promega, USA) were digested overnight with 10U *Bam*HI. The digested vector and insert were mixed in 1:2 ratio and ligated with 4 U of T4 DNA ligase. The reaction mixture was incubated for 30 min at 15°C and then, heated to 70°C for 5 min to stop the reaction. Five microliters of product was added to 100 µL of competent cells and gently mixed. The mixture was kept in ice for 30 min, then incubated at 42ºC for 2 min and again transferred to ice for 3 min. The transformants were transferred to LB containing 50 µg/mL ampicillin and incubated for 1 h at 37ºC. The cell suspension was centrifuged at 6,500 g for 10 min and 100 µL of cell suspension was spread on LA containing 100 µg/mL ampicillin for selection of transformed cells. The pGEM-T plasmid was isolated from transformed cells using minprep kit (Promega, USA) and sequenced on ABI 3130 Genetic Analyzer with Big Dye Terminator version 3.1. The sequences obtained from *Sal*I and *Bgl*II digested, self-ligated amplicons were manually assembled to determine sequence of Tn5 flanking

regions and identify the insertion site. The assembled sequence was searched on BLAST (blastn). The sequence was submitted in NCBI with GenBank accession number of KR824523.

3.9 Determination of enzyme activities

Cultures of *A. haemolyticus* TK15 and its mutant *A. haemolyticus* MG606 were grown till log phase and harvested by centrifugation. The cell pellets were washed with ice cold Tris-HCl buffer (100 mM; pH 7.2) and resuspended in the same buffer. The cells were disrupted by pulse sonication at 4°C followed by centrifugation at 12,000 g for 15 min to remove cell debris. The cell lysate was used for enzyme activity measurements.

Phosphoglucomutase (PGM) activity

PGM was measured using glucose-1-phosphate (G1P) as substrate (Ye et al., 1994). Nine hundred microliters of pre-warmed assay mixture containing 100 mM Tris-HCl buffer (pH 7.2), 5 mM $MgC1_2$, 50 µM of glucose-1,6-diphosphate, 1 mM G1P, 2 mM NAD and 1 U of glucose-6-phosphate dehydrogenase (G6PDH) was mixed with 100 µL cell lysate and the change in absorbance at 340 nm was recorded for 10 min.

UDP-glucose epimerase (UDE) activity

UDE was determined using UDP-galactose as substrate (Looijesteijn et al., 1999). Nine hundred microliters of pre-warmed assay mixture containing 50 mM Tris-HCl buffer (pH 7.2), 10 µM $MgCl_2$, 2 mM NAD and 1 U of UDP-glucose dehydrogenase was mixed with 100 µL cell lysate. The reaction was started by adding 0.2 mM UDP-glucose to the reaction mixture and change in absorbance at 340 nm was recorded for 10 min.

Phosphoglucose isomerase (PGI) activity

PGI was determined using fructose-6-phosphate (F6P) as substrate (Looijesteijn et al., 1999). Nine hundred microliters of pre-warmed assay mixture containing 50 mM potassium phosphate

(pH 6.8), 5 mM $MgCl_2$, 0.4 mM NADP and 4 U G6PDH was mixed with 100 µL cell lysate. The reaction was started by adding 5 mM F6P to the reaction mixture and change in absorbance at 340 nm was recorded.

One unit of PGM, UDE and PGI activity was defined as the amount of substrate required to produce 1 µM NAD(P)H per min per mg of protein (Looijesteijn et al., 1999; Velasco et al., 2007).

Glucosyltransferases (GST) activity

GST was determined using p-nitrophenyl glucopyranoside as substrate (Shen et al., 2010; Darkoh et al., 2011). Nine hundred microliters of pre-warmed assay mixture containing 50 mM Tris-HCl buffer (pH 7.4), 15 mM p-nitrophenyl glucopyranoside, 1 mM $MnCl_2$ and 50 mM NaCl was mixed with 100 µL cell lysate and incubated for 12 h. Aliquots (200 µL) of reaction mixture were withdrawn at 3 h intervals, mixed with 3 M Na_2CO_3 (40 µL) to quench the reaction and absorbance was measured at 410 nm.

3.10 Sodium dodecyl sulphate polyacrylamide gel electrophoresis (SDS-PAGE) and zymography

Whole cell protein profiles of TK15 and MG606 strains of *A. haemolyticus* were compared by SDS-PAGE using 12% resolving gel and 4% stacking gel (Annexure I). The 12% running gel (Annecure I) was transferred to glass slabs and overlaid with isopropanol. After 30 min of polymerization, isopropanol was removed by washing the separating gel with double distilled water. The stacking gel was overlaid on separating gel and gel comb was inserted. The gel was allowed to polymerize and comb was removed after 1 h. The glass slab assembly was transferred to running tank containing running buffer (Annexure I). The cell lysate (25 µL) was mixed with an equal volume of cracking buffer (Annexure I), boiled at 100°C for 5 min and then centrifuged

at 10,000 rpm for 30 min at 4°C. The samples and protein marker were loaded in wells and gels were electrophoresed at 60 V. As the bands crossed stacking gel, voltage was increased to 120 V and electrophoresed until bromophenol blue reached the end of resolving gel. The gel was removed from glass slabs and stained overnight with Coomassie brilliant blue R-250. The gel was destained for 4-5 h with destaining solution (Annexure I) to observe protein bands.

Native polyacrylamide gel electrophoresis was performed to detect PGM activity in cell lysates. The samples were prepared in non-denaturating buffer lacking SDS (Annexure I) and loaded into the gel containing 12% resolving gel and 4% stacking gel. The gels were prepared as described for SDS-PAGE but without addition of SDS in gel. Enzyme activity was detected in native electrophoresis gels by incubating the gels in 20 mL reaction mixture containing 100 mM Tris-HCl buffer (pH 7.2), 5 mM $MgC1_2$, 50µM of glucose-1,6-diphosphate, 1mM G1P, 2mM NAD, 1U of G6PDH, 0.01% phenazinemethosulphate and 0.05% nitrobluetetrazolium (Qian et al., 1994).

3.11 Real time PCR (RT-PCR)

pgm expression in TK15 and MG606 strains of *A. haemolyticus* were compared by RT-PCR. Total RNA was extracted from both strains using RNA isolation kit (Promega, USA). First strand cDNA synthesis was performed using random hexamer primers and MmuLV reverse transcriptase. The RNA was denatured by mixing 5 µL RNA with 3 µL of random hexamer primers and 28 µL of water. The components were kept at 65°C for 10 min and then transferred to ice for 5 min. First strand cDNA was synthesized by mixing 5 µL of 10X RT buffer, 1 µL of RNase inhibitor, 2 µL of dNTPs, 5 µL of 100 mM dithiothreitol and 1 µL of reverse transcriptase. The reaction mixture was incubated at 37°C for 1 h and then boiled for 5 min. The first strand cDNA so obtained was then amplified by PCR on ABI Step-one Real Time PCR

machine. The reaction mixture (50 µL) contained 25 µL of 2X PCR SYBR green ready mix, 19 µL of water, 2 µL each of forward and reverse primers (listed in table 3.2), 2 µL of dNTPs and 2 µL of cDNA as template. The template cDNA was amplified by 1 cycle of initial denaturation (94°C/2 min), 40 cycles of denaturation, annealing and extension (94°C/5 sec, 55°C/10 sec, 72°C/10 sec) and 1 cycle of final extension (72°C/5 min). *pgm* expression was normalized to expression of the housekeeping *tuf* gene and change in *pgm* expression was determined by $2^{-\Delta\Delta Ct}$ method (Livak and Schmittgen, 2001; Schmittgen and Livak, 2008).

3.12 Determination of intracellular metabolite concentration

Cultures of *A. haemolyticus* TK15 and its mutant *A. haemolyticus* MG606 were grown till log phase and harvested by centrifugation. The cell pellet was suspended in 75% methanol and heated to 80°C for 5 min. The concentration of G1P, glucose-6-phosphate (G6P) and UDP-glucose were determined in lyophilized powder using coupled enzyme assays (Garrigues et al., 1997; Masuda et al., 2001; Sanfelix-Haywood et al., 2011). The lyophilized material was dissolved in 1 mL water and 780 µL of this cell extract was mixed with 200 µL of reaction mixture containing 500 mM triethanolamine buffer (pH 7.6), 15 mM $MgSO_4$, 4 mM EDTA and 10 mM of NADP. The reaction was started by adding 10 µL of G6PDH (200 U/mL) and reaction was monitored fluorimetrically at 340 nm excitation and 460 nm emission. For measurement of G1P concentration, 10 µL of PGM (200 U/mL) was added and the reaction followed fluorimetrically. For UDP-glucose measurements, lyophilized cell extract was dissolved in 200 mM Tris buffer (pH 8.9) and 100 µL this cell extract was mixed with 900 µL reaction mixture containing 200 mM Tris (pH 8.9), 5 mM $MgCl_2$, and 2 mM NAD. UDP-glucose dehydrogenase (0.01 U/mL) was added into the solution and UDP-glucose content was determined by measuring the absorbance at 340 nm.

3.13 Purification of phosphoglucomutase

Log phase cells of *A. haemolyticus* MG606 were centrifuged and the pellet was washed with Buffer A (50 mM Tris-HCl buffer containing 2 mM EDTA; pH 7.2). The pellet was then resuspended in buffer A and cell suspension was pulse sonicated to disrupt cells. The cell lysate was centrifuged at 8,000 g for 10 min. To the supernatant, calculated amount of solid ammonium sulfate was added to obtain 20% saturation. The mixture was kept at 4°C for 16 h for protein precipitation and then centrifuged. The supernatant was collected and calculated amount of solid ammonium sulfate was added to the supernatant to obtain 70% saturation. The solution mixture was kept at 4°C for 16 h and precipitates formed were recovered by centrifugation. The precipitates were dissolved in buffer B (50 mM Tris-HCl containing 30 mM KCl; pH 7.2) and the solution was dialyzed with same buffer for 24 h. The dialyzed solution was purified by gel permeation chromatography using Sephacryl S-100 HR column pre-equilibriated with buffer B. The fractions were manually collected and analyzed for PGM activity. The fraction with maximum enzyme activity was further purified with a DEAE-cellulose column using Tris-HCl buffer with KCl gradient (0-0.5 mM) as eluant (Belocopitow and Marehal, 1974; Neves et al., 2006).

3.14 Determination of effect of kinetic parameters on purified enzyme activity

Temperature

Nine hundred microliters of pre-warmed assay mixture (pH 7.2) was mixed with 100 µL purified PGM (10 U/mL). PGM activity was measured over a range of different temperature (15-40°C) in individual reactions and activity was calculated as described in section 3.9.

pH

To determine the effect of pH on PGM activity, the pH of Tris-HCl buffer was varied between 3-9. Nine hundred microliters of pre-warmed assay mixture (at different pH) was mixed with 100 µL purified PGM (10 U/mL) and PGM activity was measured as described in section 3.9.

Substrates

The substrate specificity of purified PGM was detected using G1P, M1P and F6P as substrates. Nine hundred microliters of pre-warmed assay mixture containing 100 mM Tris-HCl buffer (pH 7.2), 5 mM $MgC1_2$, 50 µM of glucose-1,6-diphosphate and 1 mM substrate was mixed 100 µL of purified PGM (10 U/mL). Aliquots of 200 µL were withdrawn, mixed with 200 µL of 2 N HCl and heated at 100°C for 5 min. The reaction mixture was centrifuged and supernatant was diluted to 1 mL with water (Ye et al., 1994). The released phosphate was estimated as described in section 3.2.4.

Inhibitors

The catalytic activity of PGM was determined in presence of ions ($MgCl_2$, $MnCl_2$, $CaCl_2$, $CoCl_2$, $NiCl_2$, LiCl and $ZnCl_2$) and other modifiers (ATP, ADP, UDP-glucose, glucose-1,6-biphosphate and F6P). Nine hundred microliters of pre-warmed assay mixture (pH 7.2) was mixed with 100 µL purified PGM (10 U/mL). PGM activity was measured in presence of 5 mM ions or other inhibitors/modifiers in individual reactions and activity was calculated as described in section 3.9.

3.15 Toxicological evaluation of *A. haemolyticus* MG606 mutant and its exobiopolymer

In vivo studies

Female Swiss mice (20-30 g; 8-12 weeks old) were acclimatized to standard laboratory conditions (22 ± 3°C; 30-70% relative humidity; 12 h light/dark cycle) for 7 days. After

acclimatization, the animals were randomly selected and grouped on the basis of their body weight into total of 10 groups consisting of 2 animals each for sighting study and 4 animals each for main study. Animals were provided food and water *ad libitum* during the entire course of the study. All studies were performed at Venus Medicine Research Centre, Baddi, India.

A. haemolyticus MG606 cells growing in log phase were harvested aseptically, suspended in phosphate buffer saline (PBS) and administered intraperitoneally at doses ranging from 7-13 log CFU/animal for sighting study and 10-14 log CFU/animal for main study. EBP was dissolved in pyrogen-free saline and administered intraperitoneally at doses ranging from 60 mg/kg to 140 mg/kg. The doses were selected based on a sighting study conducted with a wider dose range of 20 mg/kg to 200 mg/kg. Animals were observed individually after dosing at least once during the first 30 min, periodically during the first 24 h, with special attention given during the first 4 h, and daily 2 times thereafter, for a total of 7 days. Clinical signs of toxicity, Body weight change and mortality were recorded daily. The LD_{50} value was calculated by logit method.

In vitro studies

Mouse macrophage cell line RAW 264.7 and human lung adenocarcinoma epithelial cell line A549 were purchased from National Centre for Cell Sciences, Pune, India. Cells were grown in DMEM containing 10% FCS. Confluent cultures were trypisinized and transferred to T75 flasks for routine subculturing. Confluent cultures were trypsinized and seeded in 96 well plates (10,000 cells, 0.2 mL). Cells were incubated with 100-500 µg/mL EBP (dissolved in culture medium) for 24 h. Following incubation, culture medium was replaced with DMEM containing 3-(4,5-dimethylthiazol-2-yl)-2,5-diphenyltetrazolium bromide (MTT) and cell viability was calculated from the amount of formazon produced, assuming 100% viability of untreated, control cells.

3.16 Characterization of exocellular biopolymer

BET analysis

Brunauer, Emmett and Teller (BET) method was used to determine surface area and porosity of EBP using nitrogen gas as sorbent (Micromeritics ASAP 2020 analyzer). The sample was degassed and nitrogen adsorption was determined at -196°C. The surface area and micropore volume were calculated using BET analysis and Barrett, Joyner and Halenda (BJH) analysis, respectively.

Elemental analysis

The elemental composition (C, H, N and S) of powdered EBP was determined by an elemental analyzer (Flash 2000 Organic Elemental Analyzer, Thermo Scientific) equipped with flame ionization detector.

Total protein

Total protein was measured by Lowry's method (Lowry et al., 1951). Two hundred microliters of EBP solution (1 mg/mL) was mixed with 1 mL of freshly mixed complex-forming reagent (Annexure I). The solution was left undisturbed for 10 min at room temperature and absorbance was recorded at 750 nm. The amount of protein was calculated from standard curve prepared using bovine serum albumin (BSA) as standard (0.1-0.5 mg/mL). The standard curve of BSA is given in Annexure II.

Carbohydrates

Total carbohydrate content was determined by phenol sulfuric acid method (DuBois et al., 1956). Two hundred microliters of EBP solution (1 mg/mL) was mixed with 200 µL of phenol reagent (Annexure I) followed by addition of 1 mL of concentrated sulfuric acid. The tubes were left undisturbed for 10 min at room temperature. The tubes were vigorously shaken and absorbance

was recorded at 490 nm after 30 min. The total carbohydrate content was calculated from standard curve using glucose as standard (0-1 mg/mL). The standard curve of glucose is given in Annexure II.

Pyruvic acid

Pyruvic acids were determined by Friedman's method (Friedemann and Haugen, 1943). Two hundred microliters of EBP solution (1 mg/mL) was mixed with 1 mL of dilute perchloric acid (50%). The mixture was incubated at 30ºC for 30 min followed by addition of 1 mL of 2,4-dinitro phenylhydrazine (DNP) reagent (Annexure 1), 4 mL of water and 10 mL of 2.2 N NaOH. The tubes were vigorously shaken and absorbance was recorded at 416 nm. The pyruvic acid content was calculated from standard curve using pyruvic acid as standard (0-3 µg/mL). The standard curve of pyruvic acid is given in Annexure II.

Amino sugars

Amino sugars were determined by Elson and Morgan method (Elson and Morgan, 1933). Two hundred and fifty microlitres of EBP solution (1 mg/mL) was mixed with 50 µL of reagent A (Annexure I). The mixture was heated at 100ºC for 3 min followed by addition of reagent B (1.5 mL). The tubes were incubated at 37ºC for 20 min and absorbance was recorded at 585 nm. The amino sugar content was calculated from stardard curve using glucosamine as standard (0-1 mg/mL). The standard curve of glucosamine is given in Annexure II.

Uronic acids

Uronic acid content was determined by Haug and Larsen's method (Haug and Larsen, 1962). Two fifty microliters of EBP solution (1 mg/mL) was mixed with 1.5 mL of ice cold reagent A followed by addition of reagent B (50 µL). The tubes were heated at 100ºC for 15 min followed by rapid cooling after each addition. The absorbance was measured at 525 nm. The uronic acid

content was calculated from standard curve using D-glucuronic acid as standard (0-1 mg/mL). The standard curve of D-glucuronic acid is given in Annexure II.

Molecular weight analysis

Molecular weight of EBP was determined by gel permeation chromatography (GPC). EBP sample (60 µL) was resolved on Ultrahydragel 500 and Ultrahydragel 120 column in series, maintained at 30°C, using Waters Alliance HPLC-GPC (Waters 2695 separation module coupled with Waters 2414 refractive index detector). The mobile phase used was 0.2 M sodium nitrate in water. The system was previously calibrated using dextrans of different molecular weights as standard.

GC-MS analysis

The monosaccharide components of EBP were determined by hydrolysis of polymer with 2 M of trifluoroacetic acid (TFA) at 121°C for 1 h. The acid was removed from the hydrolysed sample at 40°C using rotary evaporator apparatus. After hydrolysis, the solution was neutralized with 1 N NaOH solution and lyophilized. The lyophilized extract was derivatized with N,O-Bis(trimethylsilyl) trifluoroacetamide (BSTFA) and heated for 30 min at 80°C. The reaction mixture was centrifuged, treated with sodium sulphite to remove moisture and again centrifuged (10,000 g; 10 min). The supernatant was dried under vacuum and dissolved in acetonitrile. The mixture was resolved with DB-5 column (30 m x 0.25 mm x 0.25µm; Agilent Technologies) using a gas chromatography instrument coupled with mass spectrometer (GCMS QP 2010, Shimadzu) (Senila et al., 2011; Pierre et al., 2012).

Thermogravimeteric analysis

An accurately weighed EBP sample was placed in the sample pan and mounted in the thermogravimetric analysis (TGA) apparatus (Mettler Toledo). EBP was heated from 25°C to

900°C at a rate of 15°C/min under constant nitrogen flow. The heating was continued until the no further change in weight was observed.

Viscosity determination

The dynamic viscosity of EBP solution (1 mg/mL) was determined by Brookfield viscometer (DV-11+/Pro, Brookfield) at ambient temperature (~25°C).

3.17 Evaluation of adsorptive removal capacity of phosphate by exobiopolymer

Time of contact

Equal volumes (2.5 mL) of phosphate solution (2 mg/L) and EBP solution (200 mg/L) were mixed and vortexed for 10 min. The solution was kept undisturbed for time intervals ranging from 30 min to 6 h and then filtered through 0.22 µm membrane filter. The phosphate concentration present in filtrate was determined by molybdenum blue stannous chloride method as described in section 3.2.4.

Exobiopolymer concentration

Equal volumes (2.5 mL) of phosphate solution (2 mg/L) and EBP solution (200 to 1000 mg/L) were mixed and vortexed for 10 min. The solution was kept undisturbed for 240 min and then filtered through 0.22 µm membrane filter. The phosphate concentration present in filtrate was determined by molybdenum blue stannous chloride method as described in section 3.2.4.

Phosphate concentration

Equal volumes (2.5 mL) of phosphate solution (2-10 mg/L) and EBP solution (200 mg/L) were mixed and vortexed for 10 min. The solution was kept undisturbed for 240 min and then filtered through 0.22 µm membrane filter. The phosphate concentration present in filtrate was determined by molybdenum blue stannous chloride method as described in section 3.2.4.

Adsorption isotherms

The sorption isotherm was established to evaluate the capacity of an adsorption system. Phosphate binding capacity (Qe) was calculated using the formula

$$Q_e = \frac{(C_o - C_e)V}{M}$$

Where, C_o is initial concentration of phosphate (mg/L), C_e is final phosphate concentration (mg/L) after binding with EBP, V is volume of solution (L), M is mass of EBP (g). Phosphate sorption was fitted into different isotherm equations by MATLAB and model fitting was compared by error functions (Ho, 2004; Foo and Hameed, 2010; Akpa and Unuabonah, 2011).

SEM-EDS analysis

The ultrastructure was determined using a scanning electron microscope (JSM-6510LV, JEOL) equipped with EDS (INCAx-act, Oxford Instruments). Dried purified EBP samples were applied on double-sided tape attached to SEM stubs and were gold-coated. The samples were scanned for imaging and simultaneous elemental analysis.

X- ray diffraction (XRD) spectral analysis

Powder XRD analysis of unbound and phosphate-bound EBP was performed using XRD system (X-pert Pro, PANalytical). The copper Kα radiation of 1.5406 Å wavelength was obtained from copper anode and sample was scanned at $5° \leq 2\theta \leq 85°$ and step size of (2θ) 0.0130. The generator settings were 45 kV and 40 mA.

Zeta potential measurements

Zeta potential of saturated solution of unbound and phosphate bound EBP prepared in deionized water was measured using a zeta sizer (Nano ZS, Malvern).

Potentiometric titration

An aqueous solution of EBP (0.2 mg/mL; 10 mL) was acidified to pH 2.5 with 1 N HCl. The pH of solution was recorded after successive additions of 0.1 N NaOH in 20 µL increments (Guine et al., 2006; Wei et al., 2011). The titration data was fitted using ProtoFit (Turner and Fein, 2006).

Effect of pH on phosphate binding by exobiopolymer

To determine the effect of pH on phosphate binding, EBP and phosphate were dissolved in Tris-HCl buffer of varying pH (3-10). Equal volumes (2.5 mL) of phosphate solution (2 mg/L) and EBP solution (200 mg/L) were mixed and vortexed for 10 min. The solution was kept undisturbed for 240 min and then filtered through 0.22 µm membrane filter. The phosphate concentration present in filtrate was determined by molybdenum blue stannous chloride method as described in section 3.2.4.

Effect of enzyme treatment on exobiopolymer-phosphate binding

To determine the effect of enzyme treatment, aqueous EBP solution (1 g/L) was treated with a mixture of 1 mg/L of proteolytic enzymes (containing 0.33 mg/mL each of protease [4000 U/mg], trypsin [1000-1500 U/mg] and proteinase K [30 U/mg]) or 1 mg/L of amylolytic enzymes (containing 0.33 mg/mL each of amylase [2000 U/mg], cellulase [0.3 U/mg] and beta-galactosidase [500 U/mg]) or a 1:1 mixture of both proteolytic (1 mg/L) and amylolytic (1 mg/L) enzymes. After 16 h of enzymatic hydrolysis at 37°C, the hydrolyzed EBP was lyophilized. Equal volumes (2.5 mL) of phosphate solution (2 mg/L) and hydrolyzed EBP solution (200 mg/L) were mixed and vortexed for 10 min. The solution was kept undisturbed for 240 min and then filtered through 0.22 µm membrane filter. The phosphate concentration present in filtrate was determined by molybdenum blue stannous chloride method as described in section 3.2.4.

Effect of chemical treatment on exobiopolymer-phosphate binding

Powdered EBP (50 mg) was treated with 4% v/v glutaradaldehyde, concentrated hydrochloride acid:anhydrous methanol mixture (1:100 v/v) or formaldehyde:formic acid mixture (1:2 v/v). The reaction mixture was kept undisturbed for 24 h for completion of reaction and then dialyzed against deionized water. The resultant mixture was then lyophilized and phosphate binding by treated EBP was measured (Jianlong, 2002; Micheletti et al., 2008). Equal volumes (2.5 mL) of phosphate solution (2 mg/L) and chemically modified EBP solution (200 mg/L) were mixed and vortexed for 10 min. The solution was kept undisturbed for 240 min and then filtered through 0.22 µm membrane filter. The phosphate concentration present in filtrate was determined by molybdenum blue stannous chloride method as described in section 3.2.4.

Fourier Transform Infra Red (FT-IR) spectral analysis

Unbound and phosphate-bound EBP were blended with KBr and pressed into pellets. The pellets were scanned in the range 800 to 4,000 cm^{-1} and spectrum was recorded (Cary 660 FTIR, Agilent Technologies).

Effect of competing ions on phosphate binding by exobiopolymer

Equal volumes (2.5 mL) of phosphate solution (2 mg/L) and EBP solution (200 mg/L) were mixed and vortexed for 10 min. The solution was kept undisturbed for 240 min to attain equilibrium. Potassium salts of sulphate, chloride or nitrate were then added to the equilibrium solution at 10, 50 and 100 mg/L and incubation for 1 h. The solution was then filtered through 0.22 µm membrane filter and phosphate concentration in filtrate was determined by molybdenum blue stannous chloride method as described in section 3.2.4.

3.18 Statistical modeling of exobiopolymer overproduction by *A. haemolyticus* MG606

3.18.1 Optimization of culture conditions

Temperature

To determine the effect of incubation temperature on EBP production, 1 mL of log phase culture (OD = 0.3) was inoculated in 100 mL of EBP production medium and incubated for 48 h at temperatures ranging from 20°C to 45°C. For determining cell biomass, culture was centrifuged for 12,000 g for 30 min at 4°C. The pellet formed was air-dried and weighed. EBP was extracted from culture supernatant and yield determined as described in section 3.2.3.

pH

The effect of pH of culture media on EBP production was observed in pH range of 5 to 9. The pH of EBP production medium was adjusted with 0.1 N NaOH or 0.1 N HCl. One milliliter of log phase culture (OD = 0.3) was inoculated in 100 mL of EBP production and incubated for 48 h at 30°C. Cell biomass was determined as described above. EBP yield was determined as described in section 3.2.3.

Inoculum size

To determine the effect of inoculum size on EBP production, 100 mL of EBP production medium was inoculated with 0.5 to 5 mL (OD = 0.3) of log phase culture (inoculums size 0.5% to 5%) and incubated for 48 h 30°C. Cell biomass was determined as described above. EBP yield was determined as described in section 3.2.3.

Agitation speed

To determine the effect of agitation speed on EBP production, 1 mL of log phase culture (OD = 0.3) was inoculated in 100 mL of EBP production medium and incubated for 48 h at 30°C. The

medium was mixed at agitation rates ranging from 40 rpm to 240 rpm. Cell biomass was determined as described above. EBP yield was determined as described in section 3.2.3.

Carbon sources

The effect of carbon sources such as glucose, galactose, mannitol, pyruvate, ethanol, acetate, fructose, maltose, sucrose, lactose, mannose, xylose, raffinose, succinate, malate, aspartate, glutamate and butanol on EBP yield was determined. The stock solution of carbon source was filter sterilized through 0.22 µm filter membrane and added to autoclaved media to obtain a final concentration of 0.5, 1 and 2 g/L. One milliliter of inoculum (OD = 0.3) was inoculated to 100 mL of EBP production media in Erlenmeyer flasks and incubated for 48 h at 30°C. EBP yield was determined as described in section 3.2.3.

EBP production was also observed using mixture of carbon sources to improve yield. Galactose, mannitol, acetate, ethanol, pyruvate and glutamate each were added to EBP production medium at 0.5 g/L along with 0.5 g/L glucose. EBP yield was determined as described in section 3.2.3.

Various cheap carbon sources such as sugarcane molasses, sugarcane juice, wheat flour, wheat bran, corn flour, corn bran and corn cob were used as substitutes for glucose in EBP production media. All cheap sources, except sugarcane juice, were finely ground and mixed with 20% v/v sulfuric acid. The solution was boiled for 30 min in water bath (Dumbrepatil et al., 2008). The sugar content of each raw material was measured by phenol sulphuric acid method and added at amounts equivalents to 1 g/L glucose. The pH of medium was then adjusted to 7.2 with 1 M NaOH.

Nitrogen sources

The inorganic (ammonium sulphate, ammonium chloride, ammonium phosphate) and organic (peptone, beef extract, yeast extract and tryptone) nitrogen sources were dissolved in EBP

production media at 1, 2 and 5 g/L. The culture medium (100 mL) containing the desired nitrogen sources was inoculated with 1 mL log-phase bacterial culture (OD = 0.3) and incubated for 48 h at 30°C and 120 rpm. EBP yield was determined as described in section 3.2.3. Similarly, 1:1 combinations of inorganic nitrogen sources were also dissolved in EBP production at a combined level of 2 g/L (1 g/L of each inorganic nitrogen source) and EBP yield was determined after 48 h of incubation at 30°C and 120 rpm.

3.18.2 Scale-up of exobiopolymer production to bioreactor scale

Based on the above studies for EBP production by *A. haemolyticus* MG606 in EBP production medium, variables affecting EBP production were statistically optimized to maximize EBP production. The variables (glucose concentration, acetate concentration and ammonium sulphate concentration) were selected as test variables for further optimization. These studies were conducted in 5 L bioreactor with working volume of 3 L. The bioreactor was inoculated with 1% of 16 h old culture of *A. haemolyticus* MG606 through inoculation port. Batch fermentation was carried out at 30°C which is controlled by thermocouple. The dissolved oxygen concentration was measured using polarographic electrode. Aeration was maintained constant with agitation speed of 120 rpm. Sampling was performed every 4 h to study biomass and EBP production.

Statistical optimization of parameters by response surface methodology

Response surface methodology (RSM) with central composite design (CCD) was employed to illustrate the optimal settings and interactions between most significant independent variables. The coded and non-coded values of the significant experimental variables were taken at five coded ($-\alpha$, -1, 0, +1, $+\alpha$) levels. The zero levels of all variables constitute the central points while combination of experimental variables consisting of one at its lowest level (-1) and its highest (+1) levels. The total number of experimental combinations was 2^k+2k+n, where k is number of

independent variables and n is the number of repetitions of the experiments at the central point. A total of 20 experiments were carried out using three independent variables (glucose, sodium acetate and ammonium sulphate concentration). Batch experiments were conducted as per CCD for EBP production in a 5 L fermenter (Fermac 360, Electrolab, India).

The model was developed and design based experimental data was fitted into the second order polynomial equation (Eq 1). Data was analyzed using statistical software Design Expert (Stat-Ease, USA).

$$Y = B_O + \sum_{i=1}^{k} B_i X_i + \sum_{i=1}^{k} B_{ij} X_i^2 + \sum_{i<j}^{k} \sum_{j}^{k} B_{ij} X_i X_j + e \text{..... (Eq 1)}$$

Where i is linear and j is quadratic coefficient, X_i and X_j are dimensionless value of independent variables, k is number of factors studied B is regression coefficient and e is the random error.

The statistical significance of the model was determined by F test and the significance of each coefficient was determined using Student's *t*-test. The quality of fit of the model was determined by R^2 and ANOVA. *p* values were used as a tool to elucidate the interaction among the significant variables.

Kinetic modeling

Kinetic studies were performed for biomass and product formation on the RSM optimized concentrations of glucose, sodium acetate and ammonium sulphate. Batch EBP fermentation was modeled by logistic equation for cell growth and Luedeking-Piret equation for EBP production.

Logistic equation (Eq 2) was used to calculate maximum specific growth rate (μ_m) and Luedeking-Piret equation (Eq 3) was used to model EBP production kinetics.

$$\frac{dX}{dt} = \mu_m \left(1 - \frac{X}{X_m}\right) X \qquad \text{..... (Eq 2)}$$

Where μ_m is maximum specific growth rate (h^{-1}), X is instantaneous biomass (mg/L) and X_m is maximum specific biomass (mg/L)

$$\frac{dP}{dt} = \alpha \frac{dX}{dt} + \beta X \quad \text{..... (Eq 3)}$$

Where α and β are growth and non-growth associated constants, respectively. These constants are influenced by fermentation conditions such as nutritional sources and physical parameters like temperature and pH.

The integration of equation 3 and substitution of values from equation 2 gives equation 4

$$P_t = P_0 + \alpha X_o \left\{ \frac{e^{\mu_m t}}{\left[1-\left(\frac{X_o}{X_m}\right)\left(1-e^{\mu_m t}\right)\right]} - 1 \right\} + \beta \frac{X_o}{X_m} \ln \left\{ 1 - \frac{X_o}{X_m}\left(1 - e^{\mu_m t}\right) \right\} \text{..... (Eq 4)}$$

Where, P_t is the instantaneous EBP concentration, P_0 is initial EBP concentration (t=0), and X_0 is initial biomass (t=0).

The values of growth associated (α) and non-growth associated (β) constants were determined under conditions optimized of RSM. The equations were solved and kinetic parameters were estimated using Microsoft Excel.

3.19 Development of biosensor and hydrogel based systems

3.19.1 Development of biosensor

Biosensor fabrication and configuration

A biosensor based on miniature circuit (U1) shown in figure 3.2 was developed. The circuit comprises of LED and sensor for 690 nm which detect the color intensity of biosensor probe. The circuit is attached to a microcontroller and the signals are detected as milliamperes (mA).

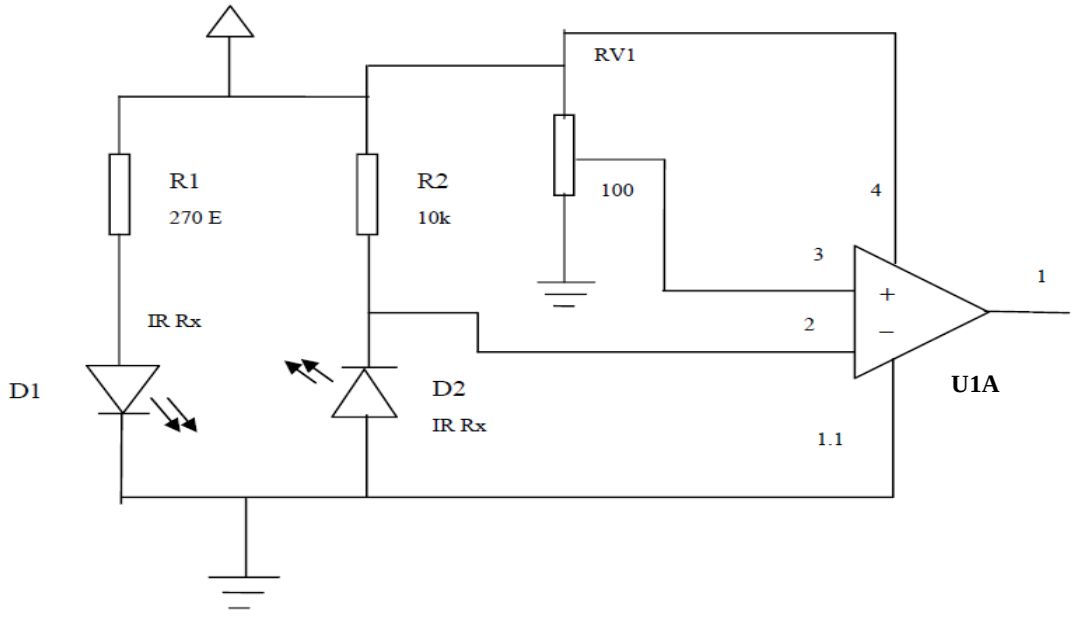

Figure 3.2: Circuit diagram of biosensor.
R1- Variable resistance, R2- Resistance, RV1- Potentiometer, U1A- Operational amplifier, D1- Diode, IR- Sensor transmitter

Optimization of biosensor probe

The biosensor probe was fabricated using cellulose acetate membranes with an approximate surface area of 5 cm^2. An aliquot of 100 μL of aqueous EBP solution (1-6 mg/mL) was applied on membrane and air-dried. The membrane was fitted into syringe filter and 1 mL of phosphate standard solution (1-10 mg/L) or deionized water (blank) was passed through biosensor probe with the help of a 5 mL syringe. The filtrate was collected and analyzed for phosphate content as described in section 3.2.4. The amount of phosphate retained on probe was calculated as difference between initial phosphate concentration (10 mg/L) and phosphate concentration in filtrate and expressed as percent retention.

In order to determine the effect of EBP concentration flow rate, membranes coated with 1-6 mg/mL the syringe filter was attached to a peristaltic pump and flow rate was calculated from the

time required to pump 5 mL of 10 mg/L phosphate. The flow rate through EBP-coated membranes was normalized to flow rate through uncoated membranes and expressed as percent flow rate.

Calibration of biosensor

The biosensor probe coated with 4 mg/mL EBP was fitted into syringe filter and 1 mL of phosphate standard solution (1-15 mg/L) was passed through biosensor probe with the help of a 5 mL syringe. The probe was then removed from holder and treated with 250 µL of ammonium molybdate (2.5%) and 50 µL stannous chloride (2.5%) for color development (APHA, 1998). The membranes were placed between LED and sensor of the biosensor and biosensor response (in mA) was recorded.

Validation of biosensor

The biosensor performance was validated by determining precision (intra-assay/intraday and inter-assay/inter-day variability), accuracy (recovery) and long-term stability. The biosensor response (mA) for different samples was determined as described under calibration of biosensor and phosphate concentration was calculated from standard curve.

Intra-assay variability is the variability in analytical results observed after repeated analysis of a test sample in a single day. Phosphorus standard solutions (1-10 mg/L) were analyzed three times on the same day and the difference between actual and analyzed concentrations was expressed as percent relative standard deviation (%RSD).

Inter-assay variability is the variability in analytical results after repeated analysis of a test sample over several days. Phosphorus standard solutions (1-10 mg/L) were analyzed on 3 consecutive days and the difference between actual and analyzed concentrations was expressed as %RSD.

Accuracy or recovery refers to the proximity between measured and actual concentration of the analyte. Accuracy is expressed as percent and calculated as (Measured concentration/Actual concentration)x100. Phosphorus standard solutions (1-10 mg/L) were analyzed and the difference between actual and analyzed concentrations was expressed as %recovery.

Long-term stability is a measure of the stability of analytical method over duration of weeks to months. Phosphorus standard solutions (1-10 mg/L) were analyzed once weekly for weeks and the difference between actual and analyzed concentrations was expressed as %RSD.

Stability of biosensor probe

Biosensor probes coated with 4 mg/ml EBP were stored at 4°C and ambient temperature (~25°C) for upto 4 weeks. Membranes were drawn at weekly intervals and 10 mg/L phosphate standard solution was analyzed as described under calibration of biosensor.

3.19.2 Preparation of hydrogels

EBP was dissolved in sodium alginate solution to achieve a final concentration of 1.25% w/v EBP and 2% w/v sodium alginate. The solution was added dropwise in 4% w/v calcium chloride solution under stirring and beads were recovered by centrifugation (500 g; 5 min). The calcium alginate hydrogel beads containing EBP are referred as CAB-EBP.

Calcium alginate beads were prepared following the same protocol except that EBP was not added to sodium alginate solution. The calcium alginate hydrogel beads not containing EBP are referred as CAB-Blank.

Characterization of hydrogel beads

The size of atleast 200 CAB-EBP was determined by manual measurements using an optical microscope equipped with an ocular micrometer. The surface morphology of CAB-EBP was determined by SEM

Column sorption studies

Calcium alginate beads, equivalent to 1 g EBP, were washed extensively with water and packed in 28 mm column. The packed column bed was washed with water for 4-6 hours at a flow rate of 10 mL/min. Synthetic water containing 1-10 mg/L phosphate was circulating at 10 mL/min and effluent phosphate concentration was determined by stannous chloride method as described in section 2.4 above. Additionally, 1 mg/L phosphate was circulated at 10, 20 and 30 mL/min. The breakthrough curves were fitted to Thomas model by non-linear curve fitting using MATLAB.

4. RESULTS

4.1 Isolation, screening and identification of phosphate-binding, exocellular biopolymer producing bacteria

Bacterial cells possess an inherent ability to produce extracellular biopolymers (EBP) in the form of capsule or slime as a mechanism of defense against toxic compounds and physical stress. The scope of EBP for commercial applications have expanded significantly over the current years based on strong insights on their diverse technological and putative environmental functionalities (Horn et al., 2013; Jing et al., 2013).

4.1.1 Isolation and screening of bacteria producing phosphate binding exobiopolymer

Sampling sites were especially selected on the basis of high phosphate concentration based on a previous analysis of phosphate levels in waste water. It was anticipated that samples from these areas may host bacteria possessing effective phosphate removal mechanisms. A total of 280 isolates were obtained, out of which 130 isolates were further selected on the basis of their prominent mucoid appearance on Luria agar. Phosphate removal ability of EBP produced by these 130 isolates was determined and only 5 isolates were found to produce phosphate-binding EBP. Phosphate removal capacity of EBP produced by these 5 isolates is represented in table 4.1. Out of these, phosphate removal capability was the highest in EBP produced by TK15 followed by TK8. The isolate TK15, showing highest phosphate removal by EBP (approximately 40%), was selected for the further study.

Table 4.1: EBP yield and phosphate removal by isolates

Isolates	EBP yield (mg/L)	Phosphate removal (%)
TK5	250	21
TK8	298	35
TK15	450	40
TK25	320	27
TK42	402	32

4.1.2 Morphological and biochemical identification of TK15

The bacterial isolate, TK15, was identified to the species level by both phenotypic as well as genotypic characterization. Morphological and biochemical properties of isolated colonies of TK15 isolate were determined. Morphologically, the strain TK15 formed opaque, creamy colonies with smooth edges and raised from the centre**.** Light microscopic analysis showed the cells were rod-like in exponential phase of growth and coccus-like in stationary phase and were Gram-negative, non-motile and non-sporulating. The biochemical analysis indicated strain TK15 was a catalase-positive, oxidase-negative obligate aerobe. TK15 was also observed to be hemolytic in nature (Table 4.2). Based on the keys described in *Bergey's Manual of Determinative Bacteriology* (Bergey and Holt, 1994), the results revealed that bacterial strain TK15 belongs to class gammaproteobacteria.

Table 4.2 Morphological and biochemical characterization of isolate TK15

Colony characteristics	**Observation**	**Biochemical test**	**Observation**
Configuration	Circular	Gram staining	Negative
Size (mm)	2.0-3.0	Indole test	Negative
Margin	Entire	Methyl red test	Negative
Elevation	Convex	Voges Proskauer test	Negative
Surface	Smooth	Citrate utilization	Positive
Pigment	Cream	Casein hydrolysis	Positive
Opacity	Opaque	Starch hydrolysis	Negative
Cellular characteristics		Gas production from glucose	Negative
Cell shape	Rod	H_2S production	Negative
Size (µm)	1.0-1.5	Catalase test	Positive
Spore	Non-sporulating	Oxidase test	Negative
Motility	Non-motile		

4.1.3 Molecular characterization of strain TK15

16S rDNA sequencing

The 16S rDNA sequence obtained was compared with sequences in NCBI database using Basic Local Alignment Search Tool (BLAST). The sequence was aligned by multiple sequence alignment. The phylogenetic tree with the sum of branch length = 0.25080515 based on 16S rDNA sequence was partitioned into two Clades – Clade I and Clade II. Clade I further resulted into subclade I grouping 5 strains of *Acinetobacter haemolyticus.* The isolate TK15 was clustered within the subclade of *A. haemolyticus* with significant bootstrap support value thereby confirming its placement in *A. haemolyticus. A. beijerinckii* was clustered basal to the sub clade I. Clade II clustered *A. johnsonii* and *Acinetobacter* sp with strong bootstrap support value. *Psychrobacter vallis* and *Escherichia coli* were used as out-group to root the tree (Figure 4.1). The sequence was deposited in GenBank database with Accession No KP701480 (Annexure I).

ARDRA genetic fingerprinting

To determine the authenticity of strain, amplified ribosomal DNA restriction analysis (ARDRA), a PCR-based genomic fingerprinting method, was performed. The 1.5 kb PCR product of 16S rDNA was digested with tetra cutter enzymes *Sau*3A and *Alu*1 and restriction fragment pattern specific to strain was generated. The strain gives same restriction pattern when analyzed for number of generations, hence verified its purity. As shown in figure 4.2 the three bands generated by *Sau*3A digested and three characteristic bands were seen after digestion with *Alu*1 (Koeleman et al., 1998; Vaneechoutte et al., 1995).

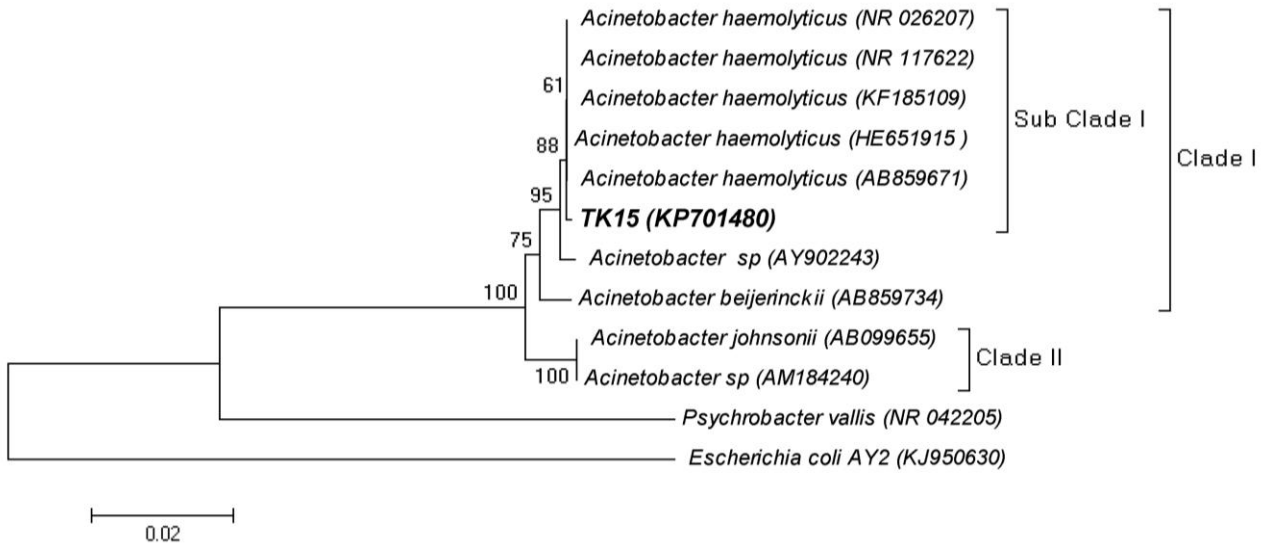

Figure 4.1 Neighbour-joining tree of the isolate TK15 based on bacterial 16S rDNA sequence. A neighbor-joining tree was constructed by aligning the sequences with other selected members from the prokaryotic domain. Listed beside each organism or strain name is the GenBank accession number.

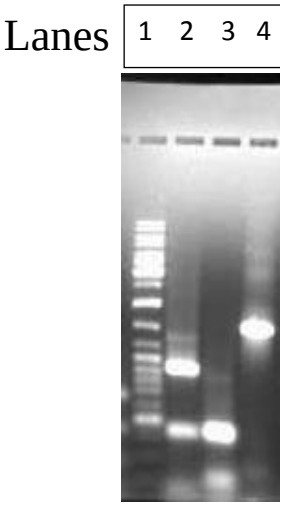

Figure 4.2 16S rDNA restriction analysis (ARDRA) profile of *A. haemolyticus* TK15 strain; Lane 1: Molecular weight DNA ladder (100 bp), lane 2: Amplicon digested with *Sau*3A, lane 3: Amplicon digested with *Alu*1, lane 4: Undigested 1.5 kb 16S DNA amplified product.

4.1.4 Virulence/pathogenicity assessment of *A. haemolyticus* TK15

Many Acinetobacter strains, including *A. haemolyticus*, are opportunistic pathogens and their virulence largely depends on the virulence factors expressed by the strain. These factors enable the bacteria to cause infection by overcoming the host's defense mechanisms. To determine the virulence potential of *A. haemolyticus* TK15 strain, various virulence markers such as lipase activity, protease production, biofilm production and antibiotic resistance were determined.

Table 4.3: Virulence markers for *A. haemolyticus* TK15

Virulence markers	Response	Antibiotic	Sensitivity
Haemolysis	Positive	Ampicillin	Resistant
Lipase	Negative	Chloramphenicol	Resistant
Protease	Negative	Ciprofloxacin	Resistant
Cell motility	Negative	Gentamicin	Resistant
Biofilm production	Positive	Kanamycin	Sensitive
AHL production	Negative	Rifampicin	Sensitive
		Streptomycin	Sensitive

Antibiotic resistant pattern of *A. haemolyticus* TK15 revealed sensitivity towards kanamycin, rifamicin and streptomycin (Table 4.3). Although the strain was found to be haemolytic and produced haemolysin, it did not produce lipase, protease and short chain AHLs. Haemolysin production contributes to haemolysis which leads to tissue injury and indicates potential invasion of cells into the blood stream. Lipase and protease contribute to pathogenicity by degrading proteins and lipids while AHL is an important signaling molecule in quorum sensing and absence of these enzymes and AHLs in *A. haemolyticus* TK15 indicates its low virulence potential (Tayabali et al., 2012).

4.2 Mutagenesis of *A. haemolyticus* TK15 and selection of exobiopolymer overproducing mutant

The isolate *A. haemolyticus* TK15 produced small amounts of EBP and hence, mutagenesis was attempted to enhance EBP production and phosphate binding capacity. The mutants generated by physical and chemical mutagenesis were deemed unsuitable for further follow up for two reasons. First, the increase in EBP yield was marginal in these mutants and EBP production was increased only two folds. Second, the mutants were unstable and EBP yield was comparable to the parent strain after 10 generations. Therefore, transposon mutagenesis was attempted. Out of a total of 998 transconjugants, 6 transconjugants showing phosphate binding with EBP were selected (Table 4.4). An insertional mutant showing approximately 2 fold higher EBP yield, along with higher phosphate binding efficiency, compared to the parent strain (TK15) was selected. The insertional mutant was designated as strain MG606. This mutant was found to be stable since EBP yield and phosphate binding efficiency remained unaltered after 50 generations (Figure 4.3).

Table 4.4 Maximum yield and phosphate removal ability of exobiopolymer from selected mutants.

Isolates	EBP yield (mg/L)	Phosphate removal (%)
MG148	750	45
MG256	500	33
MG402	480	16
MG606	810	57
MG836	500	51

Data is mean±SD of triplicate samples.

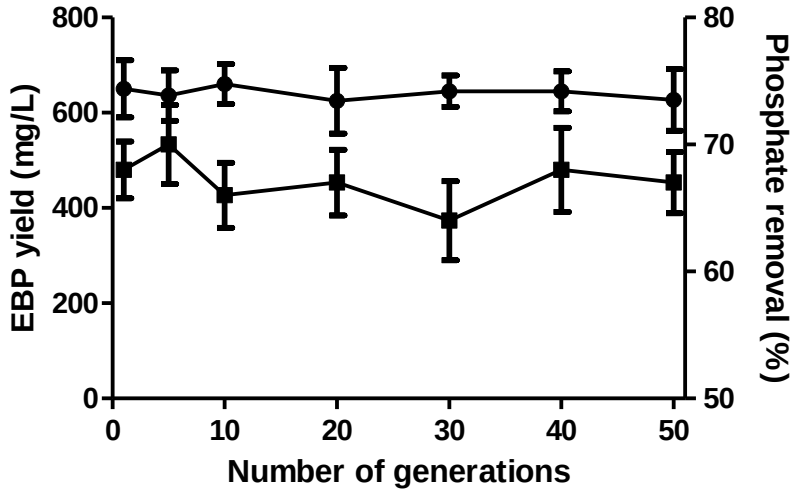

Figure 4.3: Yield of exobiopolymer produced by mutant MG606 of *A. haemolyticus* and its functional stability (■ - Phosphate removal (%), ● - EBP yield (mg/L))

4.2.1 Mechanism underlying exobiopolymer overproduction in *A. haemolyticus* MG606

Identification of Tn5 flanking regions

The transposition of Tn5 element in chromosome of *A. haemolyticus* was confirmed by PCR amplification using Tn5-specific primers. As expected, a 625 bp amplicon was generated in MG606 strain and positive control (pGS9 vector) while no amplification was observed in wild type strain TK15 (Figure 4.4). The mechanism of EBP overproduction in MG606 strain was investigated by determining the site of Tn5 insertion by inverse PCR. The sequences obtained from *Sal*I and *Bgl*II digested, self-ligated amplicons were manually assembled to determine sequence of Tn5 flanking regions and identify the insertion site. The assembled sequence was searched in BLAST (blastn). The assembled sequence of Tn5 flanking region revealed high sequence similarity with *A. haemolyticus* sequences and included partial sequence of a bifunctional phosphoglucomutase/phosphomannomutase (PGM/PMM). The Tn5 insertion site was mapped to GAGAAAGTC sequence, located between positions -89 to -97 upstream of PGM/PMM (Figure 4.5).

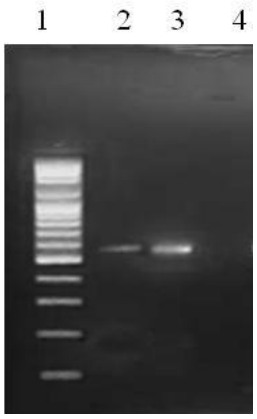

Figure 4.4 Presence of transposon (Tn5) in mutant of *A. haemolyticus* MG606. Lane 1- Molecular weight marker (100 bp ladder); Lane 2- positive control from pGS9 vector amplification; Lane 3- Tn5 amplified product from the mutant Lane 4- Absence of Tn5 amplicon in wild type

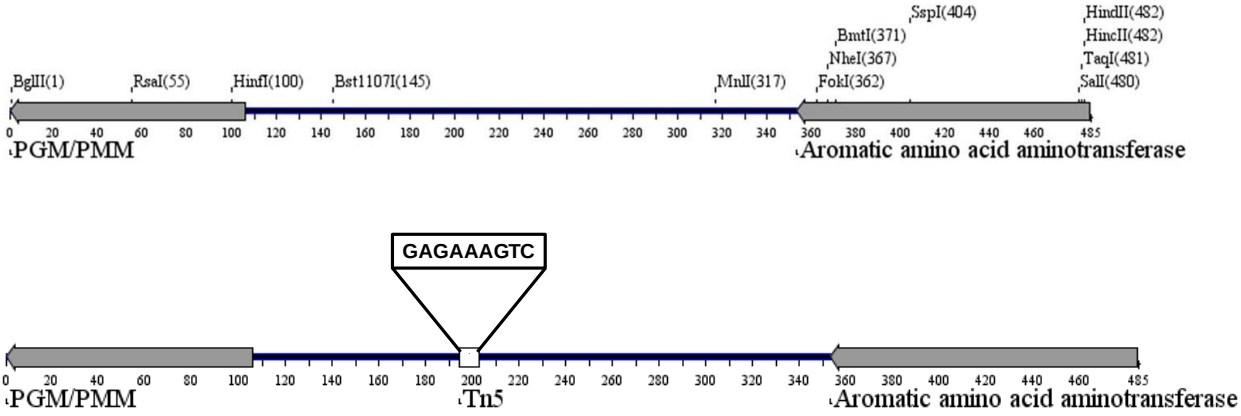

Figure 4.5 Localization of site of insertion of Tn5

Quantification of enzyme activities

Tn5 insertion upstream of PGM/PMM could potentially alter transcription of PGM/PMM therefore, PGM/PMM activities were compared in TK15 and MG606 strains by spectrophotometric assays. Additionally, activities of other enzymes involved in glucose assimilation in EBP, viz, glucose-6-phosphate isomerase (G6PI), UDP-glucose-4-epimerase (UDE) and glucosyltransferases (GST), were also compared.

The specific activity of PGM was observed to be 1.5-fold higher in MG606 compared to TK15

and the difference was statistically significant ($p<0.05$). On the other hand, specific activities of UDE, GST and PGI did not show an appreciable change (upregulation or downregulation) in enzyme activities between MG606 and TK15 strains. A comparison of activities of UDE, GST and PGI between MG606 and TK15 showed that the difference in enzyme activities was statistically insignificant ($p>0.05$) (Table 4.5).

Table 4.5 Enzyme activities of *A. haemolyticus* TK15 and MG606 strains

	TK15 (U/mg protein)	**MG606 (U/mg protein)**	**Fold change**
Phosphoglucomutase	30.34 ± 3.60	45.11 ± 4.21**	1.49 ± 0.14
UDP-glucose epimerase	70.89 ± 3.89	66.11 ± 5.71	0.94 ± 0.08
Glycosyltransferases	0.0020 ± 0.0005	0.0021 ± 0.0005	1.06 ± 0.23
Phosphoglucoisomerases	1.43 ± 0.24	1.45 ± 0.21	1.01 ± 0.15

Data is mean±SD of triplicate samples. **$p<0.01$ compared to *A. haemolyticus* TK15 as determined by Student's *t*-test.

The increase in specific activity of PGM was further confirmed by determining expression of active PGM protein by zymography. The PGM band was of considerably higher intensity in lanes loaded with cell lysates of MG606 strain compared with lanes loaded with cell lysates of TK15 strain. Further, zymograms revealed a single band of PGM in both strains with identical mobility in native PAGE gels. The intensities of PGM bands appearing in both strains were compared by densitometry and a 1.5-2 fold increase in PGM activity ($p<0.05$) was observed in MG606 compared to TK15 strain (Figure 4.6).

Detection of pgm transcription level

The increase in enzyme activity could result from an increase in transcription of PGM-encoding gene. Therefore, the expression of PGM-encoding gene, *pgm*, was determined by RT-PCR. The upregulation of *pgm* expression was investigated by RT-PCR analysis and *pgm* expression was

normalized to the housekeeping *tuf* gene. Since the sequence of PGM is not reported in *A. haemolyticus*, primers were designed for *pgm* and *tuf* genes based on gene sequences of a closely related species, *A. baumannii*. The results of RT-PCR reactions were analyzed by comparison of Ct values between the reaction sets.

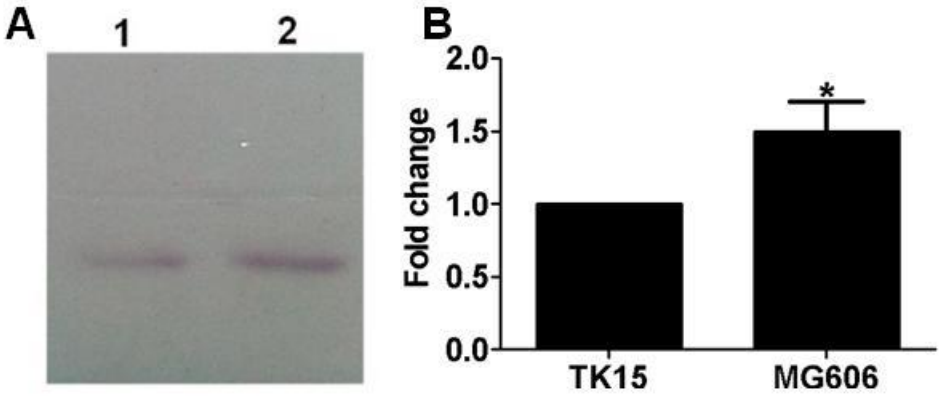

Figure 4.6 Comparison of phosphoglucomutase protein expression. (A) Zymogram of PGM in TK15 (Lane 1) and MG606 (Lane 2) strains. (B) Quantitative analysis of PGM activities in TK15 and MG606 strains.

Data is mean±SD of triplicate samples. *p<0.05 compared to *A. haemolyticus* TK15 as determined by paired *t*-test.

As observed in table 4.6, the Ct values for *pgm* were lower in MG606 compared to TK15. The Ct values of *pgm* were normalized to Ct values of *tuf* gene (ΔCt) and compared by $2^{-\Delta\Delta Ct}$ method. The *pgm* expression was found to be upregulated 1.3-1.7 fold in MG606 compared with TK15. Although *pgm* expression was higher in MG606, statistical comparison of ΔCt values revealed no significant difference (p>0.05) in both strains. The melt curves of *pgm* and *tuf* gene showed a single peak (Figure 4.7) in both strains suggesting a single amplicon was generated indicating specificity of the primers used. In order to further validate the specificity of the primers used, the PCR product was resolved by electrophoresis on 2% agarose gel. The PCR reaction product for

pgm and *tuf* transcripts resolved into a single band on agarose gel and matched the expected size of amplicon (*pgm*: 147 bp, *tuf*: 220 bp) (Figure 4.8).

Table 4.6 Transcription levels of *pgm* and *tuf* genes determined by real time PCR.

Strain	Gene	Ct	ΔCt
MG606	*pgm*	26.9750±0.2116	0.1697±0.2321
	tuf	26.8053±0.0954	
TK15	*pgm*	27.7902±0.2867	0.7459±0.6140
	tuf	27.0443±0.5430	

Data is mean±SD of triplicate samples.

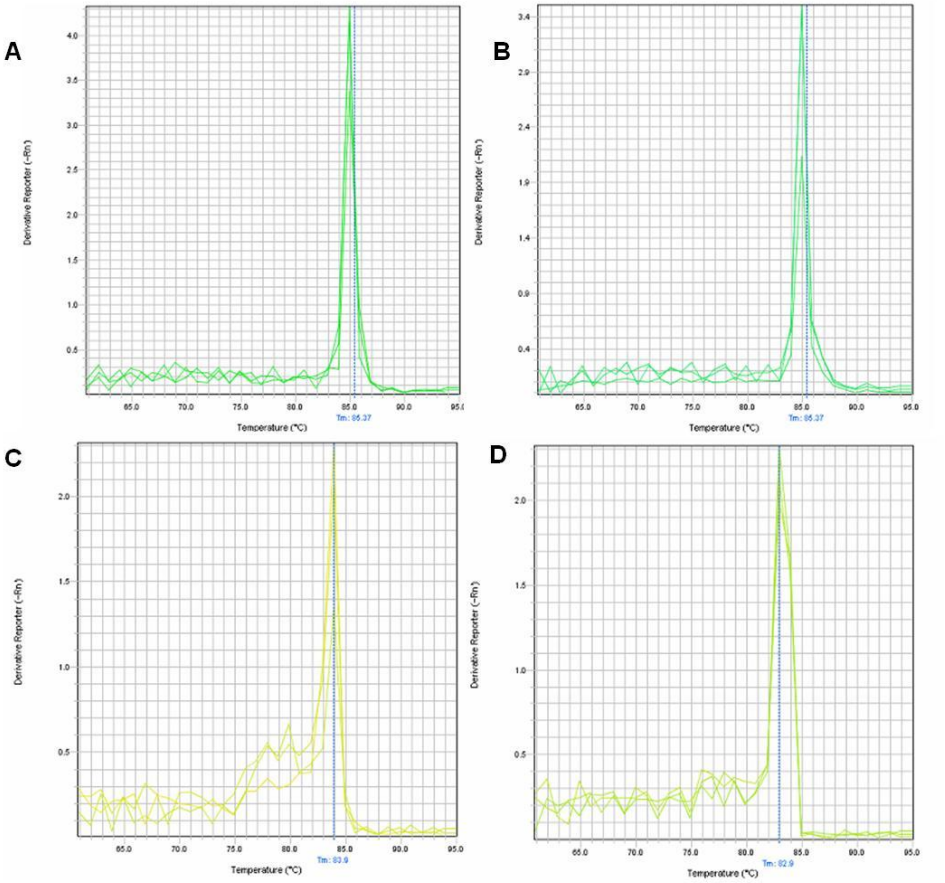

Figure 4.7: RT-PCR melt curves for *pgm* (A and B) and *tuf* (C and D) transcripts in *A. haemolyticus* MG606 and TK15 strains

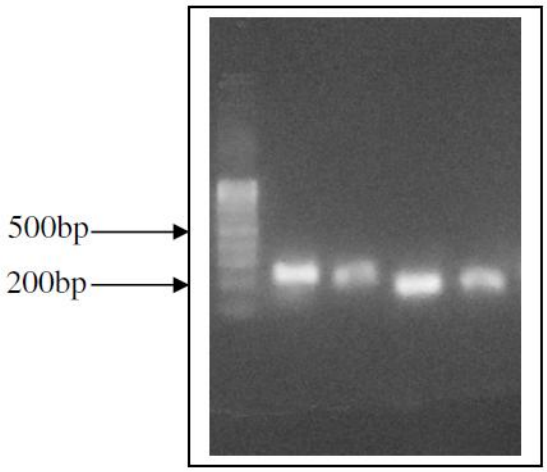

Figure 4.8: Agarose gel electrophoresis of RT-PCR reaction products. Lane 1: 100 bp DNA ladder, lane 2: *tuf* gene PCR product in *A. haemolyticus* TK15, lane 3: *tuf* gene PCR product in *A. haemolyticus* MG606, lane 4: *pgm* gene PCR product in *A. haemolyticus* TK15, lane 5: *pgm* gene PCR product in *A. haemolyticus* MG606

Intracellular concentration of sugar precursors

PGM activity has been correlated with intracellular concentrations of its substrates, G1P and G6P, and its downstream metabolite, UDP-glucose. Therefore, intracellular concentrations of the two phosphosugars and UDP-glucose were compared between TK15 and MG606. Intracellular concentrations of G1P and G6P were comparable in both strains ($p>0.05$) while UDP-glucose levels were significantly higher ($p<0.05$) in MG606 compared to TK15 (Table 4.7).

Table 4.7 Intracellular concentration of sugar precursors in TK15 and MG606 strains of *A. haemolyticus*.

	TK15 (µM/mg protein)	**MG606 (µM/mg protein)**
Glucose-1-phosphate	25 ± 6	28 ± 8
Glucose-6-phosphate	23 ± 6	19 ± 4
UDP-glucose	0.05 ± 0.008	0.08 ± 0.006*

Data is mean±SD of triplicate samples.

*$p<0.05$ compared to *A. haemolyticus* TK15 as determined by Student's *t*-test.

4.2.2 Purification of phosphoglucomutase/phosphomannomutase

PGM was sequentially purified by graded ammonium sulfate precipitation, gel permeation chromatography on Sephacryl S-100 HR column and ion exchange chromatography on DEAE-cellulose column. The fold concentration of PGM at each purification step is summarized in table 4.8, PGM was purified 34.3 folds at the last step as determined by specific activity measurements. The purified enzyme was resolved on SDS-PAGE and appeared as a single band of approximately 51 kDa (Figure 4.9).

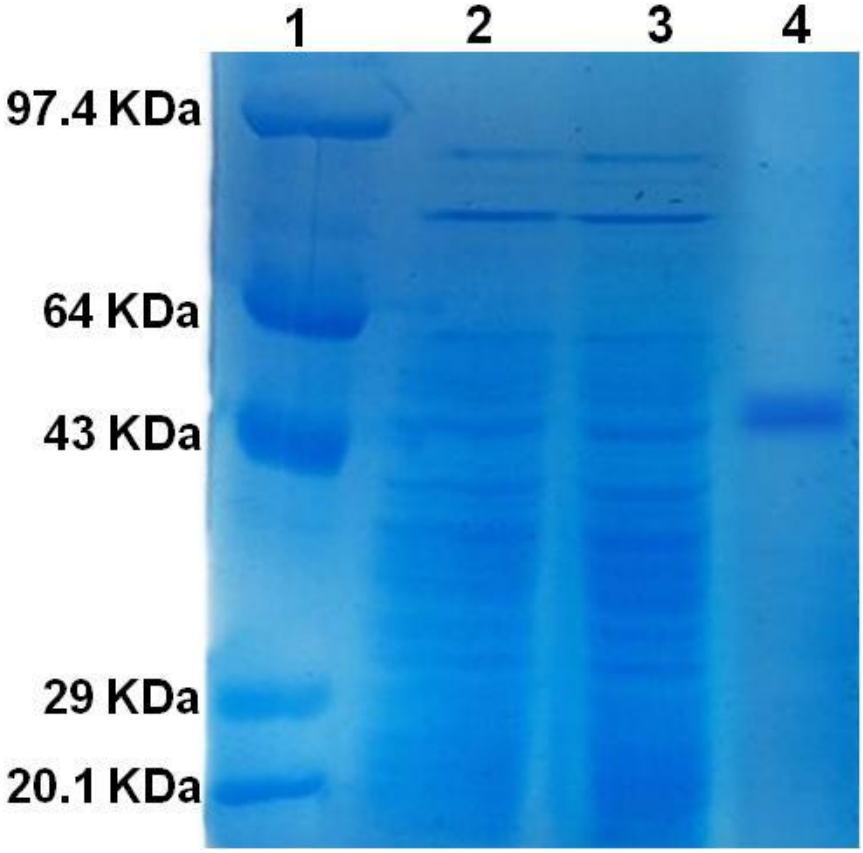

Figure 4.9 SDS-PAGE of cell lysates and purified phosphoglucomutase. Lane 1: Protein molecular weight markers lane 2: whole cell protein profile of TK15, lane 3: whole cell protein profile of MG606, lane 4: purified PGM.

Table 4.8 Purification of phosphoglucomutase from *A. haemolyticus* MG606.

Purification step	Total Protein (mg)	Specific activity (U/mg)	% Recovery	Fold purification
Cell lysate	800	45.1	100	1.0
Ammonium sulfate precipitation	320	90.4	91	2.0
Gel filtration	10.2	975	68	21.6
Ion exchange	3.5	1548	33	34.3

4.2.3 Characterization of phosphoglucomutase/phosphomannomutase

Kinetic properties of enzyme

The substrate specificity of PGM was determined by monitoring conversion of 1-phosphohexoses to their corresponding 6-phospho counterparts. Specifically, the conversion of mannose 1-phosphate (M1P) and fructose 1-phosphate (F1P) to mannose 6-phosphate (M6P) and fructose 6-phosphate (F6P), respectively, was determined by spectrophotometric assays. With M1P as substrate, the specific activity of purified enzyme was approximately 30% of the activity observed with G1P as substrate. On the other hand, no detectable conversion from F1P to F6P was observed with the purified enzyme (Table 4.9)

Table 4.9 Substrate specificity of purified enzyme

Substrate	Specific activity
Glucose-1-phosphate	45.11 ± 4.21
Mannose-1-phosphate	13.51 ± 1.23
Fructose-1-phosphate	ND

Data is mean±SD of triplicate samples. ND = not detected

The kinetic parameters of purified enzyme were determined by Lineweaver-Burk plots. An

apparent Km and Vmax of 0.028 mM and 0.15 mM/min, respectively, was observed with G1P as substrate. On the other hand, the apparent Km and Vmax were relatively lower with M1P as substrate and calculated to be 0.017 mM and 0.038 mM/min, respectively (Figure 4.10).

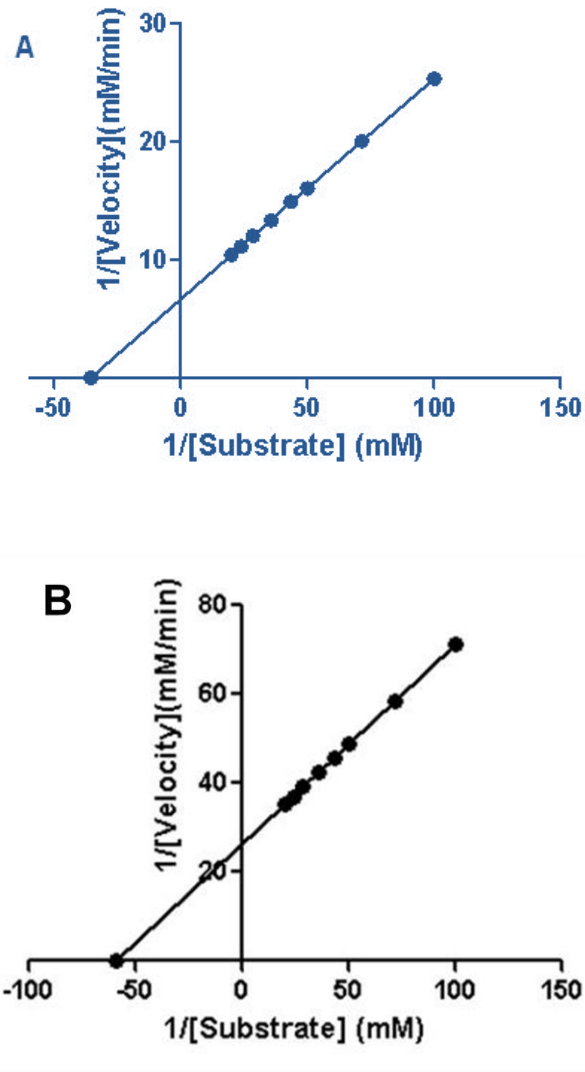

Figure 4.10 Lineweaver-Burk plots of purified enzyme with (A) G1P and (B) M1P as substrates

Effect of temperature

The optimal temperature of purified enzyme was determined by monitoring enzyme activity between 15 to 40°C at 5°C increments and thereafter at 50°C. A temperature-dependent increase in enzyme activity was observed until 35°C followed by a progressive decline in activity at 40

and 50°C (Figure 4.11A).

Effect of pH

The optimal pH of purified enzyme was determined by monitoring enzyme activity between pH 3 to 9 at 1 pH increments and an additional observation at pH 7.5. A pH-dependent increase in enzyme activity was observed until pH 7.5 followed by a progressive decline in activity at pH 8 and 9 (Figure 4.11B).

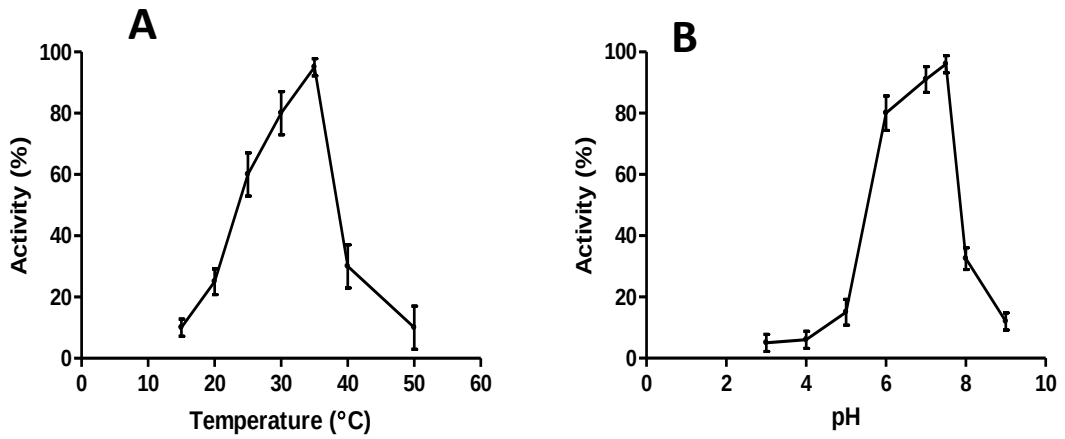

Figure 4.11 Effect of temperature (A) and pH (B) on purified phosphoglucomutase activity.

Effect of PGM activity modifiers

Several chemicals and ions can modulate enzyme activity through a plethora of mechanisms such as cofactor displacement, comptetion with substrate, allosteric inhibition, covalent modification, etc. Therefore, in order to further characterize the purified PGM, effect of metal ions, chelators, substrate analogs and other non-specific inhibitors was determined.

Metals ions exhibited a strong inhibitory effect on PGM activity. Zinc and lithium ions completely inhibited the enzyme at the tested concentration and no enzyme activity was detected. This was closely followed by nickel which inhibited the enzyme almost completely and the

detectable enzyme activity was 4% compared to the uninhibited enzyme control. Cobalt and calcium were observed to be relatively weaker inhibitors of PGM activity and PGM activity was reduced to one-third and one-half of the activity observed in control, respectively. Contrastingly, magnesium showed no inhibition of enzyme activity while the ion chelator EDTA exhibited very small inhibitory activity.

PGM activity was determined with G1P as substrate and inhibitory effect of substrate analog was determined. The highest inhibitory activity was observed with glucose-1,6-biphosphate which reduced the activity to 10% of that observed in control. Fructose-6-phosphate was found to be a relatively weaker inhibitor since over 60% of activity was retained after inhibition. G6P did not inhibit enzyme activity at the concentration tested (Table 4.10).

Table 4.10 Effect of modifiers on activity of purified phoglucomutase of *A. haemolyticus* MG606

Modifier (5 mM)	Inhibition (%)	Modifier (5 mM)	Inhibition (%)
Magnesium	0±0	UDP-glucose	65±5
Calcium	50±4	ADP	50±2
Cobalt	78±6	ATP	20±1
Nickel	96±4	Fructose-6-phosphate	38±1
Lithium	100±0	Glucose-6-phosphate	0±0
Zinc	100±0	Glucose-1,6-biphosphate	90±3
EDTA	8±1		

Data is mean±SD of triplicate samples.

UDP-glucose = Uridine diphosphate glucose, ADP = adenosine diphosphate, ATP = adenosine triphosphate, EDTA = ethylene diamine tetraacetic acid

The biochemical reactions in EBP production pathway are energy-dependent and rely on a

constant supply of ATP for synthesizing EBP. Further, UDP-glucose synthesis is the next step, after 1- to 6-phosphosugar interconversion by PGM, in EBP biosynthetic pathway and intracellular pools of UDP-glucose influence EBP production. Therefore, the effect of ADP, ATP and UDP-glucose on PGM activity was determined and PGM inhibition followed the order: UDP-glucose > ADP > ATP

4.2.4 Pathogenicity/virulence evaluation of *A. haemolyticus* MG606

The studies on pathogenicity/virulence of *A. haemoyticus* MG606 is a prerequisite for establishing safety profile and regulatory clearance of MG606. Therefore, acute toxic effect of *A. haemolyticus* MG606 was determined in mouse lethality assay following systemic administration (intraperitoneal).

Effect on body weight

The body weight of animals was recorded on the day of injection (day 0) and each day thereafter until day 7.

Sighting study: Mean body weights in all treatment groups tended to be lower on day 7 compared to day 0 of injection. However, the reduction in mean body weight was insignificant in animals injected with 7, 9 and 11 log CFU/animal. An increase in dose to 12 log CFU/animal resulted in 14.3% reduction in body weight on days 6 and 7 post-injection compared to day 0. A further increase in dose to 13 log CFU/animal resulted in 9.6% reduction in body weight on day 1 post-injection while body weight measurements could not be performed on subsequent days due to dose-related mortality within 24 hours of administration (Table 4.11).

Main study: Mean body weight of animals tended to be lower in on day 7 of injection compared to initial (day 0) body weights. However, the differences in body weights were insignificant in

animals injected with 10 log CFU/animal. An increase in dose to 11, 12 and 13 log CFU/animal resulted in 11.1, 6 and 3.8% reduction in body weight, respectively, on day 7 post-injection compared to day 0. A further increase in dose to 14 log CFU/animal resulted in 10.6% reduction in body weight on day 1 post-injection while body weight measurements could not be performed on subsequent days due to dose-related mortality within 24 hours of administration (Table 4.12).

Table 4.11 Mean body weight in sighting study

Dose (log CFU/animal)	Days							
	0	1	2	3	4	5	6	7
7	26.5±3.5	26.5±3.5	25.5±3.5	26.5±3.5	26±2.8	26±4.2	26±4.2	25.5±3.5
9	26.5±3.5	25.5±3.5	25.5±2.1	26±2.8	26±2.8	25±2.8	24.5±3.5	24.5±3.5
11	27.5±4.9	25.5±4.9	24±5.7	27±NA	28±NA	28±NA	27±NA	27±NA
12	28±1.4	26±1.4	26±NA	25±NA	25±NA	25±NA	24±NA	24±NA
13	26±0.0	23.5±0.7	D	D	D	D	D	D

D: All animals died; NA: Not applicable as only single animal was left

Table 4.12 Mean body weight in main study

Dose (log CFU/animal)	Days							
	0	1	2	3	4	5	6	7
10	26±1.6	24.5±2.1	23.5±2.1	23.5±2.1	24.3±2.1	23.5±2.1	24.3±2.5	24±2.4
11	26.3±1.3	25.3±1.5	24.5±0.6	24.3±1.2	23.7±0.6	23.3±0.6	23.3±0.6	23.3±0.6
12	26.3±1.3	24.3±1.3	24±2.0	23.7±NA	24±NA	24.7±NA	24.7±NA	24.7±NA
13	26±1.2	23.3±1.7	24±NA	24±NA	25±NA	24±NA	25±NA	25±NA
14	26±1.2	23.3±1.0	D	D	D	D	D	D

D: All animals died; NA: Not applicable as only single animal was left

Effect on rectal temperature

The rectal temperature of animals was recorded prior to injection (0 hour) followed by regular observations at 60, 120, 180, 240 and 480 min post-injection. The rectal temperatures were also recorded 24 and 48 hours post-injection.

Sighting study: The rectal temperature of animals receiving 7 and 9 log CFU/animal did not change during the 48 hour observation period. However, a decrease in rectal temperature was observed in animals receiving 11 and 12 log CFU/animal which lasted upto 8 hours. A further increase in dose to 13 log CFU/animal resulted in a decrease in rectal temperature which lasted upto 8 hrs followed by the death of animals within 48 hours (Table 4.13).

Table 4.13 Rectal temperature of mice in sighting study

		Rectal Temperature (Degree Celcius) →								
Dose/animal (Log CFU)	**↓Animal No. Time points →**	**0 min**	**60 min**	**120 min**	**180 min**	**240 min**	**480 min**	**24 hrs**	**48 hrs**	**72 hrs**
7	H	36.1	35.9	36	35.7	35.9	35.3	35.8	36.3	L
	B	35.8	35.6	35.8	35.5	35.5	35.3	36	36.2	L
9	T	35.1	35.3	35	34.9	35.2	35.3	35.7	35.5	L
	UM	36.2	36	36	35.8	35	36.2	36.5	36.3	L
11	H	35	35.2	35	34.3	34	33.2	33.9	34.1	D
	B	35.7	35.3	35.5	34.6	34	33.4	34.1	34	L
12	T	35.4	35.2	35	34.3	33.8	32.6	NR	D	D
	UM	36	36.2	35.8	35.6	34.5	34	35.3	35.7	L
13	H	35.9	35.5	35.6	35	34.8	33.6	34	D	D
	B	35.2	35.3	34.9	34.4	34	32.9	33.9	D	D

L: Animal live, D: Animals dead, NR: Not readable

Main study: The rectal temperature of animals receiving 10 log CFU/animal did not change during the 48 hour observation period. However, a decrease in rectal temperature was observed in one animal each in 11 and 12 log CFU/animal groups followed by death within 72 hours. A further increase in dose to 13 log CFU/animal induced hypothermia in 3 out of 4 animals while 14 log CFU/animal induced hypothermia in all animals. The hypothermic animals in 13 and 14 log CFU/animal died within 48 hours of dose administration (Table 4.14).

Table 4.14 Rectal temperature of mice in main study

		Rectal Temperature (Degree Celcius) →								
Dose/animal (Log CFU)	**↓Animal No. Time points →**	**0 min**	**60 min**	**120 min**	**180 min**	**240 min**	**480 min**	**24 hrs**	**48 hrs**	**72 hrs**
10	H	35.8	35.6	35.4	35.7	35.1	35	35.3	35.4	L
	B	35.3	35.3	35	35.7	35.5	35.5	35.9	35.8	L
	T	35	35.3	35.1	34.8	35.2	34.9	35.4	35.2	L
	UM	35.9	36	36.2	35.8	35.6	35.7	36.4	36.4	L
11	H	35.1	34.9	35.2	35.4	35.2	35	35.3	34	L
	B	35.6	35.4	35.2	34.7	34.2	34.3	34.8	34.8	L
	T	35.2	35.3	35.3	34.9	34.2	33.5	34.2	34	D
	UM	35.4	35.6	35.7	35.2	35	35.3	34.9	35.5	L
12	H	36.2	36	36.3	35.5	35.6	35.8	36	35.8	L
	B	35.9	35.6	35.8	35.2	35.2	35.1	35.1	35.7	L
	T	35	35.4	35.1	35.3	34.5	33.8	NR	34.8	L
	UM	35.6	35.2	35	35.2	34.3	34	33.3	D	D
13	H	36	35.8	35.3	34.2	33.8	33.1	33.3	35.5	L
	B	36.1	36.3	35.8	35.3	34	32.5	NR	D	D
	T	35.7	35.5	35.7	34.9	34.6	33.2	32.4	D	D
	UM	35.4	35.5	35	34.5	33.3	33.9	34.2	D	D
14	H	35.4	35.1	34.5	34.8	33.2	32.1	NR	D	D
	B	35.6	35.3	35.2	34.8	34.9	32.3	NR	D	D
	T	35.3	35.5	35.2	34.8	34.2	33.1	32.8	D	D
	UM	35.8	35.3	34.8	34.9	34.5	32.6	32.4	D	D

L-Animals live, D-Animals dead, NR-Not readable

Clinical signs of toxicity

Clinical signs of toxicity, listed in table 4.15, were observed in all animals of the main study. During the 7 day observation duration, *A. haemolyticus* MG606 exhibited clinical signs of toxicity in a dose-dependent manner. These signs of toxicity included anorexia, tremor, decreased grasp/hold, pilo-erection, weak grip strength, dull furcoat, hunched back, hypothermia and death. The observations are summarized in table 4.16.

Table 4.15 Parameters studied in clinical signs of toxicity

1.No abnormality detected	9. Irritable animal	17.Nasal discharge	25.Pupil size changed	33.Prostration (exhausted and collapsed)
2.Dull/Lethargic animal	10.Diarrhoea	18.Weak grip strength	26.Lack of interest in food	34.Restless/Hyperactive animal
3.Body weak and emaciated	11.Increased preening	19.Swollen eyes	27.Bizarre behavior	35.Nonresponsive to external stimuli
4.Presence of tremor	12.Unsteady gait	20.Red eyes	28.Dry/ Dirty furcoat	36.Pyrexia
5.Decreased grasp or hold	13.Panting/Gasping	21.Increased blinking	29.Dull/Lustureless furcoat	37.Avoiding light (Photophobia)
6.Drowsy or sleepy animal	14.Loss of hair	22.Vomiting	30.Repetitive circling	38.Unusual respiration pattern
7.Lacrimation	15.Laboured breathing	23.Dead animal	31.Abnormal gait pattern	39.Hunched back posture and shrunken flanks
8.Pilo-erection	16.Edema	24.Erythema	32.Bleeding from paw or tail	40.Decreased blinking (staring look) 41.Hypothermia) 42.Others (if any)

Table 4.16 Clinical signs of toxicity observed in main study

Dose (log CFU/animal)	Day→ ↓Animal No.	0	1	2	3	4	5	6	7
10	H	1	1	1	1	1	1	1	1
	B	1	8	8	1	1	1	1	1
	T	1	8	8	1	1	1	1	1
	UM	1	8	1	1	1	1	1	1
11	H	1	8, 18, 29	8	1	1	1	1	1
	B	1	8, 18, 29	29	29	1	1	1	1
	T	1	8, 18, 29, 39, 41	4, 5, 8, 18, 29, 39, 41	23	23	23	23	23
	UM	1	8, 18, 29	29	29	1	1	1	1
12	H	1	8, 18, 29	8	8	8	1	1	1
	B	1	8, 18, 29	8	8	1	1	1	1
	T	1	8, 18, 29	8	1	1	1	1	1
	UM	1	8, 18, 41	23	23	23	23	23	23
13	H	1	8, 18, 41	8, 18, 41	8, 18	8	8	8	8
	B	1	4, 5, 8, 18, 29, 39, 41	23	23	23	23	23	23
	T	1	4, 5, 8, 18, 29, 39, 41	23	23	23	23	23	23
	UM	1	4, 5, 8, 18, 29, 39, 41	23	23	23	23	23	23
14	H	1	4, 5, 8, 18, 29, 39, 41	23	23	23	23	23	23
	B	1	4, 5, 8, 18, 29, 39, 41	23	23	23	23	23	23
	T	1	4, 5, 8, 18, 29, 39, 41	23	23	23	23	23	23
	UM	1	4, 5, 8, 18, 29, 39, 41	23	23	23	23	23	23

Mortality

Sighting study: No mortality was observed over a period of 7 days in animals receiving 7 and 9 log CFU/animal. However, 50 % mortality was observed within 72 hours in animals receiving 11 and 12 log CFU/animal while 100% mortality was observed within 48 hours in 13 log CFU/animal group.

Main study: A dose-dependent trend in mortality was observed over a period of 7 days post-administration. No mortality was observed in animals receiving the lowest dose, 10 log CFU/animal, while 25, 25, 75 and 100% mortality was observed in 11, 12, 13 and 14 log CFU/animal groups, respectively. LD50 value was calculated by Logit method and found to be 12.11 log CFU/animal.

Gross necropsy

Gross necropsy was performed on animals that died during the experiment. Pin point to ecchymotic hemorrhages on heart, kidney and liver were observed in animals which died within 48 hours post-injection while no gross pathological changes were observed in surviving animals necropsied at study completion.

4.2.5 Pathogenicity/Virulence of *A. haemolyticus* MG606 exobiopolymer

The *in vivo* acute toxicity of *A. haemolyticus* MG606 EBP was determined by mouse lethality assay in female, Swiss albino mice.

Effect on body weight

The body weight of animals was recorded on the day of injection (day 0) and each day thereafter until day 7.

Sighting study: Mean body weights in all treatment groups tended to be lower on day 7

compared to day 0 of injection. However, the reduction in mean body weight was insignificant in animals injected with 20 and 60 mg/kg EBP. An increase in dose to 100 mg/kg EBP resulted in >10% reduction body weight from day 3 onwards compared to day 0. Mean body weight reached the minimum (14.8% reduction) on day 4 and remained constant thereafter till day 7. A further increase in dose to 140 and 180 mg/kg resulted in dose-related mortality within 24 hours of administration (Table 4.17).

Main study: Mean body weight of animals tended to be lower on day 7 of injection compared to initial (day 0) body weights. However, the differences in body weights were insignificant in animals injected with 60 and 80 mg/kg. An increase in dose to 100 and 120 mg/kg resulted in 14.5 and 13.8% reduction in body weight, respectively, on day 7 post-injection compared to day 0. A further increase in dose to 140 mg/kg resulted in dose-related mortality within 24 hours of administration (Figure 4.18).

Table 4.17: Mean body weight in sighting study

Dose (mg/kg bw)	**Days**							
	0	**1**	**2**	**3**	**4**	**5**	**6**	**7**
20	29.5 ± 0.7	29.0 ± 1.4	28.5 ± 0.7	30.0 ± 1.4	27.5 ± 0.7	28.0 ± 0.0	29.0 ± 0.0	28.0 ± 0.0
60	34.0 ± 2.8	33.0 ± 2.8	33.5 ± 2.1	33.5 ± 3.5	32.0 ± 2.8	32.5 ± 3.5	31.5 ± 3.5	32.0 ± 2.8
100	30.5 ± NA	28.0 ± NA	28.0 ± NA	27.0 ± NA	26.0 ± NA	27.0 ± NA	26.0 ± NA	26.0 ± NA
180	36.0 ± 0.0	D	D	D	D	D	D	D
140	32.5 ± 3.5	D	D	D	D	D	D	D

D: All animals died; NA: Not applicable as only single animal was left

Table 4.18: Mean body weight in main study

Dose (mg/kg bw)	Days							
	0	**1**	**2**	**3**	**4**	**5**	**6**	**7**
60	33.8 ± 1.7	33.5 ± 1.7	33.5 ± 1.3	33.5 ± 1.7	32.8 ± 2.2	32.8 ± 2.5	33.3 ± 1.7	33.3 ± 1.5
80	33.0 ± 1.8	32.0 ± 1.0	31.0 ± 1.0	31.3 ± 1.5	30.3 ± 1.5	30.7 ± 1.2	30.0 ± 1.0	29.7 ± 0.6
100	32.8 ± 1.0	31.0 ± NA	30.0 ± NA	30.0 ± NA	29.0 ± NA	29.0 ± NA	28.0 ± NA	28.0 ± NA
120	32.5 ± 0.6	31.0 ± NA	31.0 ± NA	29.0 ± NA	29.0 ± NA	28.0 ± NA	29.0 ± NA	28.0 ± NA
140	32.3 ± 1.7	D	D	D	D	D	D	D

D- All animals died; NA- Not applicable as only single animal was left

Effect on rectal temperature

The rectal temperature of animals was recorded prior to injection (0 hour) followed by regular observations at 30, 60, 90, 120, 180, 240 and 480 min post-injection. The rectal temperatures were also recorded 24 hours post-injection.

Sighting study: The rectal temperature of animals receiving 20 and 60 mg/kg EBP did not change significantly during the 24 hour observation period. However, a significant decrease in rectal temperature was observed in animals receiving 100, 140 and 180 mg/kg EBP animal which lasted upto 8 hours in 100 mg/kg group. The hypothermia was followed by death in one mouse of 100 mg/kg and both mice of 140 and 180 mg/kg groups within 60 min of EBP administration (Table 4.19).

Main study: The rectal temperature of animals receiving 60 mg/kg EBP did not change during the 48 hour observation period. However, a decrease in rectal temperature was observed in one animal in 80 mg/kg group followed by death within 1 hour. A further increase in dose to 100 and 140 mg/kg induced hypothermia in 3 out of 4 animals while 140 mg/kg induced hypothermia in all animals. The hypothermic animals died within 1 hour of dose administration irrespective of

the dosage except one animal in 100 mg/kg group which died between 60 and 90 min (Table 4.20).

Table 4.19 Rectal temperature of mice in sighting study.

		Rectal Temperature (Degree Celcius) →								
Dose	**↓Animal No. Time points→**	**0 min**	**30 min**	**60 min**	**90 min**	**120 min**	**180 min**	**240 min**	**480 min**	**24 h**
20	H	36.3	36.5	36.4	36.1	36.1	36.3	36.5	36.5	L
mg/kg	B	35.9	35.6	35.7	35.7	35.6	35.7	35.8	35.6	L
60	T	36.0	35.8	36.2	36	36.1	35.9	36	35.7	L
mg/kg	UM	35.4	35.6	35.6	35.4	35.7	35.6	35.5	35.7	L
100	H	35.5	33.1	NR	NR	NR	NR	NR	NR	D
mg/kg	B	36.1	34.2	32.9	NR	NR	NR	33.6	35.7	L
140	T	34.7	33.6	NR	NR	NR	NR	NR	NR	D
mg/kg	UM	35.3	33.2	NR	NR	NR	NR	NR	NR	D
180	H	36.2	33	NR	NR	NR	NR	NR	NR	D
mg/kg	B	35.8	NR	NR	NR	NR	NR	NR	NR	D

L-Animals live, D-Animals dead, NR-Not readable

Table 4.19 Rectal temperature of mice in main study.

		Rectal Temperature (Degree Celcius) →								
Dose	**↓Animal No. Time points→**	**0 min**	**30 min**	**60 min**	**90 min**	**120 min**	**180 min**	**240 min**	**480 min**	**24 h**
60	H	34.8	34.4	34.3	34.6	34.4	34.3	34.2	34.6	L
mg/kg	B	35.5	35.6	35.2	35.1	35.2	35.4	35.6	35.4	L
	T	36.3	36.1	36.3	36.4	36.1	36	36.3	36.5	L
	UM	36.1	35.8	35.6	35.9	36	36.3	35.8	36.2	L
80	H	35.6	33.6	NR	NR	NR	NR	NR	NR	D
mg/kg	B	35.7	35.4	35.2	35.2	35.5	35.4	35.2	35.2	L
	T	35.9	35.2	35.4	35.4	35.5	35.2	35.2	35.4	L
	UM	35.2	35.3	35.4	35.4	35.5	35.2	35.4	35.3	L
100	H	36.3	35.3	33.1	NR	NR	NR	NR	NR	D
mg/kg	B	35.6	33.2	NR	NR	NR	NR	NR	NR	D
	T	35.9	34	NR	NR	NR	NR	NR	NR	D
	UM	35.3	33.1	33.9	34	34.3	34.6	34.8	34.9	L
120	H	36	33.3	33.1	34.8	34.6	35.4	35.7	35.6	L
mg/kg	B	35.4	NR	NR	NR	NR	NR	NR	NR	D
	T	35.8	NR	NR	NR	NR	NR	NR	NR	D
	UM	35.6	33.2	NR	NR	NR	NR	NR	NR	D
140	H	35.7	NR	NR	NR	NR	NR	NR	NR	D
mg/kg	B	36.4	NR	NR	NR	NR	NR	NR	NR	D
	T	36.8	NR	NR	NR	NR	NR	NR	NR	D
	UM	36.6	NR	NR	NR	NR	NR	NR	NR	D

L-Animals live, D-Animals dead, NR-Not readable

Clinical signs of toxicity

Clinical signs of toxicity were observed in all animals of the main study based on parameters listed in table 4.. During the 7 day observation duration, EBP exhibited clinical signs of toxicity in a dose-dependent manner. These signs of toxicity included anorexia, tremor, decreased grasp/hold, pilo-erection, weak grip strength, dull furcoat, hunched back, hypothermia and death. The observations are summarized in Table 4.20.

Table 4.20 Clinical signs of toxicity observed in main study.

Dose (mg/kg)	Animal condition	Days							
		0	**1**	**2**	**3**	**4**	**5**	**6**	**7**
60	Live (4)	1	1, 8	1, 8	1	1	1	1	1
80	Live (3)	1	4, 5, 8, 18, 29, 39, 41, 23	23	23	23	23	23	23
	Dead (1)	1	8, 18, 29	29	29	1	1	1	1
100	Live (1)	1	8, 18, 41	8, 18, 41	8	8	8	1	1
	Dead (3)	1	4, 5, 8, 18, 29, 39, 41, 23	23	23	23	23	23	23
120	Live (1)	1	8, 18, 41	8, 18, 41	8, 18, 41	8, 18	8	8	8
	Dead (3)	1	4, 5, 8, 18, 29, 39, 41, 23	23	23	23	23	23	23
140	Live (0)	1	-	-	-	-	-	-	23
	Dead (4)	1	4, 5, 8, 18, 29, 39, 41, 23	23	23	23	23	23	23

Mortality

The mortality of animals was recorded every day until study completion.

Sighting study: No mortality was observed over a period of 7 days in animals receiving 20 and 60 mg/kg EBP. However, 50% mortality was observed within 24 h in animals receiving 100 mg/kg EBP while 100% mortality was observed within 24 h in 140 and 180 mg/kg EBP.

Main study: A dose-dependent trend in mortality was observed over a period of 7 days post-administration. No mortality was observed in animals receiving the lowest dose, 60 mg/kg while 25, 75, 75 and 100% mortality was observed in 80, 100, 120 and 140 mg/kg groups, respectively. The LD50, determined by Logit method, was found to be 92.1 mg/kg EBP.

Gross necropsy

Gross necropsy was performed on animals that died during the experiment. Pin point to ecchymotic hemorrhages on heart, kidney and liver were observed in animals which died within 48 hours post-injection while no gross pathological changes were observed in surviving animals necropsied at study completion.

in vitro cytotoxicity of exobiopolymer

The *in vitro* toxicity of EBP was determined in macrophage (RAW 264.7) and epithelial (A549) cell lines. The viability of RAW 264.7 and A549 cells was determined by MTT assay following 24 hour incubation with 100-500 µg/ml EBP. The viability of RAW 264.7 cells was not affected upto 400 µg/ml EBP concentrations while a significant reduction in viability was observed at the highest concentration. A similar trend of concentration-dependent toxicity was also observed in A549 cells.

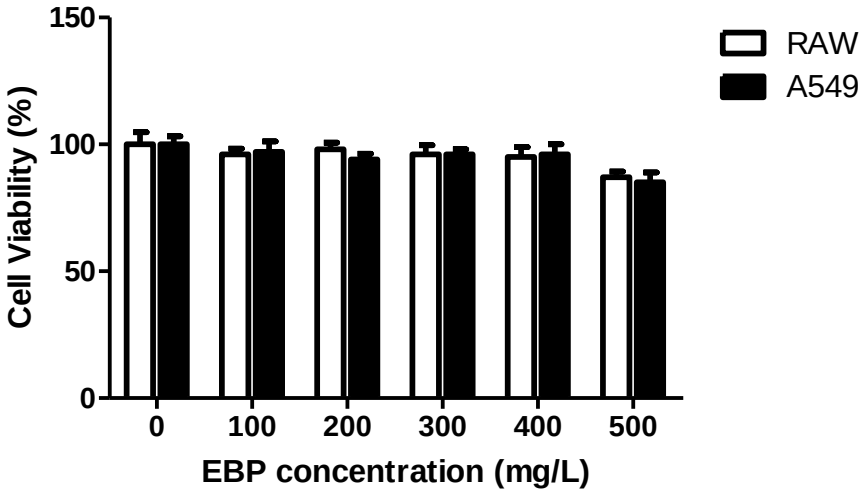

Figure 4.12 Effect of exobiopolymer concentrations on cell viability of RAW and A549 cell lines.

Data is mean±SD of two experiments run in triplicate.

***p<0.001 compared to control as determined by One way ANOVA followed by Tukey's test.

4.2.6 Properties of phosphate binding exobiopolymer of *A. haemolyticus* MG606

In order to understand the phosphate binding ability of EBP, complete characterization of EBP was performed.

Surface properties

Purified EBP was observed to be a white to off-white, fluffy and granular powder. The ultrastructure of EBP was studied under scanning electron microscope and observed to be composed of microfine granules with pores and grooves. The microfine granules were irregular shaped particles with size <10 µm in the longest dimension. A major proportion of these granules was present as irregularly shaped aggregates with size <500 µm in the longest dimension (Figure 4.13).

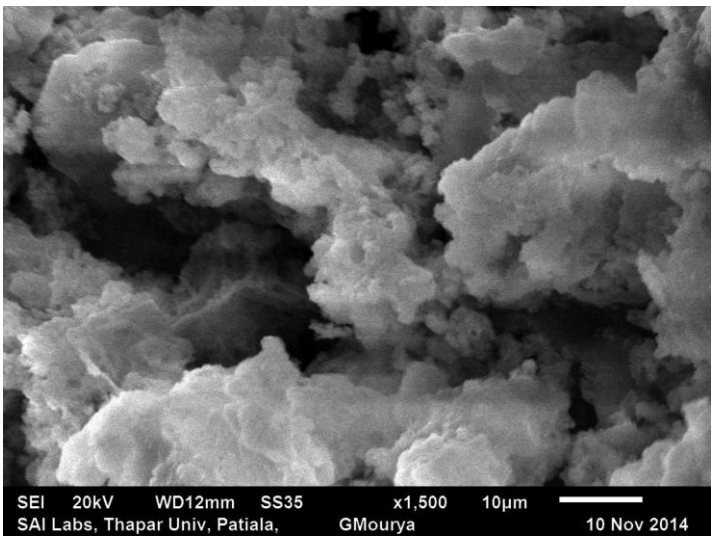

Figure 4.13 Scanning electron micrograph of exobiopolymer of *Acinetobacter haemolyticus* MG606. Magnification 1500X, bar size 10 µm.

Surface area

Surface area of EBP was studied by nitrogen adsorption by BET method and nitrogen sorption data was fitted into different models as listed in table 4.21. EBP exhibited a BET surface area of 87.8 cm^2/g, BJH pore volume of 0.7 cm^3/g and BJH average pore size of 33 nm supporting high porosity observed in SEM.

Elemental and biochemical composition of exobiopolymer

Elemental analysis of EBP revealed carbon and nitrogen were the predominant elements and carbon:nitrogen ratio was calculated to be 6:1. Additionally, hydrogen and sulfur were also present but at relatively lower levels (Table 4.22). Biochemical characterization revealed polysaccharides were the major components of EBP and constituted three-fourth of the total weight fraction. Proteins were identified as the second major components and proteins, along with amino sugars, uronic acid and pyruvic acid, constituted approximately 15% weight fraction of EBP while DNA and RNA were not detected.

Table 4.21 Surface area and porosity of exobiopolymer of *A. haemolyticus* MG606 determined by BET analysis.

Surface area	
Single point surface area at P/Po 0.250558829	84.5 m^2/g
BET surface area	87.8 m^2/g
Langmuir surface area	138.3 m^2/g
t-Plot external surface area:	90.0 m^2/g
BJH Adsorption cumulative surface area of pores	79.4 m^2/g
BJH Desorption cumulative surface area of pores	99.3 m^2/g
Pore volume	
Single point adsorption total pore volume of pores 0.995722567	0.7 cm^3/g
t-Plot micropore volume	-0.002 cm^3/g
BJH Adsorption cumulative volume of pores	0.7 cm^3/g
BJH Desorption cumulative volume of pores	0.7 cm^3/g
Pore Size	
Adsorption average pore width	33.5 nm
BJH Adsorption average pore diameter	36.6 nm
BJH Desorption average pore diameter	29.5 nm
DFT Pore Size	
Volume in pores < 1.483 nm	0.001 cm^3/g
Total volume in pores <= 294.478 nm	0.6 cm^3/g
Area in pores > 294.478 nm	21.7 m^2/g
Total area in pores >= 1.483 nm	54.0 m^2/g
DFT Surface Energy	
Total area	77.4 m^2/g

Table 4.22 Chemical and biochemical analysis of EBP produced by *A. haemolyticus* MG606

Constituent	(%)
Sugars	74.2
Proteins	8
Amino sugars	2.5
Pyruvic acid	0.98
Uronic acids	2.1
DNA	ND
RNA	ND
Carbon	10.4
Hydrogen	2.6
Nitrogen	1.7
Sulphur`	0.3
Oxygen	15.2

ND = Not detected.

Molecular weight analysis

The molecular weight of EBP was determined by gel permeation chromatography (GPC). The first peak, attributed to polysaccharides, appeared at 12 min. The molecular weight was calculated from dextran standards and found to have an average molecular weight of 48.9 KDa. The second peak, which appeared at 15 min, was identified as system/ghost peak. System peaks are commonly observed in refractive index detectors due to solvent effects and such peaks do not correspond to a component of the analyte (Trathnigg, 2000). Further, the polydispersity index was found to be 1.7 indicating monodispersive nature of polysaccharide chain thus represents presence of only one type of polysaccharide with a narrow molecular weight range (Figure 4.14). The different molecular weight indices and polydispersity index of both peaks are listed in table

4.23.

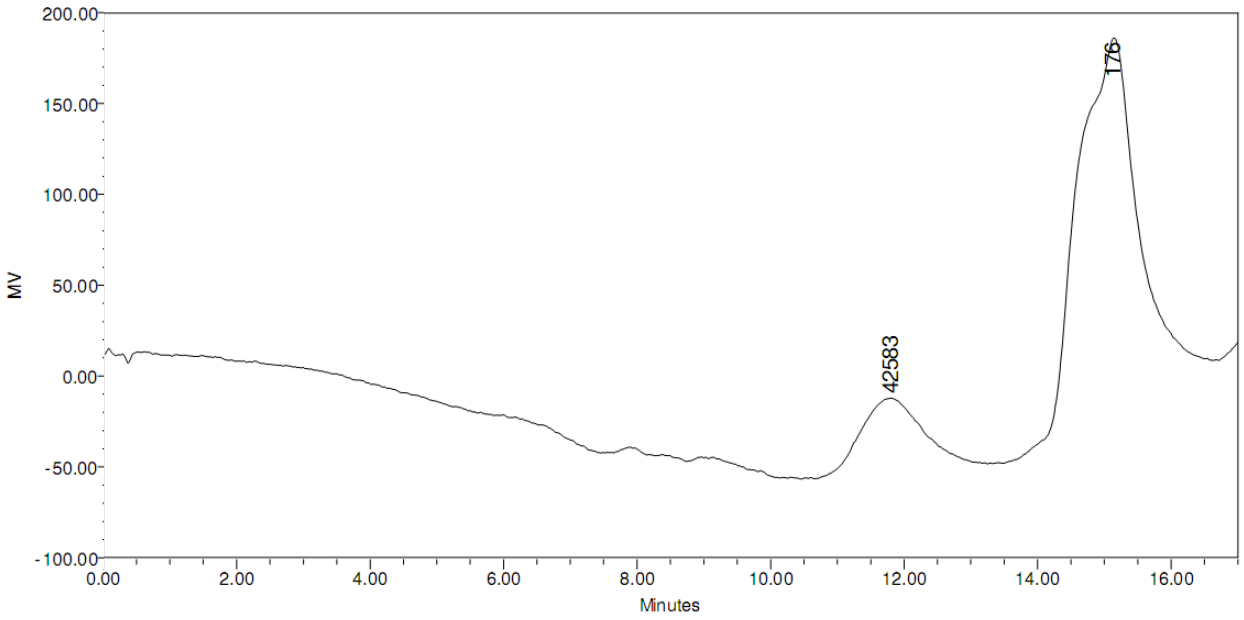

Figure 4.14 Gel permeation chromatogram showing molecular weight of exobiopolymer.

Table 4.23 Molecular weight and polydispersity index of exobiopolymer.

Peak	Mn	Mw	MP	Mz	Mz+1	Polydispersity
1	28704	48952	42583	72863	97919	1.705389
2	145	245	176	358	484	1.694085

Monosaccharide analysis

The monosaccharide composition of EBP was determined by gas chromatography mass spectroscopy. The chromatogram revealed EBP was a heteropolysaccharide composed of several pentose and hexose moieties with glucose being the most prominent monosaccharide. The relative percentage of monosaccharides was: glucose 21.9%, xylose 15.2%, arabinose 14.6%, ribose 14.6%, galactose 13.4%, allose 13.0%, lyxose 6.0% and mannose 1.2%. The retention times and relative peak areas are presented in table 4.24. Several additional peaks were observed in the chromatogram which are not included in the below table because these peaks were

attributed to either unreacted derivatizing agent or non-sugar reaction by-products. Further, all sugars were eluted within 15 min and the peaks appearing after 15 min were non-sugar impurities being eluted due to column washing (Figure 4.15).

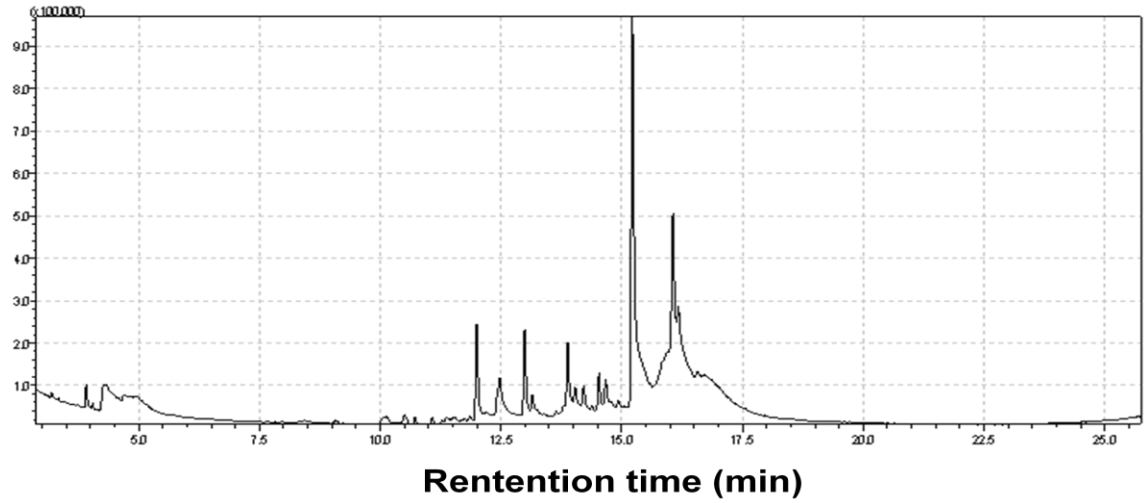

Figure 4.15 GCMS spectra showing different peaks of monosaccharide units

Table 4.24 List of monosaccharides detected during GCMS with retention time

S. No.	List of carbohydrates identified	M/Z	R.T.	Area	SI
1	Lyxose, tetra-(trimethylsilyl)-ether	73	10.128	12670	80
2	Per(trimethylsilyl)-D-fructose	73	11.374	8211	55
3	Beta.-D-Glucopyranose, 1,2,3,4,6-pentakis-O-(trimethylsilyl)	73	11.997	167389	96
4	D-Xylopyranose, 1,2,3,4-tetrakis-O-(trimethylsilyl)	73	12.475	151428	94
5	D-Ribose, 2,3,4,5-tetrakis-O-(trimethylsilyl)	73	12.99	146349	95
6	Lyxose, tetra-(trimethylsilyl)-ether	73	13.149	47696	90
7	Allose Per-TMS	73	13.883	129432	95
8	Arabinose	73	12.99	146349	95
9	Glucose	73	13.149	47696	90
10	Galactose	73	13.883	129432	95
11	D-Mannopyranose	73	14.926	12350	88

Thermal stability

Thermostability is an important parameter for commercial applications of EBP. Hence, thermogravimetry was performed to determine thermal degradation profile of EBP. The thermogram revealed a stepwise degradation of EBP with the first step appearing upto 100°C and the second step until 250°C. The weight loss in the first step may be attributed to desorption of sorbed moisture while the second step may be due to degradation of heat-labile functional groups such as carboxylate and amides. The third step signified extended upto 550°C and signified degradation of sugar molecules while the fourth step appeared until complete degradation at 895°C. The onset of degradation (Td) was observed at 295°C (Figure 4.16).

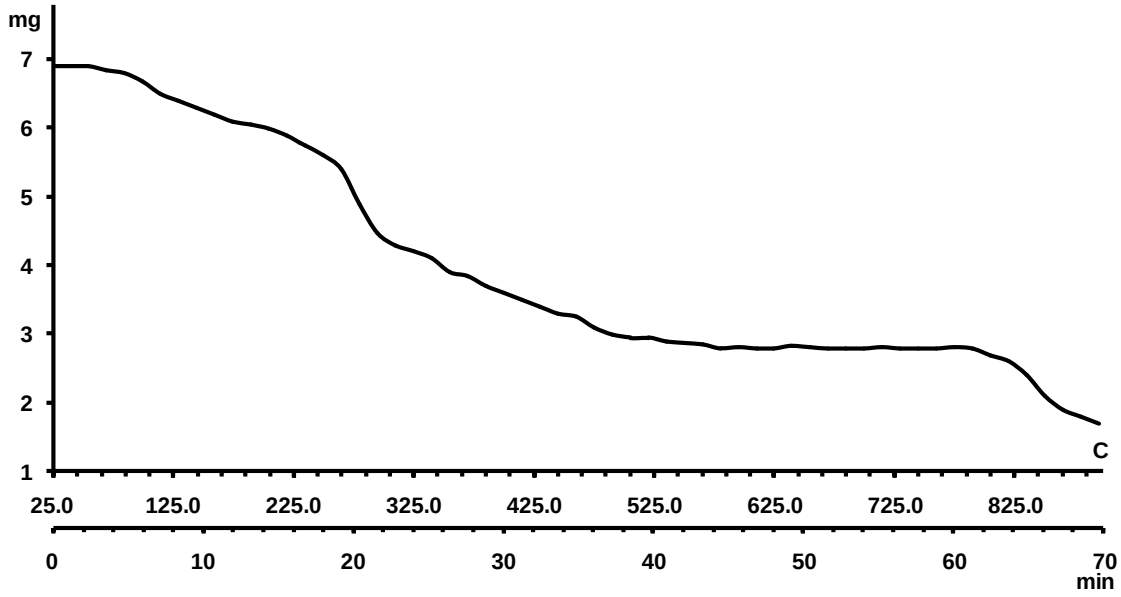

Figure 4.16 Thermogram showing thermal degradation profile of exobiopolymer of *A. haemolyticus* MG606.

Viscoelastic property

The dynamic viscosity and shear behavior of EBP solutions is an important characteristic from a commercial viewpoint. This is because shear behavior impacts the choice of carriers and other excipients as well as the maximum concentration of EBP allowable in a formulation. The

dynamic viscosity of aqueous EBP solution was determined at different shear rates. The apparent viscosity was inversely related to shear rate since apparent viscosity decreased with an increase in shear rate (Figure 4.17).

The relation between shear rate (γ, s^{-1}) and shear stress (τ, Pa) can be quantitatively defined by Power law or Ostwald-de-Waele model as follows:

$\tau=K\gamma^n$, where, K is consistency index (Pa s^n) and n is power law index or flow index value (Alves et al., 2010).

A value of n<1 represents non-Newtonian, pseudoplastic behavior while n=1 represents a Newtonian behavior. The value of flow index value was calculated to be 0.582 for EBP solutions. The observed relation between apparent viscosity and shear results suggesting pseudoplastic nature rate, together with a flow index value less than 1, suggests shear-thinning, non-Newtonian, pseudoplastic behavior of EBP solutions.

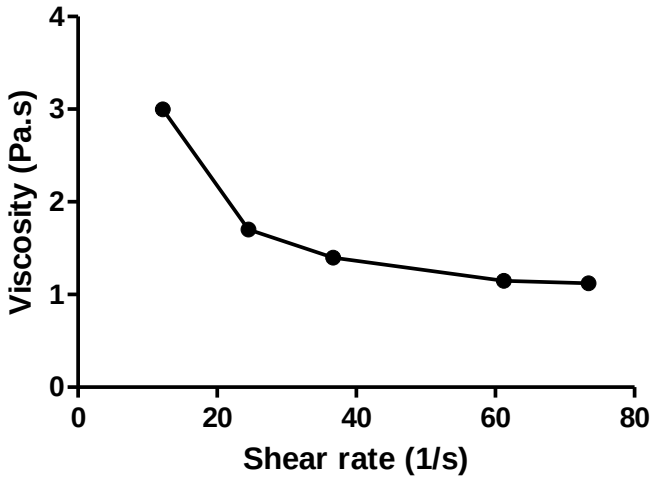

Figure 4.17 Graph showing effect of shear rate on viscosity of exobiopolymer solution

4.2.7 Adsorptive removal kinetics of phosphate by exobiopolymer

The quantitative aspects of EBP-phosphate binding were determined as a function of contact time, EBP concentration and phosphate concentration. Phosphate removal from solution was determined under optimized conditions of contact time and EBP concentration and data fitted to adsorption isotherms to determine the nature of interaction.

Optimization of contact time

The optimal contact time for phosphate removal was determined by varying contact time from 0 to 300 min at fixed phosphate concentration (1 mg/L) and different EBP concentrations (50-400 mg/L EBP). The equilibrium concentration of phosphate appeared relatively early at high EBP concentrations compared with low EBP concentrations. The equilibrium concentration was attained after 240 min contact time with 50 and 100 mg/L EBP concentration. On the other hand, binding of phosphate with EBP was relatively faster at EBP concentrations above 100 mg/L and equilibrium concentration was attained after 180 min contact time (Figure 4.18). Therefore, a contact time of 240 min was considered optimum for phosphate binding.

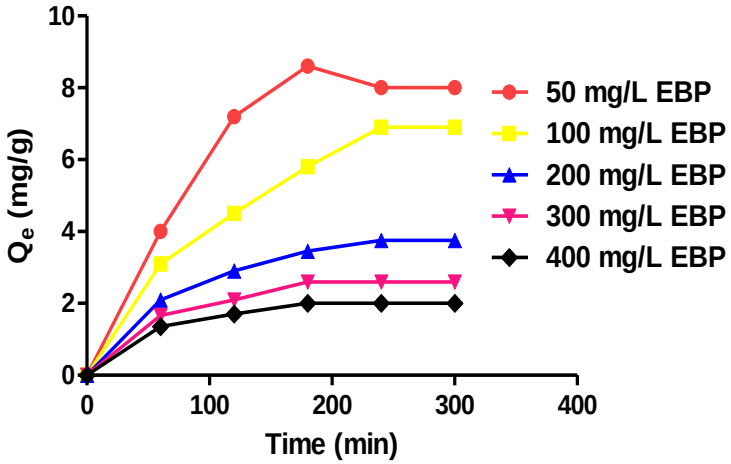

Figure 4.18 Kinetics of phosphate binding (1 mg/L) at different EBP concentrations (●- 50 mg/L, ■- 100 mg/L, ▲-200 mg/L, ▼-300 mg/L, ♦-400 mg/L)

Optimization of EBP concentration

The optimal EBP concentration for phosphate removal was determined at 1 mg/L phosphate and 240 min contact time. Percent phosphate removal and sorption efficiency (Qe) increased and decreased, respectively, with increasing EBP concentration. Percent phosphate removal increased from 40% at 50 mg/L EBP to 70% at 100 mg/L. A further increment in EBP concentration to 200 mg/L resulted in a small increase in phosphate removal to 75%. The percent removal at 200 mg/L was, apparently, the maximal removal since a similar percent removal as observed at 300 and 400 mg/L EBP concentrations as well. In contrast to percent removal, Qe value was slightly higher at 50 mg/L (Qe = 8) compared to 100 mg/L EBP (Qe = 6.8). A further increment in EBP concentration to 200 mg/L resulted in a sharp decline in Qe to 3.5. The percent removal at 200 mg/L was, apparently, the maximal removal since a similar percent removal as observed at 300 and 400 mg/L EBP concentrations as well. The Qe values steadily declined with further increase in EBP concentration to 300 and 400 mg/L (Figure 4.19A). Based on these results, 100 mg/L EBP was selected as the optimal concentration for further studies since percent phosphate removal and Qe were close-to-maximum values at this concentration.

Optimization of phosphate concentration

Following optimization of contact time and EBP concentration, phosphate removal was determined as a function of phosphate concentration. Various concentrations of phosphate (1-5 mg/L) were mixed with 100 mg/L of EBP and phosphate removal determined after 240 min. Percent phosphate removal exhibited an inverse, linear correlation (R^2 = 0.959) with phosphate concentration whereby, percent phosphate removal decreased from 68% at 1 mg/L phosphate to 50% at 5 mg/L phosphate. Contrastingly, Qe exhibited a direct correlation (R^2 = 0.959) with phosphate concentration. The lowest Qe value of 6.8 mg/g was observed at 1 mg/L phosphate

which increased linearly in a phosphate concentration-dependent manner and reached a maximum value of 25 mg/g at 5 mg/L phosphate (Figure 4.19 B).

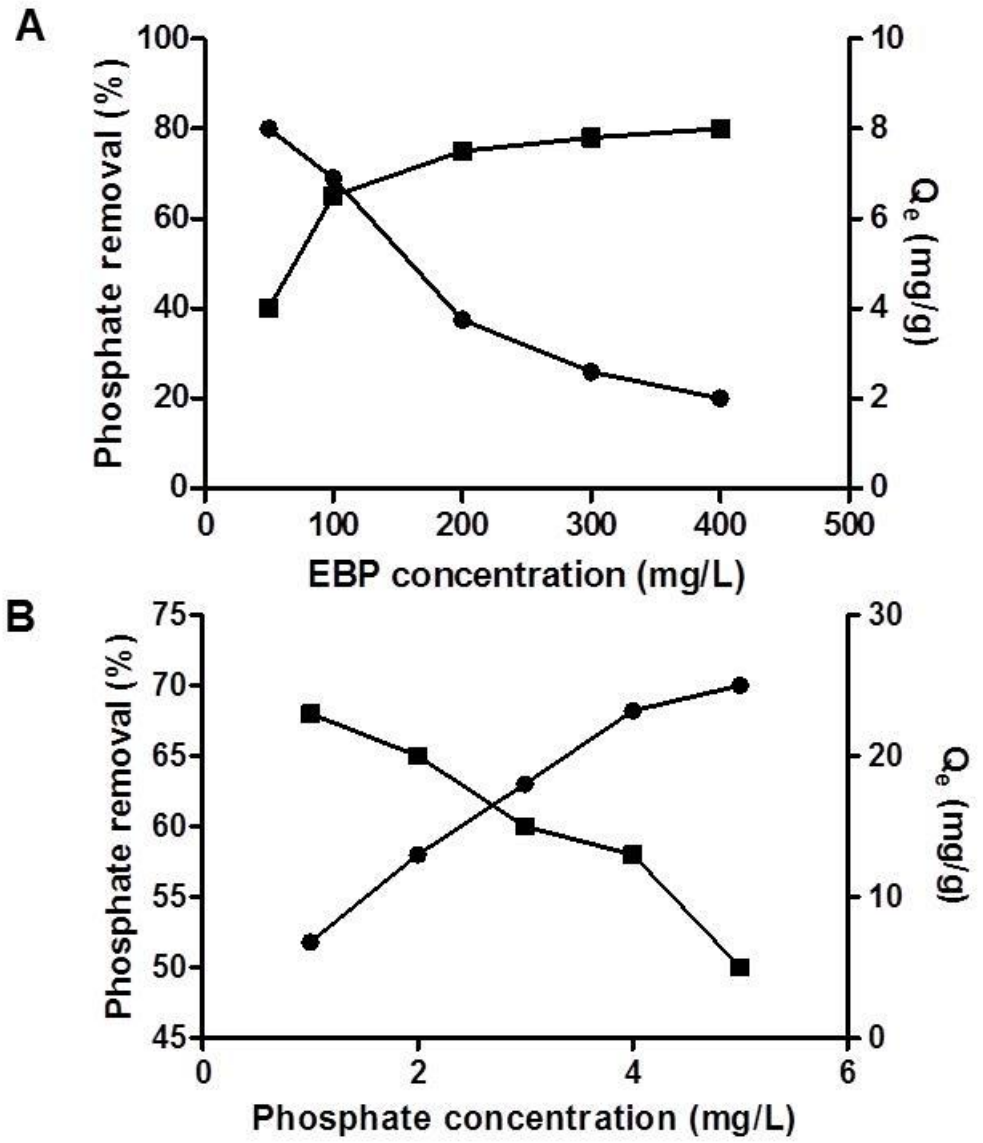

Figure 4.19 Optimization of exobiopolymer and phosphate concentration. (A) Effect of EBP concentration on percentage phosphate removal and sorption efficiency (Qe) at 1 mg/L phosphate concentration and 240 min contact time (B) Effect of phosphate concentration at 100 mg/L of EBP and 240 min of contact time (■-Phosphate removal (%), ●-Qe). Data is mean of three independent experiments run in triplicates.

Isotherm fitting

In order to further understand the nature of phosphate removal by EBP, isotherm equations were fitted to the data. The experimental data showed a good fitting with Freundlich, Langmuir, Temkin, Toth and Sips isotherms as adjudged from a high coefficient of determination (R^2>0.96) for all isotherm equations (Figure 4.20; Table 4.25). Since coefficient of determination was high for all isotherm equations and the best fitting equation could not be determined, the models were compared by error functions. Specifically, the difference between experimental and predicted values for each model was compared by SSE, HYBRID, MPSD and χ^2analysis. The values of all error functions were consistently lower in Langmuir model suggesting that Langmuir model best described phosphate removal by EBP. The models were also compared based on AICc values and the value was observed to be the lowest in Langmuir model which further verified Langmuir as the best-fitting model (Table 4.25).

The separation factor, R_L, is an important extension of the Langmuir model and provides significant cues about the favorable nature of sorbent binding to sorbate. The separation factor is calculated by the equation

$$R_L = \frac{1}{1 + K_L C_0} = \frac{1}{1 + Q_0 b C_0}$$

Where $K_L$is the Langmuir constant (L/mg), Q_0 = maximum monolayer coverage capacity (mg/g), b = Langmuir isotherm constant (L/g) and C_0 is the initial phosphate concentration (mg/L). A value of R_L= 0 indicates irreversible binding while $0<R_L\leq1$ indicates favorable nature of sorbent binding. Substituting the values of Q_0 and b from table 4.25, the value of R_L was calculated to be 0.035. Since the R_L was greater than zero, this indicated the favorable nature of phosphate binding to EBP.

Table 4.25: Adsorption isotherms parameters and correlation coefficients based on experimental data

S. No.	Isotherm	Isotherm equation	Parameter[a]	Value	R^2	*SSE*	*HYBRID*	*MPSD*	χ^2	*AICc*
1	Langmuir	$Q_e = \frac{Q_0 b C_e}{1 + bC_e}$	Q_0	41.29	0.987	2.92	6.15	5.59	0.15	9.87
			B	0.665						
2	Freundlich	$Q_e = K_f C_e^{1/n}$	K_f	15.78	0.961	8.86	13.37	14.05	0.56	15.42
			N	1.765						
3	Temkin	$Q_e = B_T(\ln A_T + \ln C_e)$	B_T	9.262	0.985	3.26	7.46	6.11	0.18	10.42
			A_T	6.251						
4	Toth	$Q_e = \frac{K_t C_e}{(a_t + C_e)^{1/t}}$	K_t	0.481	0.988	3.02	10.99	8.19	0.17	32.07
			a_t	1.408						
			T	0.0115						
5	Sips	$Q_e = \frac{K_s C_e^{t_s}}{(1 + a_s C_e^t)}$	K_s	79.8	0.970	15.97	13.23	12.06	0.58	40.39
			a_s	0.206						
			t_s	0.858						

[a] Q_e=Adsorption capacity (mg/g), Q_0 = Maximum monolayer coverage capacity (mg/g), B = Langmuir isotherm constant, C_e = Equilibrium concentration, K_f=Freundlich constant related to adsorption capacity, n = Freundlich constant related to adsorption intensity, B_T = Temkinisotherm constant, A_T = Temkin isotherm equilibrium binding constant (L/g), K_t = Toth isotherm constant (mg/g), a_t = Toth isotherm constant (L/mg), t = Toth isotherm dimensionless constant, K_s = Sips isotherm model constant (L/g), a_s = Sips isotherm model constant, t_s = Sips isotherm model exponent, AICc = Corrected Akaike's information criterion, HYBRID = Hybrid fractional error function, MPSD = Marquardt's percent standard deviation, SSE = Sum squares error, $\chi 2$ = Non-linear Chi-square analysis

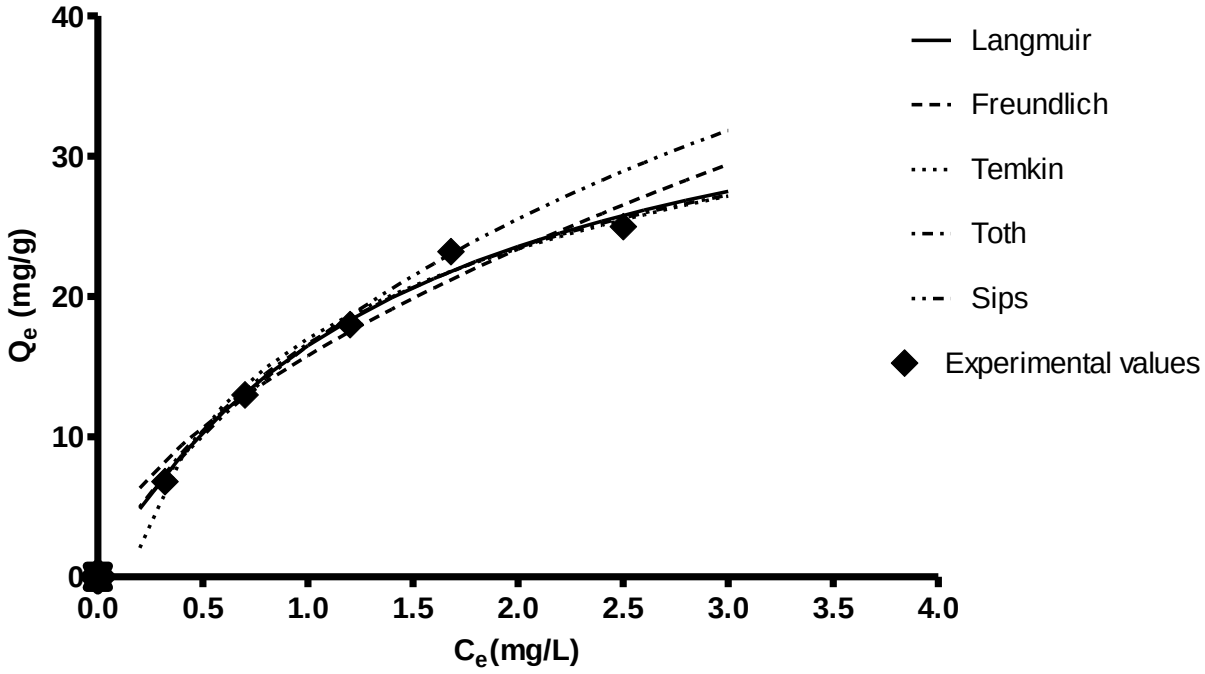

Figure 4.20 Sorption isotherm of 1-5 mg/L phosphate at 100 mg/L EBP and 240 min contact time. Data is mean of three independent experiments run in triplicates. Error bars are not shown for clarity; SD was less than 10% of mean at all concentrations.

4.2.8 Mechanism of exobiopolymer-phosphate interactions

The mechanism of exobiopolymer-phosphate interactions governing phosphate removal was determined by a combination of spectroscopic and physicochemical methods. The interacting functional groups were identified by potentiometric titrations, pH-dependent binding, FTIR spectroscopy and chemical modification of EBP. The biochemical fractions interacting with phosphate were identified by selective degradation of major fractions by enzymatic hydrolysis.

Phosphate distribution on EBP

The spatial distribution of phosphate on EBP was determined by elemental mapping using EDS. The EDS spectrum revealed carbon, nitrogen and oxygen were the major elements in unbound

EBP. Following phosphate binding, the peak for phosphorus also appeared in the EDS spectrum along with peaks for carbon, nitrogen and oxygen. Elemental mapping of phosphate-bound EBP revealed that signals for the detected elements were uniformly distributed throughout the scanned area. Further, no regions of high phosphate density were observed suggesting that phosphate binding was uniform throughout EBP (Figure 4.21).

X-Ray Diffraction spectroscopy

The X-ray diffraction (XRD) spectrum of unbound and phosphate-bound EBP was compared to determine if complex formation or precipitation of phosphate salts occurred. XRD spectrum of unbound EBP contained several broad peaks indicating the amorphous nature of EBP. The peaks were further broadened in the phosphate-bound EBP indicating an increase in amorphous nature. Further, no peaks characteristic of a phosphate complex formation or precipitate/crystal formation were observed (Figure 4.22).

Surface charge

Zeta potential is an indicator of the surface charge of a particle or molecule and is influenced by several factors such as pH, sorption, etc. Further, the changes in zeta potential following sorption of sorbate can provide valuable information on the nature of interaction. Therefore, zeta potentials of unbound and phosphate-bound EBP were compared. The unbound EBP was found to be a near-neutral polymer with zeta potential of unbound -2.98 mV. However, following phosphate binding, the surface charge of EBP shifted slightly towards negative as evident from a reduction in zeta potential to -3.11 mV.

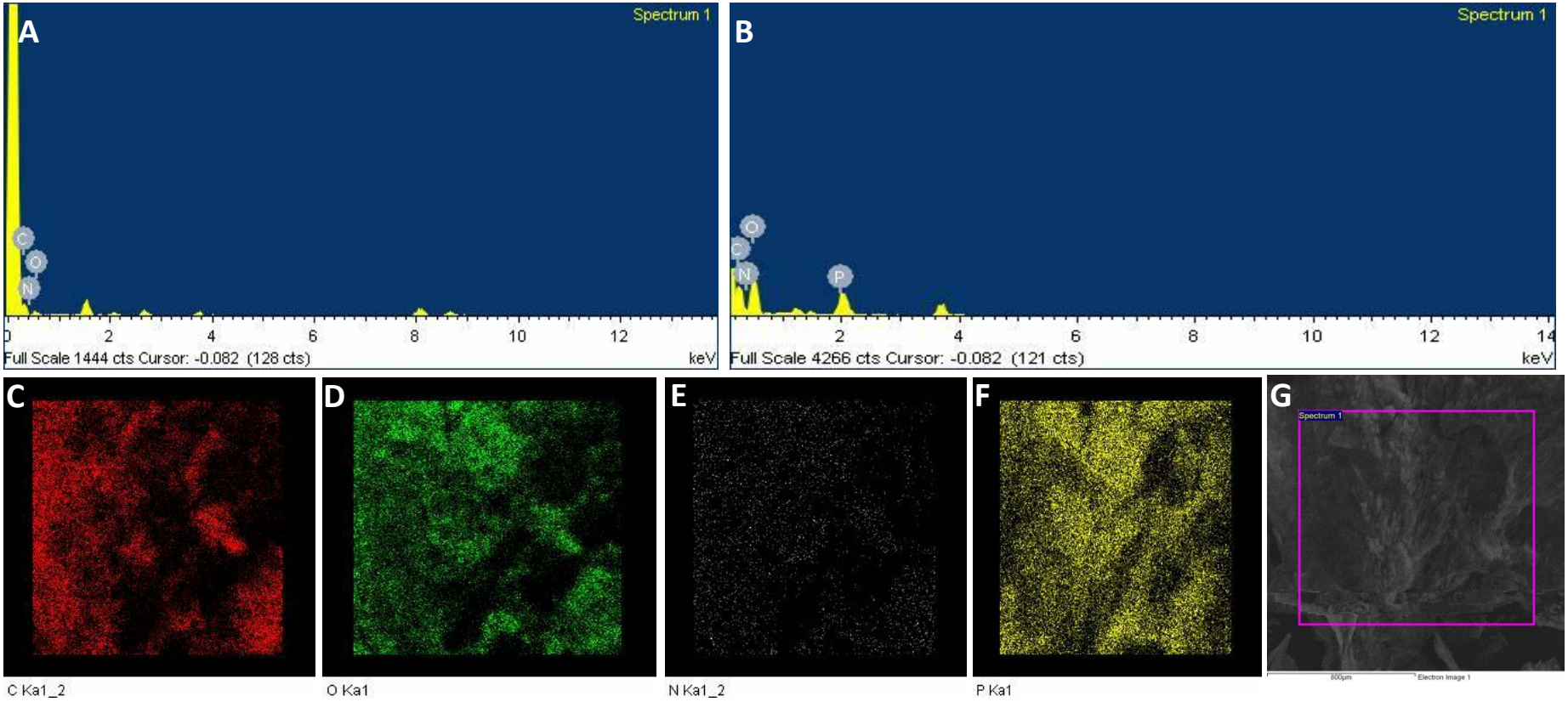

Figure 4.21 SEM-EDS spectra of unbound phosphate-bound exobiopolymer. (A) shows EDS spectrum of unbound EBP and (B) shows EDS spectrum of phosphate-bound EBP. (C-F) show elemental mapping of carbon (C), oxygen (D), nitrogen (E) and phosphorus (F). (G) shows the SEM image of EBP area scanned for elemental analysis.

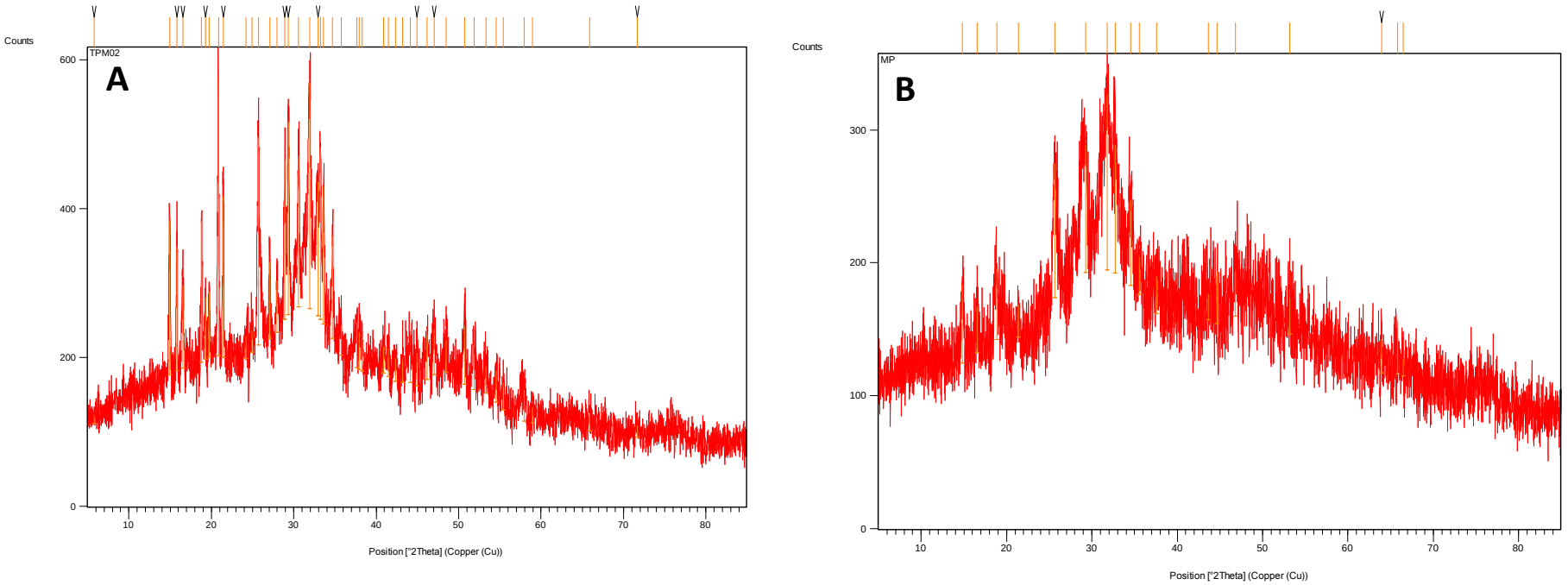

Figure 4.22 X-ray diffraction spectra of unbound (A) and phosphate-bound (B) exobiopolymer.

Functional group analysis by potentiometric titrations

Potentiometric titrations provide useful information on the nature and density of functional groups present in EBP. This information is helpful in predicting the compounds that may interact with EBP, their nature of interaction as well as pH-dependent behavior of EBP. The pH of EBP solution was adjusted to 3 and then titrated with sodium hydroxide. The titration curve is shown in figure 4.23. The pKa and site concentrations were calculated by applying diffusion layer model. The data fitted into a two-site model with pKa 3.63 and 8.61 with associated site densities of 6.61 and 8.32 mol/kg, respectively. Comparative analysis of pKa values with reported values suggest that the buffering zones corresponding to pKa 3.63 and 8.61 could be assigned to carboxylic and amino/alcohol groups, respectively (Guine et al., 2006).

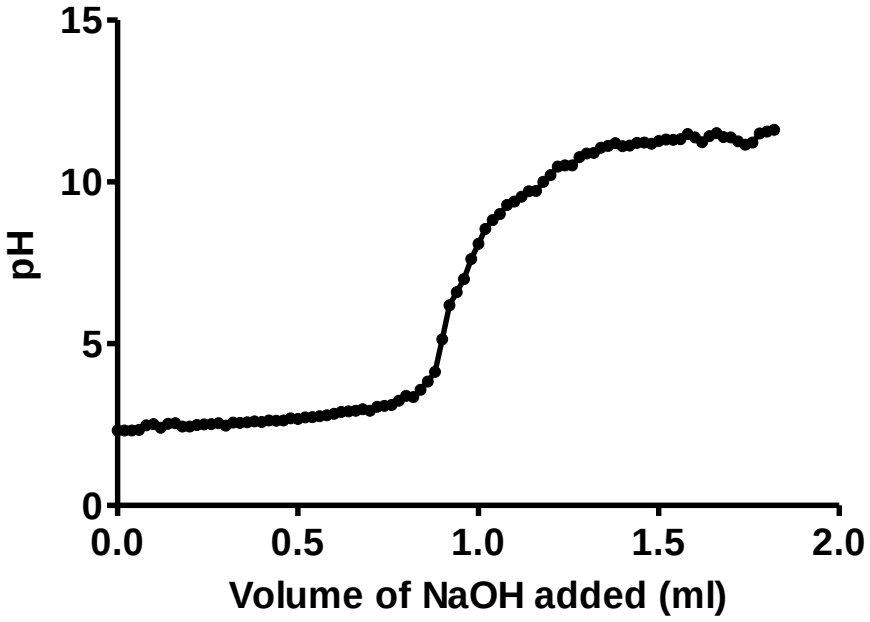

Figure 4.23 Potentiometric titration plot of exobiopolymer.

Effect of pH on phosphate binding by exobiopolymer

The pH of solution is an important factor which can influence dissociation and ionization of

functional groups of the sorbate as well as the sorbent and hence, modulate phosphate binding to EBP. Therefore, the effect of pH on phosphate removal by EBP was determined.

The percent phosphate removal and Qe was found to be the highest at pH 3 over a pH range of 3 to 10. The percent phosphate removal was close to 100%, with a Qe of approximately 10, at pH 3. The percent phosphate removal and Qe decreased with increase in pH and reached the lowest values at pH 10. The values of both parameters at pH 10 were almost half of that observed at pH 3 (Figure 4.24).

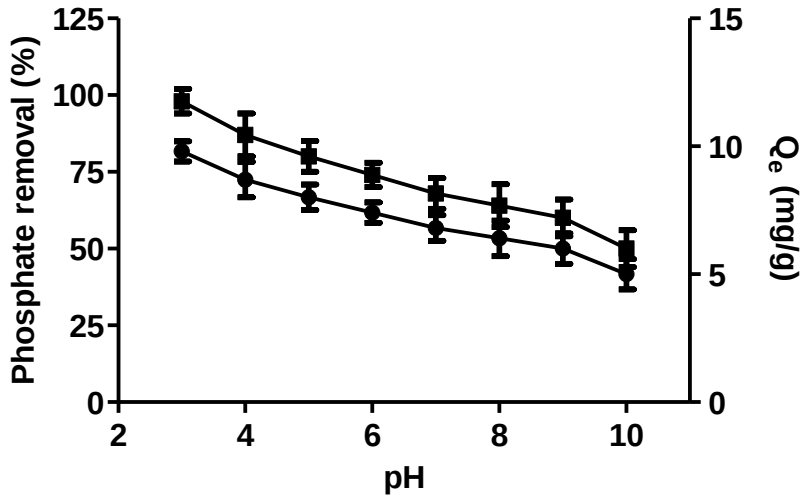

Figure 4.24 Graph of effect of pH on phosphate binding by exobiopolymer of *A. haemolyticus* MG606 (■- Phosphate removal (%), ●- Qe)

Effect of enzyme treatment

The role of polysaccharides and proteins in phosphate removal was determined by treatment of EBP with hydrolytic enzymes. Specifically, EBP was treated with an amylolytic and a proteolytic enzyme mixture, either separately or in tandem, and phosphate removal was determined in the hydrolyzed EBP.

The percent phosphate removal and Qe were reduced by 8-10% following treatment of EBP with

proteolytic enzyme mixture and the reduction was found to be statistically significant ($p<0.01$). On the other hand, the reduction in percent phosphate removal and Qe was relatively more pronounced following treatment of EBP with amylolytic enzyme mixture. Both parameters of phosphate removal were reduced to half ($p<0.001$) compared to untreated EBP (Figure 4.25).

EBP was also treated with both enzyme mixtures in tandem and phosphate removal was determined. The percent phosphate removal and Qe values were significantly ($p<.001$) lower in EBP treated with both enzyme mixtures compared to corresponding values in control EBP as well as EBP treated with both enzyme mixtures separately. Further, reduction in percent phosphate removal and Qe appeared to be the sum of reductions observed in EBPs treated with both enzyme mixtures separately (Figure 4.25).

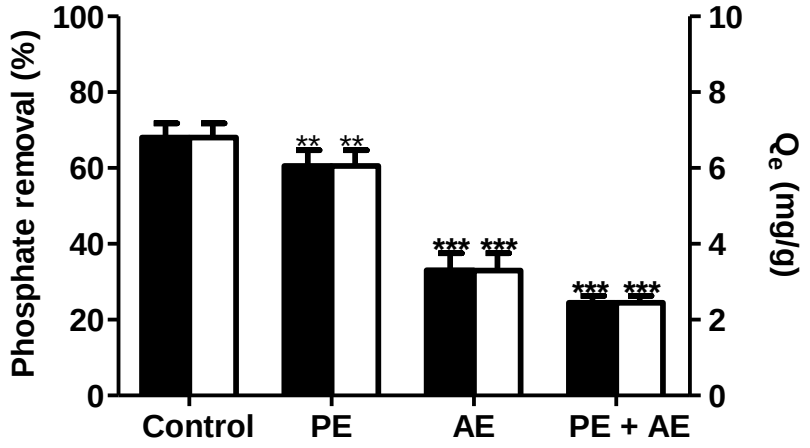

Figure 4.25 Graph of effect of enzyme treatment on phosphate binding (■- Phosphate removal, □- Qe), Data is mean of three independent experiments run in triplicates. **p<0.01, ***p<0.001 w.r.t. control. PE = Proteolytic enzyme, AE = Amylolytic enzyme

Effect of chemical treatment

The role of specific functional groups in phosphate removal was ascertained by chemical modifications of amino, amide and carboxyl groups by glutaraldehyde, formaldehyde and

methanol, respectively. The chemical modifications rendered the functional groups incompetent to bind phosphate and hence, the reduction in phosphate removal provided cues on the relative roles of different functional groups in binding phosphate.

The reductive alkylation of amino groups with glutaraldehyde resulted in approximately two-third reduction in phosphate binding. Contrastingly, methanol esterification of carboxyl groups and formaldehyde alkylation of amide groups resulted in approximately 10% and <10% reduction in phosphate removal, respectively, compared to untreated, control EBP (Figure 4.26).

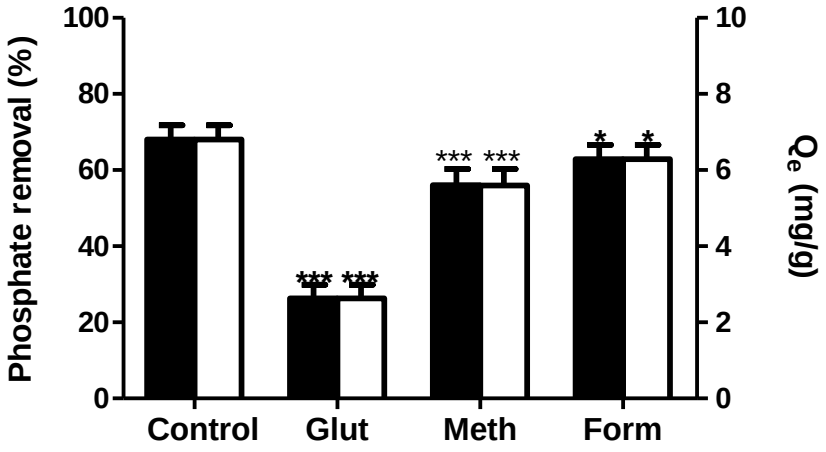

Figure 4.26 Graph of effect of chemical treatment on phosphate binding, (■- Phosphate removal, □- Qe), Data is mean of three independent experiments run in triplicates. **p<0.01, ***p<0.001 w.r.t. control. Glut=Glutaraldehyde, Meth=Methanol, Form=Formaldehyde

Fourier transform infrared spectroscpy

FTIR analysis of EBP revealed presence of a broad peak characteristic of stretching vibration of hydroxyl (O-H) and amino (N-H) groups at 3408 cm^{-1}. The peak at 1650 cm^{-1} represents N-H bending of primary amines while the peak at 1421 cm^{-1}represents C-N stretching of amines. The peak at 1032 cm^{-1} was attributed to CO ether linkage of sugars while the peak at 875 cm^{-1}

indicated presence of beta glycosidic linkage in EBP. The FTIR spectrum of phosphate-bound EBP was compared with the spectrum of unbound EBP. The comparative analysis of FTIR spectrums revealed that phosphate binding resulted in changes in peak intensities, wavenumbers and appearance of phosphate peaks. The most prominent feature was suppression of O-H and N-H stretching, N-H bending and C-N stretching peaks along with shifting of these peaks to higher wavenumbers. Further, phosphate-bound EBP exhibited additional peaks for phosphate groups which were not observed in unbound EBP. These additional peaks were attributed to P=O stretching (1107 cm^{-1}), P-O stretching (922 cm^{-1}), O-H stretching of phosphonic acids (2739 cm^{-1} and 2400 cm^{-1}) and O-H deformation (1302 cm^{-1}). The peaks for CO ether and beta glycosidic linkages were not discernible in the phosphate-bound EBP due to overlapping with P=O and P-O stretching peaks (Figure 4.27).

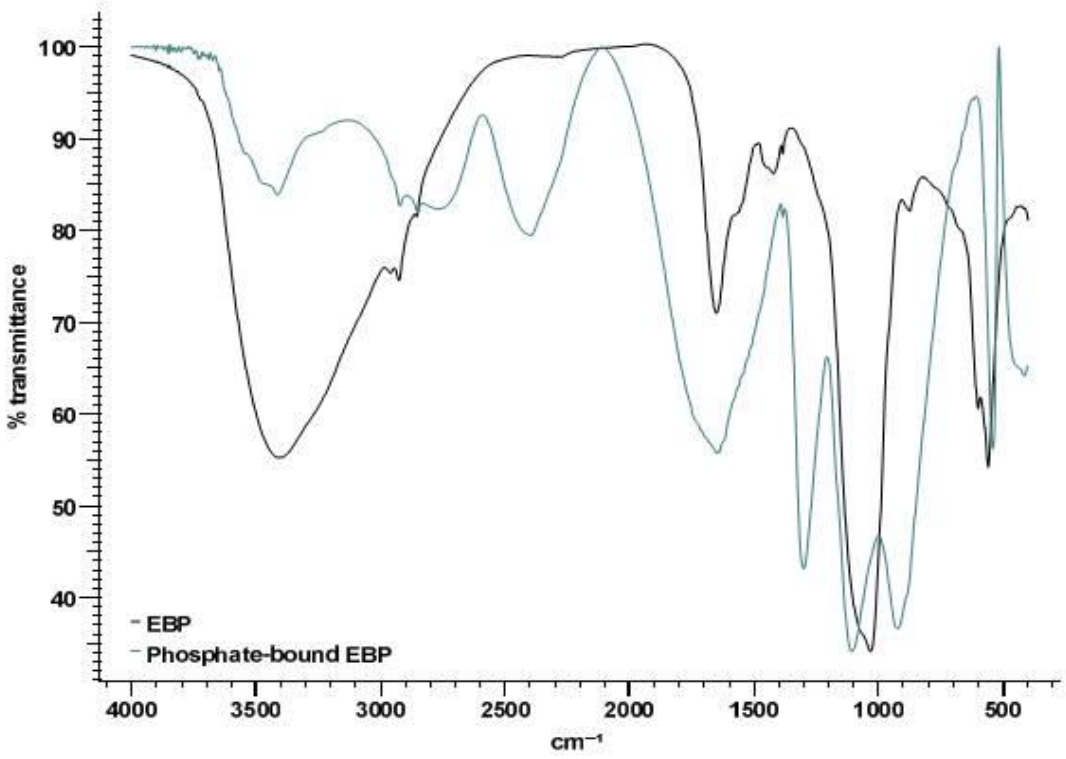

Figure 4.27 Fourier transform infrared spectra of unbound and phosphate-bound EBP.

Effect of competing anions

The selectivity and reversibility of EBP-phosphate interactions was determined by displacement of EBP-bound phosphate in presence of competing anions. Specifically, the effect of chloride, nitrate and sulfate on phosphate displacement was determined.

None of the three competing anions displaced EBP-bound phosphate at concentrations 10-fold higher than phosphate. A further increase in anion concentration to 50-fold higher than phosphate resulted in no detectable displacement in presence of chloride and nitrate while approximately 10% displacement ($p<0.001$) was observed in presence of sulfate. A further increase in anion concentration to 100-fold higher than phosphate resulted in significant displacement with all anions (Figure 4.28).

4.3 Optimization of culture conditions for maximum exobiopolymer production

4.3.1 Shake flask studies

The effect of various physical conditions such as temperature, pH, inoculum size and agitation speed as well as nutritional sources (carbon and nitrogen sources) and their concentrations were evaluated for EBP production by *A. haemolyticus* MG606 in shake flasks.

Temperature

Temperature plays an important role in EBP production and growth of bacteria. Therefore, to determine the effect of temperature on EBP yield and biomass production, *A. haemolyticus* MG606 was grown in EBP production medium at 20-45°C for 48 h. A temperature-dependent increase in EBP yield and biomass was observed from 20 to 30°C followed by a decrease in EBP production at higher temperatures. The optimal temperature for EBP and biomass production was 30°C at which maximum EBP yield and biomass production was observed (Figure 4.29A).

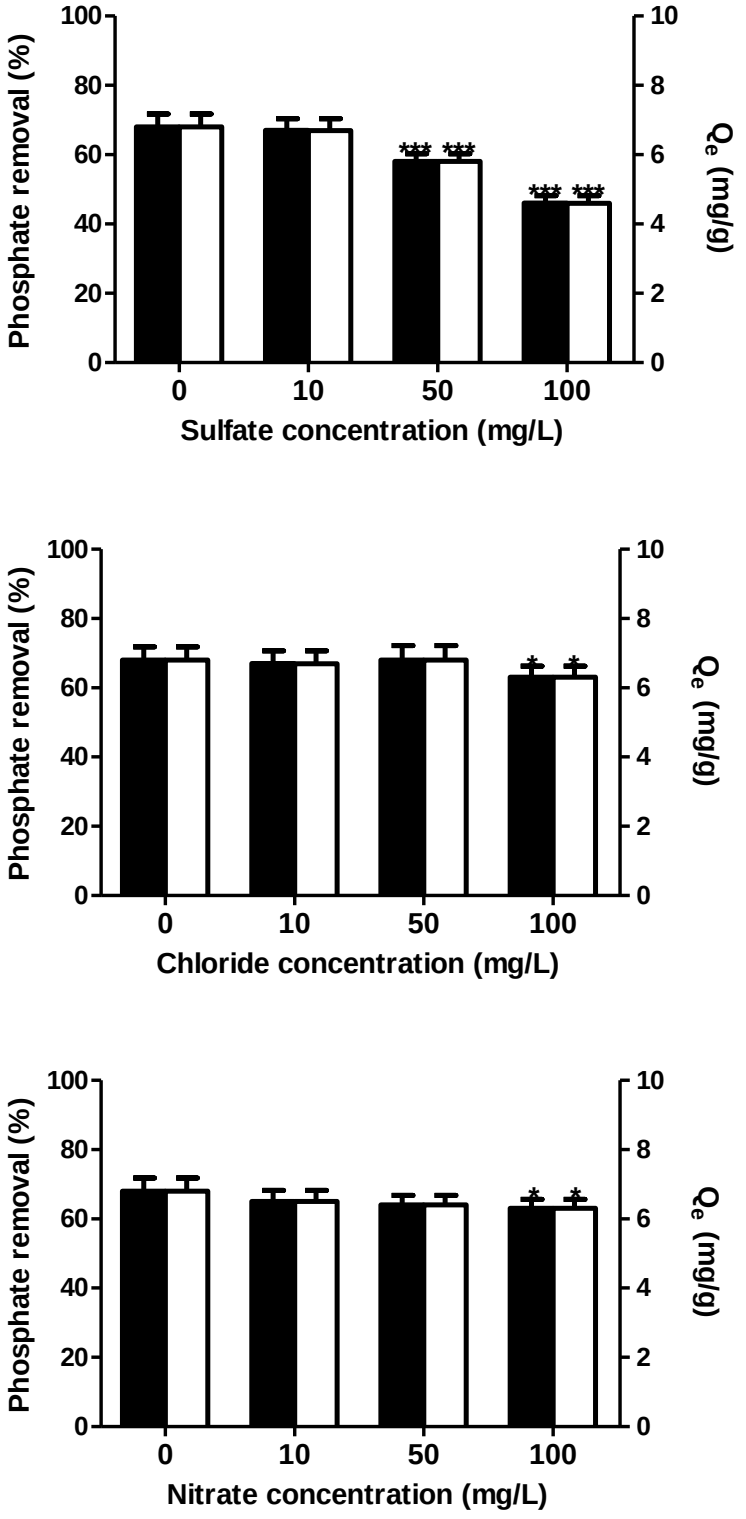

Figure 4.28 Effect of competing anions Sulfate (A), chloride (B) and nitrate (C), on phosphate binding. (■- Phosphate removal, □- Qe), Data is mean of three independent experiments run in triplicates.*p<0.05, ***p<0.001 w.r.t. control

pH

pH of culture medium is another important factor which can influence bacterial growth and metabolic processes. Hence, to determine the effect of pH, *A. haemolyticus* MG606 was grown in EBP production medium adjusted to pH 5 to 9. Following 48 h of incubation at 30°C, EBP yield and biomass was determined. A pH-dependent increase in EBP yield and biomass was observed with increase in pH from 5 to 6.5. However, a further increase in pH resulted in a pH-dependent decrease in EBP yield and biomass formation *A. haemolyticus* MG606 and reached the lowest at pH 9. The optimal pH for maximum EBP yield and biomass production was found to be 6.5 (Figure 4.29B).

Inoculum size

The inoculum size is an important consideration in microbial metabolite production since a high inoculum size will divert the metabolic flux towards biomass formation while a small inoculum size will result in slow growth and lower metabolite production. Therefore, to determine the effect of inoculums size on EBP yield and biomass, *A. haemolyticus* MG606 was inoculated in EBP production medium with 0.5-5% inoculum size and incubated for 48 h. The EBP yield was the highest at 1% inoculum size and decreased with a further increase in inoculum size. Contrastingly, the highest biomass production was observed at 2% inoculum size and then decreased with an increase in inoculums size. The optimal inoculum size for maximum EBP yield was found to be 1% (Figure 4.29C).

Agitation speed

An appropriate agitation is required for proper mixing and aeration in the culture medium. To elucidate effect of agitation speed, *A. haemolyticus* MG606 was grown in EBP production medium for 48 hours with agitation speed ranging from 40 rpm to 240 rpm. EBP yield increased

with an increase in agitation speed from 40 to 120 rpm and decreased with a further increase in agitation. A similar trend was also observed in biomass production however, maximum biomass was obtained at 160 rpm. Further, biomass production was marginally decreased with increase in agitation speed beyond 160 rpm while the decrease in EBP yield was more pronounced at higher agitation speeds. The optimal agitation speed for maximum EBP yield was found to be 120 rpm (Figure 4.29D).

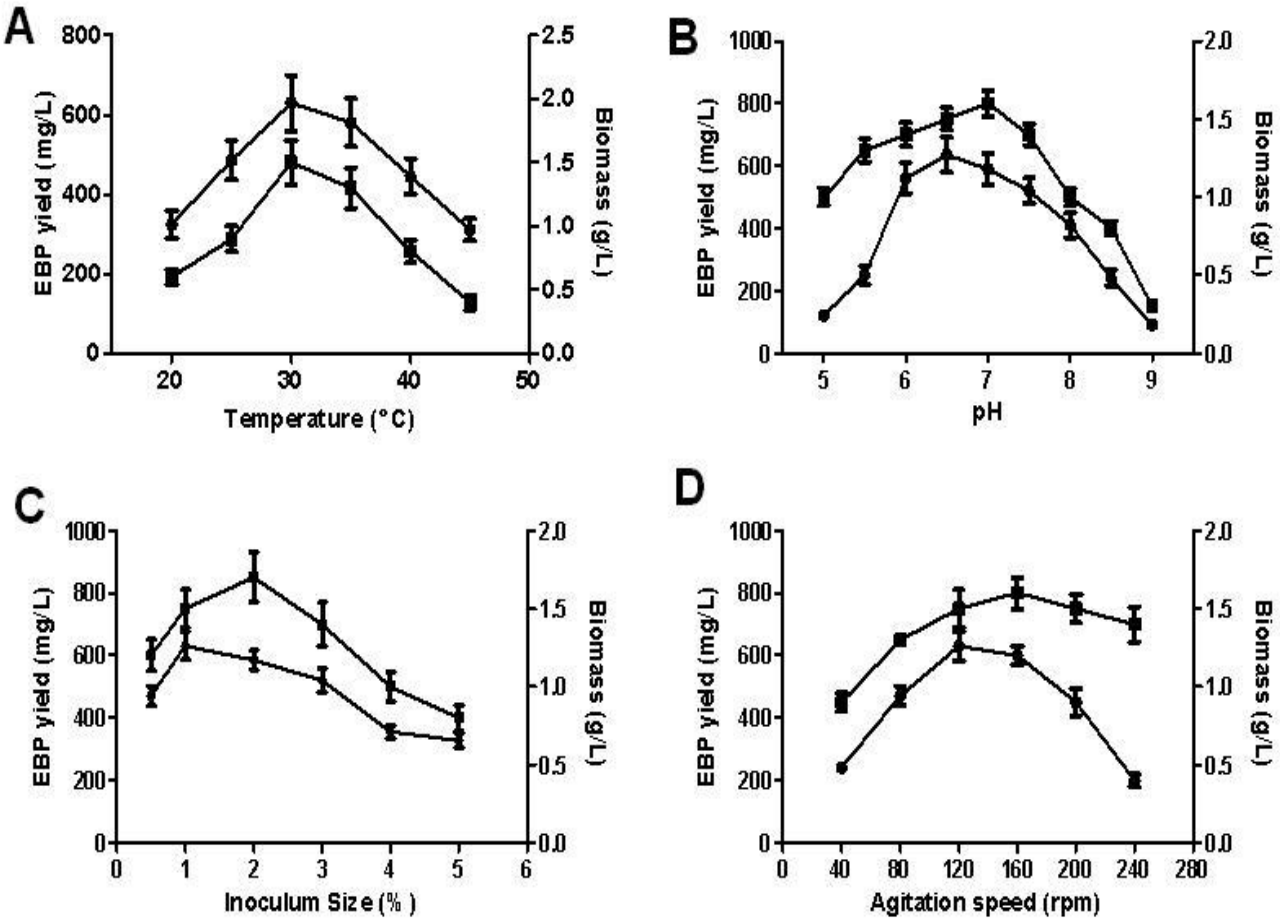

Figure 4.29: Effect of temperature (A), pH (B), inoculum size (C) and agitation speed (D) on exobiopolymer production.

Data is mean±SD of triplicate samples.

Carbon sources

A. haemolyticus MG606 was grown in EBP production medium supplemented with different carbon sources at 0.5 to 2 g/L. EBP was extracted and purified after 48 hours of incubation. The EBP yield was highest in glucose and was followed by raffinose, maltose and acetate; however, EBP yield was approximately 80% higher in glucose than in the latter three carbon sources. The EBP yield was even lower in other sugars, pyruvate and ethanol as carbon sources. No EBP production was observed with succinate, malate, aspartate, glutamate and butanol since these carbon sources did not support bacterial growth. EBP yield was observed to be concentration-dependent in all carbon sources which supported EBP production; nonetheless, the biopolymer yield was highest in glucose. In case of glucose, EBP yield increased with increase in glucose concentration from 1 g/L to 2 g/L but the difference in yield was marginal (Table 4.26). Therefore, 1 g/L was considered an optimal concentration for glucose as sole carbon source.

In order to study the effect of combination of carbon sources, the culture medium was supplemented with 1:1 combination of carbon sources (0.5 g/L of each carbon source) and EBP yield was determined after 48 h. The EBP yield was highest in presence of glucose-acetate combination compared to other combinations. The EBP yield in presence of glucose-acetate combination was significantly higher ($p<0.05$) compared to glucose and acetate as sole carbon sources at 1 g/L. A closer examination of EBP yield revealed that EBP yield in presence of glucose-acetate combination was higher compared to the additive EBP yield in presence of 0.5 g/L glucose and acetate alone. This suggested a synergistic effect of the combination on EBP production (Table 4.27). Several cheap nutritional sources were also investigated as potential carbon sources for EBP production. EBP yield in all cases was found to be lower than glucose alone and glucose-acetate combination (Table 4.28).

Table 4.26: Effect of carbon sources and their concentration on exobiopolymer yield

Carbon source	Concentration (g/L)		
	0.5	1	2
Glucose	420 ± 20	632 ± 25.9	680 ± 39.7
Galactose	120 ± 15.2	238 ± 12.5	267 ± 21.4
Mannitol	102 ± 12.5	184 ± 15	210 ± 18.5
Pyruvate	86 ± 5.7	92 ± 9.6	75 ± 10.2
Ethanol	169 ± 14.4	146 ± 7.9	105 ± 9.8
Acetate	229 ± 13.8	353 ± 21.7	487 ± 19.6
Fructose	128 ± 17.5	251 ± 23.1	389 ± 25.3
Maltose	202 ± 18.9	355 ± 29.6	410 ± 25.8
Sucrose	175 ± 14.9	233 ± 27.5	344 ± 22.9
Lactose	56 ± 8.4	107 ± 9.7	134 ± 12.1
Mannose	211 ± 20.3	307 ± 32.3	379 ± 21.9
Xylose	164 ± 10.6	284 ± 15.5	354 ± 14.3
Raffinose	176 ± 12.9	367 ± 17.8	455 ± 22.8
Succinate	0	0	0
Malate	0	0	0
Aspartate	0	0	0
Glutamate	0	0	0
Butanol	0	0	0

Table 4.27 Yield of exobiopolymer with combination of two carbon sources.

Carbon source	EBP yield (mg/L)
Glucose + Galactose	425 ± 21.2
Glucose + Mannitol	258 ± 12.3
Glucose + Acetate	752 ± 32.1
Glucose + Ethanol	158 ± 10.4
Glucose + Pyruvate	125 ± 9.8
Glucose + Glutamate	150 ± 12.8

Data is mean of triplicate samples.

Table 4.28 Yield of exobiopolymer with cheap carbon sources.

Carbon source	EBP yield (mg/L)
Sugarcane molasses	212 ± 18.3
Sugarcane juice	250 ± 12.6
Wheat flour	268 ± 15.4
Wheat bran	187 ± 16.5
Corn flour	257 ± 20.2
Corn bran	167 ± 13.5
Corn cob	120 ± 10.2

Data is mean of triplicate samples.

Nitrogen source

A. haemolyticus MG606 was grown in EBP production medium supplemented with different nitrogen sources at 2 g/L. EBP was extracted and purified after 48 h of incubation. The EBP yield was highest in presence of ammonium sulfate. The next higher EBP yield was obtained with ammonium chloride and peptone as nitrogen sources however, the EBP yield was significantly ($p<0.05$) lower in presence of ammonium chloride and peptone compared to ammonium sulfate (Table 4.29).

Table 4.29: Effect of nitrogen sources on exobiopolymer yield

Nitrogen source	Concentration (g/L)		
	1	**2**	**5**
Ammonium chloride	248 ± 16.3	450 ± 22.1	232 ± 13.7
Ammonium sulfate	567 ± 25.4	610 ± 22.5	212 ± 11.9
Ammonium phosphate	102 ± 14.2	233 ± 12	110 ± 12.6
Peptone	435 ± 24.2	512 ± 18.6	590 ± 23.7
Soyapeptone	156 ± 14.2	212 ± 10.9	304 ± 14.5
Tryptone	176 ± 9.4	265 ± 19.5	329 ± 30.2
Beef extract	189 ± 17.1	212 ± 12.4	264 ± 21.1

EBP yield in presence of combination of nitrogen sources exhibited no enhancement in comparison to ammonium sulfate alone (Table 4.30.). The effect observed was additive in nature.

Table 4.30: Effect of combination of nitrogen sources on EBP yield

Nitrogen sources	EBP yield (mg/L)
Ammonium chloride + Ammonium sulfate	470 ± 16.9
Ammonium sulfate + Ammonium phosphate	390 ± 28.3
Ammonium chloride + Ammonium phosphate	295 ± 10.7

4.3.2 Scale-up of exobiopolymer production to bioreactor scale

Based on the results of preliminary screening in shake flask, glucose, acetate and nitrogen source ammonium sulfate was selected as the main parameters for optimization during scale-up. These carbon and nitrogen sources were added at different concentrations in EBP production medium and a regression model was constructed to calculate the optimal level of glucose, acetate and ammonium sulfate.

Optimization of carbon and nitrogen source concentrations by response surface methodology

The optimum concentration of glucose, sodium acetate and ammonium sulfate as well as the interaction between these variables was determined using central composite design (CCD) of response surface methodology (RSM). The experimental results of each independent variable are listed in Table 4.31.

Statistical significance of all analysis was done by analysis of variance (ANOVA) and Fisher's F test and student *t*-test statistical tools were used to analyze the effects. Values Prob>F indicates

significant model terms having values less than 0.05 and coefficients A, B, C, AC, BC, A^2, B^2 and C^2 were found to be significant model terms. Based on the experimental data, predicted values were obtained from second order polynomial equation (Table 4.32). The equation for the model in terms of coded factors is represented below

EBP yield (mg/L) = +729.41 + 93.72*A + 65.90*B - 125.16*C - 26.36*AB - 66.31*AC - 28.59*BC - 104.83*A^2- 72.91*B^2 - 35.09*C^2

The model showed a good fit as indicated by F value of 58.06. Predicted R^2 value of 0.8562 was in close agreement with adjusted R^2 value of 0.9643 and their values close to 1 correlates predicted and experimental values. The adequate precision values measured by signal to noise ratio was observed to be 23.780 which is greater than four. This ratio indicates the adequate signal i.e the quadratic equation can be used within the range of factors in the design space. CV i.e coefficient of variance was observed to be 6.13 (represented as %) indicates the model can be reproduced as its value was less than 10%. This low CV value indicated the reliability and good precision of the experiments (Table 4.33).

EBP yield was greatly affected by interactions among significant variables. It was observed that the optimal values for glucose and acetate lied between the concentration ranges of 3.8 g/L to 6 g/L and 4 g/L to 6 g/L respectively with the ammonium sulfate concentration range of 0.1 to 0.5 g/L. The interactions among these variables are shown in figure 4.30. Further validation was carried out by doing number of experiments with in the range of tested variables which further confirms suitability of model. The predicted results were verified with experimental results and the highest EBP yield of 930 mg/L was observed at 5.454 g/L glucose, 4.506 g/L sodium acetate and 0.358 g/L ammonium sulfate concentration in media.

Table 4.31: Experimental variables and results for exobiopolymer production in terms of coded values

Run	A: Glucose (g/L)	B: Acetate (g/L)	C: Ammonium sulfate (g/L)	EBP yield (mg/L)
1	0.000	0.000	0.000	710.45
2	0.000	0.000	0.000	730.82
3	1.000	-1.000	1.000	450.2
4	-1.000	-1.000	-1.000	400.2
5	1.000	1.000	-1.000	900.1
6	0.000	0.000	0.000	743.6
7	-1.682	0.000	0.000	251.1
8	0.000	1.682	0.000	632
9	-1.000	-1.000	1.000	280.1
10	0.000	0.000	0.000	740
11	0.000	0.000	1.682	400.4
12	-1.000	1.000	1.000	470.7
13	0.000	0.000	0.000	755
14	1.682	0.000	0.000	578
15	-1.000	1.000	-1.000	570.2
16	1.000	1.000	1.000	400.4
17	1.000	-1.000	-1.000	700.6
18	0.000	-1.682	0.000	400.3
19	0.000	0.000	0.000	700
20	0.000	0.000	-1.682	840.2

Table 4.32: Statistical analysis showing ANOVA for EBP production by *A. haemolyticus* MG606 for three independent variables.

	Sum of		Mean	F	p-value	
Source	**Squares**	**df**	**Square**	**Value**	**Prob> F**	
Model	667800	9	74198.44	58.06	< 0.0001	Significant
A-Glucose	119900	1	119900	93.86	< 0.0001	
B-Acetate	59307.11	1	59307.11	46.41	< 0.0001	
C-Ammonium sulfate	214000	1	214000	167.43	< 0.0001	
AB	5559.85	1	5559.85	4.35	0.0636	
AC	35178.78	1	35178.78	27.53	0.0004	
BC	6537.96	1	6537.96	5.12	0.0472	
A^2	167600	1	167600	131.13	< 0.0001	
B^2	74522.83	1	74522.83	58.32	< 0.0001	
C^2	17742.78	1	17742.78	13.88	0.0039	

Table 4.33: Model statistics

Std. Dev.	35.75	R-Squared	0.9812
Mean	582.72	Adj R-Squared	0.9643
C.V. %	6.13	Pred R-Squared	0.8562
PRESS	97848.81	Adeq Precision	23.780

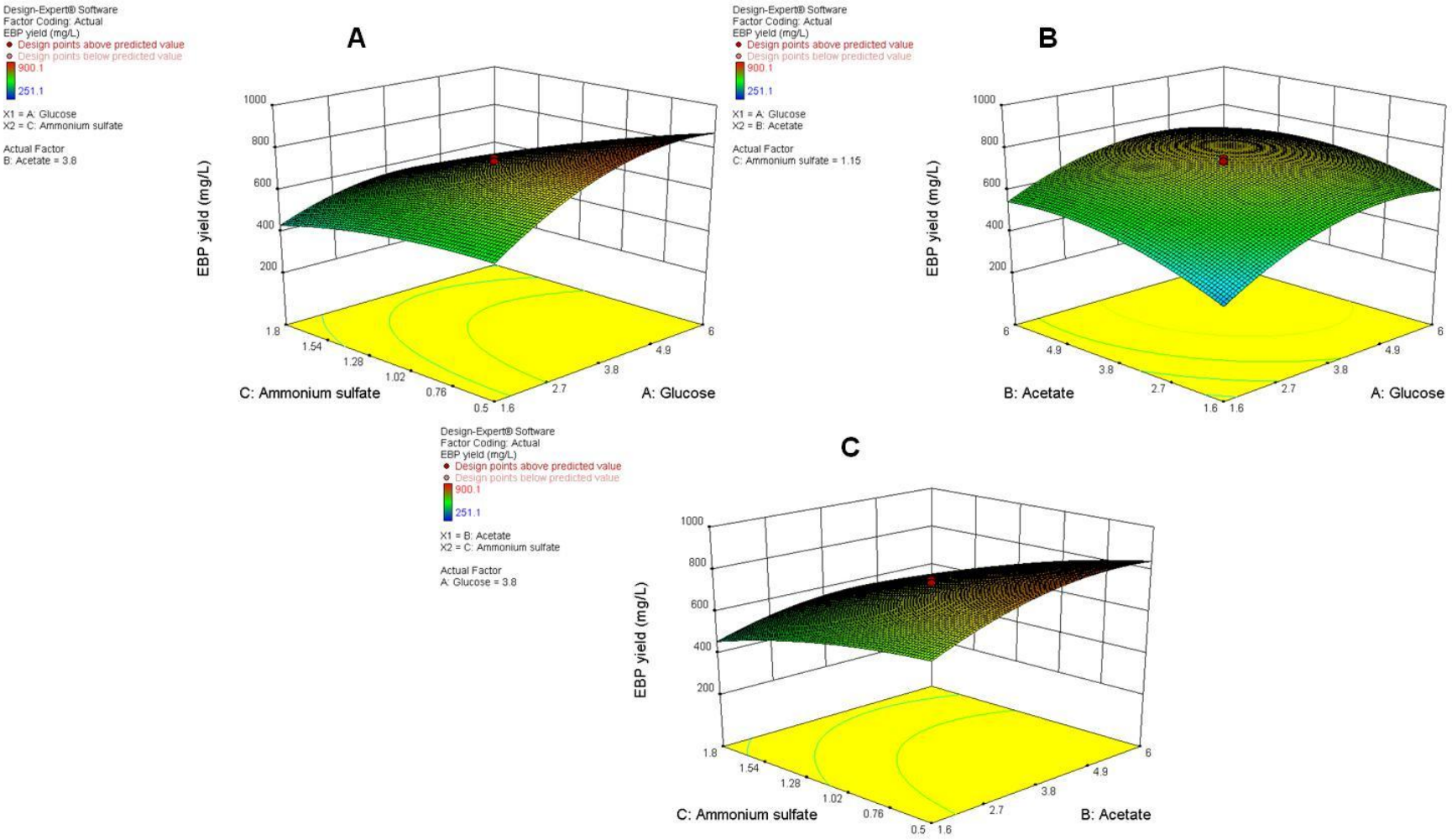

Figure 4.30 3D surface plot showing interaction (A) glucose and ammonium sulfate, (B) glucose and acetate, (C) acetate and ammonium sulfate.

Kinetic modeling of biomass and EBP production

A. haemolyticus MG606 was grown in medium with optimized glucose, sodium acetate and ammonium sulfate concentrations. The biomass production and EBP yield was fitted into Logistic and Leudeking-Piret model and the model parameters were calculated and tabulated in table 4.34 below. The models were fitted very well to the experimental data as indicated by R^2 value. Maximum specific growth rate (μ_m) was evaluated from Logistic model and it was found to be 0.35 h^{-1}. The EBP production was predicted based on model parameters listed and compared with experimental results. The predicted values agreed well with experimental values (R^2 = 0.991) as shown in figure 4.31. Based on the results, it was observed that EBP production from *A. haemolyticus* MG606 was partially growth associated as indicated by the positive α value and most of the EBP produced during stationary phase of bacteria.

Table 4.34 Estimation of model parameters from experimental data

Kinetic parameters	
μ_0	0.08
μ_m	0.35
X_0	20
X_m	2780
α	0.12
β	0.007
R^2	0.991

μ_0 = Initial specific growth rate (h^{-1}); μ_m = Maximum specific growth rate (h^{-1}); X_0 = Initial biomass concentration (mg/L); X_m = maximum biomass concentration (mg/L); α = growth associated constant in rate of product formation (mg/mg); β = Non- growth associated constant in rate of product formation (mg/mg.h)

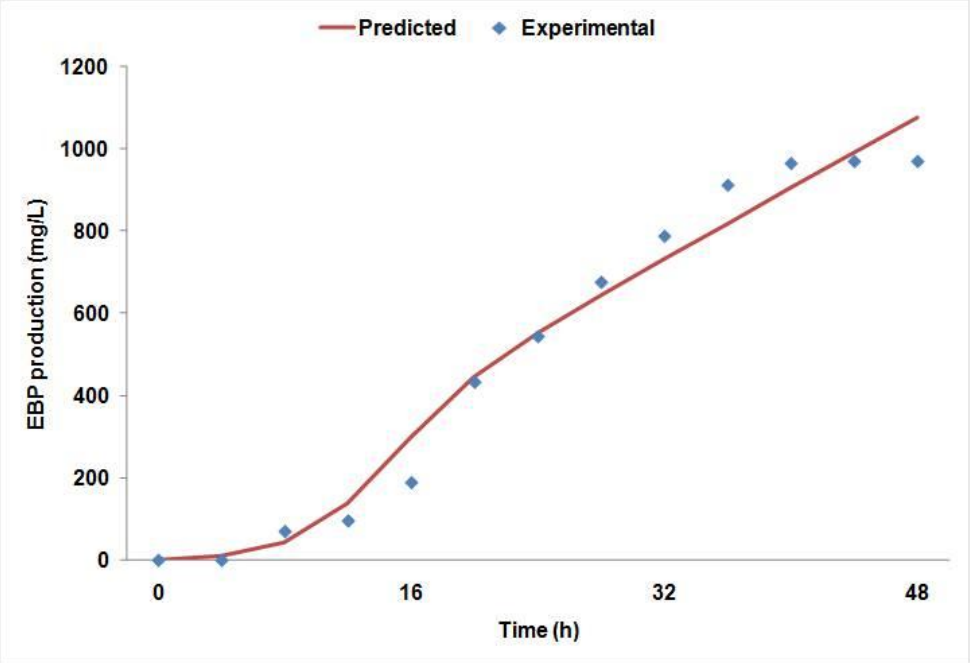

Figure 4.31 Comparison of experimental and LP model predicted values for exobiopolymer production

4.4 Application of exocellular biopolymer for monitoring phosphate levels in water and development of removal process

4.4.1 Biosensor for phosphate detection

The selective phosphate-binding characteristics of EBP were exploited to develop a biosensor probe. The EBP-coated probe retains phosphate from water which can then be detected by an optoelectric biosensor. The operational conditions of probe were optimized and biosensor performance was validated.

Optimization of biosensor probe

The biosensor probe was developed by coating cellulose acetate membrane with EBP. It is expected that the amount of EBP present in probe can influence the amount of phosphate retained on probe and hence, impact sensitivity of the detection method. Further, the amount of EBP present in probe can also impact flow rate through the membrane and hence directly influence total analysis time. Therefore, the EBP concentration on probe was optimized to obtain

maximum phosphate retention and maximum flow rate. Cellulose acetate membranes were coated with different concentrations of EBP (1-6 mg/L) and the degree of phosphate retention on probe was determined. An EBP concentration-dependent increase in percent retention was observed upto 4 mg/L EBP while a further increase in EBP to 5 and 6 mg/L offered no appreciable advantage in terms of phosphate removal (Figure 4.33A). Further, the flow rate through probes coated with 1 to 3 mg/mL EBP was comparable to flow rate through uncoated membranes while a concentration-dependent decrease in flow rate was observed at higher EBP concentrations (Figure 4.33B). Since 4 mg/mL EBP exhibited near-maximum phosphate retention with slight (approximately 15%) reduction in flow rate, 4 mg/mL EBP was considered optimal for coating membranes.

Calibration of biosensor

The biosensor response was calibrated with a broad range of phosphate concentrations (1-15 mg/L). The biosensor response, expressed as milliamperes (mA), was linear between 1 to 10 mg/L phosphate. Biosensor response was found to be linear (R^2 >0.99) in the range of 1-10 mg/L phosphate. The limit of detection was 0.5 mg/L and limit of quantification was 1 mg/L (Figure 4.34).

Validation of biosensor

The stability of biosensor measurements were determined by measuring precision (intra-assay/intraday and inter-assay/inter-day variability), accuracy (recovery) and long-term stability using cellulose acetate membranes coated with 4 mg/mL EBP. The percent relative standard deviation (%RSD) was <5% at all phosphate concentrations (1-10 mg/L) indicating high precision of biosensor. Similarly, the percent recovery was >95% at all phosphate concentrations indicating high accuracy of measurements (Table 4.35).

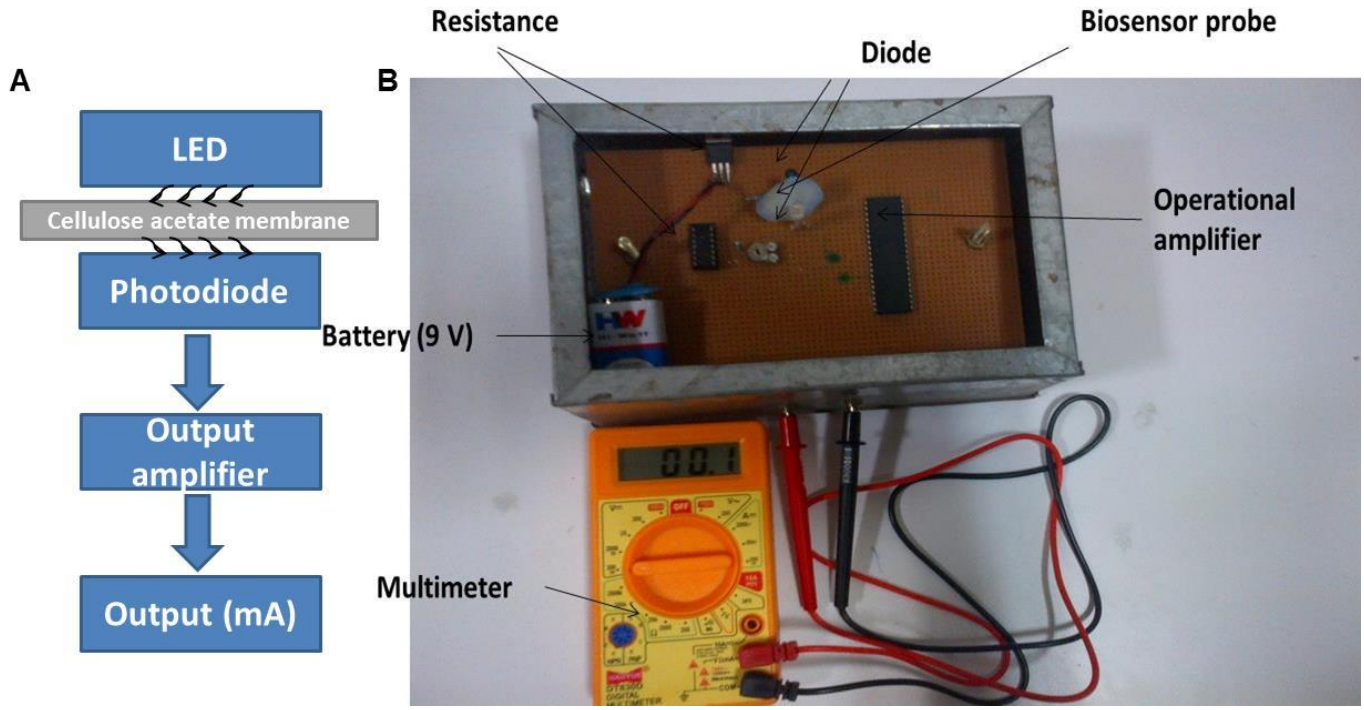

Figure 4.32 (A) Schematic diagram of the phosphate biosensor. (B) Photograph of the phosphate biosensor setup. Inset shows cellulose acetate membrane loaded in the biosensor

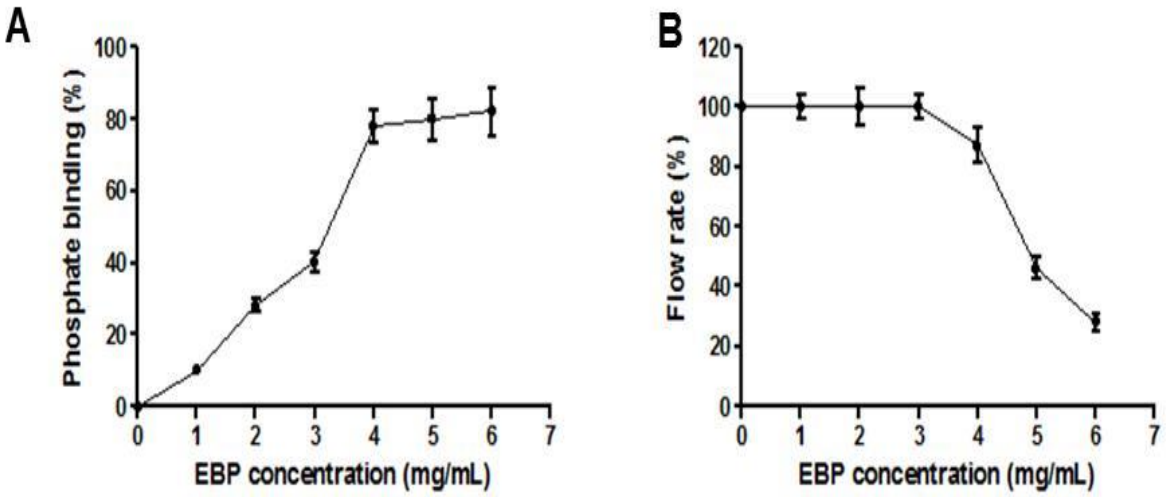

Figure 4.33 Effect of exobiopolymer concentration on phosphate binding (A) and flow rate of phosphate samples (B) on EBP-coated cellulose acetate membranes. Data is expressed as mean±SEM of 5 samples/concentration.

The long-term stability of biosensor was determined over 4 weeks. The %RSD was <5% at all phosphate concentrations and recording intervals suggesting the biosensor is stable for atleast 4 weeks (Table 4.36). The high stability of biosensor ensures that frequent calibration is not required.

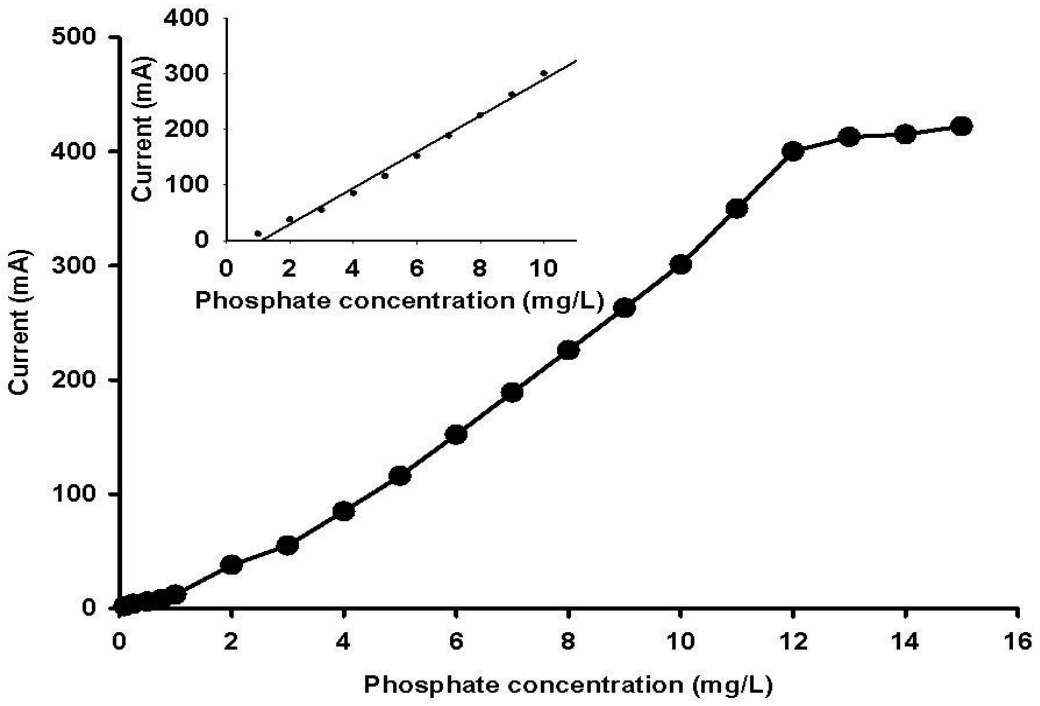

Figure 4.34. Calibration curve of biosensor at 0-15 mg/L phosphate concentration. Data is mean of 5 samples/concentration. Inset shows regression analysis of data points in the linear range of analysis.

Table 4.35. Precision and recovery of phosphate estimation by biosensor.

Phosphate concentration (mg/L)	Variability (%RSD)[a]		% Recovery[b]
	Intra-day	Inter-day	
1	2.10	1.36	96.55
2	1.78	1.57	97.78
4	1.66	1.23	97.57
6	1.05	1.00	98.16
8	1.15	1.23	101.32
10	0.98	1.14	99.15

[a]Data is %RSD of 5 samples/concentration. [b]Data is mean of 5 samples/concentration

Table 4.36. Long-term stability of phosphate estimation by biosensor

Phosphate concentration (mg/L)	Long-term stability[a]				
	Day 0	Day 7	Day14	Day 21	Day 28
1	1.34	1.36	1.89	1.71	2.06
2	0.87	0.82	1.94	1.21	2.09
4	1.46	1.87	1.63	0.91	1.75
6	1.41	1.70	1.47	1.81	1.25
8	2.01	1.09	1.22	1.95	1.76
10	1.04	1.48	0.89	0.81	0.94

[a]Data is %RSD of 5 samples/concentration.

Stability of biosensor probe

The long-term stability of biosensor probe is critical for field applications since this allows preparation of large number probes in the laboratory which can then be directly used in field. The long-term stability precludes the need for frequent probe preparation, reduces analysis time by circumventing the time required for probe preparation and increase precision by reducing inter-lot variability that could be introduced due to frequent probe preparation.

Cellulose acetate membranes coated with 4 mg/L EBP were stored at 4°C and ambient temperature (~25°C) and stability of biosensor probe was determined over 4 weeks. The difference between phosphate concentration determined with freshly prepared membranes (day 0) and the same lot after storage for upto 4 weeks was determined and expressed as %RSD. The %RSD was <5% at all recording intervals suggesting the biosensor probe is stable for atleast 4 weeks (Table 4.37).

Table 4.37. Long-term stability of biosensor probe

Storage temperature	**Long-term stability**[a]				
	Day 0	**Day 7**	**Day14**	**Day 21**	**Day 28**
4°C	1.40	1.74	2.45	1.58	2.05
Ambient	1.77	1.89	1.51	1.21	2.22

[a]Data is %RSD of 5 membranes/analysis.

4.4.2 Process of phosphate removal by hydrogel based systems

The batch equilibrium studies are an excellent indicator of sorbent performance under laboratory conditions but the method has limited practical feasibility in field applications. Column sorption studies provide a more practical solution for field applications and hence, sorption studies were

attempted with purified EBP. However, the viscous nature of EBP packing did not allow fluid flow rates above 0.1 mL/min. The small flow rate was unsuitable for practical applications and hence, alginate blended hydrogel beads of EBP were prepared.

Characterization of hydrogel beads

The particle size of calcium alginate blended EBP (CAB-EBP) hydrogel beads was determined by optical microscopy. The average particle size was found to be 1.32±0.24 mm in freshly prepared, dehydrated and rehydrated beads. SEM examination revealed the particles were porous and possessed a rough surface at microscopic scales (Figure 4.35) suggesting a large surface is available for phosphate sorption.

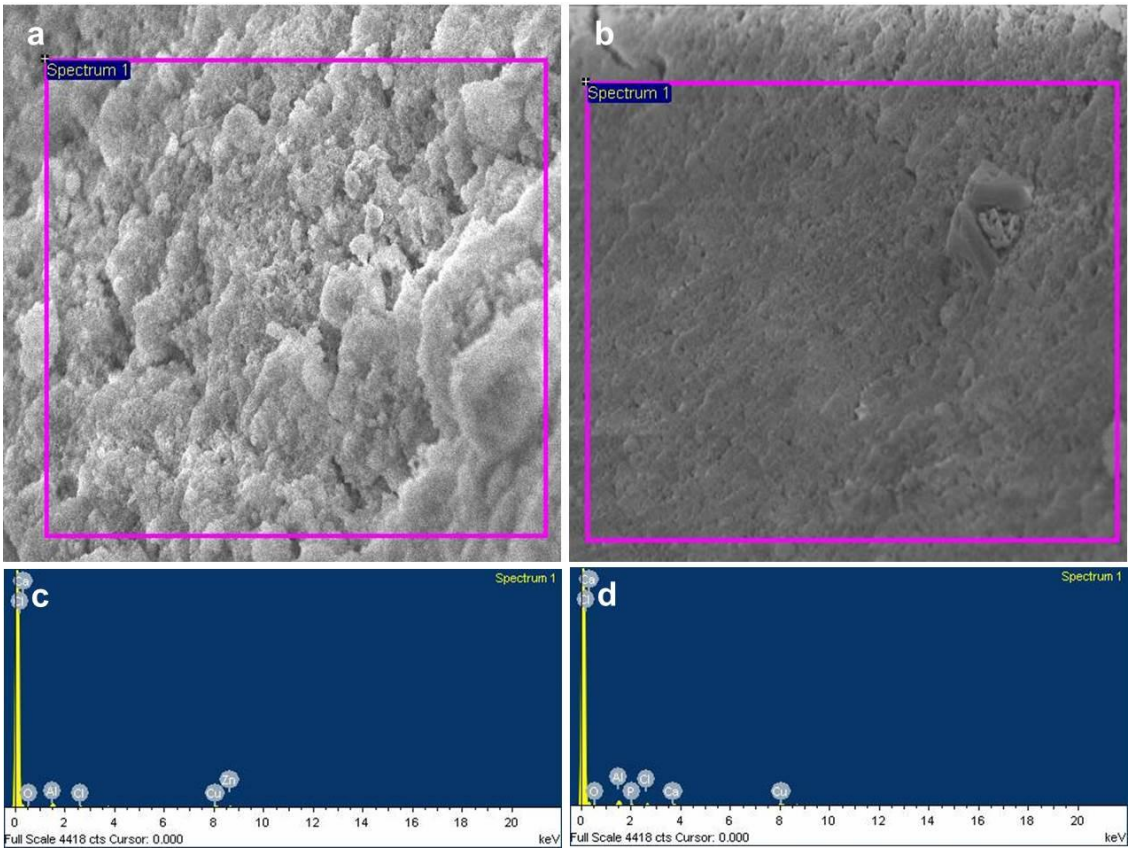

Figure 4.35: Surface morphology of unbound (A) and phosphate bound CAB-EBP (B) determined by SEM. The images are 0.5 mm✕0.5 mm (C) and (D) shows EDS spectra of the boxed fields in (A) and (B) respectively.

Following phosphate binding, the surface morphology of CAB-EBP was relatively smoother and less porous compared to unbound CAB-EBP. Phosphate binding was confirmed by presence of phosphorous peak in EDS spectrum of phosphate-bound CAB-EBP which was absent in unbound CAB-EBP. Additionally, peaks for calcium and oxygen were observed in both spectra confirming the presence of calcium alginate. Apart from these expected peaks, additional peaks corresponding to trace amounts of other elements were observed which might arise from aluminium stub (aluminium peak) and residual reaction byproducts (chlorine peak).

Effect of flow rate

The breakthrough curves at flow rates of 10, 20 and 30 mL/min revealed a typical "S" shape. The breakthrough curve was steeper, exhibited relatively early saturation and lower service time at higher flow rates compared to lower flow rates. This inverse relation between flow rate and breakpoint time occurs because the adsorption zone moved faster resulting in relatively lower contact time between the sorbate and sorbent at higher flow rates. Contrastingly, at lower flow rates, the adsorption zone is expected to move slower at lower flow rates resulting in higher residence time and hence, more efficient sorption.

Effect of influent phosphate concentration

The breakthrough curves at 1, 5 and 10 mg/L influent phosphate concentration also revealed a typical "S" shape. The breakthrough curve was steeper, exhibited relatively early saturation and lower service time at higher concentrations compared to lower concentrations.

Thomas model

Thomas model is the most commonly employed model for fitting column adsorption data which assumes Langmuir adsorption model and pseudo-second order kinetics. The non-linear form of Thomas model is expressed as (Lezehari et al., 2012)

$$\frac{Ct}{C0} = \frac{1}{1 + e^{(Kth.q.\frac{W}{Q} - Kth.C0.t)}}$$

where, C0 is initial phosphate concentration (mg/L), Ct is phosphate concentration at time "t" (mg/L), Kth is Thomas rate constant (L/min.mg), q is amount of phosphate sorbed in equilibrium per gram of sorbent (mg/g), W is weight of sorbent (g), Q is flow rate (L/min) and t is time (min).

The experimental data fitted well into the model and R^2 values were >0.98 under all operational conditions (Table 4.38). Kth values exhibited an inverse correlation with influent phosphate concentration and decreased from 0.28 L/min.mg at 1 mg/L influent concentration to 0.20 L/min.mg at 10 mg/L phosphate. Contrastingly, q increased from 18.6 mg/g at 1 mg/L phosphate to 25.1 mg/g at 10 mg/L phosphate (Figure 4.36).

The Kth and q values also exhibited dependence on the flow rate albeit in an order opposite to that observed in influent phosphate concentration. Kth values increased from 0.28 L/min.mg to 0.33 L/min.mg while 18.6 mg/g to 17.7 mg/g with an increase in flow rate from 10 mL/min to 30 mL/min.

Table 4.38 Operational and Thomas model parameters for column sorption studies

Influent phosphate concentration (mg/L)	**Flow rate (mL/min)**	**Kth (L/min.mg)**	**q (mg/g)**	**R^2**
1	10	0.28	18.6	0.988
5	10	0.23	20.4	0.990
10	10	0.20	25.1	0.986
1	20	0.30	18.5	0.996
1	30	0.33	17.7	0.994

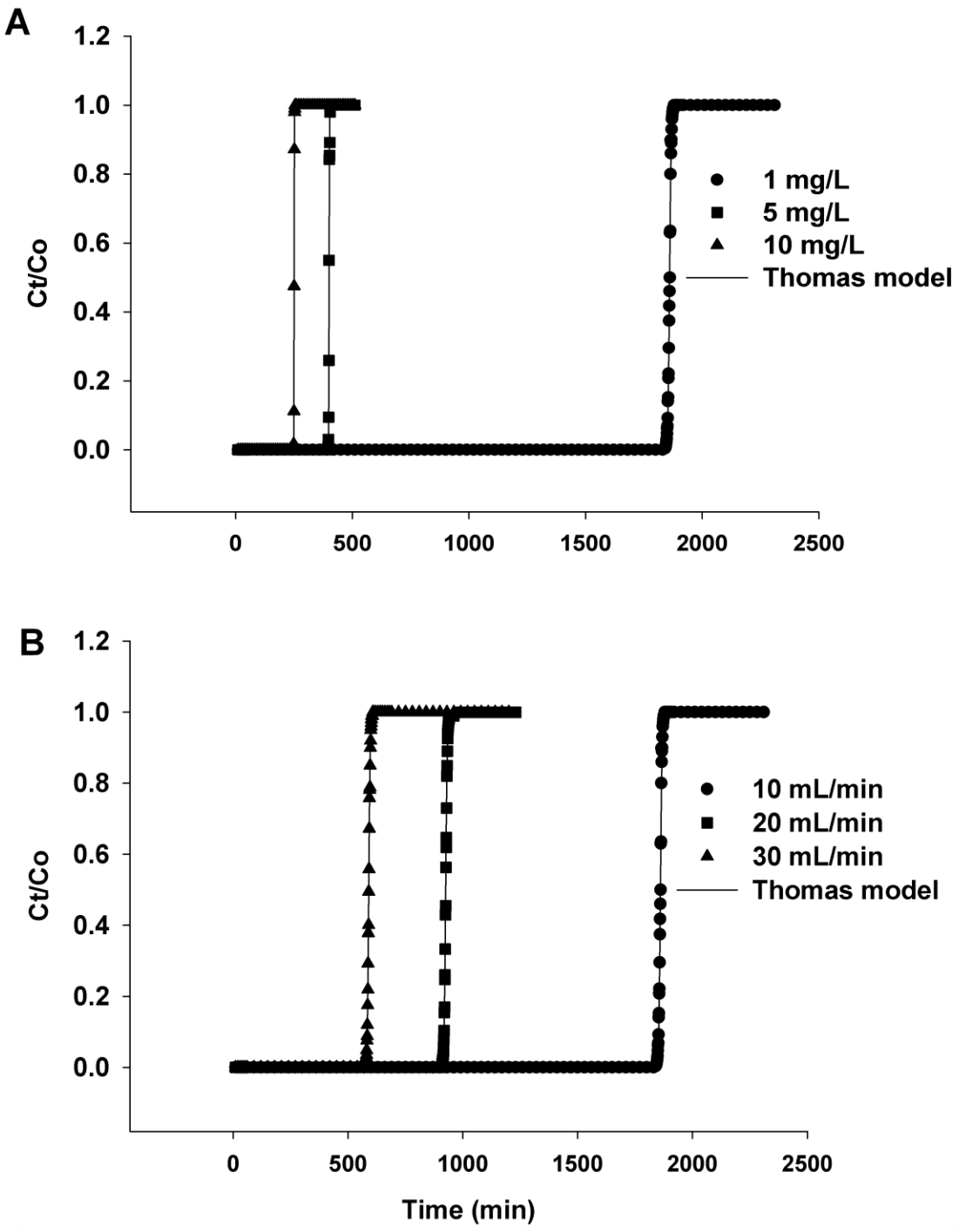

Figure 4.36 Breakthrough curves showing effect of influent phosphate concentration (A) and flow rate (B) on phosphate removal

5. DISCUSSION

The importance of curbing phosphorous is recognized as indispensable for maintaining the water quality budget. Biological methods of phosphate remediation have been strongly advocated due to the higher efficiency and process economy obtained with such methods. The current biological methods involve treatment of wastewater with activated sludge wherein phosphate accumulating organisms (PAOs) present in sludge accumulate phosphate as intracellular polyphosphate granules. In the current past, the role of exobiopolymers (EBPs) produced by sludge microorganisms were implicated in phosphate removal but a systematic study for technological exploitation remained a key impediment for commercial feasibility. A deliberation on these facts implies strategic exploration of microbial candidates with capability of proliferating phosphate binding exopolymer as an important driver for achieving a viable solution for phosphate remediation.

In view of identifying possible solutions, the current study screened potent EBP producing bacteria. Primary screening was based on colony appearance (mucoid colonies) and phosphate binding capabilities of isolates from diverse effluents with a history of high phosphate levels. The isolate producing highest quantity of EBP and exhibiting highest phosphate binding was completely characterized using established biochemical and molecular methods as *Acinetobacter haemolyticus*. Acinetobacter sp. has been frequently isolated from activated sludge and several studies have confirmed their role as predominant PAO. However, the role of EBP produced by Acinetobacter sp., or any other sludge microorganism, in phosphate removal has not been reported.

A prerequisite for commercial application of a biotechnology-derived product is the ability to produce the product in sufficiently large quantities in an economically viable setting. The isolate, designated as *A. haemolyticus* TK15, produced EBP in low yields typically relevant for analytical/investigative purposes, thus it was imperative to enhance EBP yield of TK15. The issue of low yield of secondary metabolites is not unique to TK15 and has been observed

for other microbial products in diverse genera. A plethora of strategies have been applied in a variety of microorganisms to enhance production of secondary metabolites and may be broadly classified into two categories: mutagenesis and optimization of culture conditions. Therefore, the first part of the current investigation was targeted towards augmenting EBP production by TK15 using mutagenesis followed by optimization of culture conditions.

Insertional mutagenesis by Tn5 is a random event on genomic scale. Although the insertion has been demonstrated to be biased towards GC rich regions in genome and a consensus sequence for Tn5/IS50 insertion has been proposed; nevertheless, the insertion of Tn5/IS50 insertion occurs randomly throughout the genome and potentially disrupt any gene. Several types of regulatory genes/proteins can modulate EBP production and disruption of a key regulatory gene may enhance transcription of genes involved in EBP biosynthesis. Additionally, a regulatory control on EBP production may also be exerted by intracellular levels of metabolites and disruption of the gene responsible for metabolite production may result in overexpression of EBP biosynthetic enzymes. Further, the EBP biosynthesis pathway may share metabolite(s) with another pathway and the metabolite may be "drained" to the later pathway. The disruption of a key gene of the "draining" pathway may result in enhanced flux of the metabolite towards EBP biosynthetic route. It was considered important to understand the mechanism behind increased EBP production in MG606. Insertional mutagenesis by Tn5 is a random event on genomic scale but a bias towards a 9 bp sequence with GC pairs at both ends has been demonstrated (Lodge et al., 1988). Several hotspots of Tn5 insertions have been reported all of which share the two basic features – a 9 bp sequence and GC pairs at both ends (Berg et al., 1983; Lupski et al., 1984; Boyd et al., 1993; Goryshin et al., 1998) based on *in vitro* (pRZTL1 plasmid) and *in vivo* (*E. coli* cells) Tn5 transpositions, proposed a preferred consensus sequence A-GNTYWRANC-T where the terminal G and C of the consensus sequence are flanked by A and T, respectively.

Nonetheless, insertions were also reported for sites that differed from the consensus sequence at one or more positions (Goryshin et al., 1998). Shevchenko et al reported a refined consensus sequence of G(CT)(CT)(CT)(AT)(AG)(AG)(AG)C for Tn5 insertion in cDNA clones but suggested that the insertion sequence may even be extended to 11 or 13 bp (Shevchenko et al., 2002). Green et al reported Tn5 insertion bias towards G/C rich sequences in *Candida glabrata* at sequence motifs similar, but not identical, to those suggested by Goryshin et al (Goryshin et al., 1998; Green et al., 2012). Apart from the end sequences, DNA coiling, symmetry and donor sequence also plays an important role in Tn5 insertion (Lodge and Berg, 1990; Lodge et al., 1991; Ason and Reznikoff, 2004). The Tn5 insertion site observed in *A. haemolyticus* MG606 (GAGAAAGTC) is a 9 bp sequence with GC pairs at both ends which is in agreement with the basic requirements of a Tn5 insertion site. This sequence also exhibits similarity with preferred/consensus sequences reported by others (Goryshin et al., 1998; Shevchenko et al., 2002).

Tn5 insertions in *E. coli* have been demonstrated to enhance expression of genes located downstream of Tn5 insertion site as well as distant genes. This increased expression possibly occurs through creation of a promoter at the insertion point (Berg, 1980; Berg et al., 1980; Hecker et al., 1988; Wang and Roth, 1988; Clark et al., 1994). A similar upregulation of downstream genes by an outward promoter or by creation of a new promoter site has been reported in transposons other than Tn5 as well (Ciampi et al., 1982; Simons et al., 1983; Aronson et al., 1989; Nurk et al., 1993; Giel et al., 1996; Camarena et al., 1998). Considering that Tn5 insertion in *A. haemolyticus* MG606 was observed in intergenic region and apparently did not disrupt a gene, it was deemed pertinent to determine levels of gene products located downstream of Tn5 insertion. Tn5 insertion only upregulated the vicinal gene PGM/PMM but did not affect activities of gene products translated from regions downstream of PGM/PMM (G6PI and UDE) or of a distant gene (GST). These results

suggest that Tn5 insertion only affects the gene located in vicinity of insertion but has not effect on genes located further downstream or distant genes. It, therefore, seems reasonable that upregulation of PGM/PMM transcription and subsequently, the enzyme activity, accounts for the observed increase in EBP production. Therefore, the effect of insertional mutagenesis on these enzymes involved in EBP biosynthesis was further confirmed by enzyme assays. Amongst the various enzymes, only PGM activity was found to be significantly increased in MG606 while the activities of other enzymes were comparable in MG606 and TK15 strains. The enhanced PGM activity was associated with an increase in catalytically active PGM protein and PGM transcripts as determined by zymography and RT-PCR. A similar PGM-dependent increase in EBP production has been demonstrated in lactic acid bacteria, *Pseudomonas* sp and other organisms (Davies et al., 1993; Levander and Radstrom, 2001; Levander et al., 2002; Svensson et al., 2007; Sahu et al., 2014; Zimaro et al., 2014; Cimini et al., 2015; Xu et al., 2015). The strategic role of the dual substrate specific enzyme PGM in exopolysaccharide synthesis especially by *P. aeruginosa* and *A. baumaniii* strains has been reported (Davies et al., 1993; Sahu et al., 2014). Since PGM is responsible for modulating the carbon flux between EBP and energy producing pathways, an increase in PGM activity may be presumed to divert carbon flux towards EBP-producing pathway, which, in turn, may lead to increased EBP production (Levander and Radstrom, 2001; Boels et al., 2003; Panagiotou et al., 2005; Zhai et al., 2015). The results of this study corroborated previous observations (Levander and Radstrom, 2001; Boels et al., 2003; Zhang et al., 2014) suggesting PGM to be crucial in EBP synthesis by *A. haemolyticus* and upregulation of PGM expression could result in increased EBP production.

PGM expressed by *Acinetobacter* sp. has not been isolated and characterized till date except a recent preliminary report describing cloning of PGM from *A. baumannii* (Sahu et al., 2014). Therefore, we purified the enzyme and characterized its catalytic parameters. The enzyme

was found to be a bifunctional with PGM and phosphomannomutase (PMM) activities. The purified PGM could catalyze conversion of G1P and M1P to the respective 6-phosphosugars with a Km of 0.028 mM and 0.017 mM; the low Km for both substrates indicated that the enzyme catalyzed reaction at low intracellular substrate concentrations. Further, the lower Km for M1P also suggested slightly higher affinity for M1P compared to G1P. The PGM/PMM reported in *P. aeruginosa*, *E. coli* and other species possessed similar optimal temperature and pH values of 35^0C and 7.5, observed in *A. haemolyticus* (Joshi and Handler, 1964; Ye et al., 1994; Wang and Zhang, 2010).

The successful commercial application of biotech-derived products is subject to regulatory approvals. These regulatory approvals become even more difficult when dealing with genetically modified organisms and their products, requiring safety assessment of the organism and its product(s) (OECD, 2011; Vazquez-Salat, 2013; Devos et al., 2014; Twardowski and Malyska, 2015; Zadravec et al., 2015). Therefore, a major concern in environmental application of EBP is the potential virulence of *Acinetobacter* sp. and toxicity of exoproducts. Hence, microbial virulence and EBP toxicity was determined using mouse lethality assay. *A. haemolyticus* MG606 exhibited LD50 of 12.11 logCFU/animal. This extremely high LD50 value suggested that the mutant is practically avirulent since similar LD50 values have also been reported in probiotics (Hong et al., 2008; Sorokulova et al., 2008; Szabo et al., 2011). The avirulent nature of *A. haemolyticus* is also supported by the fact that this bacterium has recently been isolated from healthy human skin (Patil and Chopade, 2001; Jagtap et al., 2010). Human infections by *A. haemolyticus* are extremely rare and only three reports have documented the role of this bacterium in diarrhea, bacteremia and endocarditis (Castellanos Martinez et al., 1995; Choi et al., 2006; Grotiuz et al., 2006). However, the issue of species misidentification in these reports could not be ruled out (Peleg et al., 2008). Virulence studies in mouse models of *Acinetobacter* sp. infection have

demonstrated virulent strains have relatively lower LD50 (5 to 6 log CFU/animal) compared to low virulent strains (7 to 8 log CFU/animal) (Avril and Mesnard, 1991; Breslow et al., 2011). Therefore, considering the experimental data in mouse lethality assay along with lack of conclusive evidence on virulence of *A. haemolyticus* in humans, it may be inferred that the mutant does not pose a biohazard and can be employed for large scale production of EBP.

In contrast to bacterial virulence, there is a dearth of studies on biological effects of bacterial EBPs. A critical comparison on functional as well as safety aspects during the course of our study was not possible due to the non-availability of a similar well characterized EBP of microbial origin. In fact, the limited amount of literature available on microbial EBPs is restricted to polysaccharides which are either currently being used or are potential candidates for applications in food and pharmaceutical industry. Nonetheless, available literature on a clinically used bacterial polysaccharide, dextran, suggests that LD50 of EBP (92.1 mg/kg) is comparable to LD50 of high molecular weight dextrans (100-500 mg/kg) and *S. cerevisiae* neutral mannan (75 mg/kg) (Nagase et al., 1984; CIR, 2012).

Bacterial EBPs are constituted of a heterogeneous system comprising polysaccharides, proteins, nucleic acids and other, relatively less conspicuous fractions. Despite the presence of several biochemical components, the polysaccharide fraction has remained focus of investigation. This interest in polysaccharide stems from two major reasons: first, polysaccharide fraction comprises the major weight fraction of EBP and second, physicochemical properties of EBP are governed by molecular weight and composition of the polysaccharide produced (Brandenburg et al., 2003; Satpute et al., 2010; More et al., 2014). The diversity in polysaccharide composition can be realized from the fact that molecular weight could range from a few thousand to millions of daltons while monomer repeating units could range from one monosaccharide (homopolysaccharide) to several monosaccharides (heteropolysaccharide) (Satpute et al., 2010; Nwodo et al., 2012; More et

al., 2014). In fact, the differences are profound to the extent that even EBPs produced by different strains of the same species may be completely unrelated in terms of molecular weight and monomer composition of polysaccharide fraction (Mozzi et al., 2006).Though studies on EBP produced by *Acinetobacter* sp. are handful, the available literature does indicate large variations in polysaccharide composition. These studies were primarily restricted to characterization of high molecular weight heteropolysaccarides such as ethapolan (500 kDa to >2 MDa) produced by *Acinetobacter* sp. 12S, emulsan (approximately 1 MDa) produced by *A. calcoaceticus*, alasan (approximately 1 MDa) produced by *A. radioresistens* and biodispersan (51 kDa) produced by *A. calcoaceticus* (Rosenberg et al., 1988b; Shabtai, 1990; Pirog et al., 2004; Pirog et al., 2009; Satpute et al., 2010). Despite the significant differences in their molecular weights and proportion of different monosaccharides, these polysaccharides shared a commonality in their composition – all of these were heteropolysaccharides composed of hexose sugars or their corresponding uronic acids/amino sugars with insignificant or undetectable amounts of pentose sugars (Pirog et al., 2004; Pirog et al., 2009; Bales et al., 2013; Sen et al., 2014). *A. haemolyticus* also produces EBP with bioemulsifier properties (Patil and Chopade, 2001; Jagtap et al., 2010) but the composition of polysaccharide fraction has not been reported. The polysaccharide was found to be a 48.9 kDa heteropolysaccaride composed of hexoses and pentoses in equal proportions. Although pentose sugars have been reported in small amounts in EBP produced by *A. baumannii* strains (Bales et al., 2013), the significant contribution of pentoses (approximately 50%) to polysaccharide composition suggests *A. haemolyticus* MG606 unique in comparison to the other members of Acinetobacter genus. In addition to composition, the nature of linkages between monosaccharides is crucial to understand the characteristics of biopolymer and is routinely performed by methylation analysis, reductive cleavage analysis, nuclear magnetic resonance spectroscopy and selective enzymatic hydrolysis (Cui, 2005; Ruiz-

Matute et al., 2011). The hydrolysis of EBP by amylase and cellulase suggest presence of (1→4)-linked α-glucans and (1→4)-linked β-glucans, respectively. Additionally, the presence of peaks at 1032 cm^{-1} and 875 cm^{-1} in FTIR spectrum also suggest presence of (1,3)- and/or (1,6)-linked β-glucans (Sandula et al., 1999; Synytsya et al., 2009).

The sorption process involves binding of sorbate molecules to sorbent binding sites by physicochemical processes. The affinity of sorbate towards binding sites is a function of the avidity of physicochemical interactions in the sorbate-sorbent system while the kinetics of sorption depends on variables such as contact time, sorbent concentration and sorbate concentration. The kinetics of phosphate-EBP interactions revealed a positive correlation between phosphate removal and contact time as well as EBP concentration. This is due to the fact that an increase in contact time provides sufficient time for the sorption to achieve equilibrium. On the other hand, an increase in EBP concentration provides higher number of binding sites available for phosphate binding which results in more efficient binding (percent phosphate removal) due to reduced competition between phosphate ions for available binding sites. In parallel, an increase in EBP concentration also results in higher number of unoccupied binding sites for a fixed phosphate concentration which results in lower phosphate removal efficiency (Qe value) at higher EBP concentrations. The effect of increasing phosphate concentration, at fixed EBP concentration, was opposite to that observed at increasing EBP concentrations at fixed phosphate concentration. The percent phosphate removal decreased while Qe increased with increasing phosphate concentration. This opposite effect in percent phosphate removal and Qe values appears because the available binding sites are saturated at lower phosphate concentrations which manifest itself as lower percent removal at high phosphate concentrations. On the other hand, the number of unoccupied binding sites is reduced with increasing phosphate concentration resulting in higher Qe values at increasing phosphate concentration.

The sorption process is frequently described by empirical methods called isotherm equations. Such a mathematical treatment of sorption data provides valuable insights on nature and mechanism of sorption process. However, these empirical models suffer from the limitation that the original models were an oversimplification of the sorption process. Another shortcoming of traditional model-fitting methods was overreliance on coefficient of determination (R^2) to compare model fitting among different isotherm equations. Although R^2 is helpful when comparing model fitting for two or three isotherm equations, it is not uncommon that several models could simultaneously describe the sorption data when compared based on R^2 values (Ho, 2004; Foo and Hameed, 2010; Akpa and Unuabonah, 2011; Chu, 2014). A similar result was also observed in our case where all the five isotherm equations showed $R^2 > 0.95$. In order to address this problem, several error functions have been described over the past few decades and improvised in recent years. These error functions are based on robust statistical tools to identify the best fitting isotherm equation when R^2 could not be solely relied on. Based on the error functions, phosphate binding was observed to follow Langmuir isotherm equation. A similar, Langmuir type adsorption of phosphate has also been demonstrated on polymers and inorganic sorbents (Dai et al., 2011; Cai et al., 2012; Yu et al., 2012; Zheng et al., 2012; Yang et al., 2015; Yu and Chen, 2015; Yuan et al., 2015; Zhang et al., 2015b). The calculated maximum phosphate removal capacity, derived from Langmuir isotherm, was 25 mg phosphate/g EBP. Interestingly, the phosphate removal capacity of EBP is for up to one magnitude higher than most natural and derivatized biopolymers as well as mineral sorbents which show binding capacities in the range of 2 to 10 mg/g (Chitrakar et al., 2006; Jellali et al., 2010; Jellali et al., 2011; Wahab et al., 2011; Riahi et al., 2014; Yuan et al., 2015). The higher phosphate binding capacity, therefore, support the application of EBP as a replacement for relatively less efficient sorbents.

The mechanisms of phosphate removal differ between natural polymers and mineral sorbents and hence, account for the observed differences in extent and kinetics of phosphate removal. The key mechanisms involved in phosphate removal are electrostatic interactions, ligand exchange and precipitation. A predominance of one of these mechanisms or co-existence of multiple mechanisms can influence the kinetics of phosphate removal. For example, phosphate removal by ligand exchange and electrostatic interactions follows a rapid association kinetics (Jellali et al., 2010; Jellali et al., 2011; Wahab et al., 2011; Tofan-Lazar and Al-Abadleh, 2012; Riahi et al., 2014) while surface precipitation accounts for the slow sorption process (Li and Stanforth, 2000; Ler and Stanforth, 2003; Yuan et al., 2015). The kinetics of phosphate removal by EBP was initially fast and major proportion of phosphate was removed within 60 min. This initial rapid removal is attributed to sorption on high-affinity sites which are saturated within the first 60 min. The rapid removal was followed by a relatively slower removal which reached equilibrium within 4 hours. This slow removal process possibly arises due to three mechanisms: repulsion of phosphate due to increase in surface negative charge, binding of phosphate to low-affinity sites and diffusion of phosphate in particle aggregates (Luengo et al., 2006; Luengo et al., 2007; Wang et al., 2013a). Although surface precipitation could be another possible reason for the slower sorption process, there are strong evidences, both direct and circumstantial to believe that surface precipitation is not involved. SEM-EDS analysis revealed a uniform coverage of EBP surface with phosphate with no evidence of "patches" of phosphorus-containing particles or crystal formation (Elghniji et al., 2014; Wang et al., 2015). Further, precipitation mechanism requires presence of a counter cation to form cation-phosphate complexes and precipitates (Li and Stanforth, 2000; Ler and Stanforth, 2003; Yagi and Fukushi, 2012; Wu et al., 2013; Jeong et al., 2014; Yan et al., 2015). The absence of a cation signal in EDS spectrum and of a cation-phosphate complex/crystal signal in XRD spectrum of phosphate-bound EBP refuted

the presence of surface precipitates or complex formation (Smith et al., 2009; Koilraj and Kannan, 2010; Liu and Hesterberg, 2011; Yao et al., 2013). Hence, it is plausible to exclude the possibility of surface precipitation occurring on EBP.

Phosphate exists as ions in solution and therefore, it is plausible to assume that electrostatic interactions between phosphate and positively charged groups on EBP might play a role in phosphate sorption. Therefore, it may be assumed that phosphate-bound EBP will possess a higher negative charge density as compared to phosphate unbound EBP. This assumption was supported by the observation that surface charge (zeta potential) of EBP decreased from -2.98 mV in unbound EBP to -3.11 mV in phosphate-bound EBP. In fact the electrostatic interaction was further supported by pH-dependent binding studies and potentiometric titrations of EBP. Potentiometric titrations of EBP revealed presence of an acidic (pKa = 3.63) and a basic (pKa = 8.61) binding site corresponding to carboxylic and amino/alcoholic groups, respectively (Guine et al., 2006). A similar two-site model of EBP has been reported in EBP produced by other bacteria as well (Lenoble et al., 2008; Gonzalez et al., 2010). The presence of carboxylic acid, amino and alcoholic groups in EBP revealed by EBP is in concurrence with biochemical estimations and elemental analysis which demonstrated high levels of uronic acids (contributing carboxylic acid groups), proteins and amino sugars (contributing amino groups) and polysaccharides (contributing alcoholic groups). It may be argued that under acidic pH conditions, the basic groups are protonated and ionization of acidic groups will be suppressed while the reverse will be true under basic conditions. This pH-dependent modulation of surface charge is expected to impact association of phosphate with EBP, therefore phosphate binding experiments were initiated over a broad pH range encompassing highly acidic to highly basic pH values. As anticipated, phosphate binding decreased with an increase in pH supporting the role of a charge-dependent, electrostatic interaction mechanism (Wang et al., 2013b). Nitrogen-containing groups are the most

probable candidate for an electrostatic interaction mechanism due to the abundance of nitrogen in EBP and the interacting groups are presumably present in the form of proteins and amino sugars. In order to validate their role in phosphate binding, the proteins were degraded by proteolytic enzymes while amino and amide groups were chemically derivatized to inhibit their interaction with phosphate. Expectedly, treatment of EBP with proteolytic enzymes or amino group derivatization with glutaraldehyde or amide group derivatization with formaldehyde resulted in significant reduction in phosphate removal. The inhibition of phosphate removal was several folds higher with glutaraldehyde compared to proteolytic or formaldehyde treatment suggesting that non-protein nitrogen moieties like amino sugars play a major role in phosphate removal. A similar role of proteins and amino sugars in heavy metal removal has also been documented (Micheletti et al., 2008; More et al., 2014).

The small decrease in zeta potential of phosphate-bound EBP relative to other sorbents (Ler and Stanforth, 2003; Zhong et al., 2007) and the incomplete inhibition of phosphate removal in glutaraldehyde treated EBP suggested that mechanisms other than electrostatic interactions with amino groups also play a role in phosphate removal. FTIR is a powerful tool in elucidating mechanism of interactions in multimolecular mixtures. The changes in peak intensities and peak shapes, peak shifts, appearance of new peaks and disappearance of peaks provides valuable information on nature of interaction (physical interaction or chemical reaction) as well as identification of interacting functional groups in a large variety of binary, tertiary and multimolecular systems. FTIR remains an important tool in understanding sorbate-sorbent interactions (Elzinga and Sparks, 2007; Wahab et al., 2011; Tofan-Lazar and Al-Abadleh, 2012; Zhang et al., 2015a) on account of its versatility and ease of operation and reliability. Therefore, to identify functional groups and elucidate other potential mechanisms involved in phosphate removal, FTIR spectrum of unbound and phosphate-bound EBP were compared. FTIR spectrum revealed that hydroxyl, carboxyl and amino peaks were suppressed

and shifted to higher wavenumbers in phosphate-bound EBP – the effect being most pronounced in hydroxyl peaks. The higher degree of peak shape and position changes for hydroxyl peaks is attributed to the predominant presence, and hence pronounced interaction, of polysaccharide hydroxyl groups with phosphate. The role of hydroxyl and carboxyl groups in phosphate sorption has been documented in iron (oxy)hydroxides such as goethite (Chitrakar et al., 2006; Luengo et al., 2006; Zhong et al., 2007; Kubicki et al., 2012), akaganeite (Chitrakar et al., 2006), ferrihydrite (Wang et al., 2013c) and hematite (Elzinga and Sparks, 2007; Tofan-Lazar and Al-Abadleh, 2012; Liu et al., 2013b), aluminum oxides (Wu et al., 2014a; Yan et al., 2015), natural and metal-loaded polysaccharides (Eberhardt et al., 2006; Biswas et al., 2007; Wahab et al., 2011; Riahi et al., 2014) and other sorbents (Xue et al., 2009; Jellali et al., 2010; Jellali et al., 2011). Phosphate sorption on these, hydroxyl-containing, sorbents is achieved via ligand exchange mechanism which can be described by below equations.

$$—R\text{-}OH + H_2PO^{4-} \longrightarrow —R\text{-}HPO_4 + H_2O$$

$$—R\text{-}COOH + H_2PO^{4-} \longrightarrow —R\text{-}COHPO_4 + H_2O$$

The predominant shifting of hydroxyl peaks to higher wavenumbers in FTIR spectrum of phosphate-bound EBP suggest that phosphate sorption on EBP also occurs via ligand exchange mechanism as described by the above equation. Since polysaccharide fraction comprises major weight proportion of EBP and contains the highest density of hydroxyl groups, it is reasonable to expect that polysaccharide fraction participates in phosphate removal and is further substantiated by the observed reduction in phosphate removal in EBP hydrolysed by amylolytic enzymes treatment (Li et al., 2010b; Xi and Chen, 2014).

The operational feasibility of the EBP arguably would be dependent on the outcomes of phosphate removal in field or real time water samples. Simulation studies have been often

used effectively to show the eventual real effects on natural systems, therefore phosphate removal studies in phosphate-spiked water samples were carried out to understand the nature and the mechanism of phosphate binding to EBP. However it must be noted that practical applicability of EBP for wastewater treatment may be compromised by presence of other, potentially competing anions. The presence of competing anions assumes even more attention since several competing anions, notably sulfate, chloride and nitrate, are present in concentrations reaching several orders of magnitude higher than phosphate. Several inorganic and organic sorbents have been demonstrated to sorb phosphate with high affinity and desorbed only in presence of very high concentrations of competing anions. Often, anion binding to hydroxyl groups via ligand-exchange and to proteins via ionic interactions has been observed to follow the sequence: phosphate >sulfate> chloride = nitrate (Collins, 2004; Chitrakar et al., 2006; Biswas et al., 2007; Jellali et al., 2011; Wahab et al., 2011; Medda et al., 2012; Riahi et al., 2014; Keranen et al., 2015). A similar affinity of phosphate and competing anions was observed in EBP as well indicating that anion sorption on EBP occurs in a charge density-dependent manner. Further, the high specificity of phosphate binding with EBP in artificial waste samples spiked with individual competing anions is conducive to its field applications as a selective phosphate bioremediant.

The favorable nature of phosphate binding by EBP warrants its application as a potential bioremediant to tackle the looming phosphate pollution problem. However, production of requisite amounts of EBP under economically viable conditions is a prerequisite for its successful commercialization. Microorganisms generally elaborate small amounts of EBP which result in high production and downstream costs. Therefore, culture conditions and medium composition are generally tweaked to enhance EBP production and achieve economy in production process. It is believed that under optimal culture conditions (pH, temperature, agitation speed, etc.), biomass production is increased which results in

augmentation of EBP production (Patil et al., 2011; Sam et al., 2011; More et al., 2014). The culture conditions of maximal EBP production coincided with maximal or near-maximal biomass production in *A. haemolyticus* MG606 indicating that biopolymer production is dependent on biomass as observed in other microorganisms (Seviour et al., 2011; Kreyenschulte et al., 2014; More et al., 2014).

Microorganisms exhibit significant flexibility in nutritional requirements and can utilize diverse carbon and nitrogen sources. However, this flexibility is unseen in EBP biosynthesis since biopolymer production occurs in presence of specific carbon and nitrogen sources only (Ravella et al., 2010; More et al., 2014). Single substrates are often used as source of carbon and energy and the major proportion of carbon flux is diverted to metabolic pathways for growth and maintenance. However, under stress conditions, microorganisms switch to a relatively dominant physiological state whereby the carbon flux is diverted to EBP producing pathways. In contrast to the stress conditions, EBP production may also be stimulated by incorporation of suitable carbon sources in culture medium since the substrate may induce expression of genes conducive for EBP production (Audy et al., 2010; Liu et al., 2011a; Andersen et al., 2013; Shi et al., 2014). Similarly, nitrogen sources may also influence expression of EBP producing genes and hence a systematic selection of nitrogen source and concentration is desirable for enhanced EBP production (Seviour et al., 2011; Lee et al., 2013; Shi et al., 2014). Therefore, the effect of single and bicomponent mixtures of carbon and nitrogen sources on EBP production was evaluated in shake flasks. The EBP yield was highest in presence of glucose as the sole carbon source while acetate synergistically enhanced EBP production by glucose in glucose-acetate combination. A similar augmentation of EBP production in glucose-acetate mixtures has been reported in *Acinetobacter* sp. and *Nostoc flagelliforme* (Pirog et al., 2007; Yu, 2012). Although the exact mechanisms responsible for intensification of EBP production remain elusive, it is believed

that glucose-acetate mixture could increase gluconeogenesis compared to single carbon sources leading and hence, augment EBP production in *Acinetobacter* sp. (Pirog et al., 2002; Pirog et al., 2007). Further, EBP yield was highest in presence of ammonium sulfate as sole inorganic nitrogen source while bicomponent mixtures of nitrogen sources provided no additional benefits in terms of EBP yield. Therefore, based on shake flask experiments, a mixture of glucose and acetate was selected as carbon source and ammonium sulfate as nitrogen source.

Shake flask experiments are valuable in initial screening of a multitude of parameters. The critical parameters identified in shake flasks are further optimized to achieve maximum production at bioreactor scale. Design of experiment strategies harness the power of statistical tools for identification of optimal conditions and provide mathematical solutions to predict behavior of variables. Such statistical approaches have been commonly applied to identify and optimize significant parameters which influence EBP production (Seviour et al., 2011; Kreyenschulte et al., 2014). The initial screening of variables in shake flasks suggested that carbon and nitrogen sources are important determinants of EBP production by *A. haemolyticus* MG606. Therefore, concentrations of glucose, acetate and ammonium sulfate were optimized by response surface methodology. The EBP yield was approximately 1.5-fold higher in batch mode bioreactor using optimized media composition as compared to shake flask, demonstrating the influence of carbon and nitrogen source concentrations on EBP yield. These observations are in concurrence with other reports demonstrating higher yield of EBP in batch mode bioreactor as compared to shake flask method (Kreyenschulte et al., 2014; Saat et al., 2014). The unstructured kinetic models, such as Luedeking-Piret model, are widely used in fitting product formation kinetics for different types of fermentation processes. The kinetics of EBP production by *A. haemolyticus* MG606 could be described by Luedeking-Piret model and EBP production was found to be partially growth associated.

Similar results were obtained by other researchers for the biosynthesis of biopolymers (Seviour et al., 2011; Saat et al., 2014).

The goal of phosphate remediation is fully realized upon its accurate detection in the environment and biosensors developed for this purpose could satisfy the basic criteria of rapidity, accuracy and economics. In attempts to address limitations of currently available biosensors for phosphate, a simple EBP based biosensor was developed which could detect phosphate over a range of 1-10 mg/L and possessed stability for up to 28 days. Possibly with further modifications, the newly developed EBP biosensor will qualify for commercial viability.

Though at a laboratory scale, equilibrium studies provide valuable information on sorption process their applicability under field conditions are restricted by practical and economical concerns. The fixed bed column is a viable alternative which offers significant advantages over equilibrium studies and enhances amenability for field applications (Zeng et al., 2004; Krishnan and Haridas, 2008; Mohapatra et al., 2008; Huang et al., 2009; Xu et al., 2011c; Choi et al., 2012; Jalali and Peikam, 2013; Jiang et al., 2013; Pitakteeratham et al., 2013; Jeong et al., 2014; Keranen et al., 2015; Yang et al., 2015). One of the major advantages of fixed bed column is the reusability of sorbent which significantly reduces the overall cost of process. Another advantage of such assemblies is the availability of robust mathematical models which allow prediction of sorption behavior under different operational conditions. Thomas model is one of the most frequently applied model in fixed bed column studies and is related to Langmuir model of equilibrium sorption (Choi et al., 2012; Xu et al., 2013b). The sorption behavior of EBP in column studies also followed Thomas model and exhibited sorption capacity of 24.8 mg phosphate/g which is in good agreement with the value obtained in equilibrium sorption studies.

CONCLUSIONS

In summary, the work was aimed towards the following objectives:

1. Isolation, screening and identification of EBP-producing bacteria capable of phosphate binding

2. Development of mutants for enhanced EBP production

3. Statistical optimization of cultural parameters for high EBP yielding mutants

The overall aim of the present study was to isolate an EBP producing strain with potential applications in phosphate sensing and remediation.

The salient findings in this study are as follows:

1. Wastewater samples from 8 sources resulted in a total of 280 bacterial isolates of which 130 isolates were selected based on mucoid appearance. The strain exhibiting highest EBP production and highest phosphate removal was further investigated. The isolate was characterized by biochemical and molecular methods were and designated as *Acinetobacter haemolyticus* TK15. Screening for virulence markers revealed the strain to be non-virulent in nature.
2. Transposon mutagenesis was attempted to raise EBP-overproducing mutants and a total of 998 transconjugants were produced. Five transconjugants exhibited phosphate binding and the mutant exhibiting highest phosphate removal capacity with enhanced exobiopolymer production was selected. The selected mutant was designated as *A. haemolyticus* MG606.
3. Sequencing of Tn5 flanking region in *A. haemolyticus* MG606 showed the insertion occurred in a 9 bp motif located between positions -89 to -97 upstream of phosphoglucomutase/phosphomannomutase (PGM/PMM), a key biosynthetic enzyme

in EBP production pathway. PGM/PMM activity in cell lysates was found to be 1.5 fold higher in *A. haemolyticus* MG606 compared to *A. haemolyticus* TK15.

4. The specific activities of other enzymes involved in glucose assimilation in exobiopolymer (glucose-6-phosphate isomerase, UDP-glucose-4-epimerase and glucosyltransferases) were comparable (p>0.05) in *A. haemolyticus* MG606 and *A. haemolyticus* TK15.
5. PGM activity, determined by zymography, was 1.5-2 fold higher in the mutant compared to the isolate. Similarly, *pgm* expression was determined by real time PCR and found to be upregulated 1.3-1.7 fold in the mutant compared to the isolate.
6. For assuring safety during applications, *in vivo* toxicity studies were performed in Swiss albino mice. The LD_{50} for *A. haemolyticus* MG606 and its EBP were 12. 11 log CFU/animal and 92.1 mg/kg EBP, respectively. In vitro toxicity assessment in RAW 264.7 and A549 cell lines revealed no toxicity for up to 400 µg/mL EBP.
7. Surface structure of exobiopolymer was compact with abundant pores and grooves with high surface area. Biochemical characterization revealed the presence of polysaccharide and protein as major fractions with amino sugars, uronic acids and pyruvic acid as minor ones. Chemically, the exobiopolymer was heteropolysaccharide comprising of glucose, xylose, arabinose, ribose, galactose, allose, lyxose and mannose. The exobiopolymer was thermostable with viscoelastic properties showing shear-thinning, non-Newtonian, pseudoplastic behavior in solutions.
8. The optimum concentration of exobiopolymer for phosphate removal was found to be 100 mg/L over a contact time of 240 min. The results were validated mathematically using different sorption models. Langmuir isotherm was found to be favourable with maximum sorption efficiency (Qe) of 25 mg/g of exobiopolymer at the phosphate concentration of 5 mg/L.

9. To order to elucidate the mechanism of phosphate binding by exobiopolymer, battery of studies were performed. Uniform distribution of phosphate over EBP was demonstrated by SEM/EDS analysis. Significant reductions in phosphate binding by EBP after treatment with amylolytic and proteolytic enzymes suggest the role of polysaccharides and proteins in phosphate binding.
10. Based on the results of FTIR analysis, it was concluded that phosphate binds through electrostatic interactions with amino groups and with OH groups via a ligand exchange mechanism. The role of amino groups in phosphate binding was further confirmed by treating exobiopolymer with glutaraldehyde, an amine reactive compound which showed significant reduction in phosphate binding as compared to esterification of carboxyl groups with methanol or blockade of amide groups with formaldehyde.
11. The optimal culture conditions for the exobiopolymer production were found to be at the temperature of 35°C, pH of 6.5 when inoculum size of 1% is used at the agitation rate of 120 rpm.
12. *A. haemolyticus* MG606 uses glucose as preferable carbon source and ammonium sulphate as nitrogen source. Apart from C6 carbon sources, EBP yield was found to be maximum when acetate was used as a carbon source along with glucose at the concentration of 0.5 g/L.
13. The optimal concentrations of glucose, acetate and ammonium sulphate were statistically optimized with Response Surface Methodology and Central Composite Design. EBP yield was found to be highest at 5.454 g/L glucose, 4.506 g/L sodium acetate and 0.358 g/L ammonium sulphate in media.

14. The biomass production and EBP yield was fitted into Leudeking-Piret model and EBP production was found to be partially growth associated with α and β value of 0.12 and 0.007 respectively.
15. A biosensor was fabricated which utilizes phosphate-binding capacity of EBP to concentrate phosphate in water samples followed by analysis with stannous chloride method. The development of miniaturized sensors provides a convenient means of sample analysis at the site of collection. The limit of detection and limit of quantification was found to be 0.5 and 1 mg/L of phosphate, respectively. The fabricated biosensor probe was stable for up to 28 days.
16. A scalable phosphate removal system as key application of the EBP was achieved by alginate blended EBP hydrogels, used for column packing. The elution and sorption of phosphate on alginate-EBP hydrogel beads followed Thomas model. Breakthrough curves revealed that column service time decreases with an increase in influent phosphate concentration from 1 mg/L to 10 mg/L phosphate and with increase in flow rate from 10 mL/min to 30 mL/min.

In conclusion the present study conclusively demonstrated the potential of the *A. haemolyticus* EBP for practical purposes, especially for removal and maintaining the water quality budget of phosphate. Further studies are warranted for understanding the other facets of this interesting exobiopolymer.

REFERENCES

1. Adam, K., Krogstad, T., Vrale, L., Sovik, A. K. and Jenssen, P. D. (2007). Phosphorus retention in the filter materials shellsand and filtralite P (R)–batch and column experiment with synthetic P solution and secondary wastewater. Ecological Engineering 29: 200-208.

2. Adrio, J. L. and Demain, A. L. (2006). Genetic improvement of processes yielding microbial products. FEMS Microbiology Reviews 30: 187-214.

3. Aftab, M. N., Ikram Ul, H. and Baig, S. (2012). Systematic mutagenesis method for enhanced production of bacitracin by *Bacillus licheniformis* mutant strain UV-MN-HN-6. Brazilian Journal of Microbiology 43: 78-88.

4. Akinbile, C. O., Ogunrinde, T. A., Che Bt Man, H. and Aziz, H. A. (2015). Phytoremediation of domestic wastewaters in free water surface constructed wetlands using *Azolla pinnata*. International Journal of Phytoremediation (DOI: 10.1080/15226514.15222015.11058330).

5. Akpa, O. M. and Unuabonah, E. I. (2011). Small-sample corrected Akaike information criterion: an appropriate statistical tool for ranking of adsorption isotherm models. Desalination 272: 20-26.

6. Altundogan H. S, T. F. (2002). Removal of phosphorus from aqueous solutions by using bauxite. Effect of pH on the adsorption of various phosphates. Journal of Chemical Technology and Biotechnology 77: 77-85.

7. Alves, V. D., Freitas, F., Torres, C. A. V., Cruz, M., Marques, R., Grandfils, C., Gonacalves, M. P., Oliveira, R. and Reis, M. A. M. (2010). Rheological and morphological characterization of the culture broth during exopolysaccharide production by *Enterobacter* sp. Carbohydrate Polymers 81: 758-764.

8. Amiri-Jami, M., Wang, H., Kakuda, Y. and Griffiths, M. W. (2006). Enhancement of polyunsaturated fatty acid production by Tn5 transposon in *Shewanella baltica*. Biotechnology Letters 28: 1187-1192.

9. Andersen, J. M., Barrangou, R., Abou Hachem, M., Lahtinen, S. J., Goh, Y. J., Svensson, B. and Klaenhammer, T. R. (2013). Transcriptional analysis of

oligosaccharide utilization by *Bifidobacterium lactis* Bl-04. BMC Genomics 14: 312.

10. APHA (American Public Health Association) (1998). Standard methods for the examination of water and wastewater, 20 ed. Washington, DC.

11. Arbib, Z., Ruiz, J., Alvarez-Diaz, P., Garrido-Perez, C. and Perales, J. A. (2014). Capability of different microalgae species for phytoremediation processes: wastewater tertiary treatment, CO_2 bio-fixation and low cost biofuels production. Water Research 49: 465-474.

12. Arnaldos, M. and Pagilla, K. (2010). Effluent dissolved organic nitrogen and dissolved phosphorus removal by enhanced coagulation and microfiltration. Water Research 44: 5306-5315.

13. Aronson, B. D., Levinthal, M. and Somerville, R. L. (1989). Activation of a cryptic pathway for threonine metabolism via specific IS3-mediated alteration of promoter structure in *Escherichia coli*. Journal of Bacteriology 171: 5503-5511.

14. Ason, B. and Reznikoff, W. S. (2004). DNA Sequence bias during Tn5 transposition. Journal of Molecular Biology 335: 1213-1225.

15. Audy, J., Labrie, S., Roy, D. and LaPointe, G. l. (2010). Sugar source modulates exopolysaccharide biosynthesis in *Bifidobacterium longum* subsp. longum CRC 002. Microbiology 156: 653-664.

16. Avril, J. L. and Mesnard, R. (1991). Factors influencing the virulence of *Acinetobacter*. In: The Biology of *Acinetobacter*. Ed. K. J. Towner, E. Bergogne-Berezin and C. A. Fewson, Springer, US.

17. Awan, M. S., Tabbasam, N., Ayub, N., Babar, M. E., Mehboob ur, R., Rana, S. M. and Rajoka, M. I. (2011). Gamma radiation induced mutagenesis in *Aspergillus niger* to enhance its microbial fermentation activity for industrial enzyme production. Molecular Biology Reports 38: 1367-1374.

18. Awuah, E., Oppong-Peprah, M., Lubberding, H. J. and Gijzen, H. J. (2004). Comparative performance studies of water lettuce, duckweed, and algal-based

stabilization ponds using low-strength sewage. Journal of Toxicology and Environmental Health, Part A 67: 1727-1739.

19. Aydin, I., Aydin, F., Saydut, A. and Hamamci, C. (2009). A sequential extraction to determine the distribution of phosphorus in the seawater and marine surface sediment. Journal of Hazardous Materials 168: 664-669.

20. Babatunde, A. O. and Zhao, Y. Q. (2010). Equilibrium and kinetic analysis of phosphorus adsorption from aqueous solution using waste alum sludge. Journal of Hazardous Materials 184: 746-752.

21. Bajaj, I. and Singhal, R. (2011). Poly (glutamic acid) an emerging biopolymer of commercial interest. Bioresource Technology 102: 5551-5561.

22. Bajaj, S. B., Survase, S. A., Saudagar, P. S. and Singhal, R. S. (2007). Gellan gum: fermentative production, downstream processing and applications. Food Technology and Biotechnology 45: 341-354.

23. Bales, P. M., Renke, E. M., May, S. L., Shen, Y. and Nelson, D. C. (2013). Purification and characterization of biofilm-associated EPS exopolysaccharides from ESKAPE organisms and other pathogens. PLoS One 8: e67950.

24. Barat, R., Montoya, T., Seco, A. and Ferrer, J. (2011). Modelling biological and chemically induced precipitation of calcium phosphate in enhanced biological phosphorus removal systems. Water Research 45: 3744-3752.

25. Barquist, L., Boinett, C. J. and Cain, A. K. (2013). Approaches to querying bacterial genomes with transposon-insertion sequencing. RNA Biology 10: 1161-1169.

26. Bauer, A. W., Kirby, W. M., Sherris, J. C. and Turck, M. (1966). Antibiotic susceptibility testing by a standardized single disk method. American Journal of Clinical Pathology 45: 493-496.

27. Beutel, M. W. (2012). Water quality in a surface-flow constructed treatment wetland polishing tertiary effluent from a municipal wastewater treatment plant. Water Science & Technology 66: 1977–1983.

28. Bellier, N., Chazarenc, F. and Comeau, Y. (2006). Phosphorus removal from wastewater by mineral apatite. Water Research 40: 2965-2971.

29. Belocopitow, E. and Marehal, L. R. (1974). Metabolism of trehalose in *Euglena gracilis*. European Journal of Biochemistry 46: 631-637.

30. Berg, D. E. (1980). Control of gene expression by a mobile recombinational switch. PNAS 77: 4880-4884.

31. Berg, D. E., Schmandt, M. A. and Lowe, J. B. (1983). Specificity of transposon Tn5 insertion. Genetics 105: 813-828.

32. Berg, D. E., Weiss, A. and Crossland, L. (1980). Polarity of Tn5 insertion mutations in *Escherichia coli*. Journal of Bacteriology 142: 439-446.

33. Bergey, D. H. and Holt, J. G. (1994). Bergey's Manual of Determinative Bacteriology, Williams & Wilkins, Baltimore, USA

34. Bhavani, A. L. and Nisha, J. (2010). Dextran - the polysaccharide with versatile uses. International Journal of Pharma and Bio Sciences 1: 569-573.

35. Bi, D., Guo, X., Cai, Z., Gao, X., Li, Y., Guo, J., Long, X., Zhong, Z. and Liang, Y. (2012). Characteristics of various forms of phosphorus and their relationships in the sediments of Haizi Lake, China. Water Science and Technology 66: 2688-2694.

36. Biswas, B. K., Inoue, K., Ghimire, K. N., Ohta, S., Harada, H., Ohto, K. and Kawakita, H. (2007). The adsorption of phosphate from an aquatic environment using metal-loaded orange waste. Journal of Colloid and Interface Science 312: 214-223.

37. Bitrian, M., Solari, C. M., Gonzalez, R. H. and Nudel, C. B. (2012). Identification of virulence markers in clinically relevant strains of *Acinetobacter* genospecies. International Microbiology 15: 79-88.

38. Blackall, L. L., Crocetti, G. R., Saunders, A. M. and Bond, P. L. (2002). A review and update of the microbiology of enhanced biological phosphorus removal in wastewater treatment plants. Antonie Van Leeuwenhoek 81: 681-691.

39. Blackall, L. L., Seviour, E. M., Bradford, D., Rossetti, S., Tandoi, V. and Seviour, R. J. (2000). *'Candidatus Nostocoida limicola*', a filamentous bacterium from activated sludge. International Journal of Systematic and Evolutionary Microbiology 50: 703-709.

40. Boels, I. C., Kleerebezem, M. and de Vos, W. M. (2003). Engineering of carbon distribution between glycolysis and sugar nucleotide biosynthesis in *Lactococcus lactis*. Applied and Environmental Microbiology 69: 1129-1135.

41. Boels, I. C., Ramos, A., Kleerebezem, M. and de Vos, W. M. (2001). Functional analysis of the *Lactococcus lactis* galU and galE genes and their impact on sugar nucleotide and exopolysaccharide biosynthesis. Applied and Environmental Microbiology 67: 3033-3040.

42. Boeriu, C. G., Springer, J., Kooy, F. K., van den Broek, L. A. M. and Eggink, G. (2013). Production methods for hyaluronan. International Journal of Carbohydrate Chemistry 2013: 14.

43. Bonin, C. P. and Reiter, W. D. (2000). A bifunctional epimerase-reductase acts downstream of the MUR1 gene product and completes the de novo synthesis of GDP-L-fucose in *Arabidopsis*. The Plant Journal 21: 445-454.

44. Bosse, J. T., Zhou, L., Kroll, J. S. and Langford, P. R. (2006). High-throughput identification of conditionally essential genes in bacteria: from STM to TSM. Infectious Disorders Drug Targets 6: 241-262.

45. Boswell, C. D., Dick, R. E., Eccles, H. and Macaskie, L. E. (2001). Phosphate uptake and release by *Acinetobacter johnsonii* in continuous culture and coupling of phosphate release to heavy metal accumulation. Journal of Industrial Microbiology & Biotechnology 26: 333-340.

46. Bouwman, L., Goldewijk, K. K., Hoek, K. W. V. D., Beusen, A. H. W., Vuuren, D. P. V., Willems, J., Rufino, M. C. and Stehfest, E. (2013). Exploring global changes in nitrogen and phosphorus cycles in agriculture induced by livestock production over the 1900-2050 period. PNAS 110: 20882-20887.

47. Boyd, L. A., Woytowich, A. and Selvaraj, G. (1993). Target sequence specificity of transposon Tn5 in the absence of major hotspots in the plasmid pBR322: identification of a new hotspot. Plasmid 30: 155-158.

48. Brandenburg, K., Andra, J., Muller, M., Koch, M. H. J. and Garidel, P. (2003). Physicochemical properties of bacterial glycopolymers in relation to bioactivity. Carbohydrate Research 338: 2477-2489.

49. Breslow, J. M., Meissler, J. J., Hartzell, R. R., Spence, P. B., Truant, A., Gaughan, J. and Eisenstein, T. K. (2011). Innate immune responses to systemic *Acinetobacter baumannii* infection in mice: neutrophils, but not interleukin-17, mediate host resistance. Infection and Immunity 79: 3317-3327.

50. Buthelezi, S., Olaniran, A. and Pillay, B. (2010). Production and characterization of bioflocculants from bacteria isolated from wastewater treatment plant in South Africa. Biotechnology and Bioprocess Engineering 15: 874-881.

51. Cai, P., Zheng, H., Wang, C., Ma, H., Hu, J., Pu, Y. and Liang, P. (2012). Competitive adsorption characteristics of fluoride and phosphate on calcined Mg-Al-CO_3 layered double hydroxides. Journal of Hazardous Materials 213-214: 100-108.

52. Camarena, L., Poggio, S., Campos, A., Bastarrachea, F. and Osorio, A. (1998). An IS4 insertion at the glnA control region of *Escherichia coli* creates a new promoter by providing the −35 region of its 3′-end. Plasmid 39: 41-47.

53. Carpenter, S. R. and Bennett, E. M. (2011). Reconsideration of the planetary boundary for phosphorus. Environmental Research Letters 6: 014009.

54. Castellanos Martinez, E., Telenti Asensio, M., Rodriguez Blanco, V. M., Rodriguez Suarez, M. L., Morena Torrico, A. and Cortina Llosa, A. (1995). Infective endocarditis of an interventricular patch caused by *Acinetobacter haemolyticus*. Infection 23: 243-245.

55. Cerning, J., Renard, C. M., Thibault, J. F., Bouillanne, C., Landon, M., Desmazeaud, M. and Topisirovic, L. (1994). Carbon source requirements for

exopolysaccharide production by *Lactobacillus casei* CG11 and partial structure analysis of the polymer. Applied and Environmental Microbiology 60: 3914-3919.

56. Chai, Y., Beauregard, P. B., Vlamakis, H., Losick, R. and Kolter, R. (2012). Galactose metabolism plays a crucial role in biofilm formation by *Bacillus subtilis*. MBio 3: e00184-001812.

57. Chalot, M., Blaudez, D., Rogaume, Y., Provent, A. S. and Pascual, C. (2012). Fate of trace elements during the combustion of phytoremediation wood. Environmental Science & Technology 46: 13361-13369.

58. Chassenieux, C., Durand, D., Jyotishkumar, P. and Thomas, S. (2013). Biopolymers: State of the art, new challenges, and opportunities. In: Handbook of biopolymer based materials: From blends and composites to gels and complex networks. Ed. S. Thomas, D. Durand, C. Chassenieux and P. Jyotishkumar, Wiley-VCH.

59. Chatterjee, A., Cui, Y., Liu, Y., Dumenyo, C. K. and Chatterjee, A. K. (1995). Inactivation of rsmA leads to overproduction of extracellular pectinases, cellulases, and proteases in *Erwinia carotovora* subsp. *carotovora* in the absence of the starvation/cell density-sensing signal, N-(3-oxohexanoyl)-L-homoserine lactone. Applied and Environmental Microbiology 61: 1959-1967.

60. Chen, H., Wu, J., Yang, L. and Xu, G. (2013). A combination of site-directed mutagenesis and chemical modification to improve diastereopreference of *Pseudomonas alcaligenes* lipase. Biochimica et Biophysica Aacta 1834: 2494-2501.

61. Chen, J., Kong, H., Wu, D., Chen, X., Zhang, D. and Sun, Z. (2007). Phosphate immobilization from aqueous solution by fly ashes in relation to their composition. Journal of Hazardous Materials 139: 293-300.

62. Cheng, K. C., Demirci, A. and Catchmark, J. M. (2011). Pullulan: biosynthesis, production, and applications. Applied Microbiology and Biotechnology 92: 29-44.

63. Chew, S. C., Kundukad, B., Seviour, T., van der Maarel, J. R., Yang, L., Rice, S. A., Doyle, P. and Kjelleberg, S. (2014). Dynamic remodeling of microbial biofilms by functionally distinct exopolysaccharides. MBio 5: e01536-01514.

64. Chiemchaisri, C., Panchawaranon, C., Rutchatanunti, S., Kludpiban, A., Ngo, H. H. and Vigneswaran, S. (2003). Development of floating plastic media filtration system for water treatment and wastewater reuse. Journal of Environmental Science and Health. Part A, Toxic/hazardous Substances & Environmental Engineering 38: 2359-2368.

65. Chien, C.C., Lin, B.C. and Wu, C.H. (2013). Biofilm formation and heavy metal resistance by an environmental *Pseudomonas* sp. Biochemical Engineering Journal 78: 132-137.

66. Childers, D. L., Corman, J., Edwards, M. and Elser, J. J. (2011). Sustainability challenges of phosphorus and food: solutions from closing the human phosphorus cycle. BioScience 61: 117-124.

67. Chimenos, J. M., Fernandez, A. I., Hernandez, A., Haurie, L., Espiell, F. and Ayora, C. (2006). Optimization of phosphate removal in anodizing aluminium wastewater. Water Research 40: 137-143.

68. Chimenos, J. M., Fernandez, A. I., Villalba, G., Segarra, M., Urruticoechea, A., Artaza, B. and Espiell, F. (2003). Removal of ammonium and phosphates from wastewater resulting from the process of cochineal extraction using MgO-containing by-product. Water Research 37: 1601-1607.

69. Chislock, M. F., Doster, E., Zitomer, R. A. and Wilson, A. E. (2013). Eutrophication: causes, consequences, and controls in aquatic ecosystems. Nature Education Knowledge 4: 10.

70. Chitrakar, R., Tezuka, S., Sonoda, A., Sakane, K., Ooi, K. and Hirotsu, T. (2006). Phosphate adsorption on synthetic goethite and akaganeite. Journal of Colloid and Interface Science 298: 602-608.

71. Cho, J., Song, K. G. and Ahn, K. H. (2009). Contribution of microfiltration on phosphorus removal in the sequencing anoxic/anaerobic membrane bioreactor. Bioprocess and Biosystem Engineering 32: 593-602.

72. Choi, J. W., Hong, S. W., Kim, D. J. and Lee, S. H. (2012). Investigation of phosphate removal using sulphate-coated zeolite for ion exchange. Environmental Technology 33: 2329-2335.

73. Choi, K. H. and Kim, K. J. (2009). Applications of transposon-based gene delivery system in bacteria. Journal of Microbiology and Biotechnology 19: 217-228.

74. Choi, S. H., Choo, E. J., Kwak, Y. G., Kim, M. Y., Jun, J. B., Kim, M. N., Kim, N. J., Jeong, J. Y., Kim, Y. S. and Woo, J. H. (2006). Clinical characteristics and outcomes of bacteremia caused by Acinetobacter species other than *A. baumannii*: comparison with *A. baumannii* bacteremia. Journal of Infection and Chemotherapy 12: 380-386.

75. Chu, K. H. (2014). Discrimination of rival isotherm equations for aqueous contaminant removal systems Advances in Environmental Research 3: 131-149.

76. Ciampi, M. S., Schmid, M. B. and Roth, J. R. (1982). Transposon Tn10 provides a promoter for transcription of adjacent sequences. PNAS 79: 5016-5020.

77. Cimini, D., Carlino, E., Giovane, A., Argenzio, O., Dello Iacono, I., De Rosa, M. and Schiraldi, C. (2015). Engineering a branch of the UDP-precursor biosynthesis pathway enhances the production of capsular polysaccharide in *Escherichia coli* O5:K4:H4. Biotechnology Journal (DOI: 10.1002/biot.201400602).

78. CIR (Cosmetic Ingredients Review) (2012). Safety assessment of microbial polysaccharide gums as used in cosmetics, Washington DC.

79. Cirigliano, M. C. and Carman, G. M. (1985). Purification and characterization of liposan, a bioemulsifier from *Candida lipolytica*. Applied and Environmental Microbiology 50: 846-850.

80. Civerolo, E. L., Collmer, A., Davis, R. E., Gillaspie, A. G., Kuykendall, L. D., Roy, M. A. and Baker, C. J. (1987). Use of plasmid vector pGS9 to introduce

transposon Tn5 into pathovars of *Pseudomonas Syringae*. Plant Pathogenic Bacteria, 4: 434-438.

81. Clark, A. J., Satin, L. and Chu, C. C. (1994). Transcription of the *Escherichia coli* recE gene from a promoter in Tn5 and IS50. Journal of Bacteriology 176: 7024-7031.

82. Cloete, T. E. and Oosthuizen, D. J. (2001). The role of extracellular exopolymers in the removal of phosphorus from activated sludge. Water Research 35: 3595-3598.

83. Collins, K. D. (2004). Ions from the Hofmeister series and osmolytes: effects on proteins in solution and in the crystallization process. Methods 34: 300-311.

84. Combie, J. (2006). Properties of levan and potential medical uses. In: Polysaccharides for drug delivery and pharmaceutical applications, American Chemical Society, Lavington, Rock Hill, SC.

85. Compton, J., Mallinson, D., Glenn, C., Filippelli, G., Follmi, K., Shields, G. and Zanin, Y. (2000). Variations in the global phosphorus cycle. In: SEPM Special Publication 66, Marine Authigenesis: From Microbial to Global, Ed. C. Glenn, L. Prevot-Lucas and J. Lucas.

86. Cui, S. W. (2005). Structural analysis of polysaccharides. In: Food Carbohydrates Chemistry, Physical Properties, and Applications, CRC Press, Boca Raton.

87. Cupp-Enyard, C. (2008). Sigma's non-specific protease activity assay - casein as a substrate. Journal of Visualized Experiments: JoVE899.

88. Cursino, L., Athinuwat, D., Patel, K. R., Galvani, C. D., Zaini, P. A., Li, Y., De La Fuente, L., Hoch, H. C., Burr, T. J. and Mowery, P. (2015). Characterization of the *Xylella fastidiosa* PD1671 gene encoding degenerate c-di-GMP GGDEF/EAL domains, and its role in the development of Pierce's disease. PLoS One 10: e0121851.

89. Dai, J., Yang, H., Yan, H., Shangguan, Y., Zheng, Q. and Cheng, R. (2011). Phosphate adsorption from aqueous solutions by disused adsorbents: Chitosan hydrogel beads after the removal of copper(II). Chemical Engineering Journal 166: 970-977.

90. Dams-Kozlowska, H., Mercaldi, M. P., Panilaitis, B. J. and Kaplan, D. L. (2008). Modifications and applications of the *Acinetobacter venetianus* RAG-1 exopolysaccharide, the emulsan complex and its components. Applied Microbiology and Biotechnology 81: 201-210.

91. Darkoh, C., Kaplan, H. B. and Dupont, H. L. (2011). Harnessing the glucosyltransferase activities of *Clostridium difficile* for functional studies of toxins A and B. Journal of Clinical Microbiology 49: 2933-2941.

92. Davies, D. G., Chakrabarty, A. M. and Geesey, G. G. (1993). Exopolysaccharide production in biofilms: substratum activation of alginate gene expression by *Pseudomonas aeruginosa*. Applied and Environmental Microbiology 59: 1181-1186.

93. De Vuyst, L. and Degeest, B. (1999). Heteropolysaccharides from lactic acid bacteria. FEMS Microbiology Reviews 23: 153-177.

94. De Vuyst, L., Vanderveken, F., Van de Ven, S. and Degeest, B. (1998). Production by and isolation of exopolysaccharides from *Streptococcus thermophilus* grown in a milk medium and evidence for their growth-associated biosynthesis. Journal of Applied Microbiology 84: 1059-1068.

95. Degeest, B., Janssens, B. and De Vuyst, L. (2001). Exopolysaccharide (EPS) biosynthesis by *Lactobacillus sakei* 0-1: production kinetics, enzyme activities and EPS yields. Journal of Applied Microbiology 91: 470-477.

96. Deng, S., Bai, R., Hu, X. and Luo, Q. (2003). Characteristics of a bioflocculant produced by *Bacillus mucilaginosus* and its use in starch wastewater treatment. Applied Microbiology and Biotechnology 60: 588-593.

97. Derkx, P. M., Janzen, T., Sorensen, K. I., Christensen, J. E., Stuer-Lauridsen, B. and Johansen, E. (2014). The art of strain improvement of industrial lactic acid bacteria without the use of recombinant DNA technology. Microbial Cell Factories 13 S5.

98. Devos, Y., Aguilera, J., Diveki, Z., Gomes, A., Liu, Y., Paoletti, C., du Jardin, P., Herman, L., Perry, J. N. and Waigmann, E. (2014). EFSA's scientific activities and

achievements on the risk assessment of genetically modified organisms (GMOs) during its first decade of existence: looking back and ahead. Transgenic Research 23: 1-25.

99. Di Luca, G. A., Maine, M. A., Mufarrege, M. M., Hadad, H. R. and Bonetto, C. A. (2015). Influence of *Typha domingensis* in the removal of high P concentrations from water. Chemosphere 138: 405-411.

100. Dietze, A., Gnirss, R. and Wiesmann, U. (2002). Phosphorus removal with membrane filtration for surface water treatment. Water Science and Technology 46: 257-264.

101. Dimopoulou, M., Vuillemin, M., Campbell-Sills, H., Lucas, P. M., Ballestra, P., Miot-Sertier, C., Favier, M., Coulon, J., Moine, V., Doco, T., Roques, M., Williams, P., Petrel, M., Gontier, E., Moulis, C., Remaud-Simeon, M. and Dols-Lafargue, M. (2014). Exopolysaccharide (EPS) synthesis by *Oenococcus oeni*: from genes to phenotypes. PLoS One 9: e98898.

102. Ding, W., Zhu, R., Hou, L. and Wang, Q. (2014). Matrix-bound phosphine, phosphorus fractions and phosphatase activity through sediment profiles in Lake Chaohu, China. Environmental Science: Processes & Impacts 16: 1135-1144.

103. Djordjevic, D., Wiedmann, M. and McLandsborough, L. A. (2002). Microtiter plate assay for assessment of *Listeria monocytogenes* biofilm formation. Applied and Environmental Microbiology 68: 2950-2958.

104. Domingos, A. K., Saad, E. B., Wilhelm, H. M. and Ramos, L. P. (2008). Optimization of the ethanolysis of *Raphanus sativus* (L. Var.) crude oil applying the response surface methodology. Bioresource Technology 99: 1837-1845.

105. Doughari, H. J., Ndakidemi, P. A., Human, I. S. and Benade, S. (2011). The ecology, biology and pathogenesis of *Acinetobacter* spp.: an overview. Microbes and Environments 26: 101-112.

106. Drizo, A., Frost, C. A., Grace, J. and Smith, K. A. (1999). Physico-chemical screening of phosphate-removing substrates for use in constructed wetland systems. Water Research 33 3595-3602.

107. DuBois, M., Gilles, K. A., Hamilton, J. K., Rebers, P. A. and Smith, F. (1956). Colorimetric method for determination of sugars and related substances. Analytical Chemistry 28: 350-356.

108. Dubey, S., Singh, A. and Banerjee, U. C. (2011). Response surface methodology of nitrilase production by recombinant *Escherichia coli*. Brazilian Journal of Microbiology 42: 1085-1092.

109. Dumbrepatil, A., Adsul, M., Chaudhari, S., Khire, J. and Gokhale, D. (2008). Utilization of molasses sugar for lactic acid production by *Lactobacillus delbrueckii* subsp. delbrueckii mutant Uc-3 in batch fermentation. Applied and Environmental Microbiology 74: 333-335.

110. Dunne, C., Moenne-Loccoz, Y., de Bruijn, F. J. and O'Gara, F. (2000). Overproduction of an inducible extracellular serine protease improves biological control of *Pythium ultimum* by *Stenotrophomonas maltophilia* strain W81. Microbiology 146: 2069-2078.

111. Eberhardt, T. L., Min, S.-H. and Han, J. S. (2006). Phosphate removal by refined aspen wood fiber treated with carboxymethyl cellulose and ferrous chloride. Bioresource Technology 97: 2371-2376.

112. EC (European Commission) (2013). Consultative communication on the sustainable use of phosphorus. (http://ec.europa.eu/environment/consultations/phosphorus_en. htm) (Assessed on 28 July 2015).

113. EFHS biology I: Biogeochemical cycles (http://moodleblogs.dearbornschools.org/WP3-QKZLJJ81/chapter/phosphorus-cycle) (Assessed on 28 July 2015).

114. Elghniji, K., Saad, M. E. K., Araissi, M., Elaloui, E. and Moussaoui, Y. (2014). Chemical modification of TiO_2 by H_2PO_4 /HPO_4^{2-} anions using the sol-gel route with controlled precipitation and hydrolysis: enhancing thermal stability. Materials Science-Poland 32: 617-625.

115. Elson, L. A. and Morgan, W. T. (1933). A colorimetric method for the determination of glucosamine and chondrosamine. The Biochemical Journal 27: 1824-1828.

116. Elzinga, E. J. and Sparks, D. L. (2007). Phosphate adsorption onto hematite: an in situ ATR-FTIR investigation of the effects of pH and loading level on the mode of phosphate surface complexation. Journal of Colloid and Interface Science 308: 53-70.

117. EPA (Environment Protection Agency) (2013). Emerging technologies for wastewater treatment and in-plant wet weather management EPA 832-R-12-011.

118. Erickson, A. J., Gulliver, J. S. and Weiss, P. T. (2012). Capturing phosphates with iron enhanced sand filtration. Water Research 46: 3032-3042.

119. Escalante, A., Villegas, J., Wacher, C., Garcia-Garibay, M. and Farres, A. (2002). Activity of the enzymes involved in the synthesis of exopolysaccharide precursors in an overproducing mutant ropy strain of *Streptococcus thermophilus*. FEMS Microbiology Letters 209: 289-293.

120. Fang, Z., Long, X., Tang, R., Zhou, C., Feng, Y. and Wang, S. (2011). The phosphorus incorporation property of extracellular polymer substances. Acta Scientiae Circumstantiae 31: 2374-2379.

121. Filippelli, G. M. (2002). The global phosphorus cycle. Reviews in Mineralogy and Geochemistry 48: 391-425.

122. Filippelli, G. M. (2008). The global phosphorus cycle: past, present, and future. Elements 4: 89-95.

123. Foo, K. Y. and Hameed, B. H. (2010). Insights into the modeling of adsorption isotherm systems. Chemical Engineering Journal 156: 2-10.

124. Foucault, Y., Leveque, T., Xiong, T., Schreck, E., Austruy, A., Shahid, M. and Dumat, C. (2013). Green manure plants for remediation of soils polluted by metals and metalloids: ecotoxicity and human bioavailability assessment. Chemosphere 93: 1430-1435.

125. Franklin, M. J., Nivens, D. E., Weadge, J. T. and Howell, P. L. (2011). Biosynthesis of the *Pseudomonas aeruginosa e*xtracellular polysaccharides, alginate, Pel, and Psl. Frontiers in Microbiology 2: 1-16.

126. Freitas, F., Alves, V. D. and Reis, M. A. (2011). Advances in bacterial exopolysaccharides: from production to biotechnological applications. Trends in Biotechnology 29: 388-398.

127. Frengova, G. I., Simova, E. D. and Beshkova, D. M. (2004). Improvement of carotenoid-synthesizing yeast *Rhodotorula rubra* by chemical mutagenesis. Zeitschrift fur Naturforschung. C, Journal of Biosciences 59: 99-103.

128. Friedemann, T. E. and Haugen, G. E. (1943). Pyruvic acid. II. The determination of keto acids in blood and urine. Journal of Biological Chemistry 147: 415-442.

129. Fuhs, G. W. and Chen, M. (1975). Microbiological basis of phosphate removal in the activated sludge process for the treatment of wastewater. Microbial Ecology 2: 119-138.

130. Gamar-Nourani, L., Blondeau, K. and Simonet, J. M. (1998). Influence of culture conditions on exopolysaccharide production by *Lactobacillus rhamnosus* strain C83. Journal of Applied Microbiology 85: 664-672.

131. Garcia-Ochoa, F., Santos, V. E., Casas, J. A. and Gomez, E. (2000). Xanthan gum: production, recovery, and properties. Biotechnology Advances 18: 549-579.

132. Garrigues, C., Loubiere, P., Lindley, N. D. and Cocaign-Bousquet, M. (1997). Control of the shift from homolactic acid to mixed-acid fermentation in *Lactococcus lactis*: predominant role of the NADH/NAD+ ratio. Journal of Bacteriology 179: 5282-5287.

133. Gebremariam, S. Y., Beutel, M. W., Christian, D. and Hess, T. F. (2011). Research advances and challenges in the microbiology of enhanced biological phosphorus removal--a critical review. Water Environment Research 83: 195-219.

134. Gerardo, M. L., Zacharof, M. P. and Lovitt, R. W. (2013). Strategies for the recovery of nutrients and metals from anaerobically digested dairy farm sludge using cross-flow microfiltration. Water Research 47: 4833-4842.

135. Gersberg, R. M. and Allen, D. W. (1985). Phosphorus uptake by *Klebsiella pneumoniae* and *Acinetobacter calcoacetics*. Water Science and Technology 17: 113-118.

136. Ghafoor, A., Hay, I. D. and Rehm, B. H. (2011). Role of exopolysaccharides in *Pseudomonas aeruginosa* biofilm formation and architecture. Applied and Environmental Microbiology 77: 5238-5246.

137. Ghazi, S., Sepahy, A. A., Azin, M., Khaje, K. and Khavarinejad, R. (2014). UV mutagenesis for the overproduction of xylanase from *Bacillus mojavensis* PTCC 1723 and optimization of the production condition. Iranian Journal of Basic Medical Sciences 17: 844-853.

138. Ghosh, M., Ganguli, A. and Mallik, M. (2006). Evidence of indigenous NAH plasmid of naphthalene degrading *Pseudomonas putida* PpG7 strain implicated in limonin degradation. Journal of Microbiology and Biotechnology 44: 473-479.

139. Ghosh, M., Ganguli, A. and Pathak, S. (2009). Application of a novel biopolymer for removal of *Salmonella* from poultry wastewater. Environmental Technology 30: 337-344.

140. Giacometti, A., Cirioni, O., Ghiselli, R., Bergnach, C., Orlando, F., D'Amato, G., Mocchegiani, F., Silvestri, C., Del Prete, M. S., Skerlavaj, B., Saba, V., Zanetti, M. and Scalise, G. (2004). The antimicrobial peptide BMAP-28 reduces lethality in mouse models of staphylococcal sepsis. Critical Care Medicine 32: 2485-2490.

141. Gibson, K. E., Campbell, G. R., Lloret, J. and Walker, G. C. (2006). CbrA is a stationary-phase regulator of cell surface physiology and legume symbiosis in *Sinorhizobium meliloti*. Journal of Bacteriology 188: 4508-4521.

142. Giel, M., Desnoyer, M. and Lopilato, J. (1996). A mutation in a new gene, bglJ, activates the bgl operon in *Escherichia coli* K-12. Genetics 143: 627-635.

143. Gonzalez, A. G., Shirokova, L. S., Pokrovsky, O. S., Emnova, E. E., Martinez, R. E., Santana-Casiano, J. M., Gonzalez-Davila, M. and Pokrovski, G. S. (2010). Adsorption of copper on *Pseudomonas aureofaciens*: protective role of surface exopolysaccharides. Journal of Colloid and Interface Science 350: 305-314.

144. Goryshin, I. Y., Miller, J. A., Kil, Y. V., Lanzov, V. A. and Reznikoff, W. S. (1998). Tn5/IS50 target recognition. PNAS 95: 10716-10721.

145. Green, B., Bouchier, C., Fairhead, C., Craig, N. L. and Cormack, B. P. (2012). Insertion site preference of Mu, Tn5, and Tn7 transposons. Mobile DNA 3: 3.

146. Grinberg, T. A., Pirog, T. P., Malashenko, Y. R. and Vlasov, S. A. (1995). Ethapolan: a new microbial exopolysaccharide for oil industry. Energy & Fuels 9: 1086-1089.

147. Grobben, G. J., Chin-Joe, I., Kitzen, V. A., Boels, I. C., Boer, F., Sikkema, J., Smith, M. R. and de Bont, J. A. (1998). Enhancement of exopolysaccharide production by *Lactobacillus delbrueckii* subsp. *bulgaricus* NCFB 2772 with a simplified defined medium. Applied and Environmental Microbiology 64: 1333-1337.

148. Grotiuz, G., Sirok, A., Gadea, P., Varela, G. and Schelotto, F. (2006). Shiga toxin 2-producing *Acinetobacter haemolyticus* associated with a case of bloody diarrhea. Journal of Clinical Microbiology 44: 3838-3841.

149. Gu, D., Xu, H., He, Y., Zhao, F. and Huang, M. (2015). Remediation of urban river water by *Pontederia cordata* combined with artificial aeration: Organic matter and nutrients removal and root-adhered bacterial communities. International Journal of Phytoremediation 2015: 0.

150. Gu, X., Lee, S. G. and Bar-Peled, M. (2011). Biosynthesis of UDP-xylose and UDP-arabinose in *Sinorhizobium meliloti* 1021: first characterization of a bacterial UDP-xylose synthase, and UDP-xylose 4-epimerase. Microbiology 157: 260-269.

151. Guibaud, G., Tixier, N., Bouju, A. and Baudu, M. (2003). Relation between extracellular polymerase composition and its ability to complex Cd, Cu and Pb. Chemosphere 52: 1701-1710.

152. Guine, V., Spadini, L., Sarret, G., Muris, M., Delolme, C., Gaudet, J. P. and Martins, J. M. (2006). Zinc sorption to three gram-negative bacteria: combined titration, modeling, and EXAFS study. Environmental Science & Technology 40: 1806-1813.

153. Gupta, P., Roy, S. and Mahindrakar, A. B. (2012). Treatment of water using water hyacinth, water lettuce and vetiver crass - a review. Resources and Environment 2: 202-215.

154. Hanada, S., Liu, W. T., Shintani, T., Kamagata, Y. and Nakamura, K. (2002). *Tetrasphaera elongata* sp. nov., a polyphosphate-accumulating bacterium isolated from activated sludge. International Journal of Systematic and Evolutionary Microbiology 52: 883-887.

155. Harper, A. D. and Bar-Peled, M. (2002). Biosynthesis of UDP-xylose. Cloning and characterization of a novel *Arabidopsis* gene family, UXS, encoding soluble and putative membrane-bound UDP-glucuronic acid decarboxylase isoforms. Plant Physiology 130: 2188-2198.

156. Hasan, S. W., Elektorowicz, M. and Oleszkiewicz, J. A. (2014). Start-up period investigation of pilot-scale submerged membrane electro-bioreactor (SMEBR) treating raw municipal wastewater. Chemosphere 97: 71-77.

157. Haug, A. and Larsen, B. (1962). Quantitative determination of the uronic acid composition of alginates. Acta Chemica Scandinavica 16: 1908-1918.

158. Hecker, M., Riethdorf, S., Bauer, C., Schroeter, A. and Borriss, R. (1988). Expression of a cloned beta-glucanase gene from *Bacillus amyloliquefaciens* in an *Escherichia coli* relA strain after plasmid amplification. Molecular and General Genetics 215: 181-183.

159. Hidalgo-Cantabrana, C., Sanchez, B., Milani, C., Ventura, M., Margolles, A. and Ruas-Madiedo, P. (2014). Genomic overview and biological functions of exopolysaccharide biosynthesis in *Bifidobacterium* spp. Applied and Environmental Microbiology 80: 9-18.

160. Ho, Y.S. (2004). Selection of optimum sorption isotherm. Carbon 42: 2115-2116.

161. Hofmann, C., Boll, R., Heitmann, B., Hauser, G., Durr, C., Frerich, A., Weitnauer, G., Glaser, S. J. and Bechthold, A. (2005). Genes encoding ezymes responsible for biosynthesis of L-lyxose and attachment of eurekanate during avilamycin biosynthesis. Chemistry & Biology 12: 1137-1143.

162. Hong, H. A., Huang, J. M., Khaneja, R., Hiep, L. V., Urdaci, M. C. and Cutting, S. M. (2008). The safety of *Bacillus subtilis* and *Bacillus indicus* as food probiotics. Journal of Applied Microbiology 105: 510-520.

163. Horn, N., Wegmann, U., Dertli, E., Mulholland, F., Collins, S. R., Waldron, K. W., Bongaerts, R. J., Mayer, M. J. and Narbad, A. (2013). Spontaneous mutation reveals influence of exopolysaccharide on *Lactobacillus johnsonii* surface characteristics. PLoS ONE 8: e59957.

164. Hou, L., Liu, M., Ding, P., Zhou, J., Yang, Y., Zhao, D. and Zheng, Y. (2011). Influences of sediment dessication on phosphorus transformations in an intertidal marsh: formation and release of phosphine. Chemosphere 83: 917-924.

165. Huang, G., Zhang, L. and Birch, R. G. (2000). Rapid amplification and cloning of Tn5 flanking fragments by inverse PCR. Letters in Applied Microbiology 31: 149-153.

166. Huang, X., Liao, X. and Shi, B. (2009). Adsorption removal of phosphate in industrial wastewater by using metal-loaded skin split waste. Journal of Hazardous Materials 166: 1261-1265.

167. Iyer, A., Mody, K. and Jha, B. (2006). Emulsifying properties of a marine bacterial exopolysaccharide. Enzyme and Microbial Technology 38: 220-222.

168. Jagtap, S., Yavankar, S., Pardesi, K. and Chopade, B. (2010). Production of bioemulsifier by *Acinetobacter* species isolated from healthy human skin. Indian Journal of Experimental Biology 48: 70-76.

169. Jalali, M. and Peikam, E. N. (2013). Phosphorus sorption-desorption behaviour of river bed sediments in the Abshineh river, Hamedan, Iran, related to their composition. Environmental Monitoring and Assessment 185: 537-552.

170. Janczarek, M. and Urbanik-Sypniewska, T. (2013). Expression of the *Rhizobium leguminosarum* bv. trifolii pssA gene, involved in exopolysaccharide synthesis, is regulated by RosR, phosphate, and the carbon source. Journal of Bacteriology 195: 3412-3423.

171. Jarvie, H. P., Sharpley, A. N., Withers, P. J., Scott, J. T., Haggard, B. E. and Neal, C. (2013). Phosphorus mitigation to control river eutrophication: murky waters, inconvenient truths, and "postnormal" science. Journal of Environmental Quality 42: 295-304.

172. Jellali, S., Wahab, M. A., Anane, M., Riahi, K. and Bousselmi, L. (2010). Phosphate mine wastes reuse for phosphorus removal from aqueous solutions under dynamic conditions. Journal of Hazardous Materials 184: 226-233.

173. Jellali, S., Wahab, M. A., Hassine, R. B., Hamzaoui, A. H. and Bousselmi, L. (2011). Adsorption characteristics of phosphorus from aqueous solutions onto phosphate mine wastes. Chemical Engineering Journal 169: 157-165.

174. Jeong, J. Y., Ahn, B. M., Kim, Y. J. and Park, J. Y. (2014). Continuous phosphorus removal from water by physicochemical method using zero valent iron packed column. Water Science and Technology 70: 895-900.

175. Jeong, S., Moon, H. S., Shin, D. and Nam, K. (2013). Survival of introduced phosphate-solubilizing bacteria (PSB) and their impact on microbial community structure during the phytoextraction of Cd-contaminated soil. Journal of Hazardous Materials 263 Pt 2: 441-449.

176. Jia, C., Li, P., Li, X., Tai, P., Liu, W. and Gong, Z. (2011). Degradation of pyrene in soils by extracellular polymeric substances (EPS) extracted from liquid cultures. Process Biochemistry 46: 1627-1631.

177. Jiang, C., Jia, L., He, Y., Zhang, B., Kirumba, G. and Xie, J. (2013). Adsorptive removal of phosphorus from aqueous solution using sponge iron and zeolite. Journal of Colloid and Interface Science 402: 246-252.

178. Jianlong, W. (2002). Biosorption of copper(II) by chemically modified biomass of *Saccharomyces cerevisiae*. Process Biochemistry 37: 847-850.

179. Jing, X., Mao, D., Geng, L. and Xu, C. (2013). Medium optimization, molecular characterization, and bioactivity of exopolysaccharides from *Pleurotus eryngii*. Archives of Microbiology 195: 749-757.

180. Johansson, L. (1999). Industrial by-products and natural substrata as phosphorus sorbents. Environmental Technology 20: 309-316.

181. Jones, K. M. (2012). Increased production of the exopolysaccharide succinoglycan enhances *Sinorhizobium meliloti* 1021 symbiosis with the host plant *Medicago truncatula*. Journal of Bacteriology 194: 4322-4331.

182. Joshi, J. G. and Handler, P. (1964). Phosphoglucomutase. I. purification and properties of phosphoglucomutase from *Escherichia coli*. Journal of Biological Chemistry 239: 2741-2751.

183. Judson, N. and Mekalanos, J. J. (2000). Transposon-based approaches to identify essential bacterial genes. Trends in Microbiology 8: 521-526.

184. Kaur, V., Bera, M. B., Panesar, P. S., Kumar, H. and Kennedy, J. F. (2014). Welan gum: microbial production, characterization, and applications. International Journal of Biological Macromolecules 65: 454-461.

185. Keranen, A., Leiviska, T., Hormi, O. and Tanskanen, J. (2015). Removal of nitrate by modified pine sawdust: effects of temperature and co-existing anions. Journal of Environmental Management 147: 46-54.

186. Khanam, R. and Prasuna, R. G. (2013). Strain improvement of *Trametes hirsuta* by physical and chemical mutagenesis for better laccases production. Journal of Environmental Science and Engineering 55: 388-396.

187. Kim, H. C. (2015). High-rate MIEX filtration for simultaneous removal of phosphorus and membrane foulants from secondary effluent. Water Research 69: 40-50.

188. Kim, H. C., Timmes, T. C. and Dempsey, B. A. (2015). Simultaneous removal of phosphorus and EfOM using MIEX, coagulation, and low-pressure membrane filtration. Environmental Technology (DOI: 10.1080/09593330.2015.1055819).

189. Kim, J. O and Chung, J. (2014). Implementing chemical precipitation as a pretreatment for phosphorus removal in membrane bioreactor-based municipal wastewater treatment plants. KSCE Journal of Civil Engineering 18: 956-963.

190. Kimura, M. (1980). A simple method for estimating evolutionary rates of base substitutions through comparative studies of nucleotide sequences. Journal of Molecular Evolution 16: 111-120.

191. Klausen, M. M., Thomsen, T. R., Nielsen, J. L., Mikkelsen, L. H. and Nielsen, P. H. (2004). Variations in microcolony strength of probe-defined bacteria in activated sludge flocs. FEMS Microbiology Ecology 50: 123-132.

192. Koeleman, J. G. M., Stoof, J., Biesmans, D. J., Savelkoul, P. H. M. and Vandenbroucke-Grauls, C. M. J. E. (1998). Comparison of Amplified Ribosomal DNA Restriction Analysis, Random Amplified Polymorphic DNA Analysis, and Amplified Fragment Length Polymorphism fingerprinting for identification of *Acinetobacter* genomic species and typing of *Acinetobacter baumannii*. Journal of Clinical Microbiology 36: 2522-2529.

193. Koilraj, P. and Kannan, S. (2010). Phosphate uptake behavior of ZnAlZr ternary layered double hydroxides through surface precipitation. Journal of Colloid and Interface Science 341: 289-297.

194. Koo, H., Xiao, J., Klein, M. I. and Jeon, J. G. (2010). Exopolysaccharides produced by *Streptococcus mutans* glucosyltransferases modulate the establishment of microcolonies within multispecies biofilms. Journal of Bacteriology 192: 3024-3032.

195. Korbekandi, H., Darkhal, P., Hojati, Z., Abedi, D., Hamedi, J. and Pourhosein, M. (2010). Overproduction of clavulanic acid by UV mutagenesis of *Streptomyces clavuligerus*. Iranian Journal of Pharmaceutical Research 9: 177-181.

196. Kreyenschulte, D., Krull, R. and Margaritis, A. (2014). Recent advances in microbial biopolymer production and purification. Critical Reviews in Biotechnology 34: 1-15.

197. Krishnan, K. A. and Haridas, A. (2008). Removal of phosphate from aqueous solutions and sewage using natural and surface modified coir pith. Journal of Hazardous Materials 152: 527-535.

198. Kubicki, J. D., Paul, K. W., Kabalan, L., Zhu, Q., Mrozik, M. K., Aryanpour, M., Pierre-Louis, A. M. and Strongin, D. R. (2012). ATR-FTIR and density functional theory study of the structures, energetics, and vibrational spectra of phosphate adsorbed onto goethite. Langmuir 28: 14573-14587.

199. Kumar, A., Seringhaus, M., Biery, M. C., Sarnovsky, R. J., Umansky, L., Piccirillo, S., Heidtman, M., Cheung, K. H., Dobry, C. J., Gerstein, M. B., Craig, N. L. and Snyder, M. (2004). Large-scale mutagenesis of the yeast genome using a Tn7-derived multipurpose transposon. Genome Research 14: 1975-1986.

200. Kumar, A. S., Mody, K. and Jha, B. (2007a). Bacterial exopolysaccharides--a perception. Journal of Basic Microbiology 47: 103-117.

201. Kumar, M., Badruzzaman, M., Adham, S. and Oppenheimer, J. (2007b). Beneficial phosphate recovery from reverse osmosis (RO) concentrate of an integrated membrane system using polymeric ligand exchanger (PLE). Water Research 41: 2211-2219.

202. Kurane, R. and Matsuyama, H. (1994). Production of a bioflocculant by mixed culture. Bioscience, Biotechnology and Biochemistry 58: 1589-1594.

203. Laverty, G., Gorman, S. P. and Gilmore, B. F. (2014). Biomolecular mechanisms of *Pseudomonas aeruginosa* and *Escherichia coli* biofilm formation. Pathogens 3: 596-632.

204. Lee, H. I., Donati, A. J., Hahn, D., Tisa, L. S. and Chang, W. S. (2013). Alteration of the exopolysaccharide production and the transcriptional profile of free-living *Frankia* strain CcI3 under nitrogen-fixing conditions. Applied Microbiology and Biotechnology 97: 10499-10509.

205. Lee, K. Y. and Mooney, D. J. (2012). Alginate: properties and biomedical applications. Progress in Polymer Science 37: 106-126.

206. Lee, N., Nielsen, P. H., Aspegren, H., Henze, M., Schleifer, K. H. and la Cour Jansen, J. (2003). Long-term population dynamics and in situ physiology in activated sludge systems with enhanced biological phosphorus removal operated

with and without nitrogen removal. Systematic and Applied Microbiology 26: 211-227.

207. Lenoble, V., Garnier, C., Masion, A., Ziarelli, F. and Garnier, J. M. (2008). Combination of 13C/ 113Cd NMR, potentiometry, and voltammetry in characterizing the interactions between Cd and two models of the main components of soil organic matter. Analytical and Bioanalytical Chemistry 390: 749-757.

208. Leo, C. P., Yahya, M. Z., Kamal, S. N., Ahmad, A. L. and Mohammad, A. W. (2013). Potential of nanofiltration and low pressure reverse osmosis in the removal of phosphorus for aquaculture. Water Science and Technology 67: 831-837.

209. Ler, A. and Stanforth, R. (2003). Evidence for surface precipitation of phosphate on goethite. Environmental Science & Technology 37: 2694-2700.

210. Levander, F. and Radstrom, P. (2001). Requirement for phosphoglucomutase in exopolysaccharide biosynthesis in glucose and lactose-utilizing *Streptococcus thermophilus*. Applied and Environmental Microbiology 67: 2734-2738.

211. Levander, F., Svensson, M. and Radstrom, P. (2002). Enhanced exopolysaccharide production by metabolic engineering of *Streptococcus thermophilus*. Applied and Environmental Microbiology 68: 784-790.

212. Lezehari, M., Baudu, M., Bouras, O. and Basly, J. P. (2012). Fixed-bed column studies of pentachlorophenol removal by use of alginate-encapsulated pillared clay microbeads. Journal of Colloid and Interface Science 379: 101-106.

213. Li, J., Xing, X. H. and Wang, B. Z. (2003). Characteristics of phosphorus removal from wastewater by biofilm sequencing batch reactor (SBR). Biochemical Engineering Journal 16: 279-285.

214. Li, L. and Stanforth, R. (2000). Distinguishing adsorption and surface precipitation of phosphate on goethite (alpha-FeOOH). Journal of Colloid and Interface Science 230: 12-21.

215. Li, M., Sheng, G. P., Wu, Y. J., Yu, Z. L., Banuelos, G. S. and Yu, H. Q. (2014a). Enhancement of nitrogen and phosphorus removal from eutrophic water by

economic plant annual ryegrass (*Lolium multiflorum*) with ion implantation. Environmental Science and Pollution Research International 21: 9617-9625.

216. Li, N., Ren, N. Q., Wang, X. H. and Kang, H. (2010a). Effect of temperature on intracellular phosphorus absorption and extra-cellular phosphorus removal in EBPR process. Bioresource Technology 101: 6265-6268.

217. Li, X. Y., Yang, J. J., Mao, Z. C., Ho, H. H., Wu, Y. X. and He, Y. Q. (2014b). Enhancement of biocontrol activities and cyclic lipopeptides production by chemical mutagenesis of *Bacillus subtilis* XF-1, a Biocontrol Agent of *Plasmodiophora brassicae* and *Fusarium solani*. Indian Journal of Microbiology 54: 476-479.

218. Li, Y., Chen, B. and Zhu, L. (2010b). Enhanced sorption of polycyclic aromatic hydrocarbons from aqueous solution by modified pine bark. Bioresource Technology 101: 7307-7313.

219. Li, Z., Zhong, S., Lei, H. Y., Chen, R. W., Yu, Q. and Li, H. L. (2009). Production of a novel bioflocculant by *Bacillus licheniformis* X14 and its application to low temperature drinking water treatment. Bioresource Technology 100: 3650-3656.

220. Lindback, T., Secic, I. and Rorvik, L. M. (2011). A contingency locus in prfA in a *Listeria monocytogenes* subgroup allows reactivation of the prfA virulence regulator during infection in mice. Applied and Environmental Microbiology 77: 3478-3483.

221. Littler, J., Geroni, J. N., Sapsford, D. J., Coulton, R. and Griffiths, A. J. (2013). Mechanisms of phosphorus removal by cement-bound ochre pellets. Chemosphere 90: 1533-1538.

222. Liu, D., Wang, P., Wei, G., Dong, W. and Hui, F. (2013a). Removal of algal blooms from freshwater by the coagulation-magnetic separation method. Environmental Science and Pollution Research International 20: 60-65.

223. Liu, D., Wang, S., Xu, B., Guo, Y., Zhao, J., Liu, W., Sun, Z., Shao, C., Wei, X., Jiang, Z., Wang, X., Liu, F., Wang, J., Huang, L., Hu, D., He, X., Riedel, C. U. and Yuan, J. (2011a). Proteomics analysis of *Bifidobacterium longum* NCC2705

growing on glucose, fructose, mannose, xylose, ribose, and galactose. Proteomics 11: 2628-2638.

224. Liu, H., Chen, T., Chang, J., Zou, X. and Frost, R. L. (2013b). The effect of hydroxyl groups and surface area of hematite derived from annealing goethite for phosphate removal. Journal of Colloid and Interface Science 398: 88-94.

225. Liu, L., Liu, Y., Li, J., Du, G. and Chen, J. (2011b). Microbial production of hyaluronic acid: current state, challenges, and perspectives. Microbial Cell Factories 10: 99.

226. Liu, W., Yuan, H., Yang, J. and Li, B. (2009). Characterization of bioflocculants from biologically aerated filter backwashed sludge and its application in dying wastewater treatment. Bioresource Technology 100: 2629-2632.

227. Liu, Y., Villalba, G., Ayres, R. U. and Schroder, H. (2008). Global phosphorus flows and environmental impacts from a consumption perspective. Journal of Industrial Ecology 12: 229-247.

228. Liu, Y., Yu, S., Xue, G. and Zhao, F. (2006a). Role of extracellular exopolymers in biological phosphorus removal. Water Science and Technology 54: 257-265.

229. Liu, Y. N., Xue, G., Yu, S. L. and Zhao, F. B. (2006b). Role of extracellular exopolymers on biological phosphorus removal. Journal of Environmental Sciences (China) 18: 670-674.

230. Liu, Y. T. and Hesterberg, D. (2011). Phosphate bonding on noncrystalline Al/Fe-hydroxide coprecipitates. Environmental Science & Technology 45: 6283-6289.

231. Livak, K. J. and Schmittgen, T. D. (2001). Analysis of relative gene expression data using real-time quantitative PCR and the 2(-Delta Delta C(T)) Method. Methods 25: 402-408.

232. Loaec, M., Olier, R. and Guezennec, J. (1997). Uptake of lead, cadmium and zinc by a novel bacterial exopolysaccharide. Water Research 31: 1171-1179.

233. Lodge, J. K. and Berg, D. E. (1990). Mutations that affect Tn5 insertion into pBR322: importance of local DNA supercoiling. Journal of Bacteriology 172: 5956-5960.

234. Lodge, J. K., Weston-Hafer, K. and Berg, D. E. (1988). Transposon Tn5 target specificity: preference for insertion at G/C pairs. Genetics 120: 645-650.

235. Lodge, J. K., Weston-Hafer, K. and Berg, D. E. (1991). Tn5 insertion specificity is not influenced by IS50 end sequences in target DNA. Molecular and General Genetics 228: 312-315.

236. Long, X., Fang, Z., Tang, R., Zhou, C., Feng, Y. and Wang, S. (2012). Roles of extracellular polymer substances in biological dephosphorization. Acta Scientiae Circumstantiae 32: 784-789.

237. Looijesteijn, P. J., Boels, I. C., Kleerebezem, M. and Hugenholtz, J. (1999). Regulation of exopolysaccharide production by *Lactococcus lactis* subsp. *cremoris* by the sugar source. Applied and Environmental Microbiology 65: 5003-5008.

238. Looijesteijn, P. J. and Hugenholtz, J. (1999). Uncoupling of growth and exopolysaccharide production by *Lactococcus lactis* subsp. *cremoris* NIZO B40 and optimization of its synthesis. Journal of Bioscience and Bioengineering 88: 178-182.

239. Lotter, L. H. (1984). The role of bacterial phosphate metabolism in enhanced phosphorus removal from the activated sludge process. Water Science and Technology 17: 127-138.

240. Lowry, O. H., Rosebrough, N. J., Farr, A. L. and Randall, R. J. (1951). Protein measurement with the Folin phenol reagent. The Journal of Biological Chemistry 193: 265-275.

241. Luengo, C., Brigante, M., Antelo, J. and Avena, M. (2006). Kinetics of phosphate adsorption on goethite: comparing batch adsorption and ATR-IR measurements. Journal of Colloid and Interface Science 300: 511-518.

242. Luengo, C., Brigante, M. and Avena, M. (2007). Adsorption kinetics of phosphate and arsenate on goethite. A comparative study. Journal of Colloid and Interface Science 311: 354-360.

243. Luo, Y., Guo, W., Ngo, H. H., Nghiem, L. D., Hai, F. I., Zhang, J., Liang, S. and Wang, X. C. (2014). A review on the occurrence of micropollutants in the aquatic environment and their fate and removal during wastewater treatment. The Science of the Total Environment 473-474: 619-641.

244. Lupski, J. R., Gershon, P., Ozaki, L. S. and Nigel Godson, G. (1984). Specificity of Tn5 insertions into a 36-bp DNA sequence repeated in tandem seven times. Gene 30: 99-106.

245. Ma, L., Wang, J., Wang, S., Anderson, E. M., Lam, J. S., Parsek, M. R. and Wozniak, D. J. (2012). Synthesis of multiple *Pseudomonas aeruginosa* biofilm matrix exopolysaccharides is post-transcriptionally regulated. Environmental Microbiology 14: 1995-2005.

246. Madhuri, K. V. and Rabhakar, K. V. (2014). Recent trends in the characterization of microbial exopolysaccharides. Oriental Journal of Chemistry 30: 895-904.

247. Maeda, H., Zhu, X., Suzuki, S., Suzuki, K. and Kitamura, S. (2004). Structural characterization and biological activities of an exopolysaccharide Kefiran produced by *Lactobacillus kefiranofaciens* WT-2BT. Journal of Agricultural and Food Chemistry 52: 5533-5538.

248. Mahvi, A. H., Ebrahimi, S. J., Mesdaghinia, A., Gharibi, H. and Sowlat, M. H. (2011). Performance evaluation of a continuous bipolar electrocoagulation/electrooxidation-electroflotation (ECEO-EF) reactor designed for simultaneous removal of ammonia and phosphate from wastewater effluent. Journal of Hazardous Materials 192: 1267-1274.

249. Malamud, F., Homem, R. A., Conforte, V. P., Yaryura, P. M., Castagnaro, A. P., Marano, M. R., do Amaral, A. M. and Vojnov, A. A. (2013). Identification and characterization of biofilm formation-defective mutants of *Xanthomonas citri* subsp. citri. Microbiology 159: 1911-1919.

250. Manna, D., Wang, X. and Higgins, N. P. (2001). Mu and IS1 transpositions exhibit strong orientation bias at the *Escherichia coli* bgl locus. Journal of Bacteriology 183: 3328-3335.

251. Masuda, C. A., Xavier, M. A., Mattos, K. A., Galina, A. and Montero-Lomeli, M. (2001). Phosphoglucomutase is an in vivo lithium target in yeast. Journal of Biological Chemistry 276: 37794-37801.

252. Matsui, K., Togami, J., Mason, J. G., Chandler, S. F. and Tanaka, Y. (2013). Enhancement of phosphate absorption by garden plants by genetic engineering: A new tool for phytoremediation. BioMed Research International 2013: 7.

253. Mayer, C., Moritz, R., Kirschner, C., Borchard, W., Maibaum, R., Wingender, J. and Flemming, H. C. (1999). The role of intermolecular interactions: studies on model systems for bacterial biofilms. International Journal of Biological Macromolecules 26: 3-16.

254. McClean, K. H., Winson, M. K., Fish, L., Taylor, A., Chhabra, S. R., Camara, M., Daykin, M., Lamb, J. H., Swift, S., Bycroft, B. W., Stewart, G. S. and Williams, P. (1997). Quorum sensing and *Chromobacterium violaceum*: exploitation of violacein production and inhibition for the detection of N-acylhomoserine lactones. Microbiology 143: 3703-3711.

255. Medda, L., Barse, B., Cugia, F., Bostrom, M., Parsons, D. F., Ninham, B. W., Monduzzi, M. and Salis, A. (2012). Hofmeister challenges: ion binding and charge of the BSA protein as explicit examples. Langmuir 28: 16355-16363.

256. Micheletti, E., Pereira, S., Mannelli, F., Moradas-Ferreira, P., Tamagnini, P. and De Philippis, R. (2008). Sheathless mutant of *Cyanobacterium gloeothece* sp. strain PCC 6909 with increased capacity to remove copper ions from aqueous solutions. Applied and Environmental Microbiology 74: 2797-2804.

257. Mikkelsen, L. H. and Nielsen, P. H. (2001). Quantification of the bond energy of bacteria attached to activated sludge floc surfaces. Water Science and Technology 43: 67-75.

258. Mino, T. (2000). Microbial selection of polyphosphate-accumulating bacteria in activated sludge wastewater treatment processes for enhanced biological phosphate removal. Biochemistry 65: 341-348.

259. Mittal, H., Jindal, R., Kaith, B. S., Maity, A. and Ray, S. S. (2014). Synthesis and flocculation properties of gum ghatti and poly(acrylamide-co-acrylonitrile) based biodegradable hydrogels. Carbohydrate Polymers 114: 321-329.

260. Mittal, H., Jindal, R., Kaith, B. S., Maity, A. and Ray, S. S. (2015). Flocculation and adsorption properties of biodegradable gum-ghatti-grafted poly(acrylamide-co-methacrylic acid) hydrogels. Carbohydrate Polymers 115: 617-628.

261. Mohapatra, D., Mishra, D. and Park, K. H. (2008). A laboratory scale study on arsenic (V) removal from aqueous medium using calcined bauxite ore. Journal of Environmental Sciences (China) 20: 683-689.

262. Molle, P., Lienard, A., Grasmick, A., Iwema, A., Kabbabi, A. (2005). Apatite as an interesting seed to remove phosphorus from wastewater in constructed wetlands. Water Science and Technology 51: 193-203.

263. More, T. T., Yadav, J. S., Yan, S., Tyagi, R. D. and Surampalli, R. Y. (2014). Extracellular polymeric substances of bacteria and their potential environmental applications. Journal of Environmental Management 144: 1-25.

264. Mozzi, F., Savoy de Giori, G. and Font de Valdez, G. (2003). UDP-galactose 4-epimerase: a key enzyme in exopolysaccharide formation by *Lactobacillus casei* CRL 87 in controlled pH batch cultures. Journal of Applied Microbiology 94: 175-183.

265. Mozzi, F., Vaningelgem, F., Hebert, E. M., Van der Meulen, R., Foulquie Moreno, M. R., Font de Valdez, G. and De Vuyst, L. (2006). Diversity of heteropolysaccharide-producing lactic acid bacterium strains and their biopolymers. Applied and Environmental Microbiology 72: 4431-4435.

266. Muhammadi and Afzal, M. (2014). Optimization of water absorbing exopolysaccharide production on local cheap substrates by *Bacillus* strain

CMG1403 using one variable at a time approach. Journal of Microbiololgy 52: 44-52.

267. Muster, T. H., Douglas, G. B., Sherman, N., Seeber, A., Wright, N. and Guzukara, Y. (2013). Towards effective phosphorus recycling from wastewater: quantity and quality. Chemosphere 91: 676-684.

268. Muyima, N. Y. and Cloete, T. E. (1995). Phosphate uptake by immobilized *Acinetobacter calcoaceticus* cells in a full scale activated sludge plant. Journal of Industrial Microbiology 15: 19-24.

269. Nagase, T., Mikami, T., Suzuki, S., Schuerch, C. and Suzuki, M. (1984). Lethal effect of neutral mannan fraction of bakers' yeast in mice. Microbiology and Immunology 28: 997-1007.

270. Nakamura, K., Hiraishi, A., Yoshimi, Y., Kawaharasaki, M., Masuda, K. and Kamagata, Y. (1995). *Microlunatus phosphovoru*s gen. nov., sp. nov., a new Gram-positive polyphosphate-accumulating bacterium isolated from activated sludge. International Journal of Systematic and Evolutionary Microbiology 45: 17-22.

271. Navon-Venezia, S., Zosim, Z., Gottlieb, A., Legmann, R., Carmeli, S., Ron, E. Z. and Rosenberg, E. (1995). Alasan, a new bioemulsifier from *Acinetobacter radioresistens*. Applied and Environmental Microbiology 61: 3240-3244.

272. Neeraj, S, G. S., C., S., Sachin, C. and Chandra, M. (2009). Exopolysaccharides and lipopolysaccharide production by *Sinorhizobiobium fredii* Tn5 mutants. ARPN Journal of Agricultural and Biological Science 4: 32-38.

273. Neves, A. R., Pool, W. A., Castro, R., Mingote, A., Santos, F., Kok, J., Kuipers, O. P. and Santos, H. (2006). The alpha-phosphoglucomutase of *Lactococcus lactis* is unrelated to the alpha-D-phosphohexomutase superfamily and is encoded by the essential gene pgmH. Journal of Biological Chemistry 281: 36864-36873.

274. Nguyen, H. T. A., Ngo, H. H., Guo, W. and Nguyen, V. T. (2012). Phosphorous removal from aqueous solutions by agricultural by-products: A critical review. Journal of Water Sustainability 2: 193-207.

275. Nguyen, T. A., Ngo, H. H., Guo, W. S., Pham, T. Q., Li, F. M., Nguyen, T. V. and Bui, X. T. (2015). Adsorption of phosphate from aqueous solutions and sewage using zirconium loaded okara (ZLO): Fixed-bed column study. The Science of the Total Environment 523: 40-49.

276. Nigam, P. S., Pandey, A. (2009). Biotechnology for Agro-Industrial Residues Utilisation: Utilisation of Agro-Residues, Springer Science & Business Media, Springer Netherlands.

277. Nigam, P. S. (2013). Microbial enzymes with special characteristics for biotechnological applications. Biomolecules 3: 597-611.

278. Nishikawa, M. and Ogawa, K. (2002). Distribution of microbes producing antimicrobial ε-poly-l-lysine polymers in soil microflora determined by a novel method. Applied and Environmental Microbiology 68: 3575-3581.

279. Nogales, J., Munoz, S., Olivares, J. and Sanjuan, J. (2006). *Sinorhizobium meliloti* genes involved in tolerance to the antimicrobial peptide protamine. FEMS Microbiology Letters 264: 160-167.

280. Nunez, C., Bogachev, A. V., Guzman, G., Tello, I., Guzman, J. and Espin, G. (2009). The Na^+ translocating NADH: ubiquinone oxidoreductase of *Azotobacter vinelandii* negatively regulates alginate synthesis. Microbiology 155: 249-256.

281. Nurk, A., Tamm, A., Hôrak, R. and Kivisaar, M. (1993). In-vivo-generated fusion promoters in *Pseudomonas putida*. Gene 127: 23-29.

282. Nwodo, U. U., Green, E. and Okoh, A. I. (2012). Bacterial exopolysaccharides: functionality and prospects. International Journal of Molecular Sciences 13: 14002-14015.

283. OECD (2010). Section 1 - Information used in the assessment of environmental applications of Acinetobacter. OECD, Safety Assessment of Transgenic Organisms, Volume 4: OECD Consensus Documents.

284. OECD (2011). Guidance document on the use of information on pathogenicity factors in assessing the potential adverse health effects of micro-organisms: bacteria.

285. Oka, T. and Jigami, Y. (2006). Reconstruction of de novo pathway for synthesis of UDP-glucuronic acid and UDP-xylose from intrinsic UDP-glucose in *Saccharomyces cerevisiae*. FEBS Journal 273: 2645-2657.

286. Oliveira, M. and Machado, A. V. (2013). The role of phosphorus on eutrophication: a historical review and future perspectives. Environmental Technology Reviews 2: 117-127.

287. Oosthuizen, D. J. and Cloete, T. E. (2001). SEM-EDS for determining the phosphorus content in activated sludge EPS. Water Science and Technology 43: 105-112.

288. Panagiotou, G., Christakopoulos, P. and Olsson, L. (2005). Simultaneous saccharification and fermentation of cellulose by *Fusarium oxysporum* F3 - growth characteristics and metabolite profiling. Enzyme and Microbial Technology 36: 693-699.

289. Pant, H. K., Reddy, K. R. and Lemon, E. (2001). Phosphorus retention capacity of root bed media of subsurface flow constructed wetlands. Ecological Engineering 17: 345-355.

290. Papagianni, M. (2012). Metabolic engineering of lactic acid bacteria for the production of industrially important compounds. Computational and Structural Biotechnology Journal 3: e201210003.

291. Pasayeva, P., Gezgin, Y., Pekin, G. and Eltem, R. (2011). Phosphate uptake performance of bacteria isolated from a full-scale Izmir municipal wastewater treatment plant. Environmental Technology 32: 543-549.

292. Patel, S., Majumder, A. and Goyal, A. (2012). Potentials of exopolysaccharides from lactic acid bacteria. Indian Journal of Microbiology 52: 3-12.

293. Patil, J. R. and Chopade, B. A. (2001). Studies on bioemulsifier production by Acinetobacter strains isolated from healthy human skin. Journal of Applied Microbiology 91: 290-298.

294. Patil, S. V., Patil, C. D., Salunke, B. K., Salunkhe, R. B., Bathe, G. A. and Patil, D. M. (2011). Studies on characterization of bioflocculant exopolysaccharide of

Azotobacter indicus and its potential for wastewater treatment. Applied Biochemistry and Biotechnology 163: 463-472.

295. Pauli, A. (1994). The role of *Acinetobacter* sp. in biological phosphorus removal from forest industry wastewaters. National Board of Waters and the Environment, Finland.

296. Pauli, A. S. and Kaitala, S. (1997). Phosphate uptake kinetics by *Acinetobacter* isolates. Biotechnology and Bioengineering 53: 304-309.

297. Pehl, M. J., Jamieson, W. D., Kong, K., Forbester, J. L., Fredendall, R. J., Gregory, G. A., McFarland, J. E., Healy, J. M. and Orwin, P. M. (2012). Genes that influence swarming motility and biofilm formation in *Variovorax paradoxus* EPS. PLoS One 7: e31832.

298. Peleg, A. Y., Seifert, H. and Paterson, D. L. (2008). *Acinetobacter baumannii*: emergence of a successful pathogen. Clinical Microbiology Reviews 21: 538-582.

299. Pengthamkeerati, P., Satapanajaru, T. and Chularuengoaksorn, P. (2008). Chemical modification of coal fly ash for the removal of phosphate from aqueous solution. Fuel 87: 2469-2476.

300. Pierre, G., Graber, M., Rafiliposon, B. A., Dupuy, C., Orvain, F., De Crignis, M. and Maugard, T. (2012). Biochemical composition and changes of extracellular polysaccharides (ECPS) produced during microphytobenthic biofilm development (Marennes-Oleron, France). Microbial Ecology 63: 157-169.

301. Pirog, T. P., Korzh, Y. V. and Shevchuk, T. A. (2009). The effect of cultivation conditions on the physicochemical properties of the exopolysaccharide ethapolan. Applied Biochemistry and Microbiology 45: 50-55.

302. Pirog, T. P., Vysyatetskaya, N. V. and Korzh, Y. V. (2007). Specific features of the synthesis of the exopolysaccharide ethapolan on a mixture of energy-deficient growth substrates. Microbiology 76: 25-30.

303. Pirog, T. P., Kovalenko, M. A., Kuzminskaya, Y. V. and Votselko, S. K. (2004). Physicochemical properties of the microbial exopolysaccharide ethapolan synthesized on a mixture of growth substrates. Microbiology 73: 14-18.

304. Pirog, T. P., Kovalenko, M. A. and Kuzminskaya, Y. V. (2002). Exopolysaccharide production and peculiarities of C6-Metabolism in *Acinetobacter* sp. grown on carbohydrate substrates. Microbiology 71: 182-188.

305. Pitakteeratham, N., Hafuka, A., Satoh, H. and Watanabe, Y. (2013). High efficiency removal of phosphate from water by zirconium sulfate-surfactant micelle mesostructure immobilized on polymer matrix. Water Research 47: 3583-3590.

306. Pratush, A., Seth, A. and Bhalla, T. C. (2010). Generation of mutant of *Rhodococcus rhodochrous* PA-34 through chemical mutagenesis for hyperproduction of nitrile hydratase. Acta Microbiologica et Immunologica Hungarica 57: 135-146.

307. Priester, J. H., Olson, S. G., Webb, S. M., Neu, M. P., Hersman, L. E. and Holden, P. A. (2006). Enhanced exopolymer production and chromium stabilization in *Pseudomonas putida* unsaturated biofilms. Applied and Environmental Microbiology 72: 1988-1996.

308. Prochaska CA, Z. A. (2006). Removal of phosphate by pilot vertical-flow constructed wetlands using a mixture of sand and dolomite as substrate. Ecological Engineering 26 293–303.

309. Qian, N., Stanley, G. A., Hahn-Hagerdal, B. and Radstrom, P. (1994). Purification and characterization of two phosphoglucomutases from *Lactococcus lactis* subsp. lactis and their regulation in maltose- and glucose-utilizing cells. Journal of Bacteriology 176: 5304-5311.

310. Qiu, G., Law, Y. M., Das, S. and Ting, Y. P. (2015). Direct and complete phosphorus recovery from municipal wastewater using a hybrid microfiltration-forward osmosis membrane bioreactor process with seawater brine as draw solution. Environmental Science & Technology 49: 6156-6163.

311. Ramberg, J. E., Nelson, E. D. and Sinnott, R. A. (2010). Immunomodulatory dietary polysaccharides: a systematic review of the literature. Nutrition Journal 9: 54.

312. Ravella, S. R., Quinones, T. S., Retter, A., Heiermann, M., Amon, T. and Hobbs, P. J. (2010). Extracellular polysaccharide (EPS) production by a novel strain of yeast-like fungus *Aureobasidium pullulans*. Carbohydrate Polymers 82: 728-732.

313. Reeve, W. G., Dilworth, M. J., Tiwari, R. P. and Glenn, A. R. (1997). Regulation of exopolysaccharide production in *Rhizobium leguminosarum* biovar viciae WSM710 involves exoR. Microbiology 143: 1951-1958.

314. Rehm, B. (2009). Microbial production of biopolymers and polymer precursors: applications and perspectives, Caister Academic.

315. Rehm, B. H. A. (2010). Bacterial polymers: biosynthesis, modifications and applications. Nature Reviews Microbiology 8: 578-592.

316. Remy, C., Miehe, U., Lesjean, B. and Bartholomaus, C. (2014). Comparing environmental impacts of tertiary wastewater treatment technologies for advanced phosphorus removal and disinfection with life cycle assessment. Water Science and Technology 69: 1742-1750.

317. Ren, Y. X., Zhu, X. L., Fan, D. D., Ma, P. and Liang, L. H. (2013). Inoculation of phosphate solubilizing bacteria for the improvement of lead accumulation by *Brassica juncea*. Environmental Technology 34: 463-469.

318. Renuka, N., Sood, A., Ratha, S. K., Prasanna, R. and Ahluwalia, A. S. (2013). Nutrient sequestration, biomass production by microalgae and phytoremediation of sewage water. International Journal of Phytoremediation 15: 789-800.

319. Riahi, K., Chaabane, S. and Thayer, B. B. (2014). A kinetic modeling study of phosphate adsorption onto *Phoenix dactylifera* L. date palm fibers in batch mode. Journal of Saudi Chemical Society (DOI:10.1016/j.jscs.2013.11.007).

320. Riahi, K., Thayer, B. B., Mammou, A. B., Ammar, A. B. and Jaafoura, M. H. (2009). Biosorption characteristics of phosphates from aqueous solution onto *Phoenix dactylifera* L. date palm fibers. Journal of Hazardous Materials 170: 511-519.

321. Richau, J. A., Leitao, J. H. and Sa-Correia, I. (2000). Enzymes leading to the nucleotide sugar precursors for exopolysaccharide synthesis in *Burkholderia cepacia*. Biochemical and Biophysical Research Communications 276: 71-76.

322. Roca, C., Alves, V. D., Freitas, F. and Reis, M. A. (2015). Exopolysaccharides enriched in rare sugars: bacterial sources, production, and applications. Frontiers in Microbiology 6: 288.

323. Rocchetta, H. L., Burrows, L. L. and Lam, J. S. (1999). Genetics of O-antigen biosynthesis in *Pseudomonas aeruginosa*. Microbiology and Molecular Biology Reviews 63: 523-553.

324. Rockstrom, J., Steffen, W., Noone, K., Persson, A., Chapin, F. S., Lambin, E. F., Lenton, T. M., Scheffer, M., Folke, C., Schellnhuber, H. J., Nykvist, B., de Wit, C. A., Hughes, T., van der Leeuw, S., Rodhe, H., Sorlin, S., Snyder, P. K., Costanza, R., Svedin, U., Falkenmark, M., Karlberg, L., Corell, R. W., Fabry, V. J., Hansen, J., Walker, B., Liverman, D., Richardson, K., Crutzen, P. and Foley, J. A. (2009). A safe operating space for humanity. Nature 461: 472-475.

325. Rodriguez, H., Mendoza, A., Cruz, M. A., Holguin, G., Glick, B. R. and Bashan, Y. (2006). Pleiotropic physiological effects in the plant growth-promoting bacterium *Azospirillum brasilense* following chromosomal labeling in the clpX gene. FEMS Microbiology Ecology 57: 217-225.

326. Rosenberg, E., Rubinovitz, C., Gottlieb, A., Rosenhak, S. and Ron, E. Z. (1988a). Production of Biodispersan by *Acinetobacter calcoaceticus* A2. Applied and Environmental Microbiology 54: 317-322.

327. Rosenberg, E., Rubinovitz, C., Legmann, R. and Ron, E. Z. (1988b). Purification and chemical properties of *Acinetobacter calcoaceticus* A2 biodispersan. Applied and Environmental Microbiology 54: 323-326.

328. Ruiz-Matute, A. I., Hernández-Hernández, O., Rodríguez-Sánchez, S., Sanz, M. L. and Martínez-Castro, I. (2011). Derivatization of carbohydrates for GC and GC–MS analyses. Journal of Chromatography B 879: 1226–1240.

329. Saat, M. N., Annuar, M. S., Alias, Z., Chuan, L. T. and Chisti, Y. (2014). Modeling of growth and laccase production by *Pycnoporus sanguineus*. Bioprocess and Biosystems Engineering 37: 765-775.

330. Sahu, P. K., Iyer, P. S., Barage, S. H., Sonawane, K. D. and Chopade, B. A. (2014). Characterization of the algC gene expression pattern in the multidrug resistant *Acinetobacter baumannii* AIIMS 7 and correlation with biofilm development on abiotic surface. Scientific World Journal 2014: 593546.

331. Saitou, N. and Nei, M. (1987). The neighbor-joining method: a new method for reconstructing phylogenetic trees. Molecular Biology and Evolution 4: 406-425.

332. Sakadevan, K. and Bavor, H. J. (1998). Phosphate adsorption characteristics of soils, slags and zeolite to be used as substrates in constructed wetland systems. Water Research 32 393–399.

333. Sam, S., Kucukasik, F., Yenigun, O., Nicolaus, B., Oner, E. T. and Yukselen, M. A. (2011). Flocculating performances of exopolysaccharides produced by a halophilic bacterial strain cultivated on agro-industrial waste. Bioresource Technology 102: 1788-1794.

334. Samadi-Maybodi, A., Taheri Saffar, H., Khodadoust, S., Nasrollahzadeh Saravi, H. and Najafpour, S. (2013). Study on different forms and phosphorus distribution in the coastal surface sediments of Southern Caspian Sea by using UV-Vis spectrophotometery. Spectrochimica Acta. Part A, Molecular and Biomolecular Spectroscopy 113: 67-71.

335. Samal, S. K. and Dubruel, P. (2014). Cationic Polymers in Regenerative Medicine, Royal Society of Chemistry.

336. Sambrook, J. and Russell, D. W. (2001). Molecular Cloning: A Laboratory Manual, Cold Spring Harbor Laboratory Press.

337. Sandula, J., Kogan, G., Kacurakova, M., and Machova, E. (1999). Microbial (1→3)-β-D-glucans, their preparation, physico-chemical characterization and immunomodulatory activity. Carbohydrate Polymers 38: 247-253.

338. Sanfelix-Haywood, N., Coll-Marques, J. M. and Yebra, M. J. (2011). Role of alpha-phosphoglucomutase and phosphoglucose isomerase activities at the branching point between sugar catabolism and anabolism in *Lactobacillus casei*. Journal of Applied Microbiology 111: 433-442.

339. Sanhueza, E., Paredes-Osses, E., González, C. L. and García, A. (2015). Effect of pH in the survival of *Lactobacillus salivarius* strain UCO 979C wild type and the pH acid acclimated variant. Electronic Journal of Biotechnology (DOI:10.1016/j.ejbt.2015.06.005).

340. Satpute, S. K., Banat, I. M., Dhakephalkar, P. K., Banpurkar, A. G. and Chopade, B. A. (2010). Biosurfactants, bioemulsifiers and exopolysaccharides from marine microorganisms. Biotechnology Advances 28: 436-450.

341. Schmittgen, T. D. and Livak, K. J. (2008). Analyzing real-time PCR data by the comparative CT method. Nature Protocols 3: 1101-1108.

342. Sen, I. K., Mandal, A. K., Chakraborty, R., Behera, B., Yadav, K. K., Maiti, T. K. and Islam, S. S. (2014). Structural and immunological studies of an exopolysaccharide from *Acinetobacter junii* BB1A. Carbohydrate Polymers 101: 188-195.

343. Senila, L., Gog, A., Senila, M., Roman, C. and Silaghi-Dumitrescu, L. (2011). Analysis of carbohydrates obtained from wood by gas chromatography-mass spectrometry. Revista de Chimie (Bucharest) 62: 149-153.

344. Seringhaus, M., Kumar, A., Hartigan, J., Snyder, M. and Gerstein, M. (2006). Genomic analysis of insertion behavior and target specificity of mini-Tn7 and Tn3 transposons in *Saccharomyces cerevisiae*. Nucleic Acids Research 34: e57.

345. Seviour, R. J., McNeil, B., Fazenda, M. L. and Harvey, L. M. (2011). Operating bioreactors for microbial exopolysaccharide production. Critical Reviews in Biotechnology 31: 170-185.

346. Shabtai, Y. (1990). Production of exopolysaccharides by *Acinetobacter* strains in a controlled fed-batch fermentation process using soap stock oil (SSO) as carbon source. International Journal of Biological Macromolecules 12: 145-152.

347. Shen, R., Wang, S., Ma, X., Xian, J., Li, J., Zhang, L. and Wang, P. (2010). An easy colorimetric assay for glycosyltransferases. Biochemistry 75: 944-950.

348. Shene, C., Canquil, N., Bravo, S. and Rubilar, M. (2008). Production of the exopolysaccharides by *Streptococcus thermophilus*: effect of growth conditions on fermentation kinetics and intrinsic viscosity. International Journal of Food Microbiology 124: 279-284.

349. Shevchenko, Y., Bouffard, G. G., Butterfield, Y. S., Blakesley, R. W., Hartley, J. L., Young, A. C., Marra, M. A., Jones, S. J., Touchman, J. W. and Green, E. D. (2002). Systematic sequencing of cDNA clones using the transposon Tn5. Nucleic Acids Research 30: 2469-2477.

350. Shi, T., Aryantini, N. P., Uchida, K., Urashima, T. and Fukuda, K. (2014). Enhancement of exopolysaccharide production of *Lactobacillus fermentum* TDS030603 by modifying culture conditions. Bioscience of Microbiota, Food and Health 33: 85-90.

351. Shintani, T., Liu, W. T., Hanada, S., Kamagata, Y., Miyaoka, S., Suzuki, T. and Nakamura, K. (2000). *Micropruina glycogenica* gen. nov., sp. nov., a new Gram-positive glycogen-accumulating bacterium isolated from activated sludge. International Journal of Systematic and Evolutionary Microbiology 50: 201-207.

352. Shivakumar, S. and Vijayendra, S. V. (2006). Production of exopolysaccharides by *Agrobacterium* sp. CFR-24 using coconut water - a byproduct of food industry. Letters in Applied Microbiology 42: 477-482.

353. Simons, R. W., Hoopes, B. C., McClure, W. R. and Kleckner, N. (1983). Three promoters near the termini of IS10: pIN, pOUT, and pIII. Cell 34: 673-682.

354. Singh, A., Kaler, A., Singh, V., Patil, R. and Banerjee, U. C. (2011a). Cyclodextrins and biotechnological applications. In: Cyclodextrins in pharmaceutics, cosmetics, and biomedicine. Ed. E. Bilensoy, John Wiley & Sons, Inc., Hoboken.

355. Singh, D. and Kumar, A. (2013). Bacterial biopolymers and genetically engineered biopolymers for gel Systems application. In: Handbook of biopolymer based

materials: From blends and composites to gels and complex networks. Ed. S. Thomas, D. Durand, C. Chassenieux and P. Jyotishkumar, Wiley-VCH., Weinheim.

356. Singh, R. P., Shukla, M. K., Mishra, A., Kumari, P., Reddy, C. R. K. and Jha, B. (2011b). Isolation and characterization of exopolysaccharides from seaweed associated bacteria *Bacillus licheniformis*. Carbohydrate Polymers 84: 1019-1026.

357. Singh, R. S., Saini, G. K. and Kennedy, J. F. (2008). Pullulan: Microbial sources, production and applications. Carbohydrate Polymers 73: 515-531.

358. Smith, S. C., Douglas, M., Moore, D. A., Kukkadapu, R. K. and Arey, B. W. (2009). Uranium extraction from laboratory-synthesized, uranium-doped hydrous ferric oxides. Environmental Science & Technology 43: 2341-2347.

359. Sorokulova, I. B., Pinchuk, I. V., Denayrolles, M., Osipova, I. G., Huang, J. M., Cutting, S. M. and Urdaci, M. C. (2008). The safety of two Bacillus probiotic strains for human use. Digestive Diseases and Sciences 53: 954-963.

360. Sovik, A. K. and Klove, B. (2005). Phosphorus retention processes in shell sand filter systems treating municipal wastewater. Ecological Engineering 25: 168-182.

361. Stafford, B., Dotro, G., Vale, P., Jefferson, B. and Jarvis, P. (2014). Removal of phosphorus from trickling filter effluent by electrocoagulation. Environmental Technology 35: 3139-3146.

362. Stahl, M. and Stintzi, A. (2015). Microarray transposon tracking for the mapping of conditionally essential genes in *Campylobacter jejuni*. Methods in Molecular Biology 1279: 1-14.

363. Stante, L., Cellamare, C. M., Malaspina, F., Bortone, G. and Tilche, A. (1997). Biological phosphorus removal by pure culture of *Lampropedia* spp. Water Research 31: 1317-1324.

364. Stumm, W. a. J. J. M. (1981). Aquatic chemistry: an introduction emphasizing chemical equilibria in natural waters. Wiley Interscience, New York.

365. Sun, J. L., Zou, X., Liu, A. Y. and Xiao, T. F. (2011). Elevated yield of monacolin K in *Monascus purpureus* by fungal elicitor and mutagenesis of UV and LiCl. Biological Research 44: 377-382.

366. Suresh, N., Warburg, R., Timmerman, M. and Halvorsan, H. (1985). New strategies for the isolation of micro-organisms responsible for phosphate accumulation. Water Science and Technology 17: 99-111.

367. Sutherland, I. W. (1986). Industrially useful microbial polysaccharides. Microbiological Sciences 3: 5-9.

368. Sutherland, I. W. (1998). Novel and established applications of microbial polysaccharides. Trends in Biotechnology 16: 41-46.

369. Svensson, M., Lohmeier-Vogel, E., Waak, E., Svensson, U. and Radstrom, P. (2007). Altered nucleotide sugar metabolism in *Streptococcus thermophilus* interferes with nitrogen metabolism. International Journal of Food Microbiology 113: 195-200.

370. Svensson, M., Waak, E., Svensson, U. and Radstrom, P. (2005). Metabolically improved exopolysaccharide production by *Streptococcus thermophilus* and its influence on the rheological properties of fermented milk. Applied and Environmental Microbiology 71: 6398-6400.

371. Synytsya, A., Míckova, K., Synytsya, A., Jablonsky, I., Spevacek, J., Erban, V., Kovarikova, E., and Copikova, J. (2009). Glucans from fruit bodies of cultivated mushrooms *Pleurotus ostreatus* and *Pleurotus eryngii*: structure and potential prebiotic activity. Carbohydrate Polymers 76: 548-556.

372. Szabo, A., Takacs, I., Murthy, S., Daigger, G. T., Licsko, I. and Smith, S. (2008). Significance of design and operational variables in chemical phosphorus removal. Water Environment Research 80: 407-416.

373. Szabo, N. J., Dolan, L. C., Burdock, G. A., Shibano, T., Sato, S., Suzuki, H., Uesugi, T., Yamahira, S., Toba, M. and Ueno, H. (2011). Safety evaluation of *Lactobacillus pentosus* strain b240. Food and Chemical Toxicology 49: 251-258.

374. Tak, H. I., Ahmad, F. and Babalola, O. O. (2013). Advances in the application of plant growth-promoting rhizobacteria in phytoremediation of heavy metals. Reviews of Environmental Contamination and Toxicology 223: 33-52.

375. Tamura, K., Peterson, D., Peterson, N., Stecher, G., Nei, M. and Kumar, S. (2011). MEGA5: molecular evolutionary genetics analysis using maximum likelihood, evolutionary distance, and maximum parsimony methods. Molecular Biology and Evolution 28: 2731-2739.

376. Tayabali, A. F., Nguyen, K. C., Shwed, P. S., Crosthwait, J., Coleman, G. and Seligy, V. L. (2012). Comparison of the virulence potential of *Acinetobacter* strains from clinical and environmental sources. PLoS One 7: e37024.

377. Tchamango, S., Nanseu-Njiki, C. P., Ngameni, E., Hadjiev, D. and Darchen, A. (2010). Treatment of dairy effluents by electrocoagulation using aluminium electrodes. The Science of the Total Environment 408: 947-952.

378. Thakur I. S. (2006a) Environmental biotechnology basic concepts and applications, I.K. International Publishing House Pvt. Ltd., Bangalore.

379. Thakur I. S. (2006b) Industrial biotechnology: problems and remedies, I.K. International Publishing House Pvt. Ltd., Bangalore.

380. Thongtha, S., Teamkao, P., Boonapatcharoen, N., Tripetchkul, S., Techkarnjararuk, S. and Thiravetyan, P. (2014). Phosphorus removal from domestic wastewater by *Nelumbo nucifera* Gaertn. and *Cyperus alternifolius* L. Journal of Environmental Management 137: 54-60.

381. Tirado, R. and Allsopp, M. (2012). Phosphorus in agriculture problems and solutions. Greenpeace Research Laboratories Technical Report 6.

382. Tofan-Lazar, J. and Al-Abadleh, H. A. (2012). Kinetic ATR-FTIR studies on phosphate adsorption on iron (oxyhydr)oxides in the absence and presence of surface arsenic: molecular-level insights into the ligand exchange mechanism. Journal of Physical Chemistry A 116: 10143-10149.

383. Torres, C. A., Antunes, S., Ricardo, A. R., Grandfils, C., Alves, V. D., Freitas, F. and Reis, M. A. (2012). Study of the interactive effect of temperature and pH on

exopolysaccharide production by *Enterobacter* A47 using multivariate statistical analysis. Bioresource Technology 119: 148-156.

384. Trathnigg, B. (2000). Size-exclusion chromatography of polymers. In: Encyclopedia of Analytical Chemistry. Ed. R. A. Meyers, John Wiley & Sons Ltd., Chichester.

385. Turner, B. F. and Fein, J. B. (2006). Protofit: A program for determining surface protonation constants from titration data. Computers & Geosciences 32: 1344-1356.

386. Twardowski, T. and Malyska, A. (2015). Uninformed and disinformed society and the GMO market. Trends in Biotechnology 33: 1-3.

387. UNDESA (2012). Back to our common future: Sustainable development in the 21st Century (SD21) project. United Nations.

388. UNEP (United Nations Environment Programme) (2008). Water quality for ecosystem and human health (http://www.unwater.org/wwd10/downloads/water_quality_human_ health.pdf) (Assessed on 28 July 2015).

389. UNEP (United Nations Environment Programme) (2012a). Global Environment Outlook-5: Environment for the future we want (www.unep.org/geo/geo5.asp) (Assessed on 28 July 2015).

390. UNEP (United Nations Environment Programme) (2012b). Measuring Progress: Environmental Goals & Gaps (www.unep.org/geo/pdfs/geo5/Measuring_progress.pdf) (Assessed on 28 July 2015).

391. van Kranenburg, R., Vos, H. R., van, S., II, Kleerebezem, M. and de Vos, W. M. (1999). Functional analysis of glycosyltransferase genes from *Lactococcus lactis* and other gram-positive cocci: complementation, expression, and diversity. Journal of Bacteriology 181: 6347-6353.

392. Vaneechoutte, M., Dijkshoorn, L., Tjernberg, I., Elaichouni, A., de Vos, P., Claeys, G. and Verschraegen, G. (1995). Identification of *Acinetobacter* genomic species

by amplified ribosomal DNA restriction analysis. Journal of Clinical Microbiology 33: 11-15.

393. Vazquez-Salat, N. (2013). Are good ideas enough? The impact of socio-economic and regulatory factors on GMO commercialisation. Biological Research 46: 317-322.

394. Velasco, S. E., Yebra, M. J., Monedero, V., Ibarburu, I., Duenas, M. T. and Irastorza, A. (2007). Influence of the carbohydrate source on beta-glucan production and enzyme activities involved in sugar metabolism in *Pediococcus parvulus* 2.6. International Journal of Food Microbiology 115: 325-334.

395. Vigil, M., Marey-Perez, M. F., Martinez Huerta, G. and Alvarez Cabal, V. (2015). Is phytoremediation without biomass valorization sustainable? - comparative LCA of landfilling vs. anaerobic co-digestion. The Science of the Total Environment 505: 844-850.

396. Vohla, C., Poldvere, E., Noorvee, A., Kuusemets, V. and Mander, U. (2005). Alternative filter media for phosphorus removal in a horizontal subsurface flow constructed wetland. Journal of Environmental Science and Health 40: 1251-1264.

397. Wahab, M. A., Hassine, R. B. and Jellali, S. (2011). *Posidonia oceanica* (L.) fibers as a potential low-cost adsorbent for the removal and recovery of orthophosphate. Journal of Hazardous Materials 191: 333-341.

398. Wang, X., Liu, F., Tan, W., Li, W., Feng, X. and Sparks, D. L. (2013a). Characteristics of phosphate adsorption-desorption onto ferrihydrite: comparison with well-crystalline Fe (hydr)oxides. Soil Science 178: 1-11.

399. Wang, A. and Roth, J. R. (1988). Activation of silent genes by transposons Tn5 and Tn10. Genetics 120: 875-885.

400. Wang, G., Wilson, T. J. M., Jiang, Q. and Taylor, D. E. (2001). Spontaneous mutations that confer antibiotic resistance in *Helicobacter pylori*. Antimicrobial Agents and Chemotherapy 45: 727-733.

401. Wang, L., Putnis, C. V., Ruiz-Agudo, E., Hovelmann, J. and Putnis, A. (2015). In situ imaging of interfacial precipitation of phosphate on goethite. Environmental Science & Technology 49: 4184-4192.

402. Wang, R., Peng, Y., Cheng, Z. and Ren, N. (2014a). Understanding the role of extracellular polymeric substances in an enhanced biological phosphorus removal granular sludge system. Bioresource Technology 169: 307-312.

403. Wang, S., Yu, S., Zhang, Z., Wei, Q., Yan, L., Ai, G., Liu, H. and Ma, L. Z. (2014b). Coordination of swarming motility, biosurfactant synthesis, and biofilm matrix exopolysaccharide production in *Pseudomonas aeruginosa*. Applied and Environmental Microbiology 80: 6724-6732.

404. Wang, W., Chen, S., Bao, K., Gao, J., Zhang, R., Zhang, Z. and Sugiura, N. (2014c). Enhanced removal of contaminant using the biological film, anoxic-anaerobic-aerobic and electro-coagulation process applied to high-load sewage treatment. Environmental Technology 35: 833-840.

405. Wang, W., Zhou, J., Wei, D., Wan, H., Zheng, S., Xu, Z. and Zhu, D. (2013b). ZrO2-functionalized magnetic mesoporous SiO2 as effective phosphate adsorbent. Journal of Colloid and Interface Science 407: 442-449.

406. Wang, X., Li, W., Harrington, R., Liu, F., Parise, J. B., Feng, X. and Sparks, D. L. (2013c). Effect of ferrihydrite crystallite size on phosphate adsorption reactivity. Environmental Science & Technology 47: 10322-10331.

407. Wang, Y. and Zhang, Y. H. (2010). A highly active phosphoglucomutase from *Clostridium thermocellum*: cloning, purification, characterization and enhanced thermostability. Journal of Applied Microbiology 108: 39-46.

408. Wei, X., Fang, L., Cai, P., Huang, Q., Chen, H., Liang, W. and Rong, X. (2011). Influence of extracellular polymeric substances (EPS) on Cd adsorption by bacteria. Environmental Pollution 159: 1369-1374.

409. Welman, A. D., Maddox, I. S. and Archer, R. H. (2003). Screening and selection of exopolysaccharide-producing strains of *Lactobacillus delbrueckii* subsp. *bulgaricus*. Journal of Applied Microbiology 95: 1200-1206.

410. WHO (World Health Organization) (2004). Laboratory biosafety manual (www.who.int/csr/resources/publications/biosafety/en/Biosafety7.pdf) (Assessed on 28 July 2015).

411. Willerding, A., Luis, Oliveira, L. A. d., Moreira, F. W., Germano, M. G., Chagas, A. and sio, F. (2011). Lipase activity among bacteria isolated from Amazonian soils. Enzyme Research 2011: 5.

412. Williams, A. G. and Wimpenny, J. W. (1977). Exopolysaccharide production by *Pseudomonas* NCIB11264 grown in batch culture. Journal of General Microbiology 102: 13-21.

413. Wingender, J., Neu, T. R. and Flemming, H.-C. (1999). Microbial extracellular polymeric substances: characterization, structure, and function, Springer Science & Business Media, Berlin.

414. Wolff, M., Joly-Guillou, M. L., Farinotti, R. and Carbon, C. (1999). In vivo efficacies of combinations of beta-lactams, beta-lactamase inhibitors, and rifampin against *Acinetobacter baumannii* in a mouse pneumonia model. Antimicrobial Agents and Chemotherapy 43: 1406-1411.

415. Wu, D., Shen, Y., Ding, A., Qiu, M., Yang, Q. and Zheng, S. (2013). Phosphate removal from aqueous solutions by nanoscale zero-valent iron. Environmental Technology 34: 2663-2669.

416. Wu, D., Zhang, B., Li, C., Zhang, Z. and Kong, H. (2006). Simultaneous removal of ammonium and phosphate by zeolite synthesized from fly ash as influenced by salt treatment. Journal of Colloid and Interface Science 304: 300-306.

417. Wu, K., Liu, T., Ma, C., Chang, B., Chen, R. and Wang, X. (2014a). The role of Mn oxide doping in phosphate removal by Al-based bimetal oxides: adsorption behaviors and mechanisms. Environmental Science and Pollution Research International 21: 620-630.

418. Wu, Q., Tun, H. M., Leung, F. C.C. and Shah, N. P. (2014b). Genomic insights into high exopolysaccharide-producing dairy starter bacterium *Streptococcus thermophilus* ASCC 1275. Scientific Reports 4: (DOI:10.1038/srep04974).

419. WWAP (2015). The United Nations world water development report 2015: water for a sustainable world. Paris, UNESCO.

420. Xi, Z. and Chen, B. (2014). The effect of structural compositions on the biosorption of phenanthrene and pyrene by tea leaf residue fractions as model biosorbents. Environmental Science and Pollution Research International 21: 3318-3330.

421. Xiang, W., Xiao, E. Y. and Rengel, Z. (2009). Phytoremediation facilitates removal of nitrogen and phosphorus from eutrophicated water and release from sediment. Environmental Monitoring and Assessment 157: 277-285.

422. Xu, F., Wang, J., Chen, S., Qin, W., Yu, Z., Zhao, H., Xing, X. and Li, H. (2011a). Strain improvement for enhanced production of cellulase in *Trichoderma viride*. Prikladnaia Biokhimiia i Mikrobiologiia 47: 61-65.

423. Xu, J. W., Ji, S. L., Li, H. J., Zhou, J. S., Duan, Y. Q., Dang, L. Z. and Mo, M. H. (2015). Increased polysaccharide production and biosynthetic gene expressions in a submerged culture of *Ganoderma lucidum* by the overexpression of the homologous alpha-phosphoglucomutase gene. Bioprocess and Biosystem Engineering 38: 399-405.

424. Xu, K., Deng, T., Liu, J. and Peng, W. (2010). Study on the phosphate removal from aqueous solution using modified fly ash. Fuel 89: 3668-3674.

425. Xu, P., Capito, M. and Cath, T. Y. (2013a). Selective removal of arsenic and monovalent ions from brackish water reverse osmosis concentrate. Journal of Hazardous Materials 260: 885-891.

426. Xu, T., Bharucha, N. and Kumar, A. (2011b). Genome-wide transposon mutagenesis in S*accharomyces cerevisiae* and *Candida albicans*. Methods in Molecular Biology 765: 207-224.

427. Xu, X., Gao, Y., Gao, B., Tan, X., Zhao, Y. Q., Yue, Q. and Wang, Y. (2011c). Characteristics of diethylenetriamine-crosslinked cotton stalk/wheat stalk and their biosorption capacities for phosphate. Journal of Hazardous Materials 192: 1690-1696.

428. Xu, Z., Cai, J.G. and Pan, B.C. (2013b). Mathematically modeling fixed-bed adsorption in aqueous systems. Journal of Zhejiang University-Science A (Applied Physics & Engineering) 14: 155-176.

429. Xue, Y., Hou, H. and Zhu, S. (2009). Characteristics and mechanisms of phosphate adsorption onto basic oxygen furnace slag. Journal of Hazardous Materials 162: 973-980.

430. Yagi, S. and Fukushi, K. (2012). Removal of phosphate from solution by adsorption and precipitation of calcium phosphate onto monohydrocalcite. Journal of Colloid and Interface Science 384: 128-136.

431. Yan, Y., Koopal, L. K., Li, W., Zheng, A., Yang, J., Liu, F. and Feng, X. (2015). Size-dependent sorption of myo-inositol hexakisphosphate and orthophosphate on nano-gamma-AlO. Journal of Colloid and Interface Science 451: 85-92.

432. Yang, M., Lin, J., Zhan, Y., Zhu, Z. and Zhang, H. (2015). Immobilization of phosphorus from water and sediment using zirconium-modified zeolites. Environmental Science and Pollution Research International 22: 3606-3619.

433. Yang, Y., Lohwacharin, J. and Takizawa, S. (2014). Hybrid ferrihydrite-MF/UF membrane filtration for the simultaneous removal of dissolved organic matter and phosphate. Water Research 65: 177-185.

434. Yao, Y., Gao, B., Chen, J. and Yang, L. (2013). Engineered biochar reclaiming phosphate from aqueous solutions: mechanisms and potential application as a slow-release fertilizer. Environmental Science & Technology 47: 8700-8708.

435. Ye, R. W., Zielinski, N. A. and Chakrabarty, A. M. (1994). Purification and characterization of phosphomannomutase/phosphoglucomutase from *Pseudomonas aeruginosa* involved in biosynthesis of both alginate and lipopolysaccharide. Journal of Bacteriology 176: 4851-4857.

436. Yilmaz, M. T., Dertli, E., Toker, O. S., Tatlisu, N. B., Sagdic, O. and Arici, M. (2014). Effect of in situ exopolysaccharide production on physicochemical, rheological, sensory, and microstructural properties of the yogurt drink ayran: an

optimization study based on fermentation kinetics. Journal of Dairy Science 98: 1604-1624.

437. Yu, H. (2012). Effect of mixed carbon substrate on exopolysaccharide production of cyanobacterium *Nostoc flagelliforme* in mixotrophic cultures. Journal of Applied Phycology 24: 669-673.

438. Yu, S. H., Dong, X. L., Gong, H., Jiang, H. and Liu, Z. G. (2012). Adsorption kinetic and thermodynamic studies of phosphate onto tantalum hydroxide. Water Environment Research 84: 2115-2122.

439. Yu, Y. and Chen, J. P. (2015). Key factors for optimum performance in phosphate removal from contaminated water by a Fe-Mg-La tri-metal composite sorbent. 445: 303-311.

440. Yuan, X., Xia, W., An, J., Yin, J., Zhou, X. and Yang, W. (2015). Kinetic and thermodynamic studies on the phosphate adsorption removal by dolomite mineral. Journal of Chemistry 2015: 8.

441. Zadravec, P., Strukelj, B. and Berlec, A. (2015). Heterologous surface display on lactic acid bacteria: non-GMO alternative? Bioengineered 6: 179-183.

442. Zeng, L., Li, X. and Liu, J. (2004). Adsorptive removal of phosphate from aqueous solutions using iron oxide tailings. Water Research 38: 1318-1326.

443. Zhai, Y., Han, D., Pan, Y., Wang, S., Fang, J., Wang, P. and Liu, X.W. (2015). Enhancing GDP-fucose production in recombinant *Escherichia coli* by metabolic pathway engineering. Enzyme and Microbial Technology 69: 38-45.

444. Zhang, H. L., Fang, W., Wang, Y. P., Sheng, G. P., Xia, C. W., Zeng, R. J. and Yu, H. Q. (2013a). Species of phosphorus in the extracellular polymeric substances of EBPR sludge. Bioresource Technology 142: 714-718.

445. Zhang, H. L., Fang, W., Wang, Y. P., Sheng, G. P., Zeng, R. J., Li, W. W. and Yu, H. Q. (2013b). Phosphorus removal in an enhanced biological phosphorus removal process: roles of extracellular polymeric substances. Environmental Science & Technology 47: 11482-11489.

446. Zhang, J., Chen, N., Tang, Z., Yu, Y., Hu, Q. and Feng, C. (2015a). A study of the mechanism of fluoride adsorption from aqueous solutions onto Fe-impregnated chitosan. Physical

447. Zhang, J., Sun, Y. X., Huang, Z. F., Liu, X. Q. and Meng, G. Y. (2006). Treatment of phosphate-containing oily wastewater by coagulation and microfiltration. Journal of Environmental Sciences (China) 18: 629-633.

448. Zhang, L., Gao, Y., Li, M. and Liu, J. (2015b). Expanded graphite loaded with lanthanum oxide used as a novel adsorbent for phosphate removal from water: performance and mechanism study. Environmental Technology 36: 1016-1025.

449. Zhang, Q., Yang, B., Brashears, M. M., Yu, Z., Zhao, M., Liu, N. and Li, Y. (2014). Influence of casein hydrolysates on exopolysaccharide synthesis by *Streptococcus thermophilus* and *Lactobacillus delbrueckii* ssp. bulgaricus. Journal of the Science of Food and Agriculture 94: 1366-1372.

450. Zhang, R. and Edgar, K. J. (2014). Properties, chemistry, and applications of the bioactive polysaccharide curdlan. Biomacromolecules 15: 1079-1096.

451. Zhang, Z.Q., Lin, B., Xia, S.Q., Wang, X.J. and Yang, A. M. (2007). Production and application of a novel bioflocculant by multiple-microorganism consortia using brewery wastewater as carbon source. Journal of Environmental Sciences 19: 667-673.

452. Zhang, Z. C., Huang, X., Yang, H. J., Xiao, K., Luo, X., Sha, H. and Chen, Y. M. (2009). Study on P forms in extracellular polymeric substances in enhanced biological phosphorus removal sludge by 31P-NMR spectroscopy. Guang Pu Xue Yu Guang Pu Fen Xi 29: 536-539.

453. Zheng, T. T., Sun, Z. X., Yang, X. F. and Holmgren, A. (2012). Sorption of phosphate onto mesoporous gamma-alumina studied with in-situ ATR-FTIR spectroscopy. Chemistry Central Journal 6: 26.

454. Zheng, X. Y., Kong, H. N., Wu, D. Y., Wang, C., Li, Y. and Ye, H. R. (2009). Phosphate removal from source separated urine by electrocoagulation using iron plate electrodes. Water Science and Technology 60: 2929-2938.

455. Zhong, B., Stanforth, R., Wu, S. and Chen, J. P. (2007). Proton interaction in phosphate adsorption onto goethite. Journal of Colloid and Interface Science 308: 40-48.

456. Zhou, J., Li, J., Long, T., Wu, Z. and Liu, M. (2008). Study on the action of extracellular polymeric substances (EPS) in biological phosphorus removal from wastewater. Acta Scientiae Circumstantiae 28: 1758-1762.

457. Zhuang, W., Gao, X., Zhang, Y., Xing, Q., Tosi, L. and Qin, S. (2014). Geochemical characteristics of phosphorus in surface sediments of two major Chinese mariculture areas: the Laizhou Bay and the coastal waters of the Zhangzi Island. Marine Pollution Bulletin 83: 343-351.

458. Zhurina, M. V., Gannesen, A. V., Zdorovenko, E. L. and Plakunov, V. K. (2014). Composition and functions of the extracellular polymer matrix of bacterial biofilms. Microbiology 83: 713-722.

459. Zimaro, T., Thomas, L., Marondedze, C., Sgro, G. G., Garofalo, C. G., Ficarra, F. A., Gehring, C., Ottado, J. and Gottig, N. (2014). The type III protein secretion system contributes to *Xanthomonas citri* subsp. citri biofilm formation. BMC Microbiology 14: 96.

ANNEXURES

Annexure I

Media

EBP production media

Composition	*quantity (g/L)*
Ammonium sulphate	1.0
Calcium chloride dehydrate	0.7
Dextrose	1.0
Dipotassium hydrogen phosphate	1.0
Magnesium sulphate heptahydrate	0.3
Peptone	5.0
Potassium dihydrogen orthophosphate	1.0
Sodium chloride	0.1
Agar	3.0
pH	7.2 ± 0.2

Luria Bertani (LB) broth

Composition	*quantity (g/L)*
NaCl	10.0
Beef extract	5.0
Tryptone	10.0
Agar	10.0

SIM agar

Composition	*quantity (g/L)*
Enzymatic Digest of Casein	20
Enzymatic Digest of Animal Tissue	6.1
Ferric Ammonium Citrate	0.2
Sodium Thiosulfate	0.2
Agar	3.5
pH	7.3 ± 0.2

Urea broth

Composition	*quantity (g/L)*
Yeast extract	0.1
Dipotassium hydrogen phosphate	9.5
Potassium dihydrogen phosphate	9.1
Urea	20.0
Phenol red	0.01
pH	6.8 ± 0.2

MR-VP broth

Composition	*quantity (g/L)*
Dipeptone	7.0
Dextrose	5.0

Dipotassium phosphate	5.0
pH	6.9±0.2

Simmons Citrate Agar

Composition	*quantity (g/L)*
Magnesium sulphate	0.2
Ammonium dihydrogen phosphate	1.0
Dipotassium phosphate	1.0
Sodium citrate	2.0
Sodium chloride	5.0
Bromothymol blue	0.08
Agar	15.0
pH	6.8±0.2

Starch Agar

Composition	*quantity (g/L)*
Beef extract	3
Soluble starch	10
Agar	12
Distilled water	1 liter

Reagents and buffers

Stannous chloride solution

Stannous chloride	2.5 g
Glycerol	100 mL

Ammonium molybdate reagent

Ammonium molybdate	25 g
Distilled water	175 mL
Concentrated sulphuric acid	280 mL

Make up the volume upto 1 L

Methyl red solution

Methyl red	0.1 g
Ethanol (95%)	300 mL

Store the prepared methyl red solution at 4°C.

Barritt's reagent A

a-naphthol in absolute ethanol	5%

Barritt's reagent B

KOH in deionized water	40%

Kovac's reagent

p-dimethylaminobenzaldehyde	5 g

Amyl alcohol	75 mL
HCl	25 mL

Dissolve p-dimethylaminobenzaldehyde in the amyl alcohol and add HCl.

Phenol Sulfuric acid method

Phenol	5%
Sulfuric acid (reagent grade)	96%
Sugar standards (reagent grade)	1 mg/mL

Folin Lowry method

Reagent A (alkaline solution) (for 50 mL)

NaOH	0.1 M
Sodium carbonate	2.0g

Reagent B (for 50 mL)

Copper sulpahte pentahydrate	0.25g Na
Na_2 Tartarate.$2H_2O$	0.5g
Lowry solution	(fresh; 0.7mL/sample)
Reagent A+ Reagent B	
Folin and Ciocalteu's Phenol Reagent	1:1

Elson Morgan method

Reagent A (100 mL)

di-Potassium tetraborate tetrahydrate	6.1 g

Reagent B

4-N,N-dimethyl-p-aminobenzaldehyde	1 g
Glacial acetic acid	50 mL
Hydrochloric acid (10 N)	1.5 mL

Carbazole assay

Reagent A

Sodium tetraborate decahydrate	0.9 g
Distilled water	10 mL
Concentrated Sulphuric acid (ice cold) 98%	90 mL

Reagent B

Carbazole	100 mg
Absolute ethanol	100 mL

Friedman method

Perchloric acid	50%
DNP reagent 2,4-dinitro phenylhydrazine	500 µmoles
Hydrochloric acid (2N)	100 mL
Sodium hydroxide	2.2N

TBE buffer (10X)

Tris-HCl	0.09 M (pH 8)
Boric acid	0.9 M
EDTA	0.02 M (pH 8)

Lysozyme

Stock solution	10 mg/mL
Working solution	300 - 400 mg/mL

Agarose gel loading dye (6X)

Bromophenol blue	0.25%
Glycerol in water	30.0%

TE buffer 10X

Tris-HCl	0.1 M (pH 8)
Na2EDTA	10 M (pH 8)

Acrylamide-bisacrylamide (30%)

Acrylamide	29.2g
Bisacrylamide	0.8g
Distilled water	100 mL

4X Separating gel buffer (1.5M Tris, pH 8.8)

Tris	3g
Distilled water	100 mL

4X Stacking gel buffer (0.5M Tris, pH 6.8)

Tris	18.15g
Distilled water	100ml

2X Cracking buffer

Tris	(0.5M, pH 6.8) 2.5mL
SDS (10%)	4.0 mL
Glycerol (100%)	2.0 mL
β-mercaptoethanol	0.8 mL
Bromophenol blue (0.1%)	300 µL
Distilled water	400 µL

Make up the volume upto 10 mL

SDS (10%)

SDS	10 g
Distilled water	100 mL

Ammonium persulfate (10%)

Ammonium persulfate	0.1g
Distilled water	1.0 mL

Bromophenol blue (0.1%)

Bromophenol blue	5 mg
Distilled water	5 mL

Staining solution

Coomassie blue (R-250)	0.3 g
Methanol (AR)	80 mL
Glacial acetic acid	20 mL
Distilled water	100 mL

Destaining solution

Acetic acid	100 mL
Methanol	300 mL

Make up the volume with distilled water to 1L

Tank buffer

Tris	6.05 g
Glycine	28.80 g
SDS	1.0 g

Make up the volume to 1000 mL with distilled water

Resolving gel (12%)

Deionized water	3.3 mL
4X Separating gel buffer (1.5M Tris, pH 8.8)	2.5 mL
Acrylamide (10%)	2.5 mL
APS (10%)	70 µL
TEMED	10 µL

Stacking gel (4%)

Deionized water	3 mL
4X Stacking gel buffer (0.5M Tris, pH 6.8)	2.5 mL
Acrylamide (10%)	800 µL
APS (10%)	70 µL
TEMED	10 µL

Genomic DNA Extraction buffer

Sodium acetate	100 mM
Na_2EDTA	50 mM
NaCl	500 mM
SDS	1%

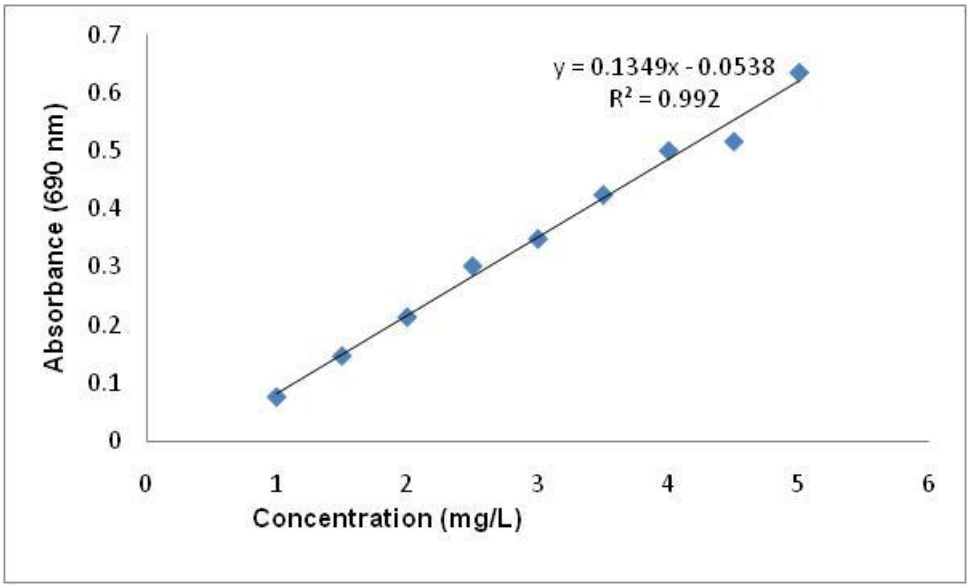

Figure A1: Standard curve of phosphate. Relationship between concentration of phosphate (as mg/L) and absorbance at 690 nm using stannous chloride method.

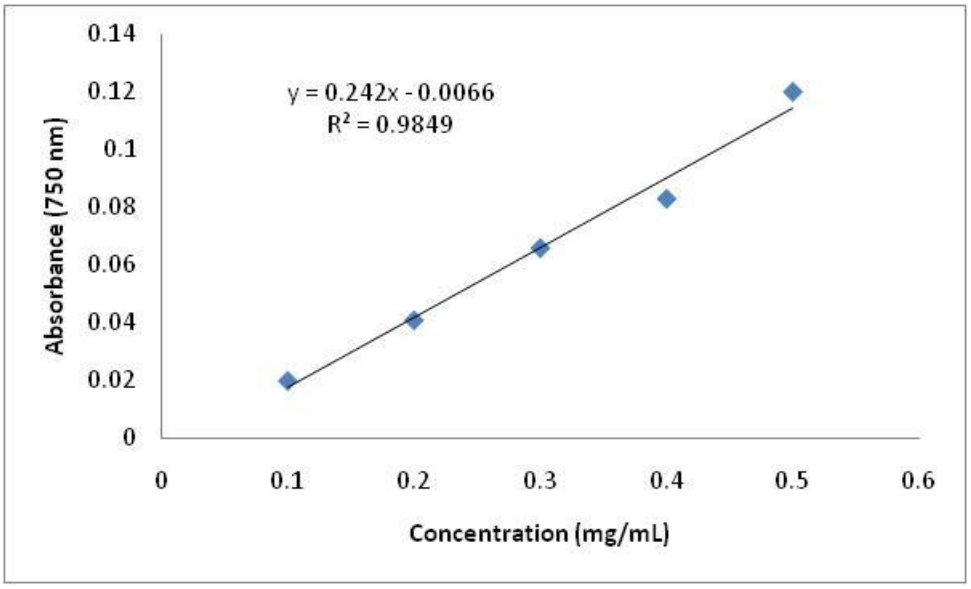

Figure A2: Standard curve of bovine serum albumin. Relationship between concentration of protein (as mg/mL) and absorbance at 750 nm using Folin Lowry method.

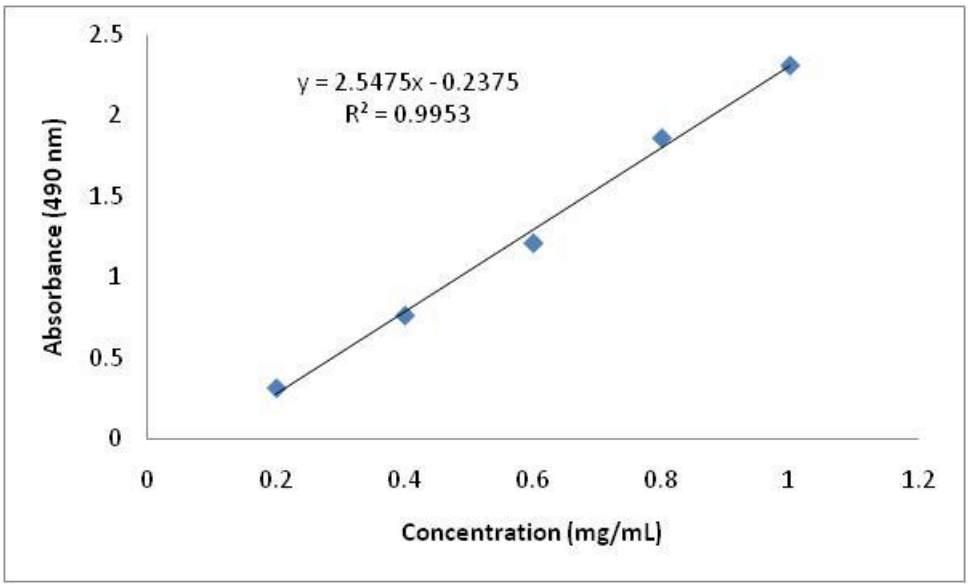

Figure A3: Standard curve of glucose. Relationship between concentration of glucose (as mg/mL) and absorbance at 490 nm using phenol sulphuric acid method.

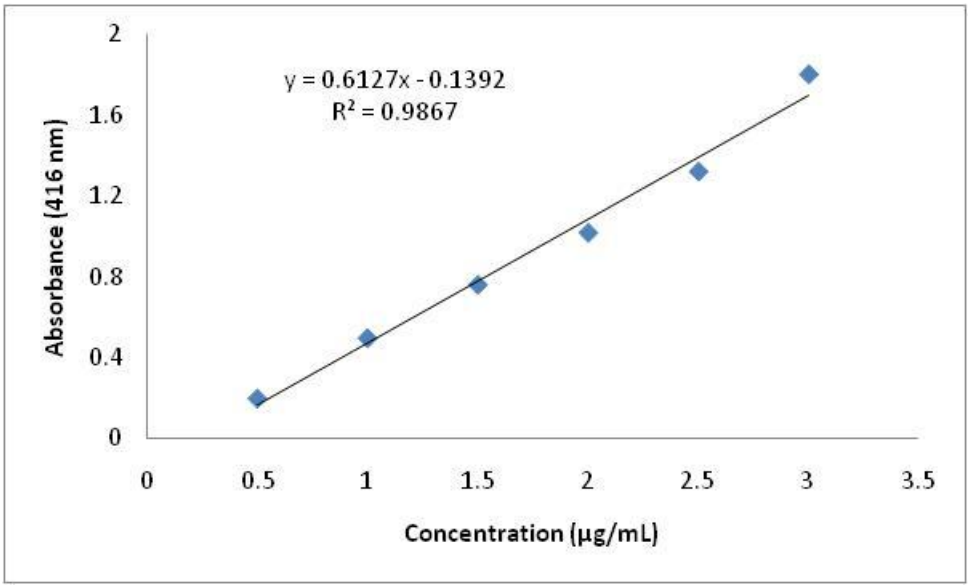

Figure A4: Standard curve of pyruvic acid. Relationship between concentration of pyruvic acid (as µg/mL) and absorbance at 416 nm using Friedman method.

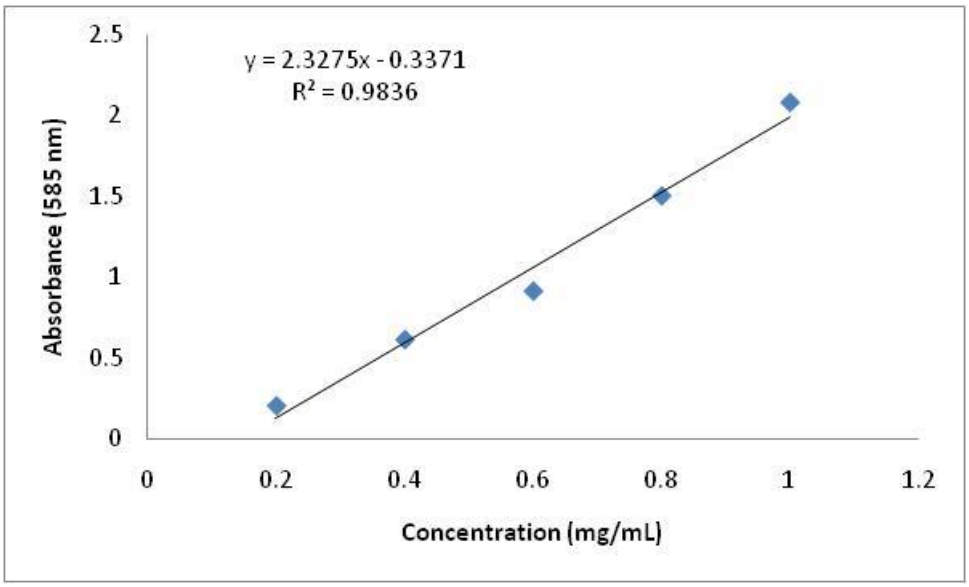

Figure A4: Standard curve of glucosamine. Relationship between concentration of glucosamine (as mg/mL) and absorbance at 585 nm using Elson-morgan method

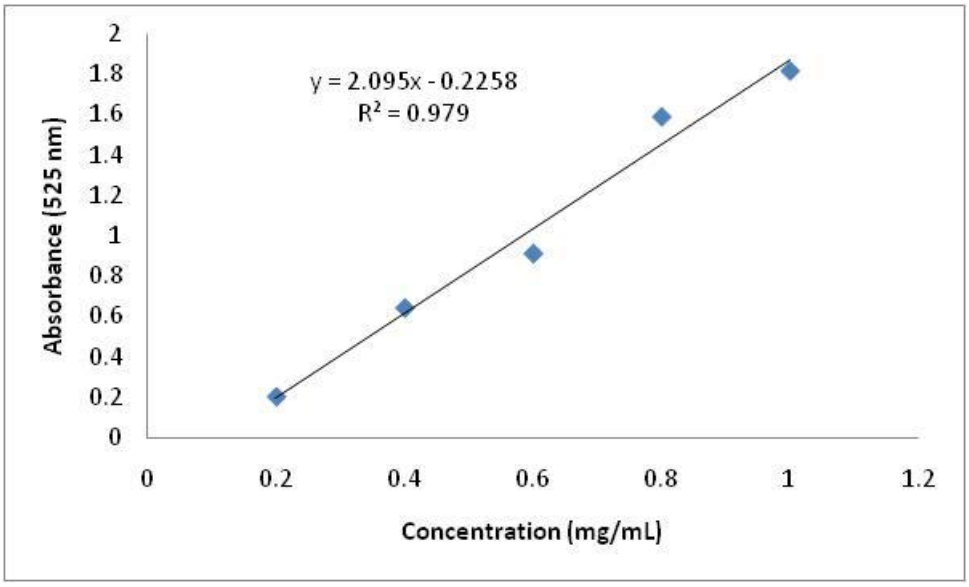

Figure A5: Standard curve of glucouronic acid. Relationship between concentration of glucouronic acid (as mg/mL) and absorbance at 525 nm using Haug and Larsen method

pGS9 suicidal vector containing Tn5 element

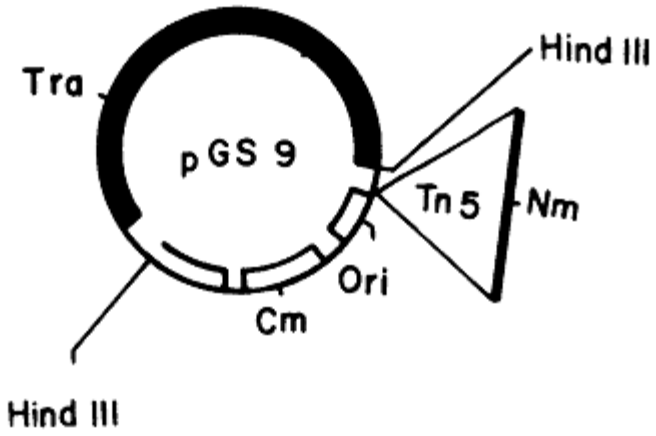

Model structure of Tn5 transposon

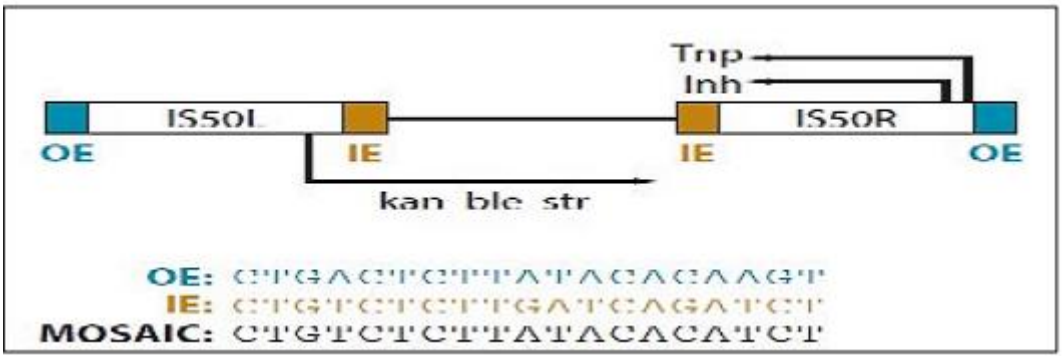

***Acinetobacter haemolyticus* strain TK15 16S ribosomal RNA gene, partial sequence**

GenBank: KP701480.1

FASTA Graphics

Go to:

LOCUS KP701480 1462 bp DNA linear BCT 30-JUN-2015
DEFINITION Acinetobacter haemolyticus strain TK15 16S ribosomal RNA gene, partial sequence.
ACCESSION KP701480
VERSION KP701480.1 GI:850224131
KEYWORDS .
SOURCE *Acinetobacter haemolyticus*
ORGANISM Acinetobacter haemolyticus
Bacteria; Proteobacteria; Gammaproteobacteria; Pseudomonadales; Moraxellaceae; Acinetobacter.
REFERENCE 1 (bases 1 to 1462)
AUTHORS Kaur,T., Ganguli,A. and Ghosh,M.
TITLE Development of exobiopolymer-based biosensor for detection of phosphate in water
JOURNAL Water Sci. Technol. 68 (12), 2619-2625 (2013)
PUBMED 24355849
REFERENCE 2 (bases 1 to 1462)
AUTHORS Kaur,T., Sharma,J., Ganguli,A. and Ghosh,M.
TITLE Application of biopolymer produced from metabolic engineered Acinetobacter sp. for the development of phosphate optoelectronic sensor
JOURNAL Compos Interfaces 21 (2), 143-151 (2014)
REFERENCE 3 (bases 1 to 1462)
AUTHORS Ghosh,M. and Kaur,T.
TITLE Direct Submission
JOURNAL Submitted (21-JAN-2015) Department of Biotechnology, Thapar University, Bhadson Road, Patiala, Punjab 147004, India
FEATURES Location/Qualifiers
source 1..1462
/organism="Acinetobacter haemolyticus"
/mol_type="genomic DNA"
/strain="TK15"
/db_xref="taxon:29430"
rRNA <1..>1462
/product="16S ribosomal RNA"
ORIGIN
1 gatgacgctg gcggcaggct taacacatgg tcgtcgagcg gggaagtgta gcttgctaca
61 ttacctagcg gcggacgggt gagtaatgct taggaatctg cctattagtg ggggacaaca
121 ttccgaaagg aatgctaata ccgcatacgt cctacgggag aaagcagggg atcttcggac

181 cttgcgctaa tagatgagcc taagtcggat tagctagttg gtggggtaaa ggcctaccaa
241 ggcgacgatc tgtagcgggt ctgagaggat gatccgccac actgggactg agacacggcc
301 cagactccta cgggaggcag cagtggggaa tattggacaa tgggcggaag cctgatccag
361 ccatgccgcg tgtgtgaaga aggccttttg gttgtaaagc actttaagcg aggaggaggc
421 tactctagtt aatacctaga gatagtggac gttactcgca gaataagcac cggctaactc
481 tgtgccagca gccgcggtaa tacagagggt gcgagcgtta atcggattta ctgggcgtaa
541 agcgtgcgta ggcggttgat taagtcggat gtgaaatccc tgagcttaac ttaggaattg
601 cattcgatac tggtcagcta gagtatggga gaggatggta gaattccagg tgtagcggtg
661 aaatgcgtag agatctggag gaataccgat ggcgaaggca gccatctggc ctaatactga
721 cgctgaggta cgaaagcatg gggagcaaac aggattagat accctggtag tccatgccgt
781 aaacgatgtc tactagccgt tggggccttt gaggctttag tggcgcagct aacgcgataa
841 gtagaccgcc tggggagtac ggtcgcaaga ctaaaactca aatgaattga cgggggcccg
901 cacaagcggt ggagcatgtg gtttaattcg atgcaacgcg aagaacctta cctggtcttg
961 acatagtaag aactttccag agatggattg gtgccttcgg gaacttacat acaggtgctg
1021 catggctgtc gtcagctcgt gtcgtgagat gttgggttaa gtcccgcaac gagcgcaacc
1081 cttttcctta tttgccagcg ggttaagccg ggaactttaa ggatactgcc agtgacaaac
1141 tggaggaagg cggggacgac gtcaagtcat catggcccct acgaccaggg ctacacacgt
1201 gctacaatgg tcggtacaaa gggttgctac ctagcgatag gatgctaatc tcaaaaagcc
1261 gatcgtagtc cggattggag tctgcaactc gactccatga agtcggaatc gctagtaatc
1321 gcggatcaga atgccgcggt gaatacgttc ccgggccttg tacacaccgc ccgtcacacc
1381 atgggagttt gttgcaccag aagtaggtag tctaaccgta aggaggacgc ttaccacggt
1441 gtggccgatg actggggtga ag
//

LOCUS Seq1 485 bp DNA linear BCT 20-MAY-2015
DEFINITION *Acinetobacter haemolyticus* MG606
phosphoglucomutase/phosphomannomutase gene, partial sequence.
ACCESSION Seq1
VERSION
KEYWORDS .
SOURCE Acinetobacter haemolyticus
ORGANISM Acinetobacter haemolyticus
Bacteria; Proteobacteria; Gammaproteobacteria; Pseudomonadales;
Moraxellaceae; Acinetobacter.
REFERENCE 1 (bases 1 to 485)
AUTHORS Kaur,T. and Ghosh,M.
TITLE Enhanced phosphate binding exobiopolymer production by a mutant
Acinetobacter haemolyticus is mediated by increased
phosphoglucomutase activity
JOURNAL Unpublished
REFERENCE 2 (bases 1 to 485)
AUTHORS Kaur,T. and Ghosh,M.
TITLE Direct Submission
JOURNAL Submitted (20-MAY-2015) Department of Biotechnology, Thapar
University, Bhadson Road, Patiala, Punjab 147004, India
COMMENT Bankit Comment: TOTAL # OF SEQS:1.
FEATURES Location/Qualifiers
source 1..485
/organism="Acinetobacter haemolyticus"
/mol_type="genomic DNA"
/strain="MG606"
/isolation_source="sludge"
/db_xref="taxon:29430"
/note="[cultured bacterial source]"
CDS complement(<1..106)
/codon_start=1
/transl_table=11
/product="Phosphoglucomutase/phosphomannomutase"
/translation="MTQLTCFKAYDIRGKLGTELNEDIAYKIGRAYGQI"
BASE COUNT 147 a 85 c 96 g 157 t
ORIGIN
1 agatctgtcc gtatgcacgg ccaattttat aggcgatgtc ttcgttcagt tctgtaccta
61 atttcccgcg aatatcatac gctttgaagc aagttagttg agtcatttaa aagagctgtt
121 tgtagtttat caatgtgttg aagtatacaa agactaagcg taattgaaca ttgattgata
181 cagaattaag caaagagaaa gtcttatttt taggtggttg agcgtttctc atttcaacca
241 ctcttagctt agaaaataaa aaaggttgtt tcacgtgaaa caacctttt tgatccataa
301 agtctccctt ttgaaaggga gatgaggagc gattatagct ccgcaagggg atgttaagct
361 gattttgcta gcacttcagc cattgctttt gcaactttat aaatattatt catatttaaa

421 cctgcaacgc agatacggcc actgcgaaca aggtaaattg catattcttc acgtaaagtg
481 tcgac
//

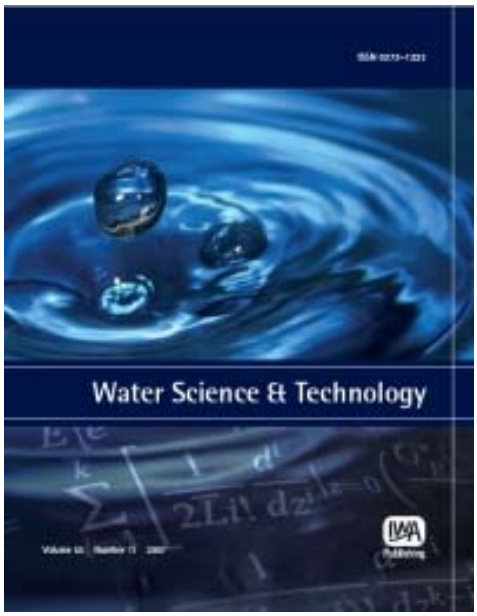

Development of exobiopolymer-based biosensor for detection of phosphate in water

Taranpreet Kaur, Abhijit Ganguli and Moushumi Ghosh

ABSTRACT

The present study was conducted to develop a biosensor by exploiting phosphate-binding capacity of exobiopolymer (EBP) produced by *Acinetobacter* sp. An environmental isolate of EBP-producing *Acinetobacter* sp. was subjected to transposon (Tn5) mutagenesis to overproduce EBP and afford improved phosphate selectivity. A mutant producing the highest amount of EBP with high phosphate-binding capacity was selected for biosensor probe fabrication. Phosphate samples were filtered through EBP-coated membranes and phosphate retained on membranes was determined by molybdenum blue method. The color produced was read using a LED 690 nm/photodiode detection system linked to an amplifier and signals were converted to appropriate phosphate concentrations. The biosensor had a limit of detection of 0.5 mg/L and a limit of quantification 1 mg/L. The biosensor as well as the probe were found to be stable for at least 28 days. In conclusion, we believe that the biosensor may have applications in monitoring of wastewater and environmental samples. Further, the enrichment of phosphate levels by EBP can help in analysis of very low phosphate concentrations.

Key words | *Acinetobacter*, biopolymer, phosphate, sensor, transposon mutagenesis

Taranpreet Kaur
Abhijit Ganguli
Moushumi Ghosh (corresponding author)
Department of Biotechnology & Environmental Sciences,
Thapar University,
Patiala-147004,
Punjab,
India
E-mail: *mghosh@thapar.edu*

INTRODUCTION

Phosphorus (P) is ubiquitously found in living organisms and plays a very important role in their growth and maintenance. The terrestrial ecosystems derive phosphorus primarily from food while the aquatic organisms rely on dissolved phosphorus to meet their needs. In recent years it has been realized that discharge of domestic and industrial wastewater and the use of fertilizers result in increased phosphorus concentration in aquatic ecosystems (USEPA 2002). This leads to increase in algal growth resulting in eutrophication of water bodies. Therefore, it is important to develop methods for efficient removal of phosphate from water and to develop sensitive systems for monitoring phosphate levels in water.

Current remediation protocols are based on physical or chemical methods for phosphate removal and include reverse osmosis, electrodialysis, treatment with aluminum sulfate or ferric chloride, etc. (Bohdziewicz *et al.* 2003; Banu *et al.* 2008). However the physical methods result in nonspecific removal of ions while chemical methods have problems in disposal and neutralization of chemicals. Bioremediation offers an attractive alternative to physical and chemical methods due to specific intracellular accumulation of phosphate by several microorganisms as well as extracellular sequestration of phosphate by microbial biopolymers. (Cloete & Oosthuizen 2001; Liu *et al.* 2006).

Spectrophotometric assays have been the mainstay in phosphate estimation in water samples, including wastewater (APHA 2007). These assays are sensitive to small amounts of phosphorus but provide false negative results or overestimation of phosphate levels due to interference by other ions. Several modifications in conventional phosphorus estimation assays have been reported to counteract interference in phosphate estimation. However, these modifications require bulky and sophisticated instruments which are unsuitable for field measurements. The development of miniaturized sensors provides a convenient means of sample analysis at the site of collection.

Acinetobacter sp. has long been identified as a major phosphate accumulating organism in sludge and other environmental samples (Kortstee *et al.* 1994; Lin *et al.* 2003; Sathasivan 2009). Several studies have reported that *Acinetobacter* can accumulate phosphates intracellularly

doi: 10.2166/wst.2013.520

(Sathasivan 2009; Khoi & Diep 2013). Investigations in our laboratory showed that the exobiopolymer (EBP) secreted by *Acinetobacter* sp. can also sequester phosphates. The present study was conducted to exploit the phosphate-sequestering potential of *Acinetobacter* EBP for development of an analytical method for phosphate estimation. A biosensor was developed which utilizes the phosphate-binding capacity of EBP to concentrate phosphate in water samples followed by analysis with the stannous chloride method.

MATERIALS AND METHODS

Chemicals and media

Ammonium sulfate, dextrose, dipotassium hydrogen phosphate, peptone, potassium dihydrogen phosphate, yeast extract, Luria Bertani (LB) broth, kanamycin and streptomycin were purchased from HiMedia (Mumbai, India). Sodium chloride and ammonium molybdate were procured from LobaChemie (Mumbai, India). Calcium chloride and magnesium sulfate were purchased from SD-fine Chem. Ltd (Mumbai, India).

Culture

Wild and mutant *Acinetobacter* sp. were cultured in LB broth at 30 °C for routine maintenance and transferred to flocculant isolation broth medium for EBP production (Ghosh *et al*. 2009).

Mutagenesis

Antibiotic-resistant strains of donor (*Escherichia coli* containing suicidal vector pGS9) and recipient (*Acinetobacter* sp.) were selected by culturing in LB broth containing kanamycin (50 μg/mL) and streptomycin (200 μg/mL), respectively. The donor and recipient were incubated in antibiotic-containing LB broth for 18 h at 30 °C under shaking (120 rpm). For conjugal mating, donor and recipient cells were mixed in the ratio of 1:1, 1:2, 2:1, 3:1 and placed onto a filter membrane supported by luria agar, and incubated for 24 at 30 °C. The filter membrane was transferred to 50 mL LB containing double antibiotics (streptomycin 200 μg/mL and kanamycin 50 μg/mL) and incubated at 30 °C for 8 h. Each of the dilutions (0.1 mL) was spread onto luria agar selective for exconjugants.

The exconjugants were screened by examining the colony morphology and mucoid colonies were selected for further studies. The EBP overproducing mutants were selected by application of Alcian Blue assay and Sudan Black staining (Liu *et al*. 1998; Kachlany *et al*. 2001).

Extraction and purification of EBP

Extraction and purification of EBP was done by the method as described earlier (Ghosh *et al*. 2009).

Characterization of EBP

The EBP was characterized by analyzing sugars (Dubois *et al*. 1956) and amino sugars (Chaplin & Kennedy 1994).

Preparation of standard phosphate solutions

Standard phosphate solution was prepared by dissolving 100 mg of potassium hydrogen orthophosphate in 1 litre of deionized water and working concentrations (0–15 mg/L) were prepared by diluting standard solution with deionized water.

Biosensor fabrication and configuration

A miniature circuit (U1) with specific LED and sensor of 690 nm was assembled, as shown in Figure 1. The circuit was attached with a microcontroller and signals detected as milliamps. For operation, the EBP-coated membranes were subjected to colorimetry and inserted between LED and sensor. Signals received were used for subsequent processing to phosphate concentration. The assembled setup used for experiments is shown in Figure 1. The biosensor setup fits into a $20 \times 14 \times 10$ cm box and weighs about 1 kg.

Biosensor analysis of phosphate

The biosensor probe was an EBP-coated cellulose acetate membrane. The membranes (approx. 5 cm^2) were coated with 100 μL of an aqueous solution of purified EBP at EBP concentrations from 0 to 6 mg/mL. One millilitre of deionized water (for blank) or phosphate solution of concentrations ranging from 1 to 15 mg/L was passed through the coated membranes. The color of the phosphate bound with EBP coated over the membranes was developed by the addition of ammonium molybdate (250 μL) and stannous chloride (50 μL) onto the membranes (APHA 2007). The membranes were subjected to analysis by the biosensor.

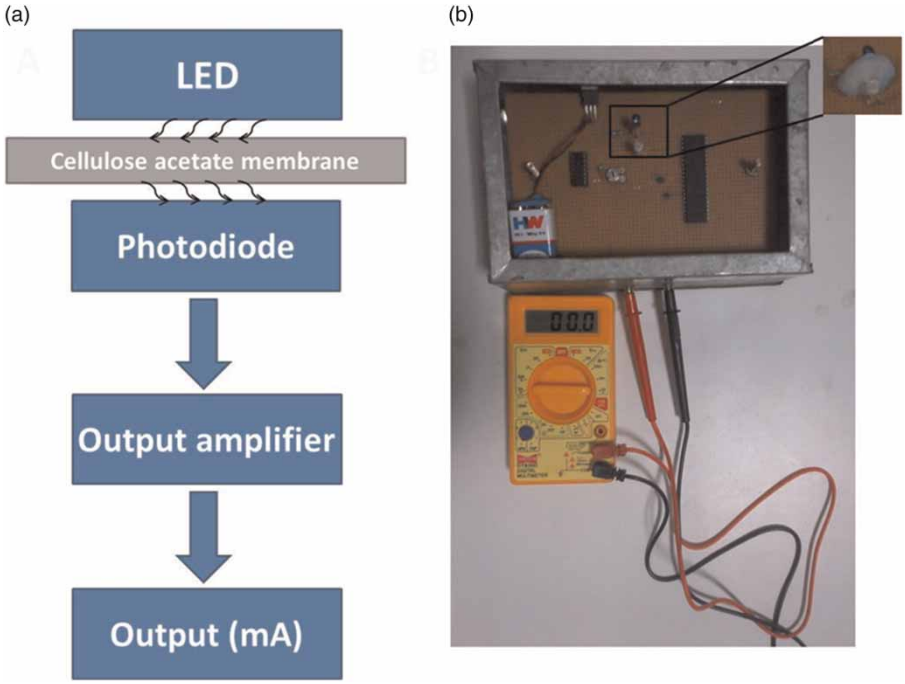

Figure 1 | (a) Schematic diagram of the phosphate biosensor. The LED emits radiations and photodiode absorbs the radiations resulting in generation of a signal. The signal intensity is proportional to color intensity on the cellulose acetate membrane. The output is amplified and the result obtained as current (mA). (b) Photograph of the phosphate biosensor setup. Inset shows cellulose acetate membrane loaded in the biosensor.

The binding efficiency of phosphate was determined by passing 1 mL of 10 mg/L phosphate solution through the membrane. The unbound phosphate remaining in the filtrate was estimated by molybdenum blue method (APHA 2007). The amount of phosphate retained on the membrane was converted to percentage of total phosphate retained on membrane and referred to as percentage phosphate binding efficiency.

Precision and accuracy

Precision or repeatability was determined by repeated analysis of spiked samples. Intra-assay variability is defined as the variability in results after repeated analysis of the same sample in one day. Standard samples in the range 1–10 mg/L were analyzed three times on the same day ($n = 5$/concentration) and percentage relative standard deviation (%RSD) was calculated.

Inter-assay variability is defined as the variability in results after repeated analysis of the sample over several days. The samples prepared for intra-day variability were analyzed for 3 consecutive days and %RSD calculated ($n = 5$/concentration). Long-term stability (4 weeks) of the sensor response was determined by analysis of samples prepared for intra-day variability on days 0, 7, 14, 21 and 28 and %RSD calculated ($n = 5$/concentration).

Accuracy or recovery refers to the closeness of the measured value to the actual value. It is calculated as (Measured concentration/Actual concentration) ×100.

Stability of biosensor probe

Cellulose acetate membranes were coated with 4 mg/mL EBP, air-dried and stored at 4 °C and ambient temperature (~25 °C) for up to 4 weeks. Membranes were used at regular intervals and phosphate concentration estimated in 10 mg/L phosphate as described above.

RESULTS AND DISCUSSION

Phosphate estimation by spectrophotometric assay is prone to interference by common environmental pollutants. Several modifications in the spectrometric methods have been developed which allow direct determination of phosphate in samples which are less susceptible to interference by environmental pollutants (Koga *et al.* 2010; Turel *et al.* 2010; Mesquita *et al.* 2011; Zimmer & Cutter 2012). Methods based

on chromatographic separation followed by spectrometric analysis of phosphates have also been reported (Rodil *et al.* 2009; Yokoyama *et al.* 2009). However, these methods use sophisticated instruments and require elaborate sample processing before analysis which makes these methods unfit for field/on-site measurements. In recent years, attempts have been made to develop phosphate biosensors using enzymes, synthetic receptors and polymers. However, a major problem associated with using enzymes is their susceptibility to poisoning/denaturation by environmental pollutants, which may lead to false negative results. Further, phosphate biosensors developed using synthetic receptors are susceptible to interference by anions commonly present in environmental samples and have not been tested for suitability for field applications (Warwick *et al.* 2013).

The present study was aimed at developing a phosphate biosensor based on the phosphate-binding capacity of EBP for two reasons. First, EBP produced by mutant strain has high selectivity for phosphate as compared to other ions. Second, phosphate binding is not substantially altered by presence of other ions. These two features ensure selectivity of phosphate retention on EBP, even in the presence of other ions/pollutants. Further, the method involves retention of phosphate during filtration through EBP-coated membrane which results in concentration of the analyte (phosphate) on membrane, thus increasing the sensitivity of the biosensor. We believe that this is the first study that reports the development of an EBP-based biosensor for phosphate estimation. Further, the method combines the advantages of selective retention of the analyte and an on-line concentration step, which has not been reported in other studies on biosensors.

Development of EBP overproducing exconjugants

The EBP production by wild type strain of *Acinetobacter* sp. is fairly low for practical applications. Hence, transposon mutagenesis was attempted to select strains producing high levels of EBP. The initial screening of mutant colonies was performed by visual inspection of colony morphology. Mucoid colonies are expected to produce EBP and, therefore selected for further screening. Based on colony morphology followed by dye staining, the mutant producing the highest amount of EBP was selected. Further, EBP from this mutant also showed the highest phosphate-binding efficiency. Hence, the mutant was selected for fabrication of the biosensor probe.

The EBP produced by mutant strain contained approximately 2-fold and 1.5-fold higher amount of sugars and amino sugars, respectively compared to EBP produced by the wild strain.

Optimization of operational conditions

The biosensor was optimized in terms of the amount of EBP coated on the membrane. Membranes were coated with 100 μL of 1–6 mg/mL of EBP and phosphate binding determined. Phosphate retention on membranes increased with an increase in the amount of EBP impregnated on membrane and reached a plateau at 4 mg/L. A further increase in EBP concentration to 5 and 6 mg/ml offered no significant increase in phosphate binding (Supplementary Figure 1, available online at http://www.iwaponline.com/wst/068/520.pdf).

The biosensor is expected to obtain a balance between sensitivity of detection/quantification and duration of analysis. All other variables remaining the same, time taken for the sample to pass through the membrane is an important factor that can impact the total time of sample analysis. Hence, the effect of EBP concentration on flow rate through the membrane was determined. The flow rate was normalized to that of uncoated membranes and expressed as percentage of flow rate through uncoated membrane. As observed in Supplementary Figure 2 (available online at http://www.iwaponline.com/wst/068/520.pdf), the flow rate through membranes remained unaffected by EBP up to a concentration of 3 mg/mL. A further increase in concentration to 4 mg/mL resulted in a slight reduction in flow rate while a further increase in EBP resulted in a sharp decline in the flow rate (Supplementary Figure 2). The observed reduction in flow rate may be attributed to blockade of membrane pores by EBP at high EBP concentrations.

Hence, considering the near-maximal binding observed at 4 mg/mL EBP and a significant reduction in flow rate at higher concentrations above 4 mg/mL, coating of membranes with 100 μL of 4 mg/mL EBP was selected for biosensor validation and sample analysis.

Calibration and validation of biosensor

One millilitre of standard phosphate solutions (1–10 mg/L) was passed through EBP-coated membranes. The membranes were treated with reagents and biosensor response was recorded as milliamperes (mA). Biosensor response was found to be linear in the range 1–10 mg/L phosphate with $R^2 > 0.99$ (Figure 2(a)). The limit of detection and limit of quantification was found to be 0.5 and 1 mg/L of phosphate, respectively.

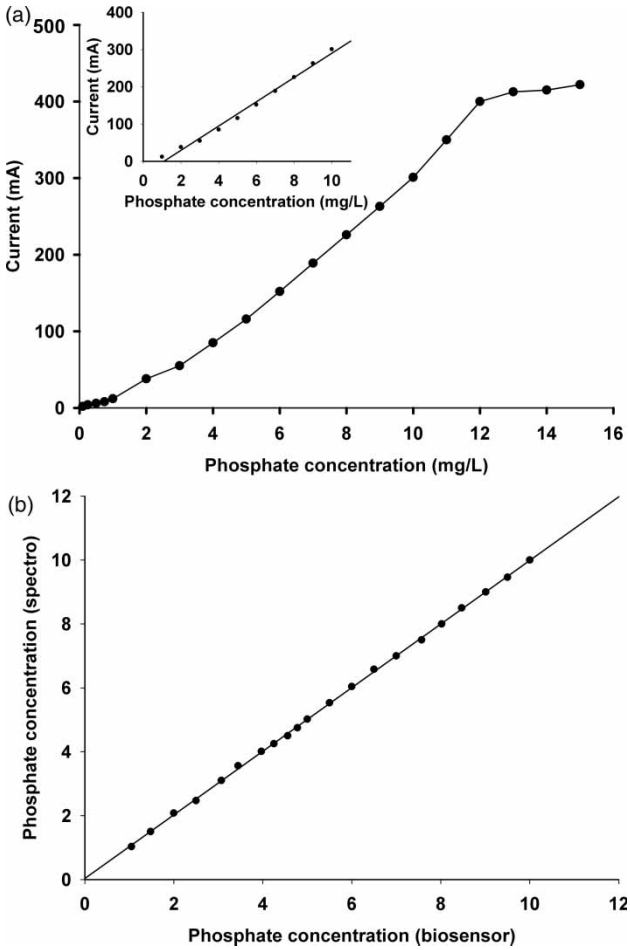

Figure 2 | (a) Calibration curve of biosensor at 0–15 mg/L phosphate concentration. Data are the mean of five samples/concentration. Inset shows regression analysis of data points in the linear range of analysis. (b) Comparison of phosphate concentration determined by biosensor and spectrophotometric method. Data are the mean of five samples/concentration.

The intra-day and inter-day variability was found to be low suggesting high precision of the biosensor (Table 1). The recovery samples were >95% at all concentrations. Further, long-term measurements over 4 weeks also showed low %RSD suggesting stability of biosensor.

Comparison of biosensor and spectrophotometric assay

The results of biosensor analysis were compared with a standard spectrophotometric method to further validate the biosensor. Standard phosphate solutions in the concentration range 1–10 mg/L were analyzed by biosensor. The same samples were also analyzed by spectrophotometric method and results obtained by both methods were compared. Regression analysis showed that phosphate concentrations determined by biosensor were in agreement with those determined by spectrophotometric method (Figure 2(b)). The coefficient of correlation was >0.99 and slope of line was close to 1 (>0.99) suggesting a good concordance between the two analytical methods.

Stability of biosensor probe

An important consideration in development of a biosensor is the long-term stability of the probe. The long-term stability of the probe is important as a large number of probes can be prepared simultaneously, offering convenience in sample analysis. Further, simultaneous preparation of probes reduces inter-analysis variations that may arise due to preparation of probes at different times.

The biosensor probes were prepared by coating membranes with 4 mg/ml EBP and stored for up to 28 days at

Table 1 | Precision, recovery and long-term stability of phosphate estimation by biosensor

	Variability (%RSD)[a]			Long-term stability[a]				
Phosphate concentration (mg/L)	Intra-day	Inter-day	% Recovery[b]	Day 0	Day 7	Day14	Day 21	Day 28
1	2.10	1.36	96.55	1.34	1.36	1.89	1.71	2.06
2	1.78	1.57	97.78	0.87	0.82	1.94	1.21	2.09
4	1.66	1.23	97.57	1.46	1.87	1.63	0.91	1.75
6	1.05	1.00	98.16	1.41	1.70	1.47	1.81	1.25
8	1.15	1.23	101.32	2.01	1.09	1.22	1.95	1.76
10	0.98	1.14	99.15	1.04	1.48	0.89	0.81	0.94

[a]Data are %RSD of five samples/concentration.
[b]Data are mean of five samples/concentration.

Table 2 | Long-term stability of biosensor probe

Storage temperature	Long-term stability[a]				
	Day 0	Day 7	Day 14	Day 21	Day 28
4 °C	1.40	1.74	2.45	1.58	2.05
Ambient	1.77	1.89	1.51	1.21	2.22

[a]Data are %RSD of five membranes/analysis.

4 °C and at ambient temperature (~25 °C). Representative membranes were drawn and 1 mL samples of 1–10 mg/L phosphate were passed. Biosensor analysis showed that the phosphate concentration determined by membranes stored for up to 28 days did not significantly differ from results obtained from freshly prepared membranes (day 0) of the same lot. The %RSD was less than 5% (Table 2).

CONCLUSION

A biopolymer-based biosensor was developed employing the molybdenum blue method for phosphate estimation. The biosensor is sensitive and accurate. Further, the biosensor is stable for long durations (at least 28 days) and does require frequent calibration. To the best of our knowledge, a biopolymer coupled to a simple electronic system with low power consumption and reproducibility has not yet been reported for detecting phosphate. The superiority of the biopolymer lies in concentrating phosphate in its matrix on account of its high affinity for phosphate and the bound phosphate is amenable to colorimetry, rendering the EBP sensor suitable in areas with low phosphate concentration. The applicability of biosensor can be extended for monitoring of environmental, industrial and household wastewater analysis.

ACKNOWLEDGEMENTS

The study was funded by a grant from the University Grants Commission (UGC), New Delhi, India. TK received a Maulana Azad National Fellowship for Minority students from UGC.

REFERENCES

APHA-AWWA-WPCF 2007 *Standard Methods for the Examination of Water and Wastewater*. American Public Health Association, Washington, DC, USA.

Banu, R. J., Do, K. U. & Yeom, I. T. 2008 Phosphorus removal in low alkalinity secondary effluent using alum. *International Journal of Environmental Science and Technology* **5** (1), 93–98.

Bohdziewicz, J. E. & Sroka, I. 2003 Application of ultrafiltration and reverse osmosis to the treatment of the wastewater produced by the meat industry. *Polish Journal of Environmental Studies* **12** (3), 269–274.

Chaplin, M. F. & Kennedy, J. F. 1994 *Carbohydrate Analysis: A Practical Approach*. ILR Press, Oxford, New York.

Cloete, T. E. & Oosthuizen, D. J. 2001 The role of extracellular exopolymers in the removal of phosphorus from activated sludge. *Water Research* **35** (15), 3595–3598.

Dubois, M., Gilles, K. A., Hamilton, J. K., Rebers, P. A. & Smith, F. 1956 Colorimetric method for determination of sugars and related substances. *Analytical Chemistry* **28**, 350–356.

Ghosh, M., Ganguli, A. & Pathak, S. 2009 Application of a novel biopolymer for removal of *Salmonella* from poultry wastewater. *Environmental Technology* **30** (4), 337–344.

Kachlany, S. C., Levery, S. B., Kim, J. S., Reuhs, B. L., Lion, L. W. & Ghiorse, W. C. 2001 Structure and carbohydrate analysis of the exopolysaccharide capsule of *Pseudomonas putida* G7. *Environmental Microbiology* **3** (12), 774–784.

Khoi, L. Q. & Diep, C. N. 2013 Isolation and phylogenetic analysis of polyphosphate accumulating organisms in water and sludge of intensive catfish ponds in the Mekong Delta, Vietnam. *American Journal of Life Sciences* **1** (2), 61–71.

Koga, M., Matsuoka, S. & Yoshimura, K. 2010 Improved solid-phase spectrometry for the microdetermination of total and dissolved phosphate. *Analytical Sciences* **26** (9), 963–968.

Kortstee, G. J., Appeldoorn, K. J., Bonting, C. F., van Niel, E. W. & van Veen, H. W. 1994 Biology of polyphosphate-accumulating bacteria involved in enhanced biological phosphorus removal. *FEMS Microbiology Review* **15** (2–3), 137–153.

Lin, C. K., Katayama, Y., Hosomi, M., Murakami, A. & Okada, M. 2003 The characteristics of the bacterial community structure and population dynamics for phosphorus removal in SBR activated sludge processes. *Water Research* **37** (12), 2944–2952.

Liu, M., Gonzalez, J. E., Willis, L. B. & Walker, G. C. 1998 A novel screening method for isolating exopolysaccharide-deficient mutants. *Applied and Environmental Microbiology* **64** (11), 4600–4602.

Liu, Y. N., Xue, G., Yu, S. L. & Zhao, F. B. 2006 Role of extracellular exopolymers on biological phosphorus removal. *Journal of Environmental Sciences (China)* **18** (4), 670–674.

Mesquita, R. B., Ferreira, M. T., Toth, I. V., Bordalo, A. A., McKelvie, I. D. & Rangel, A. O. 2011 Development of a flow method for the determination of phosphate in estuarine and freshwaters–comparison of flow cells in spectrophotometric sequential injection analysis. *Analytica Chimica Acta* **701** (1), 15–22.

Rodil, R., Quintana, J. B., Lopez-Mahia, P., Muniategui-Lorenzo, S. & Prada-Rodriguez, D. 2009 Multi-residue analytical method for the determination of emerging pollutants in water by solid-phase extraction and liquid chromatography-tandem

mass spectrometry. *Journal of Chromatography A* **1216** (14), 2958–2969.

Sathasivan, A. 2009 Biological phosphorus removal processes for wastewater treatment. In: *Encyclopedia of Life Support Systems, Water and Wastewater Treatment Technologies* (S. Vigneswaran, ed.). Encyclopedia of Life Support Systems (EOLSS) Publishers, Oxford, UK, pp. 1–23.

Turel, M., Duerkop, A., Yegorova, A., Karasyov, A., Scripinets, Y. & Lobnik, A. 2010 Microtiter plate phosphate assay based on luminescence quenching of a terbium complex amenable to decay time detection. *Analytica Chimica Acta* **675** (1), 42–48.

USEPA 2002 Epa Ground Water & Drinking Water – Secondary Drinking Water Regulations: Guidance for Nuisance Chemicals, http://water.epa.gov/drink/contaminants/secondarystandards.cfm (accessed 21 July 2013).

Warwick, C., Guerreiro, A. & Soares, A. 2013 Sensing and analysis of soluble phosphates in environmental samples: a review. *Biosensors and Bioelectronics* **41**, 1–11.

Yokoyama, Y., Danno, T., Haginoya, M., Yaso, Y. & Sato, H. 2009 Simultaneous determination of silicate and phosphate in environmental waters using pre-column derivatization ion-pair liquid chromatography. *Talanta*. **79** (2), 308–313.

Zimmer, L. A. & Cutter, G. A. 2012 High resolution determination of nanomolar concentrations of dissolved reactive phosphate in ocean surface waters using long path liquid waveguide capillary cells (LWCC) and spectrometric. *Limnology and Oceanography: Methods* **10**, 568–580.

First received 29 May 2013; accepted in revised form 19 August 2013. Available online 24 October 2013

Supplementary information

Development of exobiopolymer-based biosensor for detection of phosphate in water

Taranpreet Kaur, Abhijit Ganguli, Moushumi Ghosh*

Department of Biotechnology & Environmental Sciences, Thapar University, Patiala-147004, Punjab, India

*Email: mghosh@thapar.edu

Additional figures

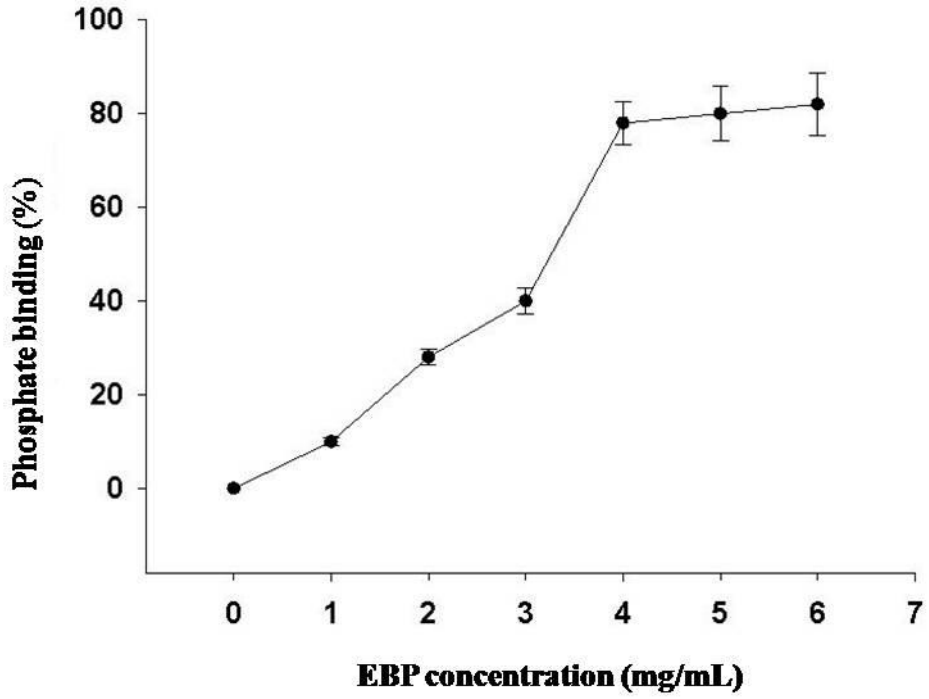

Figure 1. Effect of EBP concentration on phosphate binding on EBP-coated cellulose acetate membranes. Data is expressed as mean±SEM of 5 samples/concentration.

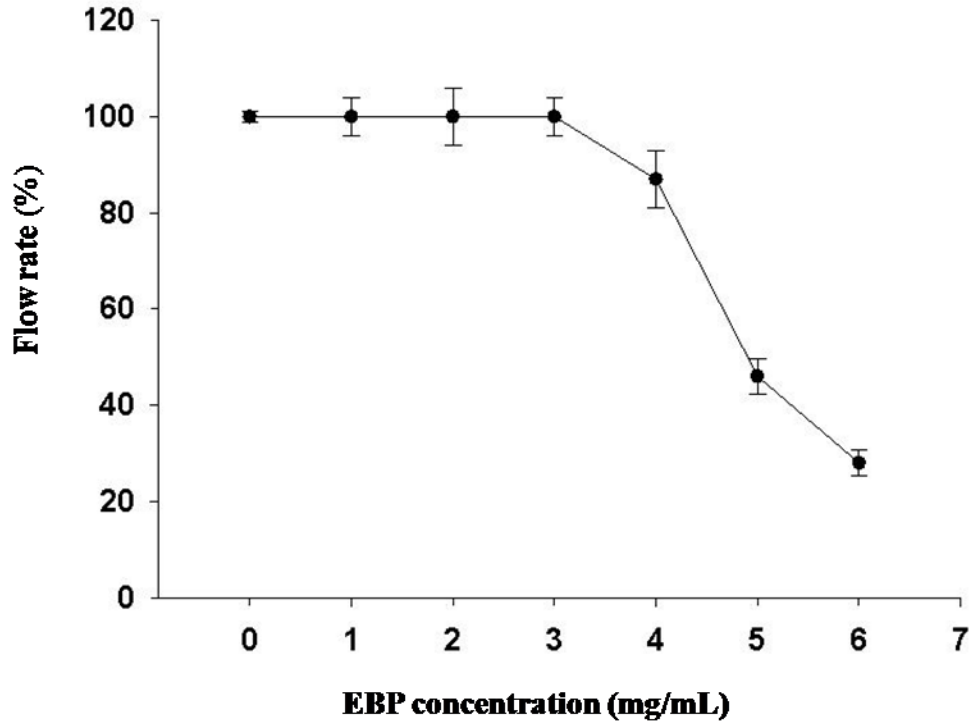

Figure 2 Effect of EBP concentration on flow rate of phosphate samples through EBP-coated cellulose acetate membranes. Data is expressed as mean±SEM of 5 samples/concentration.

Composite Interfaces
Publication details, including instructions for authors and subscription information:
http://www.tandfonline.com/loi/tcoi20

Application of biopolymer produced from metabolic engineered Acinetobacter sp. for the development of phosphate optoelectronic sensor

Taranpreet Kaur [a], Jatin Sharma [a], Abhijit Ganguli [a] & Moushumi Ghosh [a]

[a] Department of Biotechnology and Environmental Sciences, Thapar University, Patiala, 147004, Punjab, India

Published online: 30 Sep 2013.

To cite this article: Taranpreet Kaur, Jatin Sharma, Abhijit Ganguli & Moushumi Ghosh, Composite Interfaces (2013): Application of biopolymer produced from metabolic engineered Acinetobacter sp. for the development of phosphate optoelectronic sensor, Composite Interfaces, DOI: 10.1080/15685543.2013.842116

To link to this article: http://dx.doi.org/10.1080/15685543.2013.842116

Composite Interfaces, 2013
http://dx.doi.org/10.1080/15685543.2013.842116

Taylor & Francis
Taylor & Francis Group

Application of biopolymer produced from metabolic engineered *Acinetobacter* sp. for the development of phosphate optoelectronic sensor

Taranpreet Kaur, Jatin Sharma, Abhijit Ganguli and Moushumi Ghosh*

Department of Biotechnology and Environmental Sciences, Thapar University, Patiala 147004, Punjab, India

(*Received 10 December 2012; accepted 26 May 2013*)

In this study, we report the development of a phosphate sensor by exploiting phosphate-binding capability of *Acinetobacter* sp. biopolymer. An engineered strain of *Acinetobacter* sp. overproducing biopolymer was selected by Tn5 mutagenesis. The mutant showed a five-fold increase in biopolymer production and an increase in expression of intracellular biopolymer synthetic enzymes, phosphoglucomutase and glucosyl transferase. Physical and chemical analysis of biopolymer revealed a porous, compact surface morphology and a polysaccharide structure with predominance of uronic acid residues. Cellulose acetate membranes precoated with purified biopolymer were exposed to phosphate solutions and membrane-bound phosphate was determined by stannous chloride method. The colored membranes were analyzed by a LED (690 nm)/photodiode detection system. The phosphate concentration was estimated by converting the amperometric signal to phosphate concentrations from a standard plot. In conclusion, we anticipate that the developed sensor could be used for on-site phosphate analysis due to its compactness, portability, low detection levels (1 $\mu g\,L^{-1}$), and low power consumption.

Keywords: biopolymer; sensor; phosphate; *Acinetobacter*; metabolic engineering

1. Introduction

Phosphorous is an important element that regulates growth and maintenance of all organisms, spanning from the simplest to the most complex life forms. In recent years, the increased use of fertilizers and effluents from industry has resulted in an increased accumulation of phosphate, the bioavailable form of phosphorus, in water bodies. This leads to algal bloom and eutrophication. There is a need to develop efficient and economical methods for phosphate monitoring and remediation as currently available methods suffer from disadvantages of high cost, low efficiency, and disposal or neutralization of the remediation matrix.[1,2]

Biological methods of phosphate removal may prove superiority over physical and chemical methods in terms of efficiency and disposal.[3–5] *Acinetobacter* sp. is known to be a predominant organism in sludge containing high phosphorus levels *Acinetobacter* has the ability to accumulate phosphorus to very high levels with phosphate accounting for up to 10% of dry biomass. Additionally, several microorganisms, including

*Corresponding author. Email: mghosh@thapar.edu

Acinetobacter sp., also produce biopolymers which have the capacity to bind phosphorus.[6–9] The use of biopolymers for phosphate bioremediation offers several advantages over the use of live microorganisms and includes: biopolymers are stable over a wide range of temperature and therefore, do not require special arrangements during storage, transportation and handling; biopolymers can be reused after the removal of bound phosphate; and also biopolymers are non-toxic and biodegradable and are easy to dispose.

The low yield of biopolymer from microorganisms prohibits commercial application of biopolymer for phosphate bioremediation. The present study was conducted to develop a high biopolymer producing strain of *Acinetobacter* by mutagenesis. Transposon Tn5 mutagenesis has been extensively used to understand gene functions and offers several advantages like random insertion, multiple insertion sites, and stable expression in a wide variety of hosts.[10,11] Further, Tn5 has been widely used to identify genes responsible for controlling biopolymer/biofilm production in *Klebsiella pneumoniae*,[12] *Escherichia coli*,[13] and *Variovorax paradoxus*.[14] The phosphate-binding ability of biopolymer can also be used for selective concentration of phosphate from solution followed by analysis of phosphate content. This feature of biopolymer may be helpful in analysis of low enough concentrations of phosphate to evade detection by other analytical methods.

The present study was conducted to develop a strain of *Acinetobacter* sp. by transposon mutagenesis which produces high levels of biopolymer. The biopolymer was used to develop a biosensor for the detection of phosphate in dilute solutions.

2. Materials and methods

2.1. Chemicals, bacteria, and culture conditions

All chemicals used were purchased from local suppliers and were of the highest purity available. The strain *Acinetobacter* was isolated from sludge samples collected from Rainbow Denim Private Ltd Lalru, Punjab. The bacterium was allowed to grow in flocculant isolation broth (FIB) medium at 30 °C.

FIB medium was composed of peptone $5\,g\,L^{-1}$, ammonium sulphate $1\,g\,L^{-1}$, KH_2PO_4 $1\,g\,L^{-1}$, $CaCl_2.2H_2O$ $0.7\,g\,L^{-1}$, NaCl $0.1\,g\,L^{-1}$, $MgSO_4.7H_2O$ $0.3\,g\,L^{-1}$, K_2HPO_4 $1\,g\,L^{-1}$, glucose $1\,g\,L^{-1}$, and agar $3\,g\,L^{-1}$.

2.2. Extraction and purification of biopolymer

The strain *Acinetobacter* sp. was cultured for 48 h at 30 °C in FIB medium on a rotary shaker (120 rpm; Labcon, 5081U, USA). After growth, the culture was centrifuged (12,000 *g*; 30 min) at 4 °C (Sigma 2-16KC, Germany). The pellet was discarded and the supernatant was processed further for the extraction of biopolymer as described earlier.[15]

2.3. Mutagenesis

In order to develop mutants responsible for high biopolymer production, transposon mutagenesis was carried out. The method involves biparental conjugation between donor *E. coli* JB110 and recipient *Acinetobacter* sp. Antibiotics streptomycin $200\,\mu g\,mL^{-1}$ and kanamycin $50\,\mu g\,mL^{-1}$ were used as a selection marker for

Acinetobacter and *E. coli* JB110, respectively. Both donor and recipient cells were grown till mid-log phase, harvested, and washed with saline twice. The cells of donor and recipient were mixed in different ratios and placed on Luria agar plate containing filter paper discs; all plates were incubated at 30 °C for 24 h. After incubation, the filter paper discs containing cells were inoculated into Luria broth containing double antibiotic strep^{200} and kan^{50} and incubated at 30 °C for 8 h. The cells were placed on Luria agar containing double antibiotic strep^{200} and kan^{50}. Following transposition, the exconjugants were screened on the basis of their ability to overproduce biopolymer.[16]

2.4. Preparation of whole cell extracts

Whole cell-free extracts were prepared by the modified method of Mozzi et al. [17]. Log phase culture of *Acinetobacter* sp. and the mutant were harvested; pellet was resuspended in ice cold 0.1 M Tris-HC1 buffer and disrupted in an ultrasonic generator for 80 s at high intensity with cooling in ice. Cell debris was removed by centrifugation twice at 12,000 rpm for 15 min and the supernatant was used as the crude enzyme fraction. Aliquots were used for SDS PAGE and zymography.

2.5. Enzyme assays

To assess the levels of biopolymer synthetic enzymes i.e. phosphoglucomutase and glucosyl transferases, their assay from cell-free extracts of wild type and mutant stain was carried out as described by Norwal and Sutherland [18]. The assay mixture for phosphoglucomutase comprised of 1 M Tris-HCl, Cysteine NaOH, 1 M $MgCl_2$, 0.02 M NADP, and 0.1 M glucose-1-phosphate. The assay mixture of glucosyl transferases comprised of 50 mM phosphate buffer, 10 mM $MgCl_2$, 0.5 mM NADH, and 1 mM glucose.

2.6. Characterization of biopolymer

The uronic acid content of the biopolymer was determined by the method described by Stewart and Yong [19]. Infrared spectrum of the biopolymer was measured using a spectrophotometer (Perkin Elmer Spectrum, RX1 FTIR system). Monosaccharide composition of the biopolymer was analyzed by high performance liquid chromatography.

The stability of the biopolymer was assessed by loss in the biopolymer activity. Degradation of the biopolymer was carried out by thermogravimetric analysis (TGA) using a TGA apparatus (Mettler, Toledo) and the morphology was examined under a scanning electron microscope.

2.7. Dose optimization of biopolymer and phosphate

For analyzing the efficient binding of biopolymer with the phosphate, both biopolymer dose and phosphate concentration were optimized in synthetic waste water containing varying amounts of phosphate. Residual phosphate following the addition of biopolymer was analyzed by stannous chloride method and the absorbance being recorded at 690 nm. For coating biopolymer surfaces, cellulose acetate membranes were impregnated with purified biopolymer solution (optimized previously), dried briefly, and dipped into phosphate solution of different concentrations ranging from 0 to 50 $\mu g\,L^{-1}$ and were analyzed by the fabricated biosensor.

2.8. Biosensor fabrication

The biopolymer-impregnated cellulose acetate membrane was placed between LED and sensor of 690 nm. The signals were amplified by the microcontroller and recorded as mA. Phosphate concentrations were calculated from a standard plot between phosphate concentration and mA.

All experiments were carried out in triplicates and mean values with standard deviation are reported here. Statistical calculations were based on a confidence level of $\geqslant 95\%$ ($p < 0.05$ was considered statistically significant).

3. Results and discussion

The biopolymers are composed of mainly sugars, amino acids, and uronic acids [20,21] (Table 1). The biopolymers are involved in biosorption of toxic chemicals and pollutants like phosphorus. A previously isolated strain of *Acinetobacter* produced biopolymer which could effectively bind phosphate; however its quantity was low enough for practical applications. Therefore, in an effort to overproduce the biopolymer; transposon mutagenesis of wild type *Acinetobacter* sp. was attempted. Alcian blue assay allowed rapid detection of biopolymer overproducing mutants. Of the 52 mutants screened, only one mutant showed remarkable increase in biopolymer level and was used for further study. Whole-cell protein profiles of wild type and mutant *Acinetobacter* revealed highest levels of at least two proteins of molecular weight approximately 62 and 77 kDa. These results were further corroborated by zymography (Figure 1) and enzyme assays. A five-fold increase in biopolymer concentration was noted per gram (dry weight) in the mutant of *Acinetobacter* as opposed to its wild type counterpart. Optimization studies demonstrated that the biopolymer was more effective in adsorption of phosphate at a concentration of $2\,\mathrm{mg\,L^{-1}}$ (Figure 2) at ambient temperature; at higher concentrations, the adsorption remained unaltered. A biopolymer dose of $4\,\mathrm{mg\,L^{-1}}$ was highly effective in the removal of phosphate, doses above this value were not significant ($p > 0.5$) for phosphate removal (Figure 3).

To analyze the surface characteristics of the biopolymer, SEM studies were essential; the SEM observations (Figure 4) indicated that the surface morphology is a porous structure with small pore size distribution. The small pore structure may be responsible for the compactness of the polymer and the stability of the gel structure when subjected to the external forces and the maintenance of the textural properties during storage. Also, an extremely small pore size distribution may enable the web structure to have much higher capillary forces to retain water in the gel. The thermal characteristic of the

Table 1. Compositional analysis of the purified biopolymer.

S.no.	Components	Composition (%)
1	Total sugar	71.4
2	Amino sugar	02.73
3	Uronic acid	04.83
4	Protein	02.45
5	Carbon	12.19
6	Hydrogen	02.13
7	Nitrogen	0.64
8	Pyruvic acid	0.20

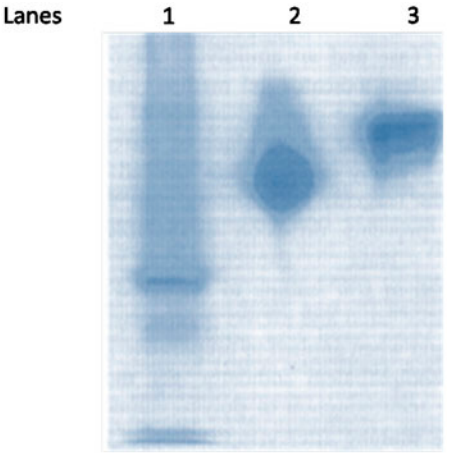

Figure 1. Zymographs of cell-free extracts of wild type and mutant *Acinetobacter* sp. Bands were counterstained with coomassie blue following detection of activity. Lane 1: wild type, Lane 2: phosphoglucomutase of mutant *Acinetobacter* sp., and Lane 3: glucosyl transferase of mutant *Acinetobacter* sp.

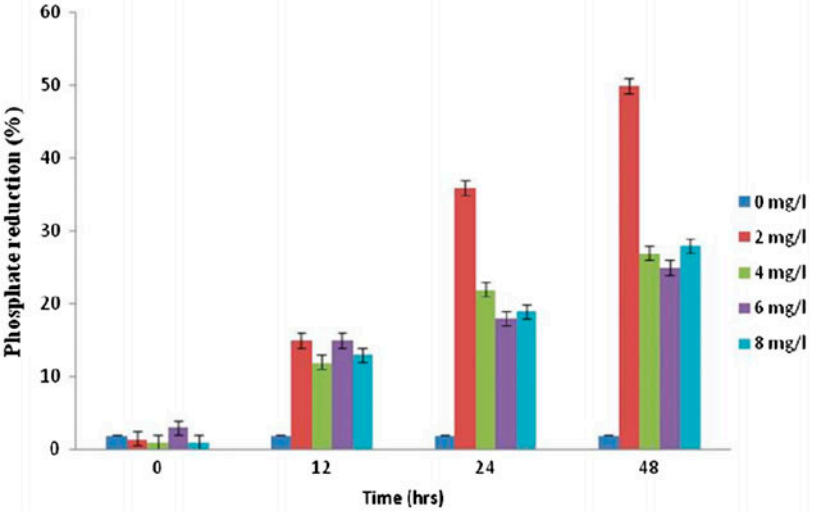

Figure 2. Effect of phosphate concentrations on phosphate removal by fixed dose of biopolymer. A phosphate concentration of $2\,mg\,L^{-1}$ shows maximum reduction in phosphate levels. Results are mean of three replicates.

biopolymer (Figure 5) revealed the onset of decomposition at 250 °C and the recorded mass loss to be 23.58%, a further mass loss between 675 and 890 °C. A degradation temperature (T_d) of 290 °C was determined from the TGA curve for the polymer. The polymer showed an initial weight loss due to moisture content between 30 and 220 °C. The initial moisture content in the sample may be attributed to the increased level of carboxyl groups in the biopolymer. The infrared spectrum of the purified biopolymer displayed a broad stretching peak at around $3423\,cm^{-1}$which is the characteristic of

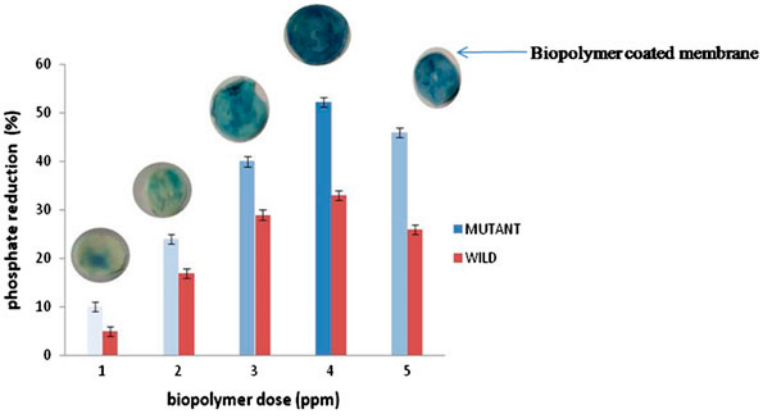

Figure 3. Effect of biopolymer concentration on phosphate removal. Results represent mean of three replicates. Biopolymer concentration of 4 mg L^{-1} is optimum for the maximum phosphate reduction.

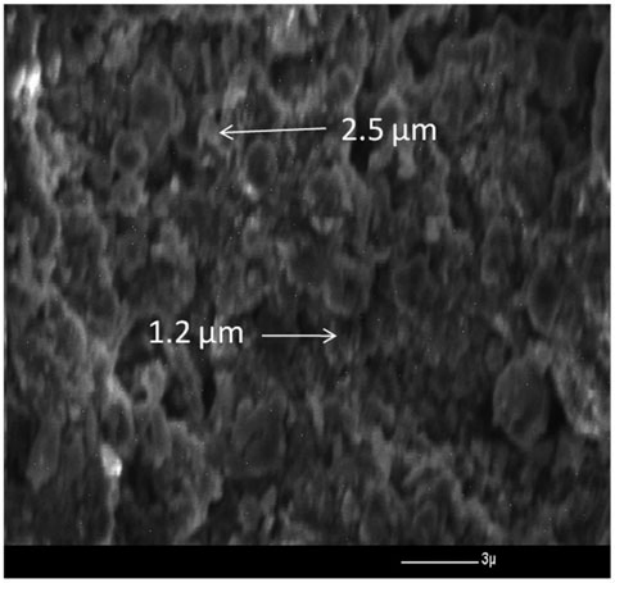

Figure 4. SEM micrograph of purified biopolymer of *Acinetobacter* sp. (wild type). Magnification 500x.

hydroxyl groups, (Figure 6); the spectrum also displayed an asymmetrical CO stretching at 1591 cm^{-1}. The absorption peak at 1077 cm^{-1} is known to be characteristic for all sugar derivatives and a weak symmetrical stretching band near 1412 cm^{-1}, which indicated the presence of uronate in this biopolymer. The hydroxyl group's present within the biopolymer had the possibility of hydrogen bonding with one or more water molecules. Thus, the polymer could imbibe water, swell, and could even dissolves partially or completely.[22,23] These results along with those obtained from HPL chromatograms (results not shown) suggested a primarily polysaccharide structure of the

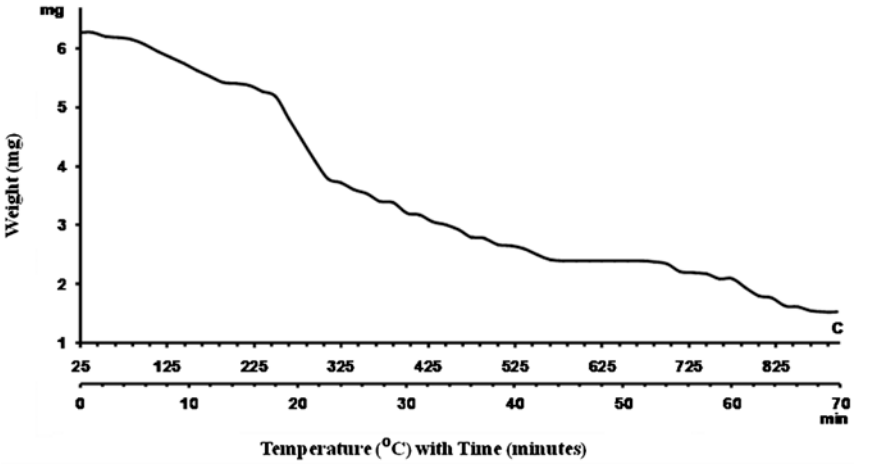

Figure 5. TGA analysis of purified biopolymer of *Acinetobacter* sp. (wild type).

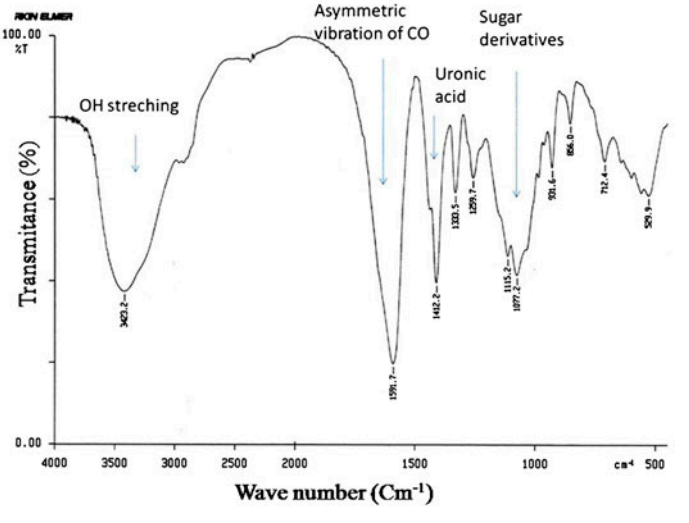

Figure 6. Infra-red spectra of purified biopolymer of wild type *Acinetobacter* sp.

biopolymer. A rapid assay of the biopolymer bound phosphate was desired; In order to quantify the bound phosphate rapidly, a miniature circuit was developed (Figure 7). For this, cellulose acetate membranes were used. The assay was found to have a limit of detection and limit of quantification of 1 and 10 $\mu g\,L^{-1}$, respectively. The biopolymer could be stabilized adequately on the membranes with no structural damage; moreover, the biopolymer-coated membranes could be stored over a period of 15 days and subsequently subjected to colorimetry for assessing the quantity of phosphate. A linear output was obtained from the sensor which correlated to the phosphate bound to the biopolymer; validation was carried out with waste water samples containing varying quantities of phosphate (Table 2).

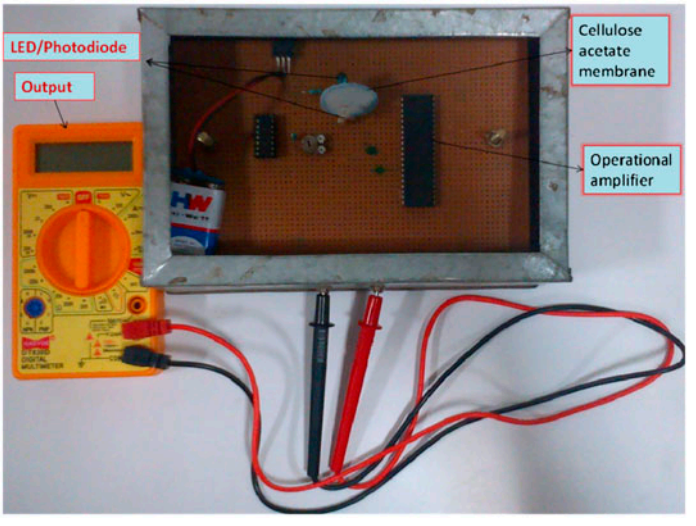

Figure 7. Photograph of the fabricated biosensor for the detection of bound phosphate.

Table 2. Correlation between biosensor response and actual phosphate estimation at concentrations from 0 to 50 $\mu g\,L^{-1}$. Values are mean ± SD of three replicates.

Phosphate conc. ($\mu g\,L^{-1}$)	Current (mA) ± SD
0	0 ± 0.0
10	13 ± 0.8
20	26 ± 1.3
30	53 ± 2.8
40	66 ± 3.1
50	124 ± 5.5

In conclusion, a biosensor is described for the estimation of phosphate in water samples, taking advantage of phosphate binding capacity of the biopolymer. The biosensor offers the advantage of being compact, portable, economic power consumption, reproducible, and stable. The high sensitivity of biosensor also qualifies its use in samples containing low phosphate concentrations.

Acknowledgments

This work was supported by the University Grants commission, New Delhi. TK thanks UGC, New Delhi for giving Maulana Azad National fellowship. The authors are thankful to RSIC, Chandigarh and JNU, New Delhi for analyzing the biopolymer samples.

References

[1] Xu K, Deng T, Liu J, Peng W. Phosphate removal from digested sludge supernatant using modified fly ash. Water Environ. Res. 2012;84:411–416.
[2] Mishra SP, Das M, Dash UN. Review on adverse effects of water contaminants like arsenic, fluoride and phosphate and their remediation. J. Sci. Ind. Res. 2010;69:249–253.
[3] Cloete TE, Oosthuizen DJ. The role of extracellular exopolymers in the removal of phosphorus from activated sludge. Water Res. 2001;35:3595–3598.

[4] Albertsen M, Hansen LB, Saunders AM, Nielsen PH, Nielsen KL. A metagenome of a full-scale microbial community carrying out enhanced biological phosphorus removal. ISME J. 2012;6:1094–1106.
[5] Onnis-Hayden A, Majed N, Schramm A, Gu AZ. Process optimization by decoupled control of key microbial populations: distribution of activity and abundance of polyphosphate-accumulating organisms and nitrifying populations in a full-scale IFAS-EBPR plant. Water Res. 2011;45:3845–3854.
[6] Van Groenestijn JW, Bentvelsen MM, Deinema MH, Zehnder AJ. Polyphosphate-degrading enzymes in *Acinetobacter* spp. and activated sludge. Appl. Environ. Microbiol. 1989;55:219–223.
[7] Boswell CD, Dick RE, Eccles H, Macaskie LE. Phosphate uptake and release by *Acinetobacter johnsonii* in continuous culture and coupling of phosphate release to heavy metal accumulation. J. Ind. Microbiol. Biotechnol. 2001;26:333–340.
[8] Sathasivan A. Biological phosphorus removal processes for wastewater treatment. In: Vigneswaran S, editor. Water and wastewater treatment technologies. Oxford (UK): Encyclopedia of Life Support Systems (EOLSS); 2009. 1–23.
[9] Liu YN, Xue G, Yu SL, Zhao FB. Role of extracellular exopolymers on biological phosphorus removal. J. Environ. Sci. (China). 2006;18:670–674.
[10] Ahmed A. Alternative mechanisms for Tn5 transposition. PLoS Genet. 2009;5:e1000619.
[11] Reznikoff WS. Transposon Tn5. Annu. Rev. Genet. 2008;42:269–286.
[12] Wu MC, Lin TL, Hsieh PF, Yang HC, Wang JT. Isolation of genes involved in biofilm formation of a *Klebsiella pneumoniae* strain causing pyogenic liver abscess. PLoS ONE. 2011;6:e23500.
[13] Puttamreddy S, Cornick NA, Minion FC. Genome-wide transposon mutagenesis reveals a role for pO157 genes in biofilm development in *Escherichia coli* O157:H7 EDL933. Infect. Immun. 2010;78:2377–2384.
[14] Pehl MJ, Jamieson WD, Kong K, Forbester JL, Fredendall RJ, Gregory GA, McFarland JE, Healy JM, Orwin PM. Genes that influence swarming motility and biofilm formation in *Variovorax paradoxus* EPS. PLoS ONE. 2012;7:e31832.
[15] Ghosh M, Pathak S, Ganguli A. Effective removal of *Cryptosporidium* by a novel bioflocculant. Water Environ. Res. 2009;81:160–164.
[16] Neeraj SC, Gaurav S, Chatterjee S, Mahesh C. Exopolysaccharides and lipopolysaccharide production by *Sinorhizobiobium fredii* Tn5 mutants infecting *Vigna radiata*. ARPN J. Agric. Biol. Sci. 2009;4:32–38.
[17] Mozzi F, Savoy de Giori G, Font de Valdez G. UDP-galactose 4-epimerase: a key enzyme in exopolysaccharide formation by *Lactobacillus casei* CRL 87 in controlled pH batch cultures. J. Appl. Microbiol. 2003;94:175–183.
[18] Norval M, Sutherland IW. The production of enzymes involved in exopolysaccharide synthesis in *Klebsiella aerogenes* types 1 and 8. Eur. J. Biochem. 1973;35:209–218.
[19] Stewart JM, Yong JD. Laboratory techniques. Solid phase peptide synthesis. 2nd ed. Rockford (IL): Pierce Chemical; 1984.
[20] Bitton G. Wastewater microbiology. New York (NY): Wiley; 1994. p. 63–65.
[21] Chaplin MF, Kennedy JF. Carbohydrate analysis: a practical approach. Washington (DC): IRL press; 1986. p. 129–136.
[22] BeMiller JN, Whistler RL. Carbohydrates. In: Fennema OR, editor. Food chemistry. 3rd ed. New York (NY): Marcel Dekker; 1996. 178–85.
[23] Mao R, Tang J, Swanson BG. Water holding capacity and microstructure of gellan gums. Carbohydr. Polym. 2001;46:365–371.

Carbohydrate Polymers 132 (2015) 72–79

Contents lists available at ScienceDirect

Carbohydrate Polymers

journal homepage: www.elsevier.com/locate/carbpol

Acinetobacter haemolyticus MG606 produces a novel, phosphate binding exobiopolymer

Taranpreet Kaur, Moushumi Ghosh*

Department of Biotechnology, Thapar University, Bhadson Road, Patiala 147004, Punjab, India

ARTICLE INFO

Article history:
Received 6 April 2015
Received in revised form 26 May 2015
Accepted 1 June 2015
Available online 8 June 2015

Keywords:
Acinetobacter haemolyticus
Exobiopolymer
Phosphate removal
Polysaccharide characterization

ABSTRACT

The present study evaluated an extracellular, novel biopolymer produced by *Acinetobacter haemolyticus* MG606 for its physicochemical properties and phosphate binding mechanism. The exobiopolymer (EBP) was characterized to be majorly polysaccharide in nature consisting of 48.9 kDa heteropolysaccharide composed of galactose, glucose, xylose, lyxose, allose, ribose, arabinose, mannose and fructose. Maximum phosphate binding efficiency of 25 mg phosphate/g of EBP was described by Langmuir isotherm and further, the physicochemical and spectroscopic studies revealed that phosphate appeared to bind predominantly with the polysaccharide fraction, and to a relatively lesser extent to protein fraction of EBP. The electrostatic interactions with amino groups and ligand exchange with hydroxyl groups of EBP were found to be primary basis for phosphate binding mechanism. The results of this study implicate the feasibility of the EBP for commercial bioremediation processes.

1. Introduction

Extracellular biopolymers (EBP) produced by microorganisms have been identified as a novel, safe, biodegradable platform for remediation of environmental pollutants. Although, their application in bioremediation is still in infancy, EBP from diverse microbial genera have been investigated for potential applications in removal of ionic contaminations, notably heavy metals, as well as organic contaminants like pesticides and oil spills. Several groups have reported affinity of EBP for cationic contaminants such as arsenic, lead, mercury, chromium and other heavy metal ions (More, Yadav, Yan, Tyagi, & Surampalli, 2014). Interestingly, a vast amount of literature exist demonstrating cation-binding capacity of EBP; however, anion-binding by EBP has largely remained unexplored due to non-consideration of seriousness of these anions unlike other toxic metal cations. The role of anions, particularly phosphate, as an environmental concern has only been realized recently (Rockstrom et al., 2009).

An increased incidence of eutrophication in water bodies has been linked to phosphorus accumulation. Phosphate remediation in wastewater can be achieved by physicochemical methods such as adsorbents, sand filters, membrane filters, precipitation and electrocoagulation. However, these methods suffer from disadvantages of long-term high processing costs and limited reusability of the removed phosphorus. These issues have paved the way for development of biological methods of phosphate removal such as enhanced biological phosphorus removal (EBPR), agricultural waste and assimilation by bacteria, algae and plants (El-Bestawy, Hussein, Baghdadi, & El-Saka, 2005; Nguyen, Ngo, Guo, & Nguyen, 2012). EBPR is currently used for the bioremediation of phosphate due to its low operating cost, reduced sludge production, easier management and reuseability of byproducts and effluent. EBPR is achieved through polyphosphate accumulating organisms (PAOs) present in sludge, which accumulates phosphate intracellularly in the form of polyphosphates (Oehmen et al., 2007). Although the role of EBP present in activated sludge and its participation in EBPR through phosphate sorption has been realized in the recent years, however, studies were either restricted to quantitative analysis of total phosphorus bound to EBP (Li, Ren, Wang, & Kang, 2010; Oosthuizen & Cloete, 2001) or mostly focussed on phosphorus speciation in EBP extracted from activated sludge (Zhang et al., 2013a,b). In the related reports, phosphate binding was studied in EBP produced by a community of PAOs and the role of specific microorganism producing the phosphate-binding EBP was not considered; also, the composition of phosphate-binding components and the mechanism of phosphate-EBP interaction were not completely elucidated.

We have earlier reported the phosphate-binding ability of EBP produced by an environmental isolate of *Acinetobacter haemolyticus* (Genbank accession number KP701480) as well as an EBP-overproducing mutant (Kaur, Ganguli, & Ghosh, 2013a; Kaur,

* Corresponding author. Tel.: +91 175 2393478; fax: +91 175 2364498/175 2393020.
E-mail address: mghosh@thapar.edu (M. Ghosh).

http://dx.doi.org/10.1016/j.carbpol.2015.06.002
0144-8617/

Sharma, Ganguli, & Ghosh, 2013b). The current investigation was aimed at identification and characterization of EBP components responsible for phosphate binding in EBP produced by the mutant strain *A. haemolyticus* MG606. Further, the nature and mechanism of phosphate interaction with the polysaccharide fraction of EBP was investigated by physical and chemical methods.

2. Materials and methods

2.1. Bacterial strain, culture conditions and EBP extraction

A. haemolyticus MG606 was grown in EBP production medium and EBP was extracted as described previously (Kaur et al., 2013b). Briefly, the bacterium was grown at 30 °C in EBP production medium composed of ammonium sulphate (1 g/L), calcium chloride dihydrate (0.7 g/L), dextrose (1 g/L), dipotassium hydrogen phosphate (1 g/L), magnesium sulphate heptahydrate (0.3 g/L), peptone (5 g/L), potassium dihydrogen orthophosphate (1 g/L), sodium chloride (0.1 g/L) and agar (3 g/L). The final pH of medium was adjusted to 7.0 ± 0.2. After 48 h of growth, the cultures were centrifuged at 12,000 × *g* for 30 min at 4 °C. The supernatant was mixed with double volume of chilled ethanol to precipitate crude EBP. The crude EBP was reprecipitated with 10% cetyl pyridinium chloride and sodium chloride and then centrifuged at 12,000 × *g* for 10 min. The pellet was washed twice with deionized water, dialyzed for 48 h with deionised water and then lyophilized to obtain purified EBP.

2.2. Physicochemical characterization of EBP

The elemental composition (C, H, N and S) and biochemical composition was determined as described previously (Kaur et al., 2013a,b).

The ultrastructure and elemental composition of EBP was determined using a scanning electron microscopy (JSM-6510LV, Jeol) equipped with EDS (INCAx-act, Oxford Instruments). The surface area and porosity of EBP was determined by Brunauer, Emmett and Teller (BET) method using Micromeritics ASAP 2020 analyzer and nitrogen gas as sorbent. The surface area was calculated using BET equation while micropore volume was calculated using Barrett, Joyner and Halenda (BJH) analysis.

Molecular weight of EBP was determined by gel permeation chromatography (GPC) on Ultrahydragel 500 and Ultrahydragel 120 column in series using Waters Alliance HPLC-GPC (Waters 2695 separation module coupled with Waters 2414 refractive index detector). The mobile phase used was 0.2 M sodium nitrate in water.

The monosaccharide components of EBP were determined by gas chromatography coupled with a mass spectrometer (GCMS) (Pierre et al., 2012; Senila, Gog, Senila, Roman, & Silaghi-Dumitrescu, 2011). Briefly, EBP was hydrolyzed with 2 M trifluoroacetic acid at 121 °C for 1 h. The hydrolyzed sample was lyophilized and dried extract was derivatized with *N,O*-bis(trimethylsilyl) trifluoroacetamide (BSTFA). The mixture was heated for 30 min at 80 °C, centrifuged and sodium sulphite was added to remove moisture present in the sample and again centrifuged at 12,000 × *g* for 10 min. The supernatant was collected, vacuum dried and injected into GCMS (GCMS QP 2010, Shimadzu) equipped with DB-5 column (30 m × 0.25 mm × 0.25 μm; Agilent Technologies).

A preweighed sample of EBP was placed in sample pan of thermogravimetric analysis (TGA) apparatus (Mettler Toledo) and heated at 15 °C/min under a constant flow of nitrogen gas. The sample was heated until no further change in weight was observed and degradation temperature was determined from TGA curve.

The dynamic viscosity of aqueous solution of EBP was determined by Brookfield viscometer (DV-11+/Pro, Brookfield). All measurements were performed at ambient temperature (25 °C).

2.3. Phosphate sorption by EBP

Standard phosphate solution was prepared by dissolving 100 mg of potassium dihydrogen phosphate in 1 L of deionised water. The working concentrations ranging from 2 mg/L to 10 mg/L were prepared by suitably diluting the stock solution with deionised water.

To determine sorption of phosphate on EBP, 2.5 mL phosphate solution (2 to 10 mg/L) was mixed with an equal volume of EBP solution (100 to 1000 mg/L), vortexed for 10 min and kept undisturbed for indicated time. The mixture was then filtered through 0.22 μm membrane filter and phosphate concentration was determined by molybdenum blue stannous chloride method using potassium dihydrogen orthophosphate as standard (0–10 mg/L) (APHA, 1998). The colour produced by reaction of ammonium molybdate with stannous chloride in presence of phosphate was measured by recording absorbance at 690 nm. The standard plot between phosphate concentration (1–5 mg/L) and absorbance was linear ($y = 0.027x + 0.005$; $R^2 = 0.991$).

The sorption data for optimized contact time and EBP concentration was fitted to isotherm equations using MATLAB (Foo & Hameed, 2010). The goodness of fit was determined based on coefficient of determination (R^2) and rigorous error functions (Foo & Hameed, 2010; Ho, 2004). The best fitting isotherm model was selected based on corrected Akaike information criterion (AICc) (Akpa & Unuabonah, 2011).

The reversibility of phosphate binding was determined by desorption studies. Phosphate-bound EBP was prepared by sorption of phosphate (1 mg/L) on EBP (100 mg/L) for 4 h. Phosphate-bound EBP was recovered by filtration, mixed with 0.1 N NaOH (1 mg EBP/10 mL) and kept undisturbed for 4 h. The desorbed phosphate was determined by measuring phosphate concentration as described above.

2.4. Mechanism of phosphate binding

2.4.1. Effect of enzyme and chemical treatment, competing anions and pH

The effect of chemical/enzyme treatment, competing anions and pH on phosphate sorption by EBP was determined at 1 mg/L phosphate and 100 mg/L EBP.

An aqueous solution of EBP (1 g/L) was incubated for 16–18 h with a cocktail of 1 mg/L proteolytic (protease [4000 U/mg], trypsin [1000–1500 U/mg] and proteinase K [30 U/mg] in equal weight proportions), 1 mg/L amylolytic (amylase [2000 U/mg], cellulose [0.3 U/mg] and beta-galactosidase [500 U/mg] in equal weight proportions) enzymes and their combination (1 mg/L proteolytic and 1 mg/L amylolytic cocktail) at 37 °C and lyophilized. For chemical modifications, 50 mg powdered EBP was mixed with 50 mL of 4% v/v glutadaldehyde or 1:100 concentrated hydrochloride acid:anhydrous methanol mixture (v/v) or 1:2 formaldehyde:formic acid (v/v) and allowed to react for 24 h. The reaction mixture was then extensively dialyzed against deionized water to remove unreacted reactants and then lyophilized (Jianlong, 2002; Micheletti et al., 2008). A low concentration of glutaraldehyde (4%, v/v) was selected to minimize interchain crosslinking, and subsequent precipitation, observed at higher glutaraldehyde concentrations. Phosphate binding was determined with treated EBP as described above.

To determine the effect of competing ions, EBP and phosphate (1 mg/L) were incubated until equilibrium was reached (240 min). Following equilibrium, potassium salts of sulphate, chloride or nitrate were added to EBP solution at 10, 50 and 100 mg/L

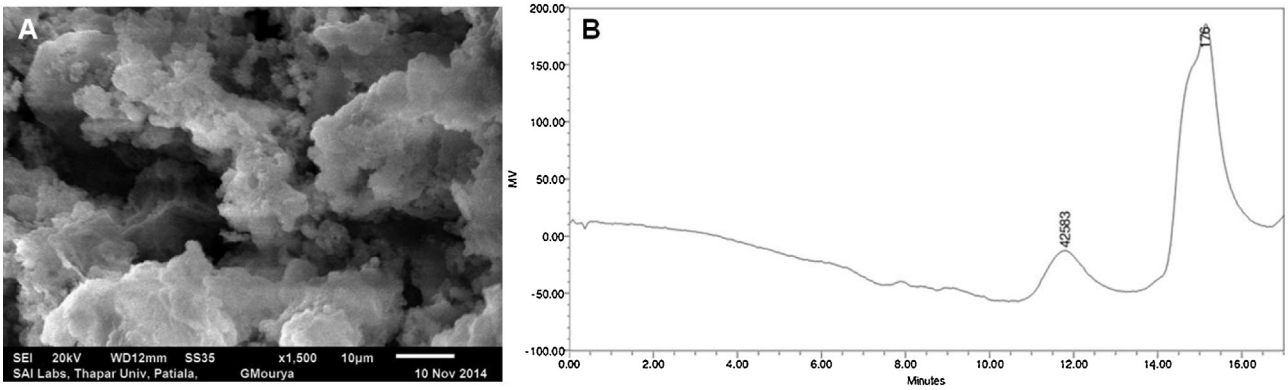

Fig. 1. Physicochemical characterization of EBP. (A) A representative scanning electron microscope micrograph showing ultrastructure of EBP (magnification 1500×). (B) Gel permeation chromatogram showing molecular weight of EBP.

concentration and further incubated for 1 h. The unbound phosphate was determined as described above.

To determine the effect of pH, EBP and phosphate solutions were prepared in Tris–HCl buffer of different pH (3–10) instead of water and phosphate sorption was determined as described above.

2.4.2. Infrared spectroscopy

The functional groups of lyophilized EBP and phosphate-bound EBP were analyzed by Fourier transform infrared (FT-IR) spectroscopy (Cary 660 FTIR, Agilent Technologies). The samples were prepared by grinding with KBr, compressed to pellets and pellets scanned in the range 800 to 4000 cm^{-1}.

2.4.3. X-ray diffraction spectroscopy

Powder X-ray diffraction (XRD) analysis of EBP was carried out using XRD system (X-pert Pro, PANalytical). The copper $K\alpha$ radiation (1.5406 Å wavelength) was obtained from copper anode and sample was scanned at $5^\circ \leq 2\theta \leq 85^\circ$, 45 kV, 40 mA and step size (2θ) 0.0130.

2.5. Potentiometric titration

The acid–base titrations were performed as described elsewhere (Guine et al., 2006; Wei et al., 2011). Briefly, 2 mg of EBP was dissolved in 10 mL water and the solution was acidified with 1 N HCl to lower the pH to approximately 2.5. The acidified solution was titrated with 0.1 N NaOH in 20 µl increments. The pH was allowed to stabilize after each addition and acidity was recorded. The titration data was fitted using ProtoFit (Turner & Fein, 2006).

2.6. Particle size and zeta potential measurements

A saturated solution of EBP was prepared in deionized water. Zeta potential was measured using zeta sizer (Nano ZS, Malvern).

2.7. Determination of phosphate removal in real time conditions

Water samples from the ponds, canals/rivers, drains and surface runoff water from fields were collected from Patiala and nearby regions in Punjab. Water analysis was performed according to American Public Health Association methods (APHA, 1998); pH of the water samples were determined at the spot, whereas, other parameters were determined after transporting the samples to the laboratory in ice.

Wastewater was filtered through a 0.45 µm filter to remove suspended particles and then mixed with an equal volume of 200 µg/L EBP solution. The mixture was filtered through 0.22 µm membrane filter after 4 h and phosphate concentration was determined by molybdenum blue stannous chloride method. The expected values of phosphate removal were calculated from Langmuir isotherm equation using parameters calculated in phosphate-spiked artificial wastewater. The difference between expected and observed phosphate removal was compared by Bland–Altman difference plot using MedCalc software. The contribution of competing anions on phosphate removal was determined by principal least square (PLS) method using Statistica software.

3. Results and discussion

3.1. Physicochemical properties of EBP

A white to off white fluffy powder of EBP was obtained. The ultrastructure of EBP, as analyzed by SEM, comprised of sheets and microfine powder granules with numerous pores and grooves (Fig. 1A). The individual particles, measuring <10 µm, formed irregularly shaped aggregates measuring <500 µm in the longest dimension. BET analysis indicated that EBP possessed a surface area of 87.8 cm^2/g, pore volume of 0.73 cm^3/g and average pore size of 33 nm thereby confirming the porous nature and high specific area of EBP as observed in SEM.

Elemental analysis of EBP revealed that carbon, hydrogen and nitrogen accounted for most of the chemical composition with minor contribution by sulphur. Biochemical characterization of EBP revealed the presence of polysaccharides and proteins as major components while amino sugars, uronic acid and pyruvic acid were identified as minor constituents (Table 1).

The molecular weight determination of EBP showed that polysaccharide fraction eluted as a single peak with a number average molecular weight (*Mn*) of 28.7 kDa, weight average molecular weight (*Mw*) of 48.9 kDa and peak molecular weight (MP) of 45.6 kDa (Fig. 1B). The second peak, corresponding to *Mw* 245 Da (*Mn* 145 Da; *MP* 176 Da; polydispersity 1.7), was identified as a system peak appearing due to solvent effects and does not depict a low molecular weight component of EBP (Trathnigg, 2000). The

Table 1
Composition of EBP of *A. haemolyticus* MG606.

Constituent	Composition (%)
Sugars	74.2
Proteins	8
Amino sugars	2.5
Pyruvic acid	0.98
Uronic acids	2.1
Carbon	10.4
Hydrogen	2.6
Nitrogen	1.7
Sulphur	0.3

polydispersity (*Mw*/*Mn* ratio) of 1.7 indicated the monodisperse nature of polysaccharide chain confirming the production of only one type of polysaccharide with a narrow molecular weight range.

The monomer composition of polysaccharide was determined by GCMS and found to be a heteropolysaccharide, mainly composed of pentose and hexose sugars in approximately equal proportions. The relative ratios of sugars determined by GCMS were approximately glucose:xylose:arabinose:ribose:galactose: allose:lyxose:mannose:fructose 3:2:2:2:2:2:1:0.2:0.1.

Microorganisms are known to produce EBP with very divergent biochemical compositions and polysaccharide characteristics, with polysaccharide molecular weights ranging from a few thousand to several hundred million (More et al., 2014). EBP produced by members of *Acinetobacter* genus have not been extensively studied, except for few studies on EBPs with emulsifier activity such as ethapolan, emulsan, alasan and biodispersan (Satpute, Banat, Dhakephalkar, Banpurkar, & Chopade, 2010). The bioemulsifiers have been demonstrated to be high molecular weight heteropolysaccharides composed of hexose sugars such as glucose, galactose, mannose and rhamnose or their corresponding uronic acids/amino sugars as the predominant components (Satpute et al., 2010; Sen et al., 2014). Interestingly, *A. haemolyticus* has also been demonstrated to produce EBP with emulsifying properties (Jagtap, Yavankar, Pardesi, & Chopade, 2010; Patil & Chopade, 2001) but the EBP has never been completely characterized. In the current study, we observed that the polysaccharide fraction eluted as a single peak with average molecular weight of 48.9 kDa. These observations corroborate findings in other species that *Acinetobacter* sp. produces a single type of polysaccharide in EBP. However, in striking contrast to existing reports, we observed that hexose sugars contributed to approximately half of the total polysaccharide composition while the remaining is contributed to pentose sugars. These results suggest that *A. haemolyticus* MG606 produces EBP with distinct properties from other *Acinetobacter* sp. Apparently, this is the first report on characterization of EBP produced by *A. haemolyticus*.

3.2. Phosphate sorption by EBP

Phosphate removal was performed by varying three parameters: contact time, EBP concentration and phosphate concentration. A contact time of 240 min and EBP concentration of 100 mg/L showed maximum phosphate binding (Supplementary Fig. S1). Therefore, phosphorus removal was determined at the optimized EBP concentration (100 mg/L) and contact time (240 min) and data fitted into isotherm equations. It was observed that Q_e increased from 6.8 mg/g at 1 mg/L phosphate to 25 mg/g at 5 mg/L phosphate due to constant number of binding sites or EBP concentration, the binding sites are saturated at higher phosphate concentration resulting in lower percentage phosphate removal and higher Q_e values. The high Q_e value (25 mg/g) observed for EBP is significantly higher (2–10 mg/g) than other organic and inorganic sorbents (Chitrakar et al., 2006; Nguyen et al., 2012). Further, effluent phosphate concentration after EBP treatment (0.2 mg/L) is comparable to magnetic separation (0.1–0.5 mg/L) and crystallization (0.3–1.0 mg/L) methods but lower than membrane filtration (0.04 mg/L), reverse osmosis (0.008 mg/L), electrodialysis (<0.005 mg/L), chemical precipitation (0.005–0.04 mg/L), EBPR (<0.02–0.1 mg/L) and constructed wetlands (0.02 mg/L) (Nguyen et al., 2012). Although batch equilibrium studies indicate a lower efficacy of EBP compared in terms of effluent phosphate concentration, the efficacy of phosphate removal can be further increased by using trickling bed filters or fixed bed columns (Kim et al., 2015; Nguyen et al., 2015; Woumfo, Siewe, & Njopwouo, 2015).

To establish an appropriate correlation of equilibrium data, the experimental data was fitted into Langmuir, Freundlich, Temkin, Toth and Sips equations by non-linear curve fitting. The isotherm equations as well as the parameters values with respective R^2, error function and AICc values are listed in Supplementary Table 1. All models exhibited a high degree of fitting and correlation with $R^2 > 0.96$ (Fig. 2; Supplementary Table 1). Hence, error functions were used for further inter-model comparison to identify the best fitting model(s). Based on sum squares errors (SSE), hybrid fractional error function (HYBRID), Marquardt's percent standard deviation (MPSD) and non-linear Chi-square analysis (χ^2), Langmuir model was observed to best describe phosphate sorption on EBP. Further, inter-model comparison with AICc values complemented observation with error functions and confirmed Langmuir equation best describes sorption of phosphate on EBP. A Langmuir-type of phosphate sorption has also been reported for polymers (Dai et al., 2011) and mineral sorbents.

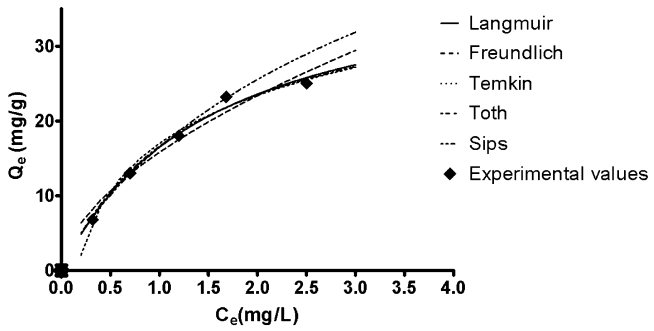

Fig. 2. Sorption isotherm of 1–5 mg/L phosphate at 100 mg/L EBP and 240 min contact time. Data is mean of three independent experiments run in triplicates. Error bars are not shown for clarity; SD was less than 10% of mean at all concentrations.

The Langmuir isotherm assumes sorption of the sorbate as a monolayer on identical binding sites. The favourable nature of the sorption process is described by separation factor, R_L, as described in the following equation:

$$R_L = \frac{1}{1 + K_L C_0} \quad (1)$$

where K_L and C_0 are refers to the Langmuir constant (L/mg) and initial phosphate concentration (mg/L), respectively.

A value of less than 1, but higher than 0, is considered favourable binding while a value of 0 is considered irreversible. The observed value of 0.03 in our study indicates favourable nature of sorption.

The reusability of sorbent and efficient recovery of sorbate are important considerations for field applications. Therefore, desorption studies were conducted to determine reusability of EBP. Phosphate was efficiently desorbed from phosphate-bound EBP under alkaline conditions (0.1 N NaOH) as evident from the difference in Q_e values before (8 mg/g) and after desorption (0.5 mg/g). Further, the sorption capacity was determined during 10 cycles of sorption/desorption and was found to be practically unaltered after 10 cycles (Supplementary Fig. S2). The desorption of phosphate under alkaline conditions is expected be a result of two phenomena: reduction in phosphate binding under alkaline conditions (further discussed in next section) and competition between phosphate and hydroxyl ions for binding sites (Chitrakar et al., 2006). The results of desorption studies suggest that after each sorption cycle, EBP can be replenished without loss of sorption capacity and the recovered phosphate can be reused for further applications.

3.3. Mechanism of phosphate binding

Polysaccharides and proteins comprise the major weight fraction of EBP and their role in sorption of inorganic and organic compounds is well documented (More et al., 2014). Therefore,

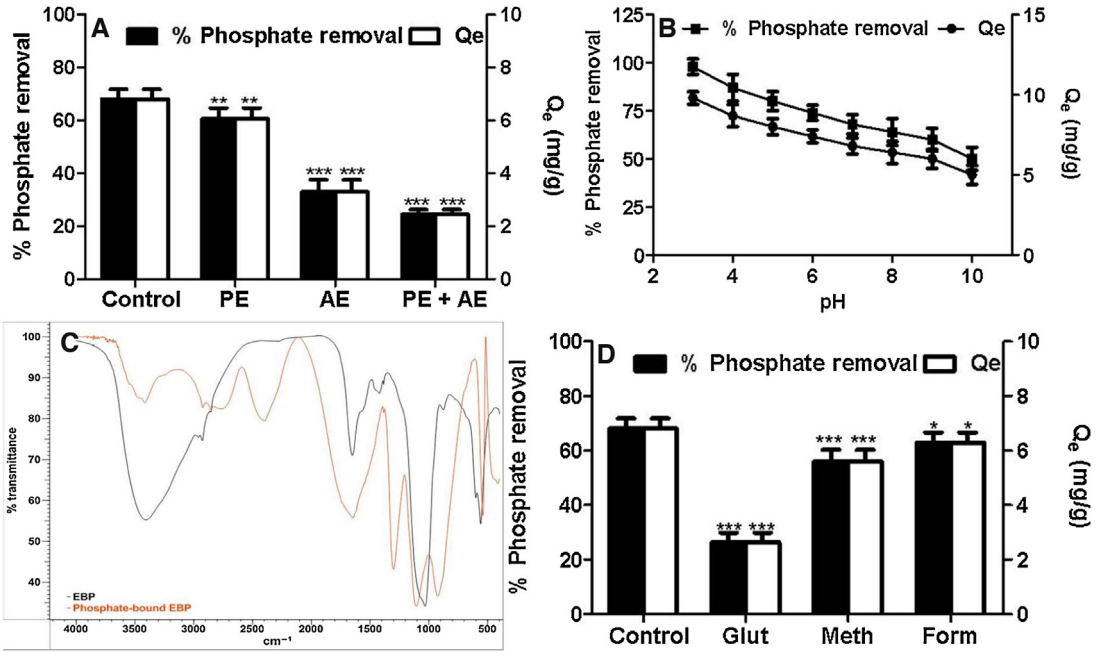

Fig. 3. Mechanism of phosphate binding. Effect of enzyme treatment (A) and pH (B) on phosphate binding. (C) FTIR of unbound and phosphate-bound EBP. (D) Effect of chemical treatment on phosphate binding. Phosphate binding was performed at 1 mg/L phosphate, 100 mg/L EBP and 240 min contact time. Data is mean of three independent experiments run in triplicates. * $p < 0.05$, ** $p < 0.01$, *** $p < 0.001$ w.r.t. control. PE = proteolytic enzyme, AE = amylolytic enzyme, Glut = glutaraldehyde-treated EBP, Meth = methanol–HCl-treated EBP, Form = formaldehyde–formic acid-treated EBP.

in order to delineate the contribution of both fractions in phosphate binding, EBP was individually treated with proteolytic and amylolytic enzymes followed by determination of phosphate binding in the hydrolysate. Following treatment with protease, it was observed that the phosphate-binding capacity of EBP was significantly reduced ($p < 0.01$) suggesting the contribution of protein fraction in phosphate binding. Similarly, treatment with amylolytic enzymes resulted in significant ($p < 0.001$) reduction in phosphate binding suggesting role of polysaccharide fraction in phosphate removal. Further, treatment with a combination of proteolytic and amylolytic enzymes resulted in a significant ($p < 0.001$) reduction in phosphate binding compared to the individual effects of both enzymes (Fig. 3A). It is worthwhile to mention here, that although phosphate binding was significantly reduced by amylolytic enzyme treatment, the binding persisted at appreciable levels. A possible reason for incomplete loss of phosphate binding may be due to incomplete degradation of the polysaccharide chain to monosaccharides, but reducing the polysaccharide chain length. Another plausible reason for the incomplete loss of phosphate binding is the presence of other components of EBP (amino sugars, uronic acids, etc.) which may also contribute to phosphate binding since phosphate binding was detected at appreciable levels even after treatment with combination of proteolytic and amylolytic enzymes. A similar role of amino sugars and uronic acids in phosphate binding has been documented in other biopolymers as well (Block et al., 2013; Deiana, Palma, Premoli, & Senette, 2007; Savica et al., 2009).

The dissociation of functional groups is influenced by pH of the reaction medium and hence pH-dependent binding of sorbate provide valuable information on the nature and type of groups involved in sorption (Shuhong et al., 2014). Phosphate binding with EBP was determined over a pH range of 3–10 and found to be maximum in the acidic medium and decreased with an increase in pH (Fig. 3B). The observed pH-dependent phosphate binding behaviour may be attributed to protonation of negatively charged functional groups, such as carboxylic groups present in proteins and uronic acids, which result in reduction in electrostatic repulsive forces. Additionally, protonation of basic functional groups such as amino groups present in proteins and amino sugars results in more efficient phosphate binding due to electrostatic interactions.

Potentiometric titrations are commonly employed to supplement information obtained from pH-dependent binding studies. Potentiometric titrations provide information on the acidity constants (p*K*a), an indicator of the nature of binding site, as well as binding site density (Wei et al., 2011). The pH titration data (Supplementary Fig. S3) was fitted using Protofit to calculate p*K*a and site concentrations. The data was fitted into diffusion layer model and observed to contain two buffering zones with p*K*a 3.63 and 8.61. The first buffering zone could be attributed to carboxylic groups present in proteins and uronic acids. The second p*K*a was observed at 8.61 which generally correspond to the buffering range of amino and alcohol groups (Guine et al., 2006). The second buffering zone could appear due to amino groups present in proteins and amino sugars as well as alcohol groups present in polysaccharides and amino sugars. It is noteworthy to mention here that alcoholic, amino and carboxylic groups were also identified as the major functional groups by FTIR spectroscopy. Based on comparison of observed deprotonation constants with reported values, we believe that the major binding sites in EBP are carboxylic acid (p*K*a 3.63) and amino/alcoholic (p*K*a 8.61) groups with corresponding site densities of 6.61 and 8.32 mol/kg, respectively.

The FTIR spectrum of unbound EBP and phosphate-bound EBP revealed several characteristic peaks, peak shifts and changes in peak shapes which provide important insights into phosphate binding mechanism of EBP. The most notable differences were observed in peaks for alcoholic (OH) and amino (NH) groups. A broad peak was observed at 3408 cm^{-1} in unbound EBP which may be attributed to stretching vibration of alcoholic (OH) groups and amino groups (NH) groups. The peaks at 1650 cm^{-1} and 1421 cm^{-1} represent N—H bending and C—N stretching of amines, respectively. These peaks were observed to be suppressed and shifted to slightly higher wavenumbers in phosphate bound EBP suggesting the role of OH and NH groups in phosphate binding. The peaks observed at 1032 cm^{-1} and 875 cm^{-1} in unbound EBP indicated CO ether

linkage of sugars and beta glycosidic linkage, respectively. However, these peaks were not observed in phosphate bound EBP due to overlap with P=O stretching and P—O stretching vibrations at 1107 cm^{-1} and 922 cm^{-1}, respectively. Additional peaks were identified in phosphate bound EBP which include O—H stretching peaks of phosphonic acids at 2739 cm^{-1} and 2400 cm^{-1} along with O—H deformation peak at 1302 cm^{-1} (Fig. 3C).

Based on the results of FTIR analysis, phosphate appears to bind through electrostatic interactions with amino groups present in proteins and amino sugars. In parallel, phosphate may also interact with OH groups present in polysaccharide fraction and amino sugars via a ligand exchange mechanism and described by below equation:

$$-R-OH + H_2PO^{4-} \rightarrow R-HPO_4 + H_2O \quad (2)$$

$$-R-COOH + H_2PO^{4-} \rightarrow R-COHPO_4 + H_2O \quad (3)$$

A similar mechanism of phosphate binding via electrostatic interactions and ligand exchange has also been suggested in plant fibres (Riahi, Chaabane, & Thayer, 2014; Wahab, Hassine, & Jellali, 2011) and phosphate mine sludge (Jellali, Wahab, Anane, Riahi, & Bousselmi, 2010). It is worth mentioning here, that the peaks for amino groups were either overlapping with peaks from OH in unbound EBP or with peaks for phosphate groups in phosphate-bound EBP hence, the contribution of amino groups in phosphate removal could not be determined with reliability. Based on the combined results of potentiometric titrations and FTIR studies, it is evident that amino and hydroxyl groups confer phosphate-binding properties to EBP. In order to verify the role of amino groups in phosphate binding, EBP was treated with glutaraldehyde, an amine reactive compound. Following glutaraldehyde treatment, phosphate binding to EBP was significantly ($p < 0.001$) reduced compared to untreated control. On the other hand, esterification of carboxyl groups with methanol or blockade of amide groups with formaldehyde showed relatively less reduction in phosphate binding than glutaraldehyde (Fig. 3D) suggesting amino groups present in proteins and amino sugars play a major role in phosphate sorption by EBP.

EBP has been reported to bind to metals through a variety of mechanisms such as precipitation with counterions, complex formation and electrostatic interactions. However, similar studies with bacterial EBP have not been reported so far. Therefore, as a first step, we performed elemental mapping of phosphorus by EDS coupled to SEM. Elemental mapping revealed that phosphorus was uniformly distributed on EBP (Supplementary Fig. S4), thus, excluding the possibility of a precipitation mechanism of binding. Comparative XRD analysis of unbound and phosphate-bound EBP also did not showed formation of phosphate complexes or crystals (Supplementary Fig. S5) further confirming that precipitation/crystallization of phosphate in salt form does not occur.

The zeta potential of unbound and phosphate-bound EBP were determined in water and found to be −2.98 mV and −3.11 mV, respectively. Based on the decrease in zeta potential after phosphate binding, it is plausible that binding of the negatively charged phosphate with EBP will impart a more negative charge on EBP suggesting an ion-exchange mechanism of binding (Zhong, Stanforth, Wu, & Chen, 2007). It may be argued that the small decrease in zeta potential after phosphate binding may be result of surface complexation or microprecipitation. However, the contribution of these two mechanisms may be ruled out by two observations. First, phosphate binding to geothite occurs by a rapid (occurring over a few minutes) ion adsorption mechanism and a relatively slower (occurring over days or weeks) precipitation mechanism (Luengo, Brigante, Antelo, & Avena, 2006). Considering that phosphate binding to EBP to be a rapid phenomenon and that phosphate concentrations were

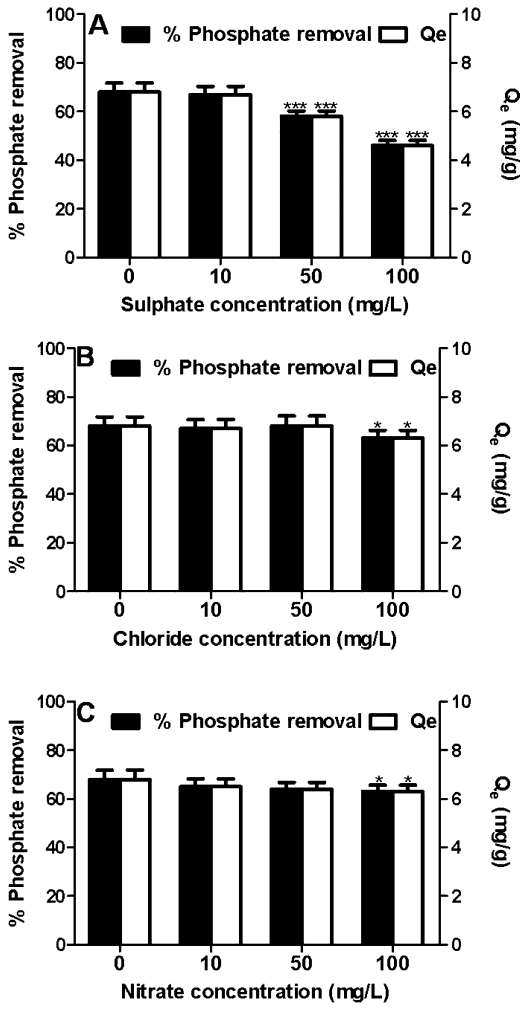

Fig. 4. Effect of competing anions, sulphate (A), chloride (B) and nitrate (C), on phosphate binding at 1 mg/L phosphate and 100 mg/L EBP. Data is mean of three independent experiments run in triplicates.* $p < 0.05$, *** $p < 0.001$ w.r.t. control.

determined following a contact time of 240 min, the possibility of precipitation mechanism can be ruled out. Second, phosphate requires a cation for precipitation or complexation reactions to occur on EBP. Since the EBP was dialyzed for several hours, we do not expect cations to be present in significant amounts to cause a considerable precipitation reaction. The absence of cations in EBP is further supported by absence of peaks for metals in the EDS spectrum.

The nature of phosphate binding to EBP was further investigated by anion displacement studies using competing anions, chloride, nitrate and sulphate. Sulphate was found to displace the maximum amount of bound phosphate among all competing anions while chloride and nitrate displaced phosphate only at a concentration 100-fold higher than phosphate (Fig. 4). These results suggest that binding of phosphate with EBP is a reversible process and the observed affinity of EBP for anions (phosphate > sulphate > chloride = nitrate) indicates that anion binding to EBP is governed by surface charge density of the anion. A similar order of anion binding has been reported for proteins, polysaccharides and inorganic adsorbents (Chitrakar et al., 2006; Medda et al., 2012; Wahab et al., 2011).

Overall, from the results the above studies, it may be inferred that phosphate primarily interacts with protein and carbohydrate components of EBP. Further, other EBP components such as amino sugars, uronic acids, etc. could also play a significant

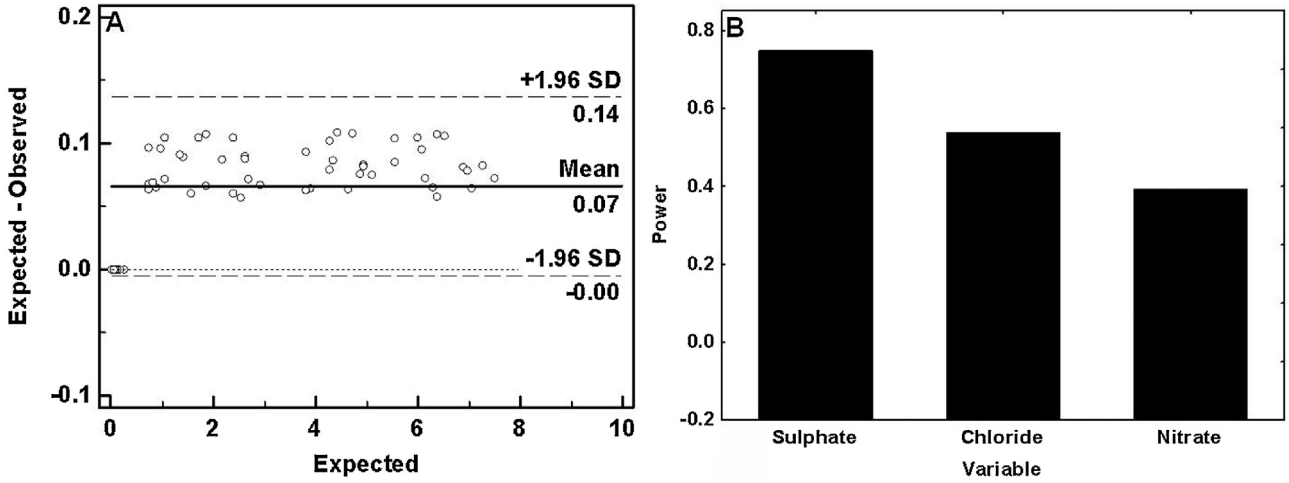

Fig. 5. Phosphate removal in wastewater samples. (A) Bland–Altman plot showing difference between predicted and observed phosphate removal ($n = 60$). (B) Partial least square showing contribution of competing anions in interference with phosphate removal.

role in phosphate binding (Block et al., 2013; Dai et al., 2011; Deiana et al., 2007; Savica et al., 2009). Phosphate may be sorbed on EBP through electrostatic interactions with amino groups as suggested by pH-dependent binding, glutaraldehyde treatment, FTIR and anion displacement studies. Further, a ligand exchange mechanism, involving hydroxyl groups, may also contribute to phosphate sorption by EBP as indicated by FTIR analysis. Based on the observations in EDS and XRD analysis, we do not anticipate that a precipitation or complexation mechanism may be involved in phosphate sorption. Phosphate removal by bacterial EBP has not been reported so far, except by microbial communities in activated sludge (Zhang et al., 2013a,b). Hence, this is the first report to document phosphate-binding capabilities and mechanism of phosphate removal by EBP produced by a well characterized strain of bacterium.

3.4. Real time phosphate removal studies

EBP has been studied for bioremediation of heavy metals and pollutants present in wastewater. Following the studies in phosphate solution, it was anticipated that EBP may be useful for removal of phosphate from water bodies. Phosphate removal was determined in 60 wastewater samples. The range of quality parameters in wastewater samples was: pH 6–8, total dissolved solids <2000 mg/L, total hardness <600 mg/L, nitrate <100 mg/L, sulphate 100–1000 mg/L, phosphate 0.02–10.00 mg/L, chloride 100–1000 mg/L and fluoride <0.5 mg/L. A significant reduction of >60% ($p < 0.001$; Wilcoxon signed rank test) in phosphate concentration was observed in all samples within a period of 4 h. However, difference plots revealed that phosphate removal in real time conditions was lower than calculated/expected removal (Fig. 5A). In order to determine the competing anions that might have resulted in the observed reduction in phosphate removal, water samples were analyzed for nitrate, chloride and sulphate. PLS analysis revealed that sulphate showed highest interference with phosphate removal followed by chloride and nitrate (Fig. 5B).

The high thermal stability ensures that EBP can be used in extreme temperatures while the shear-thinning behaviour of polymer solution makes it amenable to industrial applications since the reduction in viscosity by agitation ensures efficient mixing of formulation components during mixing operations as well as confers ease of liquid handling (Supplementary Figs. S6 and S7).

4. Conclusion

Characterization of EBP produced by *A. haemolyticus* MG606 revealed presence of polysaccharides, proteins, uronic acids, pyruvic acid and other constituents. Results of FTIR analysis and potentiometric titration indicated that major functional groups (carboxyl, hydroxyl and amines groups) on the EBP contribute to the electrostatic interaction and leading to binding mechanism for phosphate removal. The high surface area suggests availability of a large number of binding sites on surface, conducive for efficient phosphate binding. Additionally, EBP exhibits a significantly higher binding capacity (25 mg/g) than other natural and mineral sorbents (2–10 mg/g) reported, suggesting superiority of EBP over other sorbents. EBP was relatively less efficient compared to several physical and chemical methods when compared on effluent phosphate concentration basis. The efficient recovery of bound phosphate and reusability of EBP offers additional advantages unseen in most phosphate remediation techniques.

Acknowledgements

The study was supported by grant from University Grants Commission (UGC) (41-536/2012 (SR)) and (F1-17.1/2010/ MANF-SIK-PUN-4099), India. TK acknowledges UGC for providing Maulana Azad National Fellowship.

Appendix A. Supplementary data

Supplementary data associated with this article can be found, in the online version, at http://dx.doi.org/10.1016/j.carbpol.2015.06.002

References

Akpa, O. M., & Unuabonah, E. I. (2011). Small-sample corrected Akaike information criterion: An appropriate statistical tool for ranking of adsorption isotherm models. *Desalination*, *272*, 20–26.

APHA. (1998). *Standard methods for the examination of water and wastewater*. Washington, DC: American Public Health Association.

Block, G. A., Persky, M. S., Shamblin, B. M., Baltazar, M. F., Singh, B., Sharma, A., et al. (2013). Effect of salivary phosphate-binding chewing gum on serum phosphate in chronic kidney disease. *Nephron Clinical Practice*, *123*, 93–101.

Chitrakar, R., Tezuka, S., Sonoda, A., Sakane, K., Ooi, K., & Hirotsu, T. (2006). Phosphate adsorption on synthetic goethite and akaganeite. *Journal of Colloid and Interface Science*, *298*, 602–608.

Dai, J., Yang, H., Yan, H., Shangguan, Y., Zheng, Q., & Cheng, R. (2011). Phosphate adsorption from aqueous solutions by disused adsorbents: Chitosan hydrogel beads after the removal of copper(II). *Chemical Engineering Journal*, *166*, 970–977.

Deiana, S., Palma, A., Premoli, A., & Senette, C. (2007). Possible role of the polyuronic components in accumulation and mobilization of iron and phosphate at the soil–root interface. *Plant Physiology and Biochemistry*, *45*, 341–349.

El-Bestawy, E., Hussein, H., Baghdadi, H. H., & El-Saka, M. F. (2005). Comparison between biological and chemical treatment of wastewater containing nitrogen and phosphorus. *Journal of Industrial Microbiology and Biotechnology*, *32*, 195–203.

Foo, K. Y., & Hameed, B. H. (2010). Insights into the modeling of adsorption isotherm systems. *Chemical Engineering Journal*, *156*, 2–10.

Guine, V., Spadini, L., Sarret, G., Muris, M., Delolme, C., Gaudet, J. P., et al. (2006). Zinc sorption to three gram-negative bacteria: Combined titration, modeling, and EXAFS study. *Environmental Science & Technology*, *40*, 1806–1813.

Ho, Y. S. (2004). Selection of optimum sorption isotherm. *Carbon*, *42*, 2115–2116.

Jagtap, S., Yavankar, S., Pardesi, K., & Chopade, B. (2010). Production of bioemulsifier by *Acinetobacter* species isolated from healthy human skin. *Indian Journal of Experimental Biology*, *48*, 70–76.

Jellali, S., Wahab, M. A., Anane, M., Riahi, K., & Bousselmi, L. (2010). Phosphate mine wastes reuse for phosphorus removal from aqueous solutions under dynamic conditions. *Journal of Hazardous Materials*, *184*, 226–233.

Jianlong, W. (2002). Biosorption of copper(II) by chemically modified biomass of *Saccharomyces cerevisiae*. *Process Biochemistry*, *37*, 847–850.

Kaur, T., Ganguli, A., & Ghosh, M. (2013). Development of exobiopolymer-based biosensor for detection of phosphate in water. *Water Science and Technology*, *68*, 2619–2625.

Kaur, T., Sharma, J., Ganguli, A., & Ghosh, M. (2013). Application of biopolymer produced from metabolic engineered *Acinetobacter* sp. for the development of phosphate optoelectronic sensor. *Composite Interfaces*, *21*, 143–151.

Kim, B., Gautier, M., Olvera Palma, G., Molle, P., Michel, P., & Gourdon, R. (2015). Pilot-scale study of vertical flow constructed wetland combined with trickling filter and ferric chloride coagulation: Influence of irregular operational conditions. *Water Science and Technology*, *71*, 1088–1096.

Li, N., Ren, N.-Q., Wang, X.-H., & Kang, H. (2010). Effect of temperature on intracellular phosphorus absorption and extra-cellular phosphorus removal in EBPR process. *Bioresource Technology*, *101*, 6265–6268.

Luengo, C., Brigante, M., Antelo, J., & Avena, M. (2006). Kinetics of phosphate adsorption on goethite: Comparing batch adsorption and ATR-IR measurements. *Journal of Colloid and Interface Science*, *300*, 511–518.

Medda, L., Barse, B., Cugia, F., Bostrom, M., Parsons, D. F., Ninham, B. W., et al. (2012). Hofmeister challenges: Ion binding and charge of the BSA protein as explicit examples. *Langmuir*, *28*, 16355–16363.

Micheletti, E., Pereira, S., Mannelli, F., Moradas-Ferreira, P., Tamagnini, P., & De Philippis, R. (2008). Sheathless mutant of *Cyanobacterium gloeothece* sp. strain PCC 6909 with increased capacity to remove copper ions from aqueous solutions. *Applied and Environmental Microbiology*, *74*, 2797–2804.

More, T. T., Yadav, J. S. S., Yan, S., Tyagi, R. D., & Surampalli, R. Y. (2014). Extracellular polymeric substances of bacteria and their potential environmental applications. *Journal of Environmental Management*, *144*, 1–25.

Nguyen, H. T. A., Ngo, H. H., Guo, W., & Nguyen, V. T. (2012). Phosphorous removal from aqueous solutions by agricultural by-products: A critical review. *Journal of Water Sustainability*, *2*, 193–207.

Nguyen, T. A., Ngo, H. H., Guo, W. S., Pham, T. Q., Li, F. M., Nguyen, T. V., et al. (2015). Adsorption of phosphate from aqueous solutions and sewage using zirconium loaded Okara (ZLO): Fixed-bed column study. *The Science of the Total Environment*, *523*, 40–49.

Oehmen, A., Lemos, P. C., Carvalho, G., Yuan, Z., Keller, J. R., Blackall, L. L., et al. (2007). Advances in enhanced biological phosphorus removal: From micro to macro scale. *Water Research*, *41*, 2271–2300.

Oosthuizen, D. J., & Cloete, T. E. (2001). SEM–EDS for determining the phosphorus content in activated sludge EPS. *Water Science and Technology*, *43*, 105–112.

Patil, J. R., & Chopade, B. A. (2001). Studies on bioemulsifier production by *Acinetobacter* strains isolated from healthy human skin. *Journal of Applied Microbiology*, *91*, 290–298.

Pierre, G., Graber, M., Rafiliposon, B. A., Dupuy, C., Orvain, F., De Crignis, M., et al. (2012). Biochemical composition and changes of extracellular polysaccharides (ECPS) produced during microphytobenthic biofilm development (Marennes-Oleron, France). *Microbial Ecology*, *63*, 157–169.

Riahi, K., Chaabane, S., & Thayer, B. B. (2014). A kinetic modeling study of phosphate adsorption onto *Phoenix dactylifera* L. date palm fibers in batch mode. *Journal of Saudi Chemical Society*, http://dx.doi.org/10.1016/j.jscs.2013.11.007

Rockstrom, J., Steffen, W., Noone, K., Persson, A., Chapin, F. S., Lambin, E. F., et al. (2009). A safe operating space for humanity. *Nature*, *461*, 472–475.

Satpute, S. K., Banat, I. M., Dhakephalkar, P. K., Banpurkar, A. G., & Chopade, B. A. (2010). Biosurfactants, bioemulsifiers and exopolysaccharides from marine microorganisms. *Biotechnology Advances*, *28*, 436–450.

Savica, V., Calo, L. A., Monardo, P., Davis, P. A., Granata, A., Santoro, D., et al. (2009). Salivary phosphate-binding chewing gum reduces hyperphosphatemia in dialysis patients. *Journal of the American Society of Nephrology*, *20*, 639–644.

Sen, I. K., Mandal, A. K., Chakraborty, R., Behera, B., Yadav, K. K., Maiti, T. K., et al. (2014). Structural and immunological studies of an exopolysaccharide from *Acinetobacter junii* BB1A. *Carbohydrate Polymers*, *101*, 188–195.

Senila, L., Gog, A., Senila, M., Roman, C., & Silaghi-Dumitrescu, L. (2011). Analysis of carbohydrates obtained from wood by gas chromatography–mass spectrometry. *Revista de Chimie (Bucharest)*, *62*, 149–153.

Shuhong, Y., Meiping, Z., Hong, Y., Han, W., Shan, X., Yan, L., et al. (2014). Biosorption of Cu(2+), Pb(2+) and Cr(6+) by a novel exopolysaccharide from Arthrobacter ps-5. *Carbohydrate Polymers*, *101*, 50–56.

Trathnigg, B. (2000). Size-exclusion chromatography of polymers. In R. A. Meyers (Ed.), *Encyclopedia of analytical chemistry* (pp. 8008–8034). Chichester: John Wiley & Sons Ltd.

Turner, B. F., & Fein, J. B. (2006). Protofit: A program for determining surface protonation constants from titration data. *Computers & Geosciences*, *32*, 1344–1356.

Wahab, M. A., Hassine, R. B., & Jellali, S. (2011). *Posidonia oceanica* (L.) fibers as a potential low-cost adsorbent for the removal and recovery of orthophosphate. *Journal of Hazardous Materials*, *191*, 333–341.

Wei, X., Fang, L., Cai, P., Huang, Q., Chen, H., Liang, W., et al. (2011). Influence of extracellular polymeric substances (EPS) on Cd adsorption by bacteria. *Environmental Pollution*, *159*, 1369–1374.

Woumfo, E. D., Siewe, J. M., & Njopwouo, D. (2015). A fixed-bed column for phosphate removal from aqueous solutions using an andosol–bagasse mixture. *Journal of Environmental Management*, *151*, 450–460.

Zhang, H. L., Fang, W., Wang, Y. P., Sheng, G. P., Xia, C. W., Zeng, R. J., et al. (2013). Species of phosphorus in the extracellular polymeric substances of EBPR sludge. *Bioresource Technology*, *142*, 714–718.

Zhang, H. L., Fang, W., Wang, Y. P., Sheng, G. P., Zeng, R. J., Li, W. W., et al. (2013). Phosphorus removal in an enhanced biological phosphorus removal process: Roles of extracellular polymeric substances. *Environmental Science & Technology*, *47*, 11482–11489.

Zhong, B., Stanforth, R., Wu, S., & Chen, J. P. (2007). Proton interaction in phosphate adsorption onto goethite. *Journal of Colloid and Interface Science*, *308*, 40–48.

Supplementary data

Acinetobacter haemolyticus MG606 produces a novel, phosphate binding exobiopolymer

Taranpreet Kaur, Moushumi Ghosh*

Department of Biotechnology, Thapar University, Patiala, 147004, India.

* Corresponding author: Email: mghosh@thapar.edu, Tel: +91-175-2393478

Fax: +91-175-2364498, 2393020

Phosphate sorption by EBP

The effect of contact time and EBP concentration on phosphate removal was determined. We observed that phosphate sorption (1 mg/L) on EBP (100 mg/L) increased in a time-dependent manner and reached maximum at 240 min. A further increase in contact time to 300 min provided no additional advantage in terms of phosphate removal (Supplementary Figure S1A). Hence, 240 min contact time was selected for further studies.

Phosphate removal from a 1 mg/L solution was studied by varying EBP concentration from 50 to 400 mg/L with a contact time of 240 min. The percentage phosphate removal increased with an increase in EBP concentration from 50 to 400 mg/L. A closer examination of the data revealed that a near-maximum phosphate removal was achieved at 100 mg/L. An increase in EBP concentration from 100 to 200 mg/L afforded a small increment (approximately 10%) in phosphate removal and a further increase in EBP concentration upto 400 mg/L provided no additional phosphate removal. Phosphate sorption efficiency (Qe) also decreased from 8 mg/g to 2 mg/g with an increase in EBP concentration from 50 to 400 mg/L at 1 mg/L phosphate concentration (Supplementary Figure S1B). As observed in percentage phosphate removal, 100 mg/L showed a near-maximum Qe value. The contrasting results in percentage phosphate removal and Qe could be explained by considering the increase in the number of binding sites increase with an increase in EBP concentration. As a result of this, the percentage phosphate removal increases with an increase in EBP concentration. On the other hand, the number of unbound sites increase with an increase in EBP concentration at a fixed phosphate concentration which transforms into lower Qe values at higher EBP concentrations. Therefore, based on percentage phosphate removal and Qe values, 100 mg/L EBP was selected as the optimal concentration for further studies.

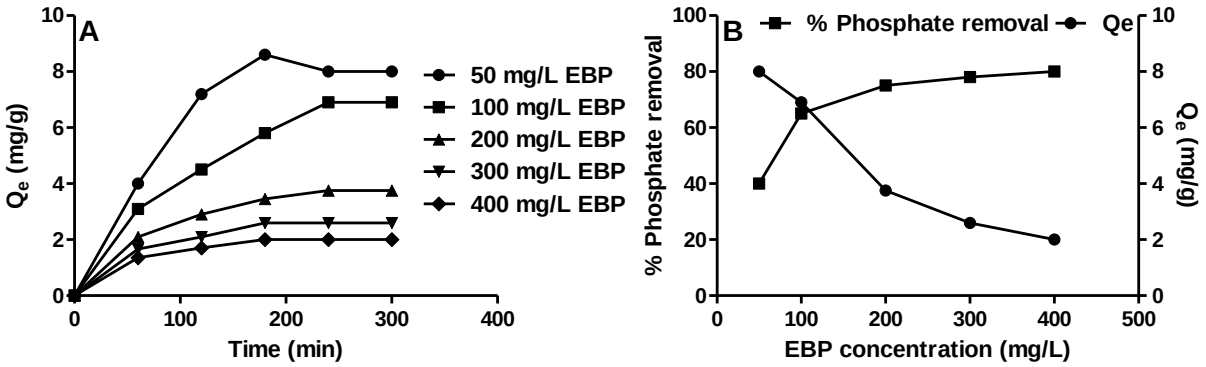

Supplementary Fig. S1. Optimization of contact time and EBP concentration. (A) Kinetics of phosphate binding (1 mg/L) at different EBP concentrations. (B) Effect of EBP concentration on percentage phosphate removal and sorption efficiency (Qe) at 1 mg/L phosphate concentration and 240 min contact time. Data is mean of three independent experiments run in triplicates. Error bars are not shown for clarity; SD was less than 10% of mean at all concentrations.

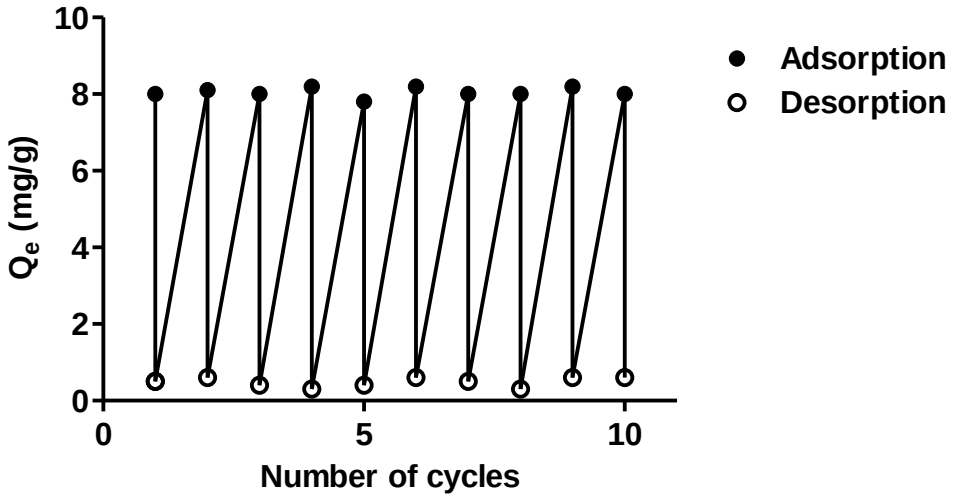

Supplementary Fig. S2. Sorption/desorption cycles of phosphate on EBP.

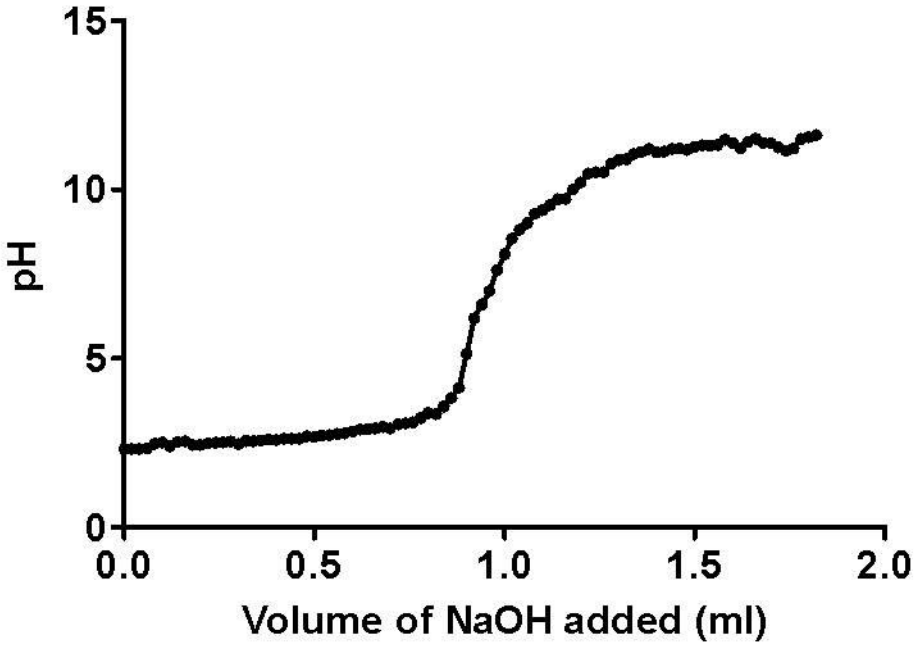

Supplementary Fig. S3. Potentiometric titration of EBP.

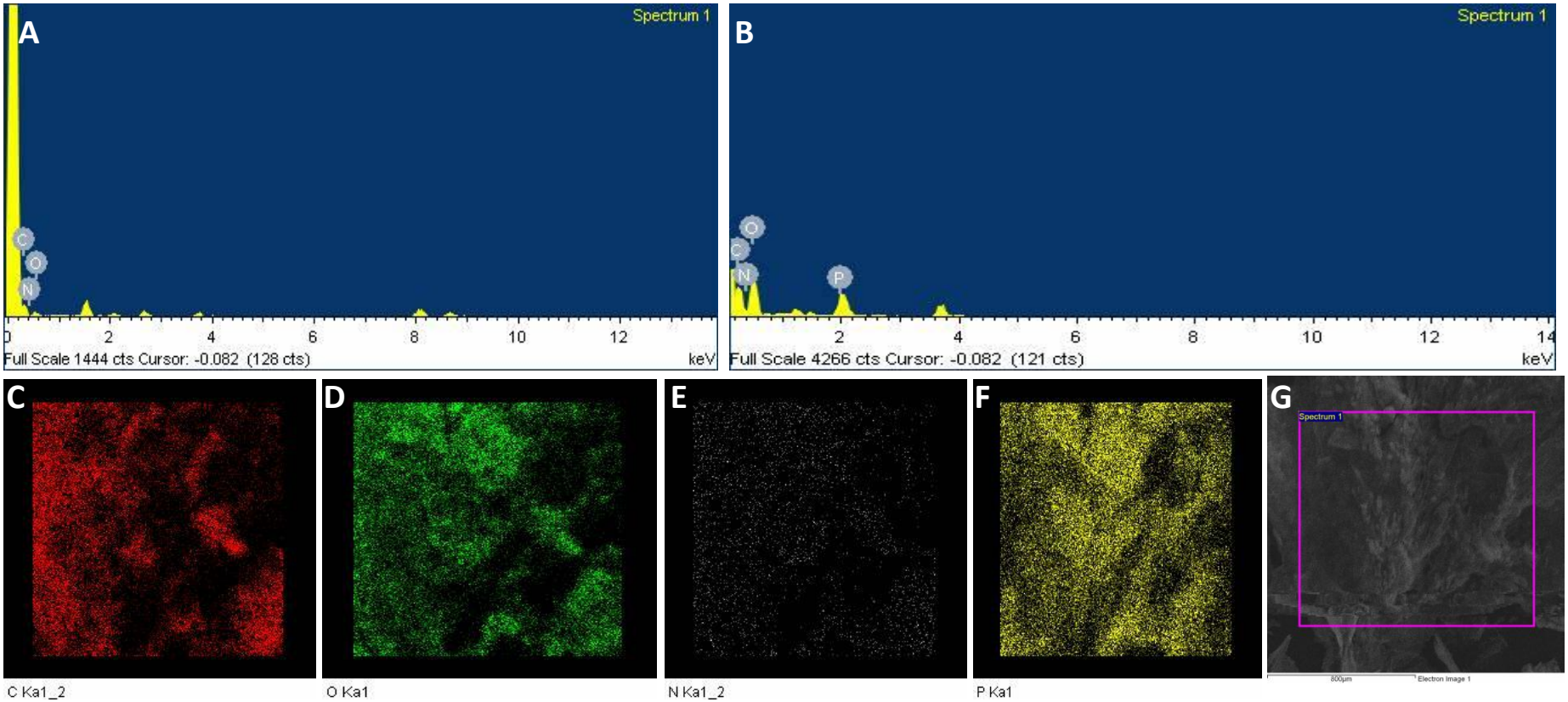

Supplementary Fig. S4. EDS analysis of unbound phosphate-bound EBP. (A) shows EDS spectrum of unbound EBP and (B) shows EDS spectrum of phosphate-bound EBP. (C-F) show elemental mapping of carbon (C), oxygen (D), nitrogen (E) and phosphorus (F). (G) shows the SEM image of EBP area scanned for elemental analysis.

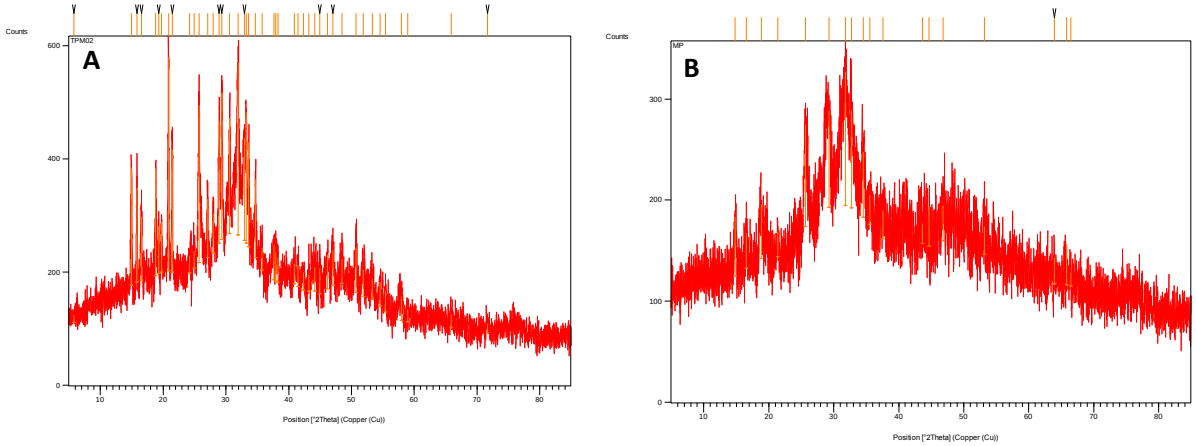

Supplementary Fig. S5. XRD spectrum of unbound (A) and phosphate-bound EBP (B).

Thermal stability of EBP

Thermogravimetric analysis (TGA) was performed on a Mettler Toledo TGA apparatus. Thermogram of EBP revealed slow decomposition possibly due to presence of thermally stable sugar moieties. The EBP showed an initial weight loss (approximately 5-7%) possibly due to loss of sorbed water/moisture and gases. Following this initial weight loss, EBP showed a further 5-7% weight loss until 250°C due to loss of sorbed volatile compounds or degradation of carboxylic groups. The onset of degradation was observed at 295°C (T_d) and thermogram showed a temperature-dependent degradation until EBP was completely decomposed at 895°C (Supplementary Fig. S6).

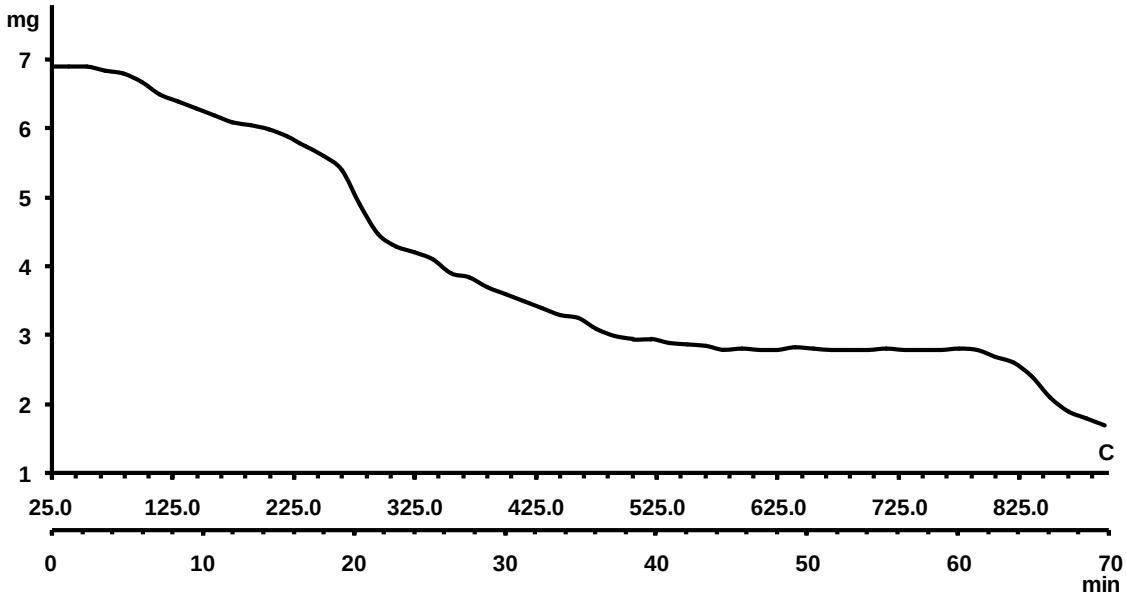

Supplementary Fig. S6. A representative thermogram showing thermal degradation of EBP.

Viscosity measurements

The dynamic viscosity of aqueous solution of EBP was determined by Brookfield viscometer (DV-11+/Pro, Brookfield). Viscosity measurements were performed at different shear stress in order to understand the viscoelastic properties of EBP. It was observed that apparent viscosity of solution decreased with increasing shear stress suggesting non-Newtonian, shear thinning behaviour of EBP solution (Supplementary Fig. S7). The quantitative relation between shear rate (γ, s^{-1}) and shear stress (τ, Pa) is generally determined by fitting Power law or Ostwald-de-Waele model (Alves et al., 2010), which is expressed as

$$\tau = K\gamma^n$$

where, K is consistency index (Pa s^n) and n is power law index or flow index value. The value of n is an indicator of the shear behaviour of solution with n = 1 representing Newtonian fluid whilst n<1 suggesting pseudoplastic behaviour. The EBP produced by

MG606 strain showed a flow index value of 0.582 suggesting pseudoplastic nature of EBP solution. A similar pseudoplastic behaviour has been demonstrated for EBP produced by other microorganisms as well (Arias et al., 2003; Castellane, Lemos, & Lemos, 2014; Ismail & Nampoothiri, 2014).

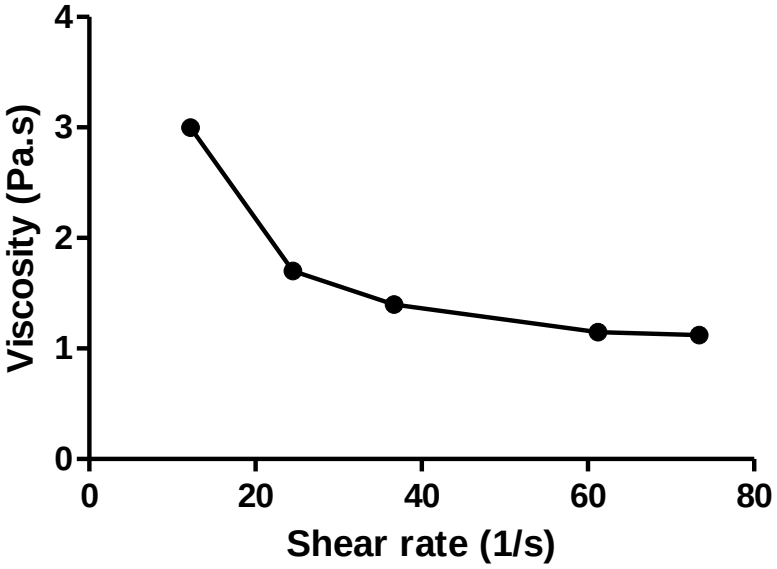

Supplementary Fig. S7. Effect of shear rate on viscosity of EBP solution.

Supplementary Table 1: Adsorption isotherms parameters and correlation coefficients based on experimental data

	Isotherm	Isotherm equation	Parameter[a]	Value	R^2	*SSE*	*HYBRID*	*MPSD*	χ^2	*AICc*
1	Langmuir	$Q_e = \frac{Q_0 b C_e}{1 + b C_e}$	Q_0	41.29	0.987	2.92	6.15	5.59	0.15	9.87
			B	0.665						
2	Freundlich	$Q_e = K_f C_e^{1/n}$	K_f	15.78	0.961	8.86	13.37	14.05	0.56	15.42
			N	1.765						
3	Temkin	$Q_e = B_T(\ln A_T + \ln C_e)$	B_T	9.262	0.985	3.26	7.46	6.11	0.18	10.42
			A_T	6.251						
4	Toth	$Q_e = \frac{K_t C_e}{(a_t + C_e)^{1/t}}$	K_t	0.481	0.988	3.02	10.99	8.19	0.17	32.07
			a_t	1.408						
			T	0.0115						
5	Sips	$Q_e = \frac{K_s C_e^{t_s}}{(1 + a_s C_e^t)}$	K_s	79.8	0.970	15.97	13.23	12.06	0.58	40.39
			a_s	0.206						
			t_s	0.858						

[a] Q_e=Adsorption capacity (mg/g), Q_0 = Maximum monolayer coverage capacity (mg/g), B = Langmuir isotherm constant, C_e = Equilibrium concentration, K_f=Freundlich constant related to adsorption capacity, n = Freundlich constant related to adsorption intensity, B_T =

Temkinisotherm constant, A_T = Temkin isotherm equilibrium binding constant (L/g), K_t = Toth isotherm constant (mg/g), a_t = Toth isotherm constant (L/mg), t = Toth isotherm dimensionless constant, K_s = Sips isotherm model constant (L/g), a_s = Sips isotherm model constant, t_s = Sips isotherm model exponent

AICc = Corrected Akaike's information criterion, HYBRID = Hybrid fractional error function, MPSD = Marquardt's percent standard deviation, SSE = Sum squares error, $\chi 2$ = Non-linear Chi-square analysis

References

Alves, V. D., Freitas, F., Torres, C. A. V., Cruz, M., Marques, R., et al. (2010). Rheological and morphological characterization of the culture broth during exopolysaccharide production by Enterobacter sp. *Carbohydrate Polymers, 81*, 758-764.

Arias, S., del Moral, A., Ferrer, M. R., Tallon, R., Quesada, E., et al. (2003). Mauran, an exopolysaccharide produced by the halophilic bacterium Halomonas maura, with a novel composition and interesting properties for biotechnology. *Extremophiles, 7*, 319-326.

Castellane, T. C., Lemos, M. V., & Lemos, E. G. (2014). Evaluation of the biotechnological potential of Rhizobium tropici strains for exopolysaccharide production. *Carbohydrate Polymers, 111*, 191-197.

Ismail, B., & Nampoothiri, K. (2014). Molecular characterization of an exopolysaccharide from a probiotic Lactobacillus plantarum MTCC 9510 and its efficacy to improve the texture of starchy food. *Journal of Food Science and Technology, 51*, 4012-4018.

Microbiological Research 181 (2015) 8–14

Contents lists available at ScienceDirect

Microbiological Research

journal homepage: www.elsevier.com/locate/micres

Characterization and upregulation of bifunctional phosphoglucomutase/phosphomannomutase enzyme in an exobiopolymer overproducing strain of *Acinetobacter haemolyticus*

Taranpreet Kaur, Moushumi Ghosh *

Department of Biotechnology, Thapar University, Patiala, Punjab 147 004, India

ARTICLE INFO

Article history:
Received 5 April 2015
Received in revised form 13 July 2015
Accepted 4 August 2015
Available online 6 August 2015

Keywords:
Acinetobacter haemolyticus
Exobiopolymer
Insertional mutant
Phosphoglucomutase

ABSTRACT

Several members of the *Acinetobacter* spp. produce exobiopolymer (EBP) of considerable biotechnological interest. In a previous study, we reported phosphate removal capacity of EBP produced by *Acinetobacter haemolyticus*. Insertional mutagenesis was attempted to develop EBP-overproducing strains of *A. haemolyticus* and mutant MG606 was isolated. In order to understand the underlying mechanism of overproduction, the EBP overproducing mutant MG606 was analyzed and compared with the wild type counterpart for its key EBP synthetic enzymes. The EBP produced by MG606 mutant was 650 mg/L compared to 220 mg/L in its wild type counterpart. Significantly high ($p < 0.05$) levels of phosphoglucomutase/phosphomannomutase (PGM/PMM) in MG606 mutant was noted, whereas activities of other enzymes responsible for EBP synthesis showed no significant change ($p > 0.05$). The up-regulation of PGM/PMM expression in mutant was further confirmed by real time reverse transcriptase (RT)-PCR of PGM/PMM transcripts. The optimal conditions for PGM/PMM activity were found to be 35 °C and pH 7.5; PGM/PMM activity was inhibited by ions such as lithium, zinc, nickel. Further, incubation of cells with a PGM inhibitor (lithium) resulted in a concentration-dependent decrease in EBP production further confirming the role of PGM/PMM overexpression in enhanced EBP production by the mutant. Overall the results of our study indicate a key role of PGM/PMM in enhanced EBP production, as evident from enhanced enzyme activity, increased PGM/PMM transcripts and reduction in EBP synthesis by a PGM inhibitor. We envisage a potential exploitation of the insights so obtained to effectively engineer strains of *Acinetobacter* for overproducing phosphate binding EBP.

1. Introduction

Microbial exobiopolymers or exobiopolymer (EBP) produced by bacteria serves to enhance the competitive success of the producer strains during different natural conditions. The composition and physicochemical properties of EBP are culture dependent and may be tweaked by modifications in culture conditions. Due to their multifunctional properties and ease of production, EBP from various microbial sources have been employed in several areas such as waste water treatment, cosmetics, crude oil recovery and downstream processing (Calvo et al., 2008; Auger et al., 2012; Ali et al., 2014).

A frequently occurring active component of EBP include polysaccharide fraction and has been identified as the major fraction of EBP in terms of weight fraction and biological/physicochemical properties (Ibarburu et al., 2007; Joshi and Kanekar, 2011; Vlamakis et al., 2013). The first step in EBP formation involves conversion of glucose-6-phosphate (G6P) to glucose-1-phosphate (G1P) by phosphoglucomutase (PGM). G1P serves as a precursor sugar nucleotide which is further used in synthesis of other precursor sugar nucleotides (Ramos et al., 2001; Jung et al., 2014). G1P is converted to uridine-5′-diphosphate glucose (UDP-glucose) by UDP-glucose phosphorylase which is then converted to UDP-galactose by epimerase (UDE). The activated monosaccharide units are brought and assembled on a lipid carrier by glycosyltransferase (GST) (Seibel et al., 2006; Bounaix et al., 2010; Kralj et al., 2011; Chai et al., 2012; Dertli et al., 2013).

Several enzymes of the EBP biosynthetic pathway have been identified as important targets for modulating EBP production. An increased expression or loss of enzyme activity results in alterations in intracellular sugar nucleotides' pool resulting in alterations in EBP production (Ramos et al., 2002). The deletion/inactivation of

* Corresponding author. Tel.: +91 175 239 3421; fax: +91 1752393020.
E-mail address: mghosh@thapar.edu (M. Ghosh).

http://dx.doi.org/10.1016/j.micres.2015.08.003
0944-5013/

one or more enzymes results in reduction or complete loss of EBP production, thus validating the utility of these enzymes as targets for metabolic engineering of EBP production. Conversely, overexpression of one or combination of these enzymes results in enhanced EBP production. For example, disruption of PGM gene resulted in complete loss of EBP production in *Lactobacillus helveticus* (Torino et al., 2005) while an overexpression of PGM resulted in increased EBP yield in *Streptococcus thermophilus* and other lactic acid bacteria (Levander et al., 2002; Svensson et al., 2005; Papagianni, 2012). Similarly, an epimerase-deficient strain of *L. lactis* was unable to synthesize EBP while an engineered strain of *S. thermophilus* overexpressing the enzyme showed higher EBP yield (Degeest and de Vuyst, 2000; Boels et al., 2001; Degeest et al., 2001; Levander et al., 2002; Mozzi et al., 2003; Chai et al., 2012). In line with observations in the role of PGM and epimerase, genetic manipulation studies have also demonstrated the key role of GST in EBP production (van Kranenburg et al., 1999; Torino et al., 2005; Koo et al., 2010). Additionally, several groups have also reported a correlation between enzyme activity and EBP production in several species. For example, activities of PGM and epimerase exhibited a positive correlation with EBP yield in *S. thermophilus* LY03 (Degeest and de Vuyst, 2000; Degeest et al., 2001; Levander et al., 2002).

The application of insertional mutagenesis using Tn5-based vectors offers a particularly interesting feature for construction of complex phenotypes such as biopolymer formation which depend on more than one enzyme. Such an approach may prove to be instrumental in enhancing the landscape of EBP synthesis and thus worthwhile to apply on *Acinetobacter* with a view of achieving a microbial cell factory for EBP production. In an earlier attempt, we enhanced phosphate binding EBP from a strain of *Acinetobacter* using insertional mutagenesis (Tn5 based vectors). Though an increase in EBP biosynthetic enzymes in the mutant clone was presumed from whole cell protein profiles (Kaur et al., 2013b), further studies were imperative for inferring the exact biochemical mechanism crucial for high EBP production. Therefore, in the present study we sought to investigate the role of key enzymes involved in EBP biosynthesis by *A. haemolyticus* MG606 and functionally characterize the responsible enzyme.

2. Materials and methods

2.1. Chemicals and enzymes

All chemicals and media used for EBP production were purchased from HiMedia (Mumbai, India) and were of highest purity available. Adenosine triphosphate (ATP), adenosine diphosphate (ADP), UDP-glucose, G1P, G6P, glucose-6-phosphate dehydrogenase (G6PDH) were purchased from Sigma (MO, USA).

2.2. EBP extraction

Wild type and MG606 mutant of *A. haemolyticus* were inoculated in EBP production medium (peptone 5 g/L, ammonium sulphate 1 g/L, KH_2PO_4 1 g/L, $CaCl_2{\cdot}2H_2O$ 0.7 g/L, NaCl 0.1 g/L, $MgSO_4{\cdot}7H_2O$ 0.3 g/L, K_2HPO_4 1 g/L, glucose 1 g/L, agar 3 g/L; pH 7.0 ± 0.2) and incubated for 48 h at 30 °C. The cultures were then centrifuged at $12{,}000 \times g$ for 30 min at 4 °C. The supernatant fraction was used to recover EBP by precipitating with double volume of chilled ethanol. The crude EBP was purified by precipitation with 10% of cetyl pyridinium chloride and sodium chloride. The pellet formed was dialyzed (molecular weight cut off 12 kDa) extensively with deionised water for 48 h. The resultant was lyophilized to obtain purified EBP.

2.3. Cell extract preparation, enzyme assays and metabolite concentration

Wild type and MG606 mutant of *A. haemolyticus* were grown at 30 °C in Luria-Bertani broth. Log phase cultures of wild and MG606 strains were harvested and centrifuged. The cell pellets were washed with ice cold 100 mM Tris–HCl buffer (pH 7.2), suspended in Tris–HCl buffer and disrupted by pulsed sonication at 4 °C. Cell debris was removed by centrifugation ($12{,}000 \times g$; 15 min) and the supernatant (cell lysate) were used for enzyme assays.

Phosphoglucomutase (PGM) activity was measured by a G6PDH-coupled reaction using G1P as substrate as described by Ye et al. (1994). Briefly, 100 μL of cell lysate was added in 900 μL of pre-warmed assay mixture containing 100 mM Tris–HCl buffer (pH 7.2), 5 mM $MgC1_2$, 50 μM of glucose-1,6-diphosphate, 1 mM G1P, 2 mM NAD and 1 U of G6PDH; increase in absorbance was measured at 340 nm for 10 min.

UDP-glucose epimerase (UDE) activity was determined using UDP-galactose as substrate and UDP-glucose dehydrogenase as the coupling enzyme (Looijesteijn et al., 1999). A 100 μL of cell lysate was added in 900 μL of pre-warmed assay mixture comprising of 50 mM Tris–HCl buffer (pH 8.5), 5 mM $MgCl_2$, 2 mM NAD and 0.01 U of UDP-glucose dehydrogenase. The reaction was initiated by the addition of 0.2 mM of UDP-galactose. The change in absorbance due to formation of NADH was monitored at 340 nm for 10 min.

Phosphoglucoisomerase (PGI) activity was determined by the reverse reaction (F6P as substrate) (Looijesteijn et al., 1999). Briefly, 100 μL of cell lysate was added in 900 μL of pre-warmed assay mixture containing 50 mM potassium phosphate (pH 6.8), 5 mM $MgCl_2$, 0.4 mM NADP and 4 U G6PDH. The reaction was initiated by adding 5 mM of F6P. One unit of enzymatic (PGM, UDE and PGI) activity is defined as the amount of substrate required for formation of 1 μM NAD(P)H per min per mg of protein (Looijesteijn et al., 1999; Velasco et al., 2007).

Glucosyltransferases (GST) activity was determined using p-nitrophenylglucopyranoside as substrate and enzyme activity was correlated with p-nitrophenol released (Darkoh et al., 2011). Briefly, 100 μL of cell lysate was added in 900 μL of pre-warmed assay mixture containing 50 mM Tris–HCl buffer (pH 7.4), 15 mM p-nitrophenylglucopyranoside, 1 mM $MnC1_2$ and 50 mM NaCl. The reaction mixture was incubated for 12 h, aliquots (200 μL) were withdrawn from the reaction mixture every 3 h. The aliquots were mixed with 40 μL of 3 M Na_2CO_3 and absorbance read at 410 nm.

Substrate specificity of PGM was determined by a direct assay for phosphate as described by Ye et al. (1994). The enzyme was incubated in 1 ml reaction mixture comprising of 100 mM Tris–HCl buffer (pH 7.2), 5 mM $MgC1_2$, 50 μM of glucose-1,6-diphosphate and 1 mM substrate. Aliquots (200 μL) were withdrawn at different time points and the reaction was quenched by mixing with an equal volume of 2 N HCl. The samples were heated (100 °C, 10 min), centrifuged and volume of supernatant adjusted to 1 ml; the released inorganic phosphate was determined by stannous chloride method (Kaur et al., 2013a).

For measurement of intracellular metabolite concentration, log phase cultures of TK15 and MG606 were harvested by centrifugation and pellet was resuspended in 75% methanol. The resulting suspension was heated at 80 °C for 5 min, cooled and lyophilized. Intracellular concentrations of glucose-1-phosphate, glucose-6-phosphate and UDP-glucose were determined in the lyophilized powder by coupled enzyme assays (Garrigues et al., 1997; Masuda et al., 2001; Sanfelix-Haywood et al., 2011).

2.4. Gel electrophoresis of whole cell extract

Total protein profiles of wild and MG606 strains of *A. haemolyticus* were analyzed by SDS-PAGE using whole cell lysates (80 μg

Table 1
Primer sequence for *pgm* and *tuf* gene.

Gene	Primer sequence
pgm	
Forward primer	5′-CCGTGTAGTGATGGTTGATAAGTTCGGTAAC-3′
Reverse primer	5′-GCTTTTTCAAGTGCCACTTCAAGTGCC-3′
tuf	
Forward primer	5′-TGGGAAGCGAAAATCCTG-3′
Reverse primer	5′-CAGTACAGGTAGACTTCTG-3′

of protein) and visualized with Coomassie Blue R-250. For zymographic analysis, proteins were separated on native PAGE (lacking SDS) and incubated in a reaction mixture, containing 100 mM Tris–HCl buffer (pH 7.2), 5 mM $MgC1_2$, 50 μM of glucose-1,6-diphosphate, 1 mM G1P, 2 mM NAD, 1 U of G6PDH, 0.01% phenazinemethosulphate and 0.05% nitrobluetetrazolium (Qian et al., 1994). Western blotting was performed as described elsewhere (Malik et al., 2012). Nitrocellulose membrane was probed with polyclonal anti-PGM mouse serum and visualized with alkaline phosphate conjugated rabbit anti-mouse antibodies.

2.5. *pgm* transcription

pgm gene expression in wild type and MG606 cells was determined by real time PCR (RT-PCR). Total RNA was extracted using RNA isolation kit (Promega, Madison, WI, USA). The extracted RNA was subjected to reverse transcription for first strand cDNA synthesis using random hexamer primers. The first strand cDNA was amplified by PCR using primers in Table 1. The reaction mixture (50 μL) contained 2× PCR SYBR green ready mix with 19 μL water, 2 μL each of forward and reverse primers and 2 μL of cDNA. All reactions were run in triplicates on ABI Step-one Real Time PCR machine. The PCR conditions were 94 °C/2 min; 94 °C/5 s; 55 °C/10 s; 72 °C/10 s; 72 °C/5 min till 40 cycles. The gene expression was normalized to housekeeping gene, *tuf*. The fold change in *pgm* expression was calculated using $2^{-\Delta\Delta Ct}$ method as described elsewhere (Livak and Schmittgen, 2001; Schmittgen and Livak, 2008).

2.6. Purification of PGM

PGM was purified from log phase cultures of mutant *A. haemolyticus* as described elsewhere with modifications (Belocopitow and Marehal, 1974; Neves et al., 2006). Cells were centrifuged, washed with Buffer A (50 mM Tris–HCl buffer containing 2 mM EDTA; pH 7.2) and pellet was resuspended in the same buffer. Cells were disrupted by pulsed sonication and the cell lysate was centrifuged as described above. Solid ammonium sulfate was gradually added to the supernatant to obtain 0.2 (=20%) saturation and kept overnight at 4 °C. The precipitate was removed by centrifugation and additional amount of solid ammonium sulfate was added to the supernatant to obtain 0.7 saturation. The solution was kept overnight at 4 °C, centrifuged and precipitate dissolved in buffer B (50 mM Tris–HCl containing 30 mM KCl; pH 7.2). The solution was dialyzed overnight with buffer B and applied on Sephacryl S-100 HR column pre-equilibrated with buffer B. The fractions were analyzed for PGM activity and active fractions were pooled. The fraction showing highest enzyme activity was applied on a DEAE-cellulose column and eluted with Tris–HCl buffer with KCl gradient (0–0.5 mM). The eluates were analyzed for PGM activity to identify the active fraction.

2.7. Factors influencing PGM activity

The effect of pH, temperature and inhibitors/activators on PGM activity was determined in mutant strain. Purified PGM was incubated with reaction mixture over a range of pH (5–8) and enzyme activity determined as described above. In order to study the effect of temperature on enzyme activity, purified PGM was mixed with reaction buffer (pH 7.5) and incubated over a range of temperature (25–40 °C).

PGM activity was also determined in presence of ions *i.e.* $MgCl_2$, $MnCl_2$, $CaCl_2$, $CoCl_2$, $NiCl_2$, LiCl and $ZnCl_2$ (5 mM) as well as other modifiers such as ATP, ADP, UDP-glucose, glucose-1,6-biphosphate and fructose-6-phosphate.

2.8. Effect of lithium on EBP production, PGM activity and growth

To observe the effect of lithium on EBP production, log phase cultures of MG606 mutant were inoculated in medium containing 1, 5 or 10 mM lithium chloride (LiCl). The EBP yield and PGM activity were determined following 48 and 3 h of incubation, respectively. The effect of lithium on growth of MG606 was monitored over 48 h at hourly intervals.

Additionally, cell lysates were prepared from naïve MG606 cells (not exposed to LiCl) as described in Section 2.3. PGM assay was performed as described in Section 2.3 except that reaction mixture was spiked with LiCl to achieve final concentrations of 1, 5 or 10 mM LiCl.

2.9. Intracellular lithium concentration

Log phase MG606 cells were incubated with 10 mM LiCl for 3 h and centrifuged in 20 ml aliquots. The cell pellet was washed with 1 ml of 10 mM $MgC1_2$ and hydrolyzed boiling for 10 min in 0.1 M HCl. Lithium concentration was determined in the hydrolysate by flame photometry (Ros et al., 1998).

2.10. Statistical analysis

The data was converted to mean ± SD and statistical analysis was performed using GraphPad Prism. The enzyme activities and *pgm* expression in TK15 and MG606 strains were compared by two-tailed Student's *t*-test. The densitometry results of zymography and western blots were compared by two-tailed paired *t*-test. Multiple group comparison was performed by One-way ANOVA followed by Tukey's test. The intergroup differences were considered significant at $p < 0.05$.

3. Results

3.1. Activity of key enzymes involved in EBP biosynthesis

The interplay between enzymes of EBP biosynthetic pathway can modulate EBP production in bacteria. Amongst the several enzymes involved in EBP production, activities of PGM, UDE, GST and PGI have been demonstrated to influence EBP production in bacteria. We have earlier reported development of an insertional mutant which produced significantly higher amounts of EBP compared to the wild strain. The EBP produced by wild type and MG606 strain was 220 mg/L and 650 mg/L, respectively.

The activities of key enzymes in the EBP biosynthetic pathway were compared in wild and MG606 by spectrophotometric enzyme assays. The specific activity of PGM was found to be 1.5-fold higher in MG606 as compared to wild strain ($p < 0.01$). Further, GST activity was slightly higher in the MG606 strain; however, the difference was statistically insignificant ($p > 0.05$). Similarly, UDE and PGI activity was found to be similar in both strains ($p > 0.05$; Table 2).

Table 2
Enzyme activities of TK15 and MG606 strains of *A. haemolyticus*.

	TK15 (U/mg protein)	MG606 (U/mg protein)	Fold change
Phosphoglucomutase	30.34 ± 3.60	45.11 ± 4.21**	1.49 ± 0.14
UDP-glucose epimerase	70.89 ± 3.89	66.11 ± 5.71	0.94 ± 0.08
Glycosyltransferases	0.0020 ± 0.0005	0.0021 ± 0.0005	1.06 ± 0.23
Phosphoglucoisomerases	1.43 ± 0.24	1.45 ± 0.21	1.01 ± 0.15

Data is mean ± SD of triplicate samples and intergroup differences were compared by Student's *t*-test.
** $p < 0.01$ w.r.t. enzyme activity in *A. haemolyticus* TK 15.

3.2. Comparison of PGM activity and transcripts in wild and mutant strains

In electrophoretograms of whole cell extracts of wild and MG606 strains, distinct differences were noted in protein expression profiles (Fig. 1A). In line with observation in spectrophotometric enzyme assays, zymograms for PGM exhibited higher ($p < 0.05$) enzyme activity in MG606 compared with wild strain (Fig. 1B). Total PGM protein content was compared by densitometric analysis of Western blots and indicated 1.5–2 fold increase ($p < 0.05$) in PGM protein content in MG606 strain (Fig. 1C).

The *pgm* transcripts were quantified by RT-PCR and normalized to *tuf* gene. The Ct values for *pgm* transcripts in wild and MG606 strains were 27.7902 and 26.975, respectively, while corresponding Ct values for *tuf* gene in the two strains were 27.0443 and 26.8053, respectively. A comparison of *pgm* transcripts in both strains by $2^{-\Delta\Delta Ct}$ method revealed 1.5 fold upregulation of *pgm* expression in MG606 with respect to wild strain. Although gene expression tended to be higher in MG606, the difference in ΔCt values between both strains was not significant ($p > 0.05$). Supplementary Fig. 1 shows the melting curves of *pgm* and *tuf* gene in both strains. The presence of a single peak in the melting curves suggests that a single amplicon was generated. The single peak also confirmed the specificity of the primers used and that the increase in fluorescence was due to amplification of a specific sequence. The results of enzyme assays, Western blotting and RT-PCR are in agreement that PGM is overexpressed in MG606 at levels 1.5–2 folds higher than in wild strain.

3.3. Intracellular concentration of sugar precursors

PGM activity has been correlated with intracellular concentrations of its substrates, G1P and G6P, and its downstream metabolite, UDP-glucose. Therefore, intracellular concentrations of the two phosphosugars and UDP-glucose were compared between TK15 and MG606. Intracellular concentrations of G1P and G6P were comparable in both strains ($p > 0.05$) while UDP-glucose levels were significantly higher ($p < 0.05$) in MG606 compared to TK15 (Table 3).

Table 3
Intracellular concentration of sugar precursors in TK15 and MG606 strains of *A. haemolyticus*.

	TK15	MG606
Glucose-1-phosphate	25 ± 6	28 ± 8
Glucose-6-phosphate	23 ± 6	19 ± 4
UDP-glucose	0.05 ± 0.008	0.08 ± 0.006*

Data is mean ± SD of triplicate samples and intergroup differences were compared by Student's *t*-test. Concentrations are expressed as μM/mg protein.
* $p < 0.05$ w.r.t. concentration in *A. haemolyticus* TK 15.

3.4. Purification, kinetic and other properties of PGM

PGM was purified sequentially by ammonium sulfate precipitation, gel permeation chromatography and ion exchange chromatography. The purified enzyme was purified 34.3 folds after the last step as adjudged by enzyme activity measurements. The fold concentration of enzyme after each purification step is summarized in Table 4.

The purified enzyme catalyzed the conversion of G1P to G6P with a Km of 0.028 mM and Vmax of 0.06 mM/min. The enzyme catalyzed conversion of mannose 1-phosphate (M1P) to mannose 6-phosphate (M6P) with a Km of approximately 0.017 mM with Vmax of 0.038 mM/min (Supplementary Fig. 2). The specific activity of enzyme toward M1P and fructose-1-phosphate was found to be approximately 30% and 0%, respectively, with respect to G1P as substrate. A similar bifunctional enzyme catalyzing interconversion of G1P and G6P as well as M1P and M6P has been demonstrated in *Pseudomonas aeuroginosa, Clostridium thermocellum* and other organisms (Joshi and Handler, 1964; Ye et al., 1994; Wang and Zhang, 2010).

3.5. Effect of temperature and pH

The effect of temperature on PGM activity in mutant strain was determined over a range of 25–40 °C. The enzyme activity increased in a temperature-dependent manner from 20 to 35 °C and reduced upon further increase of temperature to 40 °C (Fig. 2A). The effect of pH on PGM activity in mutant strain was determined over a pH

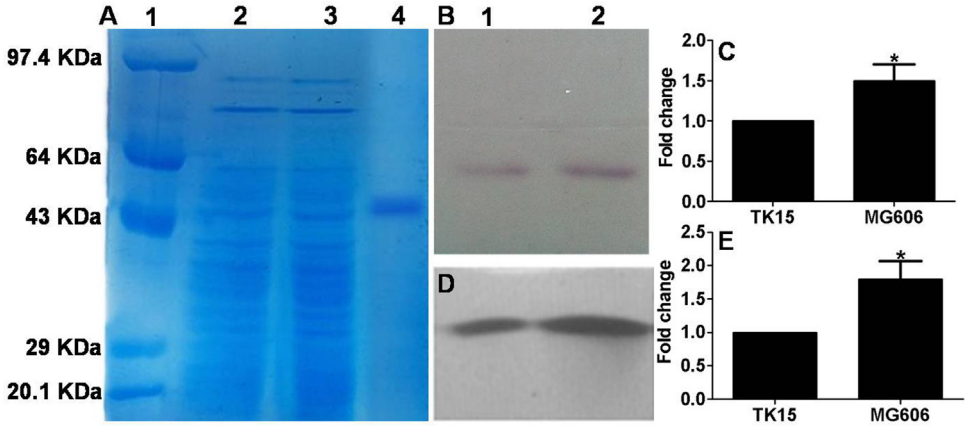

Fig. 1. (A) Coomassie blue stained 12% SDS-PAGE gels showing molecular weight markers (lane 1), whole cell protein profile of wild strain (lane 2) and MG606 mutant (Lane 3), and purified enzyme (lane 4). (B) Zymogram of PGM activity in wild strain (Lane 1) and MG606 mutant (Lane 2). (C) Quantitative comparison of PGM activities in zymograms by densitometry. (D) Western blot of PGM in wild strain (Lane 1) and MG606 mutant (Lane 2). (E) Quantitative comparison of PGM activities in western blots by densitometry. *$p < 0.05$ w.r.t. band intensity in *A. haemolyticus* TK 15.

Table 4
Purification of PGM/PMM from MG606 mutant of *A. haemolyticus*.

Purification step	Total protein (mg)	Specific activity (U/mg)	% Recovery	Fold purification
Cell lysate	800	45.1	100	1.0
Ammonium sulfate precipitation	320	90.4	91	2.0
Gel filtration	10.2	975	68	21.6
Ion exchange	3.5	1548	33	34.3

Table 5
Effect of modifiers on PGM activity in MG606 mutant of *A. haemolyticus*.

Modifier (5 mM)	Inhibition (%)
Magnesium	0 ± 0
Calcium	50 ± 4
Cobalt	78 ± 6
Nickel	96 ± 4
Lithium	100 ± 0
Zinc	100 ± 0
UDP-glucose	65 ± 5
ADP	50 ± 2
ATP	20 ± 1
Fructose-6-phosphate	38 ± 1
Glucose-1,6-biphosphate	90 ± 3
Glucose-6-phosphate	0 ± 0
EDTA	8 ± 1

Data is mean ± SD of triplicate samples.
UDP-glucose = uridine diphosphate glucose, ADP = adenosine diphosphate, ATP = adenosine triphosphate, EDTA = ethylene diamine tetraacetic acid.

range of 3–9. The enzyme activity increased in a pH-dependent manner, reaching a maximum at pH 7.5 and reduced thereafter with increase in pH to 8 (Fig. 2B). A similar weakly basic pH optima was also reported in *Escherichia coli*, *Pyrococcus horikoshii* and *Clostridium thermocellum* (Ye et al., 1994; Wang and Zhang, 2010).

3.6. Effect of PGM activity inhibitors/modifiers

The effect of chemicals/ions known to influence activity of PGM in other species was determined on purified PGM of mutant strain. Zinc, lithium, nickel and cobalt exhibited significantly high inhibition of the purified enzyme in their order of sequence. These results corroborated those reported by Ye et al. (1994) in PGM purified from *Pseudomonas aeruginosa*. Other modifiers such as glucose-1,6-biphosphate significantly inhibited PGM in contrast to G6P (Table 5).

In order to examine whether PGM overexpression actually led to an enhanced EBP production, mutant cells were grown in presence of LiCl. EBP production decreased in a concentration-dependent manner from 650 mg/L in untreated control cells to 276 mg/L in cells incubated at the highest concentration of LiCl (Fig. 3). Cell growth was unaltered in presence of 1 and 5 mM LiCl while approximately 10% reduction in cell growth was observed at the highest concentration (Supplementary Fig. 3). These results suggest that

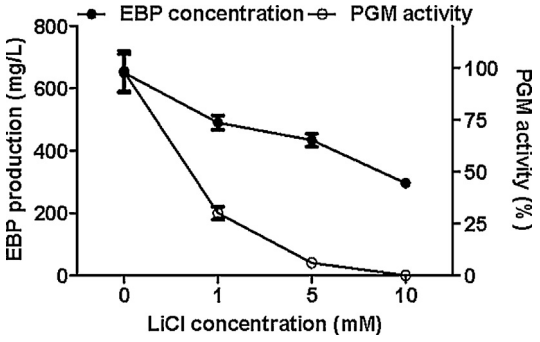

Fig. 3. Effect of lithium chloride on EBP production and PGM activity in MG606 strain.

reduction in EBP production is not due to cell death or growth inhibition but a consequence of PGM inhibition.

To validate *in vivo* inhibition of PGM by LiCl, lithium concentration was determined in cell lysates of MG606 cells. The intracellular levels of lithium were found to be 8 ± 0.7 mM following incubation with 10 mM LiCl for 3 h. The ability of LiCl to inhibit PGM activity under *in vivo* conditions was further confirmed by estimating PGM activity in cell lysates prepared from naïve MG606 cells and spiked with 0 (control), 1, 5 and 10 mM LiCl. Comparative analysis of PGM activity revealed that enzyme activity was reduced to approximately one-fourth of the control cells at 1 mM LiCl while the enzyme was completely inhibited at 5 and 10 mM LiCl (Fig. 3). These results suggest that lithium can enter inside MG606 cells and exhibit its inhibitory action on PGM.

To further investigate the effect of LiCl treatment on intracellular PGM levels, PGM activity was determined in cell lysates of LiCl-treated cells. The enzyme activity was found to increase by 5, 28 and 40% after incubation with 1, 5 and 10 mM LiCl, respectively, compared to untreated cells. This increase in PGM activity may be attributed to a stress-dependent PGM induction as observed in yeast (Masuda et al., 2001).

4. Discussion

Molecular biology tools have remained the mainstay for reprogramming industrially important microorganisms to harness their potential as cell factories. With ever expanding horizons of

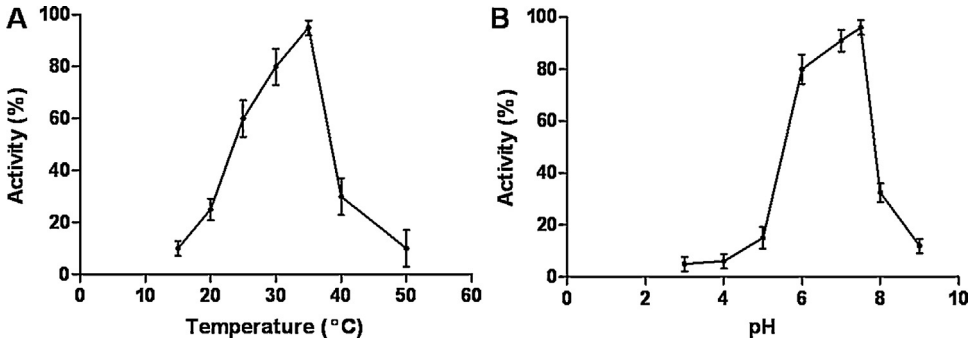

Fig. 2. Effect of temperature (A) and pH (B) on activity of PGM purified from MG606 strain.

molecular biology, and encompassing metabolic engineering, it is imperative to delineate the regulatory networks and checkpoints modulating the production of economically important metabolites by microorganisms. The genus *Acinetobacter* has gathered considerable attention in the recent past owing to several extracellular products as well as unique capabilities of biotechnological importance of many members of this genus. The importance of EBP in effective removal of phosphorous by an environmental isolate *A. haemolyticus* and its EBP-overproducing insertional mutant were reported in earlier studies by our group (Kaur et al., 2013a,b). The isolate (TK15) and the mutant (MG606) strain were found to be non-pathogenic in nature based on absence of virulence factors and rapid intramacrophage killing in RAW 264.7 cells (unpublished data) thereby supporting biotechnological application of both strains. In the present study, we sought to investigate the role of key enzymes involved in EBP biosynthesis by *A. haemolyticus* MG606 and functionally characterize the responsible enzyme.

Spectrophotometric enzyme assays revealed that PGM activity was significantly ($p < 0.05$) higher in MG606 whereas no significant change ($p > 0.05$) was noted in UDE, GST and PGI activities. The increase in PGM activity, independent of other enzymes, indicated that either PGM structure or its expression was altered due to Tn5 insertion. The electrophoretic mobility of PGM in wild and MG606 strains was identical as indicated by zymography suggesting that neither the protein structure was altered nor any additional isozyme was produced in MG606. On the other hand, results of zymography, Western blotting and RT-PCR suggested an upregulation of *pgm* transcripts resulting in overexpression of PGM. Tn5 insertion in MG606 has been mapped upstream of PGM/PMM gene (unpublished data) and hence, the observed upregulation of *pgm* expression could be attributed to Tn5 insertion. A similar activation/upregulation of genes located downstream of Tn5 insertion has been reported in *E. coli* and other microorganisms site (Berg et al., 1980, 1983; Hecker et al., 1988; Wang and Roth, 1988; Clark et al., 1994; Gutierrez et al., 1997; Guo et al., 2010). The kinetic and substrate specificity properties of purified enzyme suggest that MG606 expressed a single, bifunctional enzyme with PGM/PMM activities similar to *Clostridium thermocellum, Pseudomonas aeruginosa* and other organisms (Joshi and Handler, 1964; Ye et al., 1994; Wang and Zhang, 2010). Since PGM is responsible for modulating the carbon flux between EBP and energy producing pathways, an increase in PGM activity may be presumed to divert carbon flux toward EBP-producing pathway, which, in turn, may lead to increased EBP production (Levander and Radstrom, 2001; Boels et al., 2003). Analysis of intracellular sugar metabolites revealed elevation in UDP-glucose levels with no detectable change in G1P and G6P levels. A similar correlation between PGM activity and intracellular UDP-glucose levels has been noted in *Lactococcus lactis*, *Lactobacillus casei* and *Saccharomyces cerevisiae* (Kaur T, Ghosh M, Characterization and upregulation of bifunctional Phosphoglucomutase/Phosphomannomutase enzyme in an exobiopolymer overproducing strain of *Acinetobacter haemolyticus*, *Microbiological Research*, doi: 10.1016/j.micres.2015.08.003). These results corroborated previous observations (Levander and Radstrom, 2001; Boels et al., 2003; Zhang et al., 2014) suggesting PGM to be crucial in EBP synthesis by *A. haemolyticus* and upregulation of PGM expression could result in increased EBP production. Observations in *P. aeruginosa* suggest that PGM acts as a checkpoint in exopolysaccharide synthesis (Franklin et al., 2011; Ma et al., 2012) and upregulation of PGM activity in *A. haemolyticus* MG606 could potentially enhance carbon flux toward EBP biosynthesis pathway resulting in EBP overproduction.

The role of lithium as an *in vivo* target for inhibiting PGM has been reported in the yeast *Saccharomyces cerevisiae* and *Candida albicans* (Masuda et al., 2001; Bro et al., 2003; Csutora et al., 2005; Regenberg et al., 2006; Martins et al., 2008). The strong inhibitory effect of lithium on PGM has been attributed to the replacement of magnesium ion, the cofactor for PGM. In order to further validate the role of PGM/PMM in EBP production, we tested the effect of lithium by growing the mutant MG606 in presence of LiCl. A significant ($p < 0.05$) decline in EBP production by MG606 cells was observed further testifying the role of PGM/PMM. However, cell lysates of LiCl-treated cells showed a concentration-dependent increase in PGM activity. Although the increased PGM activity after LiCl may appear counterintuitive, the increased enzyme activity (upregulation) is not unexpected because lithium-induced PGM inhibition under *in vivo* conditions may trigger compensatory upregulation of the enzyme to maintain cellular homeostasis (Masuda et al., 2001). However, the upregulation of PGM may not be sufficient enough to completely revert the effects of lithium inhibition as evident from the apparent, concentration-dependent reduction in EBP production.

Conclusion

The present study demonstrated that in MG606 the mutant clone of *A. haemolyticus*, enhanced production of EBP with high phosphate binding ability occurs due to the upregulation of PGM/PMM. The higher enzyme activity results in formation of EBP precursor metabolites presumably favoring the metabolic flux toward EBP synthesis, resulting in higher EBP production. We believe that this is the first study demonstrating the key role of PGM upregulation in EBP production by *Acinetobacter*. Apparently, this is also the first study on characterization of PGM in an *Acinetobacter* sp.

Conflict of interest

The authors report no declarations of interest.

Acknowledgements

This work was supported by grants from University Grants Commission, New Delhi. TK is thankful to University Grants Commission (UGC), New Delhi for providing Maulana Azad National Fellowship.

Appendix A. Supplementary data

Supplementary data associated with this article can be found, in the online version, at http://dx.doi.org/10.1016/j.micres.2015.08.003

References

Ali S, Sandhya V, Venkateswar Rao L. Isolation and characterization of drought-tolerant ACC deaminase and exopolysaccharide-producing fluorescent *Pseudomonas* sp. Ann Microbiol 2014;64(2):493–502.

Auger C, Han S, Appanna VP, Thomas SC, Ulibarri G, Appanna VD. Metabolic reengineering invoked by microbial systems to decontaminate aluminum: implications for bioremediation technologies. Biotechnol Adv 2012;31(2):266–73.

Belocopitow E, Marehal LR. Metabolism of trehalose in *Euglena gracilis*. Eur J Biochem 1974;46(3):631–7.

Boels IC, Kleerebezem M, de Vos WM. Engineering of carbon distribution between glycolysis and sugar nucleotide biosynthesis in *Lactococcus lactis*. Appl Environ Microbiol 2003;69(2):1129–35.

Berg DE, Weiss A, Crossland L. Polarity of Tn5 insertion mutations in *Escherichia coli*. J Bacteriol 1980;142(2):439–46.

Berg DE, Schmandt MA, Lowe JB. Specificity of transposon Tn5 insertion. Genetics 1983;105(4):813–28.

Boels IC, Ramos A, Kleerebezem M, de Vos WM. Functional analysis of the *Lactococcus lactis* galU and galE genes and their impact on sugar nucleotide and exopolysaccharide biosynthesis. Appl Environ Microbiol 2001;67(7):3033–40.

Bounaix MS, Robert H, Gabriel V, Morel S, Remaud-Simeon M, Gabriel B, Fontagne-Faucher C. Characterization of dextran-producing *Weissella* strains isolated from sourdoughs and evidence of constitutive dextransucrase expression. FEMS Microbiol Lett 2010;311(1):18–26.

Bro C, Regenberg B, Lagniel G, Labarre J, Montero-Lomeli M, Nielsen J. Transcriptional, proteomic, and metabolic responses to lithium in galactose-grown yeast cells. J Biol Chem 2003;278(34):32141–9.

Calvo C, Silva-Castro GA, Uad I, Garcia Fandino C, Laguna J, Gonzalez-Lopez J. Efficiency of the EPS emulsifier produced by *Ochrobactrum anthropi* in different hydrocarbon bioremediation assays. J Ind Microbiol Biotechnol 2008;35(11):1493–501.

Chai Y, Beauregard PB, Vlamakis H, Losick R, Kolter R. Galactose metabolism plays a crucial role in biofilm formation by *Bacillus subtilis*. MBio 2012;3(4):e00184–212.

Clark AJ, Satin L, Chu CC. Transcription of the *Escherichia coli* recE gene from a promoter in Tn5 and IS50. J Bacteriol 1994;176(22):7024–31.

Csutora P, Strassz A, Boldizsar F, Nemeth P, Sipos K, Aiello DP, Bedwell DM, Miseta A. Inhibition of phosphoglucomutase activity by lithium alters cellular calcium homeostasis and signaling in *Saccharomyces cerevisiae*. Am J Physiol Cell Physiol 2005;289(1):C58–67.

Darkoh C, Kaplan HB, Dupont HL. Harnessing the glucosyltransferase activities of *Clostridium difficile* for functional studies of toxins A and B. J Clin Microbiol 2011;49(8):2933–41.

Degeest B, de Vuyst L. Correlation of activities of the enzymes alpha-phosphoglucomutase, and UDP-galactose 4-epimerase, and UDP-glucose pyrophosphorylase with exopolysaccharide biosynthesis by *Streptococcus thermophilus* LY03. Appl Environ Microbiol 2000;66(8):3519–27.

Degeest B, Vaningelgem F, Laws AP, De Vuyst L. UDP-N-acetylglucosamine 4-epimerase activity indicates the presence of N-acetylgalactosamine in exopolysaccharides of *Streptococcus thermophilus* strains. Appl Environ Microbiol 2001;67(9):3976–84.

Dertli E, Colquhoun IJ, Gunning AP, Bongaerts RJ, Le Gall G, Bonev BB, Mayer MJ, Narbad A. Structure and biosynthesis of two exopolysaccharides produced by *Lactobacillus johnsonii* FI9785. J Biol Chem 2013;288(44):31938–51.

Franklin MJ, Nivens DE, Weadge JT, Howell PL. Biosynthesis of the *Pseudomonas aeruginosa* extracellular polysaccharides, alginate, Pel, and Psl. Front Microbiol 2011;2:167.

Garrigues C, Loubiere P, Lindley ND, Cocaign-Bousquet M. Control of the shift from homolactic acid to mixed-acid fermentation in *Lactococcus lactis*: predominant role of the NADH/NAD+ ratio. J Bacteriol 1997;179(17):5282–7.

Guo Y, Sagaram US, Kim JS, Wang N. Requirement of the galU gene for polysaccharide production by and pathogenicity and growth In Planta of *Xanthomonas citri* subsp. citri. Appl Environ Microbiol 2010;76(7):2234–42.

Gutierrez JC, Santero E, Tortolero M. Ammonium repression of the nitrite-nitrate (nasAB) assimilatory operon of *Azotobacter vinelandii* is enhanced in mutants expressing the nifO gene at high levels. Mol Gen Genet 1997;255(2):172–9.

Hecker M, Riethdorf S, Bauer C, Schroeter A, Borriss R. Expression of a cloned beta-glucanase gene from *Bacillus amyloliquefaciens* in an *Escherichia coli* relA strain after plasmid amplification. Mol Gen Genet 1988;215(1):181–3.

Ibarburu I, Soria-Diaz ME, Rodriguez-Carvajal MA, Velasco SE, Tejero-Mateo P, Gil-Serrano AM, Irastorza A, Duenas MT. Growth and exopolysaccharide (EPS) production by *Oenococcus oeni* I4 and structural characterization of their EPSs. J Appl Microbiol 2007;103(2):477–86.

Joshi A, Kanekar P. Production of exopolysaccharide by *Vagococcus carniphilus* MCM B-1018 isolated from alkaline Lonar Lake, India. Ann Microbiol 2011;61(4):733–40.

Joshi JG, Handler P. Phosphoglucomutase I. purification and properties of phosphoglucomutase from *Escherichia coli*. J Biol Chem 1964;239:2741–51.

Jung JH, Seo DH, Holden JF, Park CS. Identification and characterization of an archaeal kojibiose catabolic pathway in the hyperthermophilic *Pyrococcus* sp. strain ST04. J Bacteriol 2014;196(5):1122–31.

Kaur T, Ganguli A, Ghosh M. Development of exobiopolymer-based biosensor for detection of phosphate in water. Water Sci Technol 2013a;68(12):2619–25.

Kaur T, Sharma J, Ganguli A, Ghosh M. Application of biopolymer produced from metabolic engineered *Acinetobacter* sp. for the development of phosphate opto-electronic sensor. Compos Interfaces 2013b;21(4):143–51.

Koo H, Xiao J, Klein MI, Jeon JG. Exopolysaccharides produced by *Streptococcus mutans* glucosyltransferases modulate the establishment of microcolonies within multispecies biofilms. J Bacteriol 2010;192(12):3024–32.

Kralj S, Grijpstra P, van Leeuwen SS, Leemhuis H, Dobruchowska JM, van der Kaaij RM, Malik A, Oetari A, Kamerling JP, Dijkhuizen L. 4,6-Alpha-glucanotransferase, a novel enzyme that structurally and functionally provides an evolutionary link between glycoside hydrolase enzyme families 13 and 70. Appl Environ Microbiol 2011;77(22):8154–63.

Levander F, Radstrom P. Requirement for phosphoglucomutase in exopolysaccharide biosynthesis in glucose- and lactose-utilizing *Streptococcus thermophilus*. Appl Environ Microbiol 2001;67(6):2734–8.

Levander F, Svensson M, Radstrom P. Enhanced exopolysaccharide production by metabolic engineering of *Streptococcus thermophilus*. Appl Environ Microbiol 2002;68(2):784–90.

Livak KJ, Schmittgen TD. Analysis of relative gene expression data using real-time quantitative PCR and the 2(−Delta Delta C(T)) Method. Methods 2001;25(4):402–8.

Looijesteijn PJ, Boels IC, Kleerebezem M, Hugenholtz J. Regulation of exopolysaccharide production by *Lactococcus lactis* subsp. cremoris by the sugar source. Appl Environ Microbiol 1999;65(11):5003–8.

Ma L, Wang J, Wang S, Anderson EM, Lam JS, Parsek MR, Wozniak DJ. Synthesis of multiple *Pseudomonas aeruginosa* biofilm matrix exopolysaccharides is post-transcriptionally regulated. Environ Microbiol 2012;14(8):1995–2005.

Malik M, Ganguli A, Ghosh M. Enhancement of bioconversion efficiency of limonin by *Pseudmonas putida* G7. Int J Food Sci Nutr 2012;63(1):59–65.

Martins LF, Montero-Lomeli M, Masuda CA, Fortes FS, Previato JO, Mendonca-Previato L. Lithium-mediated suppression of morphogenesis and growth in *Candida albicans*. FEMS Yeast Res 2008;8(4):615–21.

Masuda CA, Xavier MA, Mattos KA, Galina A, Montero-Lomeli M. Phosphoglucomutase is an in vivo lithium target in yeast. J Biol Chem 2001;276(41):37794–801.

Mozzi F, Savoy de Giori G, Font de Valdez G. UDP-galactose 4-epimerase: a key enzyme in exopolysaccharide formation by *Lactobacillus casei* CRL 87 in controlled pH batch cultures. J Appl Microbiol 2003;94(2):175–83.

Neves AR, Pool WA, Castro R, Mingote A, Santos F, Kok J, Kuipers OP, Santos H. The a-phosphoglucomutase of *Lactococcus lactis* is unrelated to the a-phosphohexomutase superfamily and is encoded by the essential gene pgmH. J Biol Chem 2006;281(48):36864–73.

Papagianni M. Metabolic engineering of lactic acid bacteria for the production of industrially important compounds. Comput Struct Biotechnol J 2012;3:e201210003.

Qian N, Stanley GA, Hahn-Hagerdal B, Radstrom P. Purification and characterization of two phosphoglucomutases from *Lactococcus lactis* subsp. lactis and their regulation in maltose- and glucose-utilizing cells. J Bacteriol 1994;176(17):5304–11.

Ramos A, Neves AR, Santos H. Metabolism of lactic acid bacteria studied by nuclear magnetic resonance. Antonie Van Leeuwenhoek 2002;82(1–4):249–61.

Ramos A, Boels IC, de Vos WM, Santos H. Relationship between glycolysis and exopolysaccharide biosynthesis in *Lactococcus lactis*. Appl Environ Microbiol 2001;67(1):33–41.

Regenberg B, Grotkjaer T, Winther O, Fausboll A, Akesson M, Bro C, Hansen LK, Brunak S, Nielsen J. Growth-rate regulated genes have profound impact on interpretation of transcriptome profiling in *Saccharomyces cerevisiae*. Genome Biol 2006;7(11):R107.

Ros R, Montesinos C, Rimon A, Padan E, Serrano R. Altered Na+ and Li+ homeostasis in *Saccharomyces cerevisiae* cells expressing the bacterial cation antipoetic NhaA. J Bacteriol 1998;180(12):3131–6.

Sanfelix-Haywood N, Coll-Marques JM, Yebra MJ. Role of alpha-phosphoglucomutase and phosphoglucose isomerase activities at the branching point between sugar catabolism and anabolism in *Lactobacillus casei*. J Appl Microbiol 2011;111(2):433–42.

Schmittgen TD, Livak KJ. Analyzing real-time PCR data by the comparative CT method. Nat Protoc 2008;3(6):1101–8.

Seibel J, Jordening H-J, Buchholz K. Glycosylation with activated sugars using glycosyltransferases and transglycosidases. Biocatal Biotransform 2006;24(5):311–42.

Svensson M, Waak E, Svensson U, Radstrom P. Metabolically improved exopolysaccharide production by *Streptococcus thermophilus* and its influence on the rheological properties of fermented milk. Appl Environ Microbiol 2005;71(10):6398–400.

Torino MI, Mozzi F, Font de Valdez G. Exopolysaccharide biosynthesis by *Lactobacillus helveticus* ATCC 15807. Appl Microbiol Biotechnol 2005;68(2):259–65.

van Kranenburg R, Vos HR, van S, Kleerebezem II, de Vos MWM. Functional analysis of glycosyltransferase genes from *Lactococcus lactis* and other gram-positive cocci: complementation, expression, and diversity. J Bacteriol 1999;181(20):6347–53.

Velasco SE, Yebra MJ, Monedero V, Ibarburu I, Duenas MT, Irastorza A. Influence of the carbohydrate source on beta-glucan production and enzyme activities involved in sugar metabolism in *Pediococcus parvulus* 2.6. Int J Food Microbiol 2007;115(3):325–34.

Vlamakis H, Chai Y, Beauregard P, Losick R, Kolter R. Sticking together: building a biofilm the *Bacillus subtilis* way. Nat Rev Microbiol 2013;11(3):157–68.

Wang A, Roth JR. Activation of silent genes by transposons Tn5 and Tn10. Genetics 1988;120(4):875–85.

Wang Y, Zhang YH. A highly active phosphoglucomutase from *Clostridium thermocellum*: cloning, purification, characterization and enhanced thermostability. J Appl Microbiol 2010;108(1):39–46.

Ye RW, Zielinski NA, Chakrabarty AM. Purification and characterization of phosphomannomutase/phosphoglucomutase from *Pseudomonas aeruginosa* involved in biosynthesis of both alginate and lipopolysaccharide. J Bacteriol 1994;176(16):4851–7.

Zhang Q, Yang B, Brashears MM, Yu Z, Zhao M, Liu N, Li Y. Influence of casein hydrolysates on exopolysaccharide synthesis by *Streptococcus thermophilus* and *Lactobacillus delbrueckii* ssp. bulgaricus. J Sci Food Agric 2014;94(7):1366–72.

Supplementary information

Characterization and upregulation of bifunctional Phosphoglucomutase/Phosphomannomutase enzyme in an exobiopolymer overproducing strain of *Acinetobacter haemolyticus*

Taranpreet Kaur, Moushumi Ghosh*

Department of Biotechnology, Thapar University, Patiala, Punjab, India – 147 004

*Corresponding author: Moushumi Ghosh, Email: mghosh@thapar.edu; Tel: +91-175-239 3421

Supplementary Figure 1: RT-PCR showing *pgm* transcripts of wild strain and MG606 mutant of *A. haemolyticus*.

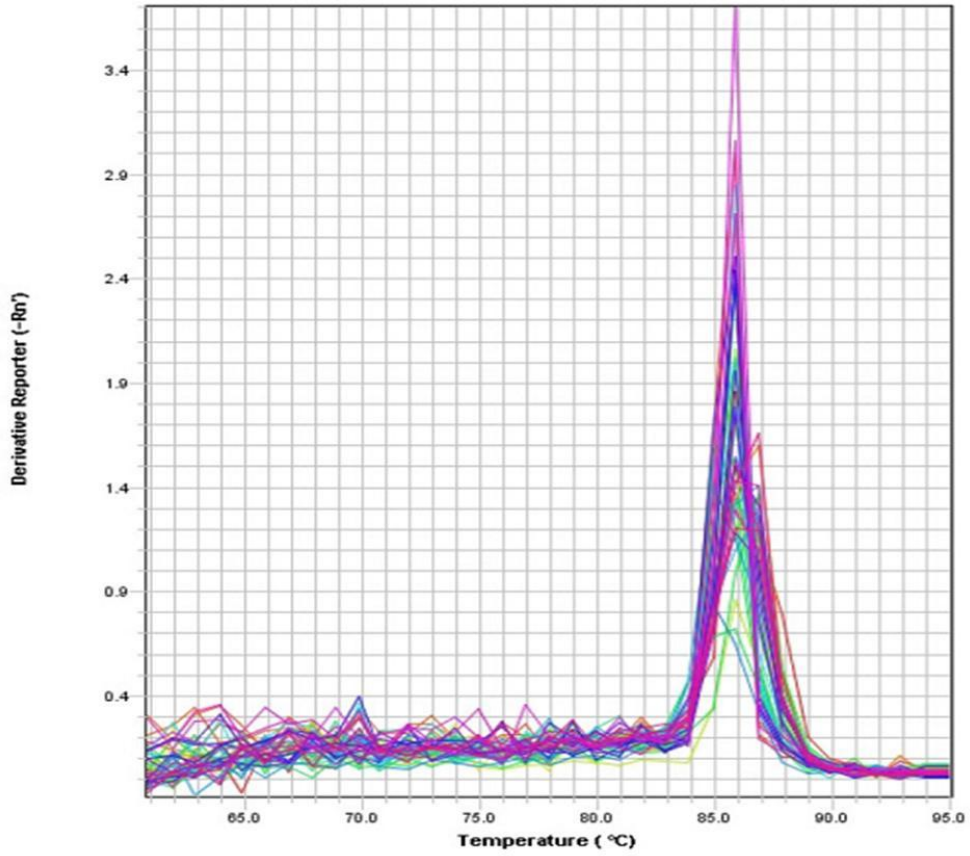

Supplementary Figure 2: Lineweaver-Burk plot of PGM using glucose-1-phosphate (A) and mannose-1-phosphate (B) as substrates.

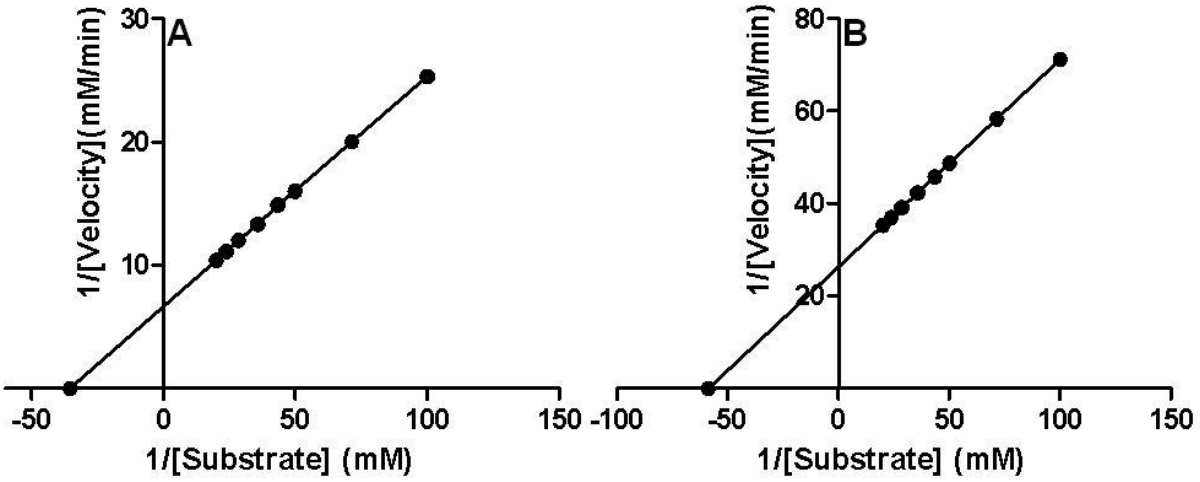

Supplementary Figure 3: Effect of lithium chloride on growth of MG606.